

H Y D R O G E N T R A N S F E R R E A C T I O N S
O F I N D O L E S

BY

HENRY STEPHEN RZEPA, B.Sc.

August, 1974

A Thesis submitted for the degree
of Doctor of Philosophy of the
University of London.

Chemistry Department,
Imperial College,
London, S.W.7.

ABSTRACT.

The validity of kinetic hydrogen isotope effects as an index of transition state symmetry is reviewed, and the results compared with other indexes such as the Brønsted exponent. The effect of quantum tunnelling of the proton on isotope effects is discussed.

A study of hydrogen exchange of sterically hindered indoles showed that bulky substituents in the 4-position slowed the exchange rate of the indolyl anion, but not the neutral molecule. This unusual result is interpreted in terms of considerable differences in the transition state symmetry of the two pathways, induced by the difference in the remote substituent (NH *vis a vis* N⁻). Deuterium isotope effects for the two pathways were very similar and no proton tunnelling was detected.

Diazocoupling to indoles was found to proceed with a fast proton transfer. A partial change in rate determining step occurred when a bulky substituent occupied the 4-position of the indole, and this was interpreted as a steric effect on the proton abstraction by base, resulting from an asymmetric σ complex.

Decarboxylation of indole-3-carboxylic acid was also found to proceed *via* a partially rate determining ring protonation, and a detailed kinetic analysis enabled isotope effects to be evaluated for these compounds. No systematic variation with substrate reactivity was found.

The base catalysed ionisation of 2-indolinones proved to be highly analogous to indoles, with bulky 4- groups slowing the rate by about 37 times more than expected. This is the largest steric effect yet found for carbon acid ionisation not involving a hindered amine as base and suggests that steric effects may have general utility in predicting the symmetry of the transition state for hydrogen transfer. Deuterium isotope effects for this reaction were evaluated with greater accuracy than for indoles and their magnitude suggests no proton tunnelling. A value for the Swain-Schaad exponent is reported.

These results suggest that isotope effects are not a good index of transition state symmetry, particularly for A-S_E2 reactions, and that a study of comparative steric effects can be more useful in certain cases.

ACKNOWLEDGEMENTS

I would like to thank my Supervisor, Dr. B.C.Challis, for the inspiration behind the work described here and the encouragement which enabled it to be completed.

I am also very grateful to Professor Sir Derek Barton, F.R.S., for the opportunity to work in an Institution of such excellence and to the Salters' Company for the award of a Scholarship.

My sincerest thanks also go to the many people who provided their services and friendship during my stay here.

I N D E X

	PAGE
PART ONE. INTRODUCTION.	
CHAPTER I. THE HYDROGEN TRANSFER REACTION. KINETIC ISOTOPE EFFECTS AND TRANSITION STATE SYMMETRY.	
1.1 Theory.	12
1.2 Experimental Results.	16
PART TWO. DISCUSSION OF THE EXPERIMENTAL RESULTS.	
CHAPTER II. HYDROGEN EXCHANGE OF INDOLES.	
2.1 Introduction.	29
2.1.1 The Kinetics of exchange.	29
2.1.2 The Brønsted Relationship.	32
2.1.3 Primary kinetic isotope effects.	33
2.1.4 Synthesis of the Substrates.	34
Results.	
2.2 General acid and base catalysed protodeuteration of 2-methylindole in aqueous buffers.	37

	PAGE
2.3 Protodetrition of 2-methylindole in 50%(w/w) aqueous methanol buffers.	44
2.4 Acid catalysed hydrogen exchange of 2-methyl-4,6-di ^t butylindole.	48
2.5 Base catalysed hydrogen exchange of 2-methyl-4,6-di ^t butylindole.	51
2.6 Hydrogen exchange of 2,4,6-tri ^t butylindole.	51
2.7 Protonation of indoles in acidic media.	54
2.8 Activation parameters for the protonation of indoles.	59
Discussion.	
2.9 2.9.1 Rate correlations for the acid catalysed exchange in aqueous solution.	61
2.10 2.9.2 Acid catalysed exchange in aqueous methanol.	63
2.10.1 Rate correlations for the base catalysed exchange in aqueous solution.	66
2.10.2 Rate correlations for the base catalysed exchange in aqueous methanol.	68
2.11 The nature of the Transition State.	77
2.11.1 Conclusions.	84
2.12 Kinetic isotope effects for aromatic hydrogen exchange.	85
2.12.1 Evaluation neglecting secondary isotope effects.	86
2.12.2 Evaluation using a theoretical value for the Swain-Schaad exponent.	87
2.12.3 Evaluation assuming an experimental value for the secondary isotope effects.	89
2.12.4 The magnitude of primary isotope effects for Indoles.	91
2.12.5 Conclusions.	95

	PAGE
CHAPTER III. THE REACTION OF ARYLDIAZONIUM IONS WITH INDOLES.	
3.1 Introduction.	97
Results.	
3.2 Reaction of aryldiazonium ions with 2-methylindole.	100
3.2.1 Verification of rate order.	101
3.2.2 Acidity dependence of coupling rate.	104
3.2.3 Deuterium isotope effects.	111
3.2.4 Activation parameters.	111
3.2.5 Linear free energy relationship.	112
3.3 Diazocoupling in aprotic solvents.	114
3.4 Coupling to sterically hindered indoles.	117
3.5 Reaction of aryldiazonium ions with 2-methyl-4,6-dit ^t butylindole.	119
3.5.1 Acidity dependence of the coupling rate.	119
3.5.2 Kinetic isotope effects.	123
3.6 Discussion.	
3.6.1 The Swain-Schaad Relationship.	127
3.6.2 Deuterium isotope effects in diazocoupling.	128
3.6.3 The nature of the transition state.	132
CHAPTER IV. THE DECARBOXYLATION OF INDOLE-3-CARBOXYLIC ACIDS.	
4.1 Introduction.	136
4.1.1 Statistical analysis of data.	140
4.1.2 The kinetic method.	144

	PAGE
Results.	
4.2 Indole-3-carboxylic acid.	
4.2.1 The rate of decarboxylation at low pH.	145
4.2.2 The rate of decarboxylation at high pH.	149
4.3 2-Methylindole-3-carboxylic acid.	153
4.4 5-Chloroindole-3-carboxylic acid.	153
Discussion.	
4.5 The rate equation for decarboxylation.	160
4.6 The magnitude of the deuterium isotope effects.	164
 CHAPTER V. HYDROGEN EXCHANGE OF 2-INDOLINONES.	
5.1 Introduction.	167
5.1.1 Synthesis of the substrates	168
5.1.2 Exchange rates by tritium or deuterium analysis.	170
5.1.3 Proton and deuterium exchange rates by halogenation.	171
Results.	
5.2 Tritium exchange of 1,3-dimethylindolin-2-one.	175
5.3 Proton and deuterium exchange rate of 1,3-dimethyl indolin-2-one.	175
Discussion.	
5.4 The exchange kinetics of 1,3-dimethylindolinone.	182
5.4.1 The accuracy of iodination rates. Air oxidation.	183
5.4.2 Iodination through the neutral enol.	185

	PAGE
5.4.3 The isotopic purity of the substrate.	186
5.5 Kinetic isotope effect for 1,3-dimethylindolinone.	188
5.6 Hydrogen exchange of 4- ^t butylindolinones. Results.	190
5.7 Kinetic isotope effects for 1,3-dimethyl-4,6-di ^t butylindolin-2-one.	192
5.8 Hydrogen exchange of 4- ^t butylindolinones. Steric effects and transition state symmetry.	196
5.9 The magnitude of isotope effects for hydrogen exchange of 2-indolinones.	200

PART THREE. THE EXPERIMENTAL DETAILS.

CHAPTER VI.

6.1 Hydrogen exchange of indoles.	
6.1.1 Preparation and purification of substrates.	205
6.1.2 Labelled indoles.	209
6.1.3 Characterisation of protonated indoles.	210
6.1.4 Calculation of buffer ratios.	212
6.1.5 Measurement of detritiation rates.	213
6.1.6 Measurement of deuterium exchange rates.	214
6.1.7 Analysis of kinetic data.	217
6.1.8 Measurement of pK_a for protonation of indoles.	224
6.1.9 Measurement of pK_E for ionisation of 3-(p-nitrophenylazo)indoles.	224

	PAGE
6.2 Reaction of aryldiazonium ions with indoles.	
6.2.1 Preparation and purification of substrates.	228
6.2.2 Preparation and purification of products.	228
6.2.3 Measurement of diazocoupling rates.	229
6.2.4 Treatment of kinetic data.	233
6.3 Decarboxylation of indole-3-carboxylic acids.	
6.3.1 Preparation of ^{14}C labelled carboxylic acids.	240
6.3.2 Measurement of decarboxylation rates in H_2O	241
6.3.3 Measurement of decarboxylation rates in D_2O	242
6.3.4 Treatment of kinetic data.	242
6.4 Hydrogen exchange of 2-indolinones.	
6.4.1 Preparation and purification of substrates.	247
6.4.2 Labelled indolinones.	250
6.4.3 Oxidation products of indolinones.	251
6.4.4 Measurement of rates.	252
6.4.5 Analysis of the kinetic data.	254

PART FOUR. APPENDIX.

CHAPTER VII.

7.1 Non-linear least squares analysis of kinetic data.	260
7.2 Non-linear least squares analysis of decarboxylation data.	265
 BIBLIOGRAPHY.	 268

P A R T O N E

INTRODUCTION

CHAPTER I

THE HYDROGEN TRANSFER REACTION. KINETIC ISOTOPE EFFECTS AND TRANSITION STATE SYMMETRY.

1.1 THEORY.

The transfer of a hydrogen atom from an acid to a base is a widespread, and apparently simple reaction. It is therefore an eminently suitable starting point for an investigation into the nature of reactions in solution. In this account it is proposed to focus on chemical kinetics and the properties of transition state (or absolute reaction rate) theory, which attempts a quantitative kinetic description of reactions.

The properties of transition states are not yet sufficiently understood that accurate general kinetic predictions can be made, though certain molecular orbital treatments of transition state geometries and energies may provide one avenue of approach. Proton transfer reactions provide another, and their usefulness stems from the relatively different properties of the three isotopes of hydrogen, which result in easily measurable changes in reaction rates and equilibria.

At present these isotopic differences define the energy of the reaction pathway rather better than any calculation can do, and for this reason attention has centered on the study of isotope effects. A suggestion by Westheimer¹ which has had great impact, was that the magnitude of kinetic

isotope effects could be directly related to the transition state properties. The results that have been obtained subsequently have been reviewed^{2,3} and an excellent summary of the theoretical treatments is available⁴. What follows here is a brief review of recent advances, particularly with reference to the validity of isotope effects as an index of transition state structure.

If the framework of transition state theory is accepted, and the proton transfer (Scheme 1.1) can be described by a three centre model (that is to say no other concerted bond breaking or making is important)

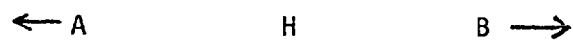


Scheme 1.1

then a consideration of only the zero point vibrational frequencies of the reactants and the transition state leads to a calculated kinetic isotope effect, k^H/k^D , of about 7 at 25°C. For simplicity, this calculation assumes that the vibrational frequencies in the transition state are independent of the isotopic mass, and the only difference arises in the zero point energies.

This picture is grossly simplified and as an illustration, a few of the factors that more sophisticated treatments include are a consideration of bending modes in the transition state and reactants, calculation of transition state vibrational frequencies using assumed potential barriers, use of 5-centre models with non-linear transition states and tunnelling and solvation factors.

Despite the inaccuracy of these calculations, there can be no doubt that the majority of experimental values are lower in magnitude than expected, and Westheimer¹ was among the first to attempt to include this observation within the framework of the above theory. Considering only two stretching vibrations which are dependent on isotopic hydrogen,



symmetric stretch

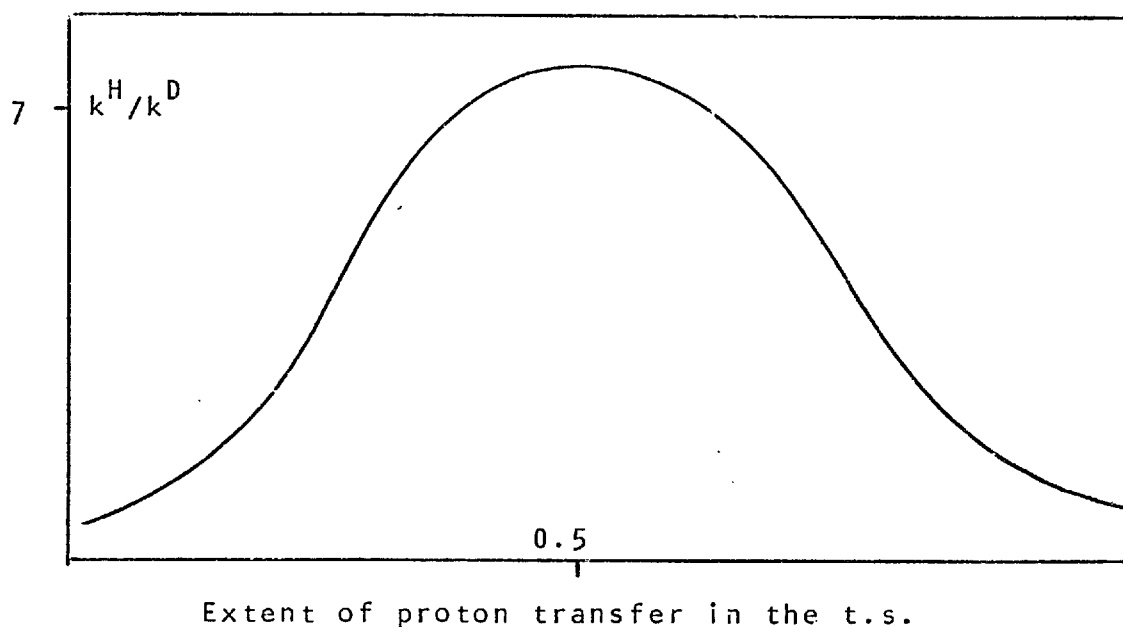


antisymmetric stretch

the antisymmetric (or imaginary) frequency represents only translational energy along the reaction ordinate. When the hydrogen is equally disposed between A and B the symmetric stretch will be independent of the isotopic mass and the full effect of the difference in zero point energies will be manifested in the isotope effect. For any other case, the symmetric stretch is isotope dependent, reducing the difference in zero point and transition state energies for the different isotope, and having an effect on the isotope rate ratio as shown in Fig. 1.1

This simple model has been criticised on the grounds that a) bending modes are not considered, of particular importance for non-linear transition states and b) no allowance is made for proton tunnelling effects.

Figure 1.1 The effect of transition state symmetry on the magnitude of isotope effects.



More O'Ferrall has produced a five centre model which considers bending vibrations in both linear⁵ and non-linear transition states,⁶ and a tunnelling correction was also applied. His results, and also similar calculations by Albery⁷ tend to show that the effect of bending vibrations is independent of transition state symmetry, validating Westheimers' original argument. It was also concluded that small tunnelling corrections have comparatively little effect, in marked contrast to the most recent calculations of Bell,⁸ who employed an electrostatic cloud charge model. Though this model does not predict the relative absolute energies of the transition states and reactants very well, it was considered to give an adequate estimate of the relative variations of the transition state energy with various applied perturbations. It was shown that neither inclusion of bending modes, nor changes in the frequency of the symmetric stretch would result in significant changes in the magnitude of the isotope effects. Inclusion

of a tunnel correction gave the variable isotope effects, which were a maximum for a symmetric state and showed a sharp variation with the absolute magnitude of the linear transition state (ie the internuclear distance), with a well defined distance for which the isotope effect was a maximum. This latter phenomenon may well account for some very large values obtained experimentally⁹. Wolfsberg and co-workers¹⁰ had reached similar conclusions from a consideration of the antisymmetric vibration in the transition state, but their conclusions were highly dependent on the choice of the properties of the potential energy surface used. This highlights the great problem in dealing with these systems, in that adjustment of a suitable number of empirical parameters can lead to virtually most required results.

1.2 EXPERIMENTAL RESULTS.

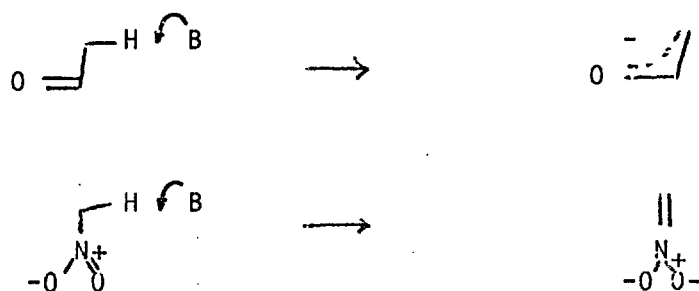
The Westheimer hypothesis has generally been interpreted in terms which are experimentally accessible. One criterion of transition state symmetry has been the free energy change in the reaction and this can be reduced to a consideration of the thermodynamic equilibrium acidities. If for the substrates, these are equal, then to a good approximation $pK_a \approx 0$ and the transition state symmetry should be a maximum. This is an extensively used index, but is only really meaningful when large relative differences in energy are being considered.

An alternative experimental index which has been much discussed recently¹¹ is the Brønsted exponent. These are derived from the catalytic efficiency of the acid or base, and relate directly to the free energy of the transition state, in contrast to isotope effects which relate to ground state energies. The classical interpretation of

the exponents α and β limits their range to $0 < \alpha$ or $\beta < 1$ and suggests that they ought to represent only local constants, which vary from $0 \rightarrow 1$ over a sufficiently large change in ΔpK_a for the system, a phenomenon anticipated by Brønsted¹² and recently reviewed¹¹. The interpretation of these exponents has been made more complex by observations that α or $\beta > 1$ or < 0 ¹³, particularly in systems where electron delocalisation can occur along 3 or 5 centre bonds, and extensive theoretical studies of this phenomenon have been made by Marcus¹⁴ and others¹⁵. Further, certain acids and bases, particularly H_3O^+ and OH^- do not correlate well in this type of treatment,¹⁶ and probably Brønsted exponents provide only a semi-quantitative description of transition state symmetry. Normally, use is made of both isotope effects and other indexes such as Brønsted exponents, and some of the results available are presented below.

a) α - Carbonyl and nitro compounds.

These classes represent the most studied systems (Scheme 1.2)

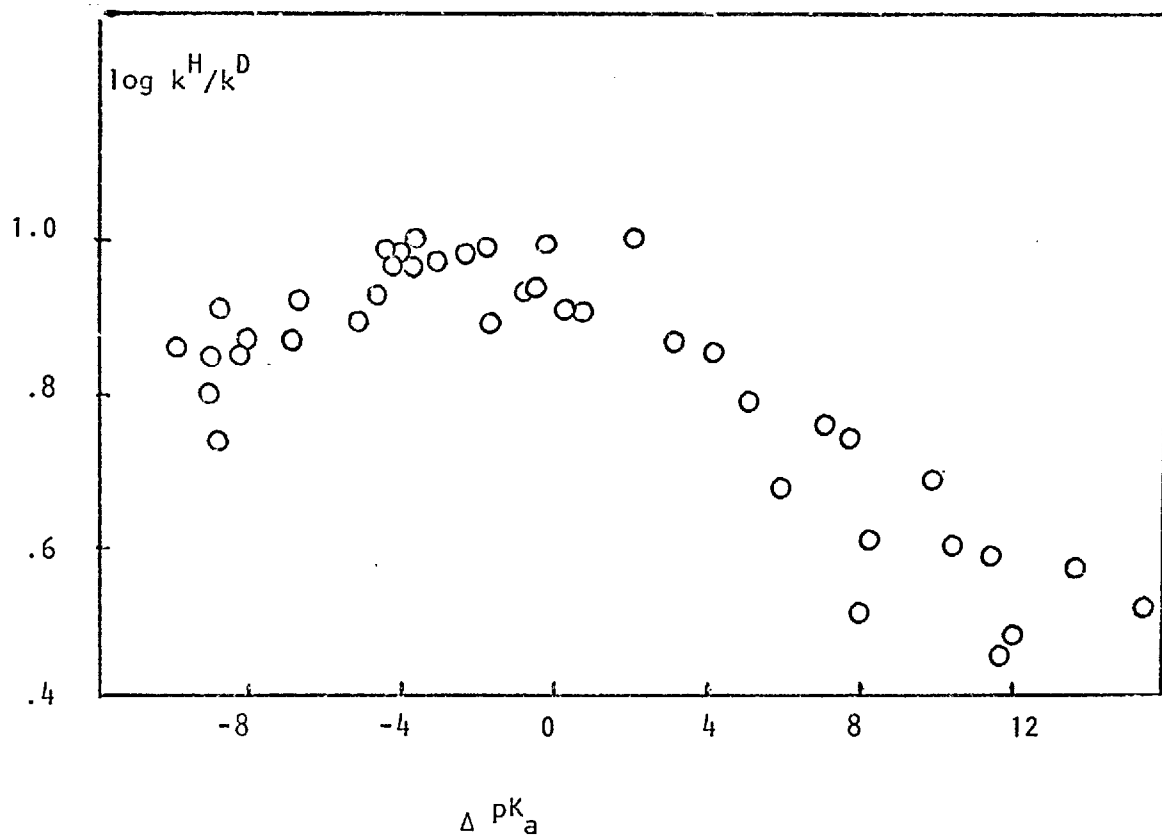


Scheme 1.2

Bell has reported numerous examples and a recent paper provides a convenient summary¹⁷. Over a range of ΔpK_a of about 18, k^H/k^D

was found to vary regularly with a maximum value of 10.3. This latter value is typical of the base 2,6 lutidine, in this case with ethyl nitroacetate as the acid. The Brønsted parameter β had the value 0.65 over the entire reactivity range and it was suggested that this parameter may be very insensitive to the changing symmetry of the transition state. If the data is considered as a whole, the maximum in the region $\Delta pK_a \approx 0$ (normally taken as verification of the Westheimer theory) was found to be diffuse and Bordwell¹⁸ has suggested that the expected curvature may in fact be so slight as to be useless for predictive purposes (Fig. 1.2).

Figure 1.2 Variation of experimental isotope effects with ΔpK_a .¹⁸



It is apparent that in order to obtain a large range of reactivity, a wide spectrum of structural variation occurs and factors other than transition state symmetry may be responsible for the observed results. This has been overcome to some extent by using aqueous dimethyl sulphoxide as a solvent, which has the property of inducing large changes in the basicity of the substrates, and also ΔpK_a . Representative of such studies are the results in Table 1.1 for the ionisation of nitroethane in various aqueous DMSO solutions.^{19a}

TABLE 1.1 Ionisation of nitroethane by OH^- in aqueous DMSO solutions at 25°. (Ref. 19a).

Mole fraction DMSO	k^H/k^D
0	9.3
0.13	8.4
0.26	7.6
0.37	6.9
0.48	6.3
0.58	5.9

Similar trends have been reported for nitroethane in dioxan by Dixon and Bruice,^{19c} and the inversion of (-) menthone^{19b} where a distinct maximum is observed. Ionisation of 2-phenylnitromethane also shows a distinct maximum at $\Delta pK_a \approx 0$, whereas the Brønsted exponent β has the constant value of 0.57. As is normally found, a large value was obtained for the isotope effect when 2,6 lutidine was used as base, and a study of the activation parameters (particularly the pre-exponential

term) revealed that tunnelling may have been responsible for much of the observed variation in isotope effects - rather than transition state symmetry.^{20a} Nevertheless Leffek^{20b} has found no evidence of tunnelling by this method for the ionisation of $(p\text{-NO}_2\text{Ar})_2\text{CH(D)}_2$ by OH^- and this criterion may not be totally adequate in assessing tunnelling contributions.

There appears to be little doubt in attributing large isotope effects of 20 or more, such as obtained for the ionisation of methyl 4-nitro valerate by 2,4,6 collidine²¹ to tunnelling. However Gold^{22a} has pointed out that for the latter system, ΔpK_a is close to zero, when tunnelling should be a maximum. Gold was able to demonstrate that it may also occur for systems where $\Delta\text{pK}_a \approx 15$ by using diethylketone, finding $k^{\text{H}}/k^{\text{D}} = 4$ (using pyridine) and 6.8 (using 2,6 lutidine). This was interpreted as demonstrating that tunnelling can still occur when the transition state is asymmetric.

Several systems have been reported, all containing CN groups, where isotope effects are remarkably low, a phenomenon which is less likely to be caused by tunnelling. Long²³ reports deuterium isotope effects of about 1.5 for ionisation of malonitrile and tert-butylmalonitrile and Melander²⁴ found $k^{\text{H}}/k^{\text{D}}$ varies from 1.2 to 1.5 for ionisation of 2-methyl-3-phenylpropionitrile in methanol/DMSO mixtures. Exchange of deuterium with solvent proceeded at the same rate as racemisation, ruling out a tight ion-pair mechanism, and the rate of reprotonation was concluded to be fast (approaching diffusion control) compared with ionisation. In both cases^{23,24} the Brønsted exponent was close to unity suggesting a very asymmetric product-like transition state, and the small isotope effects appear to be powerful evidence for the Westheimer approach¹. Using the Wolfsberg-Stern treatment¹⁰

Melander^{24b} showed that the proton must be 99% transferred to account for the isotope effect of 1.2 and suggested this may be general for all really weak carbon acids. This is certainly not the case for toluene³¹ and nitriles may be a special case.

b) Elimination reactions.

There has been considerable discussion whether many elimination reactions are concerted (E2) or proceed by a rate limiting proton transfer (E1_{cb})²⁵. The transition state of the former is multi-centered and can no longer be considered simple.

One reaction which is thought to proceed via an irreversible E1_{cb} mechanism is elimination from diaryl trichloroethanes, Ar₂CH-CCl₃²⁵, which gives a variable isotope effect when the base is varied (Table 1.2) but not the substrate.

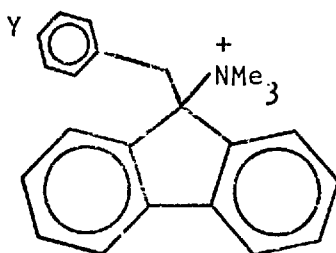
TABLE 1.2 Elimination of Diaryltrichloroethanes.²⁵

Base:	PhS ⁻	O ₂ NPhO ⁻	PhO ⁻ *	MeO ⁻	EtO ⁻
k ^H /k ^D :	3.13	4.83	6.21	4.75	3.40

* ΔpK_a ≈ 0

Seventeen other examples are collected in this paper²⁵ of "E2" eliminations catalysed by EtO⁻ and t-BuO⁻ and in all the cases the

isotope effect is larger for catalysis by the butoxide. This particular pattern of isotope effect variation is not easily explicable in terms of gross symmetry changes. Variation in the substrate reactivity was found to give variable isotope effects when substituted fluorenes were used²⁶. Variation of Y (Y = OMe \rightarrow CF₃) changed k^H/k^D from



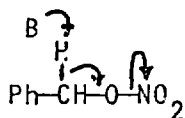
5.91 to 4.15 systematically, and this was interpreted as indicating a product like transition state. An explanation which is possibly more valid is that a change in mechanism, from E2 to E1_{cb} may occur.

An interesting, albeit preliminary report, suggests that for the elimination of benzyl nitrate by various bases, the primary hydrogen and nitrogen isotope effects vary in magnitude, but in opposite directions (Table 1.3).²⁷

TABLE 1.3 Elimination of Benzyl nitrate by various bases.²⁷

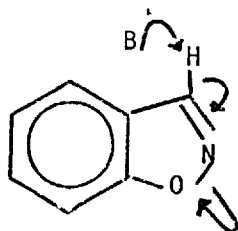
Base	HO ⁻	EtO ⁻	t-BuO ⁻
k^{14N}/k^{15N}	1.0207	1.0182	1.0154
k^H/k^D	-	5.94	6.41
Rate/s ⁻¹ M ⁻¹	0.028	0.438	481

These authors suggest that a fully concerted reaction (Scheme 1.3) may not occur, and systems of this type are certainly worth further investigation.



Scheme 1.3

Kemp and Casey^{11c} report isotope effects for a similar system (Scheme 1.4) , over a wide range of reactivity and find not only constant isotope effects but a unique value for the Brønsted exponent.



Scheme 1.4

This appears to suggest no variation in transition state symmetry over some 15 ΔpK_a units, and may arise from a compensating effect of the concerted N-O bond cleavage. Similarly constant isotope effects were observed for the elimination of p-substituted phenylethyl bromides²⁸, accompanied in this case however by some evidence of proton tunnelling. It seems likely that for a concerted process, k^H/k^D is strongly influenced by the extent of coupling of the proton transfer with other atomic motions, making the interpretation of these values all the more difficult.

c) Other non-concerted proton transfer reactions.

There are few other systems which can be studied over a large range of reactivity, but potentially free radical transfers are such a system. Pryor²⁹ has reported values for k^H/k^D for reactions of the type

$$Q\cdot + {}^t\text{BuSH} \longrightarrow \text{QH} + {}^t\text{BuS}\cdot$$

where Q represents a large variety of aromatic radicals. When the isotope effect was plotted against the heat of reaction a distinct maximum was observed not far from $\Delta H^0 = 0$. In view of the remarkable ease with which tunnelling occurs (eg oxidation of dihydrophenanthrene, $k^H/k^D \approx 250$ ^{9a}; reaction of $\text{Me}\cdot$ with MeNC , $k^H/k^D \approx 3000$ ^{9b}) these values are probably too ambiguous to be useful³⁰.

Streitwieser³¹ has studied the ionisation of numerous aromatic hydrocarbons using lithium dicyclohexylamine as base and finds little evidence of tunnelling as judged by excellent Brønsted correlations and the acceptable values for the Swain-Schaad exponent that were obtained. However, almost identical values for k^D/k^T and also k^H/k^D were obtained for toluene and triphenylmethane, yet the $\Delta \text{p}K_a$ for this system was about 10. An early transition state ($\beta \approx 0.31$) with little charge development was suggested to account for this. More interestingly, in order to account for the slightly high isotope effects ($k^H/k^D \approx 12$) complete loss of stretching vibrations in the transition state, with appearance of bending vibrations in the product was suggested. Kresge has invoked absence of initial state bending modes to explain the low isotope effect observed for the protonation of ethyl vinyl ether by HF ($k^H/k^D = 3.4$ compared with about 7 for catalysis by formic acid)³². These results enabled the transition state bending frequency γ^\ddagger to be estimated as 1100 cm^{-1}

This is close to the value estimated from theoretical calculations and suggests that normally the transition state and initial state bending frequencies are well matched and probably cancel out.

Various isotope effects in aromatic A-S_E2 reactions have been reported. These suffer from the disadvantage that k^H/k^D cannot be determined directly without several *a priori* assumptions which may themselves be invalidated by phenomena such as tunnelling. The isotope effects are also far more susceptible to experimental error. For this reason, the apparent maximum in k^H/k^D around $\Delta pK_a \approx 0$ observed for azulenes is not very compelling³³, even though other data for exchange of methoxybenzenes is included. In order to extend the range of the reactivity, Olsson studied exchange of the highly unreactive bromobenzene³⁴ for which $k^H/k^D \approx 4.4 - 5.1$. Though this is lower than the data for azulenes, it is higher than the value found for benzene itself. This relative order is not that expected from a consideration of the Westheimer theory. It should be mentioned however that accurate data is very difficult to obtain for such unreactive systems.

Exchange reactions of Indoles were studied by Challis and Millar³⁵ who found no well defined maximum in the region $\Delta pK_a = 0$, and no difference in cases where the Brønsted exponents suggested a considerable difference in symmetry of the transition state. These results are to be contrasted with isotope effects reported by Zollinger³⁶ for diazocoupling, which varied considerably with the nature of the base that removed the proton and showed a well defined maximum. It may well be that a change in the r.d.s. occurs with the stronger bases, with a corresponding increase in the uncertainty of the isotope effect.

d) Quantum mechanical tunnelling effects.

It is apparent from the numerous reports above that tunnelling is a phenomenon which may account for much of the observed variation in isotope effects. The detailed theoretical discussion and most of the evidence for tunnelling is beyond the scope of the account here and reference is made to a review by Caldin³⁷ and a chapter in the book by Jones³⁸. It is worth considering the two most important ramifications of tunnelling, namely the effect on Arrhenius parameters and the primary isotope effects.

The Arrhenius parameters have been widely studied, and it has been shown the the pre-exponential ratio A^D/A^H should have a maximum value of 2. In the presence of tunnelling this increases and perhaps one of the largest deviations reported is the value $A^D/A^H = 31$ by Caldin³⁹ for ionisation of $p\text{-O}_2\text{NPhCD}_2\text{NO}_2$ by tetramethylquanidine. For this reaction Caldin reports a value $k^H/k^D = 45$, which is similar to the value of 22 reported for the ionisation of 2-nitropropane by 2,4,6 collidine⁴⁰. Deuterium isotope effects can be even larger. Thus the value reported for the radical reaction ^{9b}



carried out in the solid state at low temperatures was estimated as 3000, and the curved Arrhenius plot for this reaction is the best example yet of this manifestation of tunnelling.

This example was quoted as an illustration that many factors other than steric hindrance combine to produce these effects. It is important when studying variation in the magnitude of isotope effects to differentiate between these gross tunnelling effects and other factors. Of particular importance in the study of aromatic hydrogen exchange is

the effect of tunnelling on the magnitude of the Swain-Schaad exponent \underline{r} . A recent definitive account of this problem⁴¹ suggests that \underline{r} will not be greatly influenced but may well decrease slightly from the normal value of 1.442⁴². Experimentally, little work has been carried out³⁸, but perhaps the most convincing results are those of Lewis⁴⁰ where even though tunnelling is unambiguously occurring ($k^H/k^D = 22$) the value of \underline{r} remains in the region 1.44. This exponent is a particularly difficult parameter to measure accurately, and it may be that the variation with tunnelling cannot easily be detected.

P A R T T W O

DISCUSSION OF THE EXPERIMENTAL
RESULTS

CHAPTER II

H Y D R O G E N E X C H A N G E O F I N D O L E S .

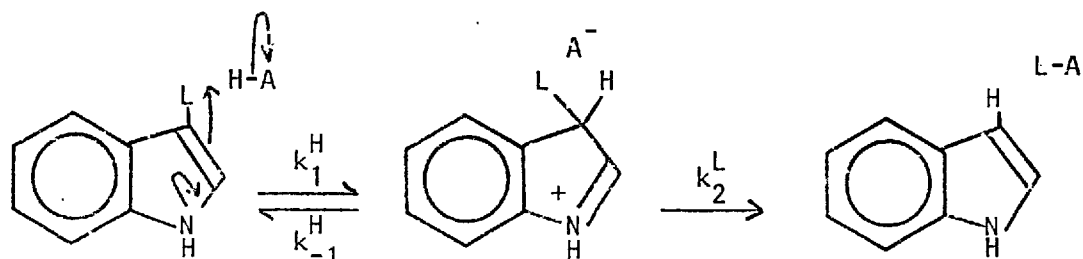
2.1 INTRODUCTION.

The hydrogen exchange of a variety of aromatic species has been studied in detail. For a full account, reference should be made to recent papers which deal with specific substrates, including a study of methoxybenzenes by Kresge⁴³, azulenes by Long³³, biphenyls and related species by Taylor⁴⁴, numerous heterocyclic compounds by Katritzky⁴⁵ and indoles themselves by Challis and Millar³⁵.

2.1.1 The kinetics of exchange.

The mechanism of exchange for indoles was shown to be a typical acid catalysed A-S_E2 process, involving a Wheland type σ intermediate (Scheme 2.1). The concentration of the intermediate (as estimated

Scheme 2.1 A-S_E2 exchange mechanism for indoles.



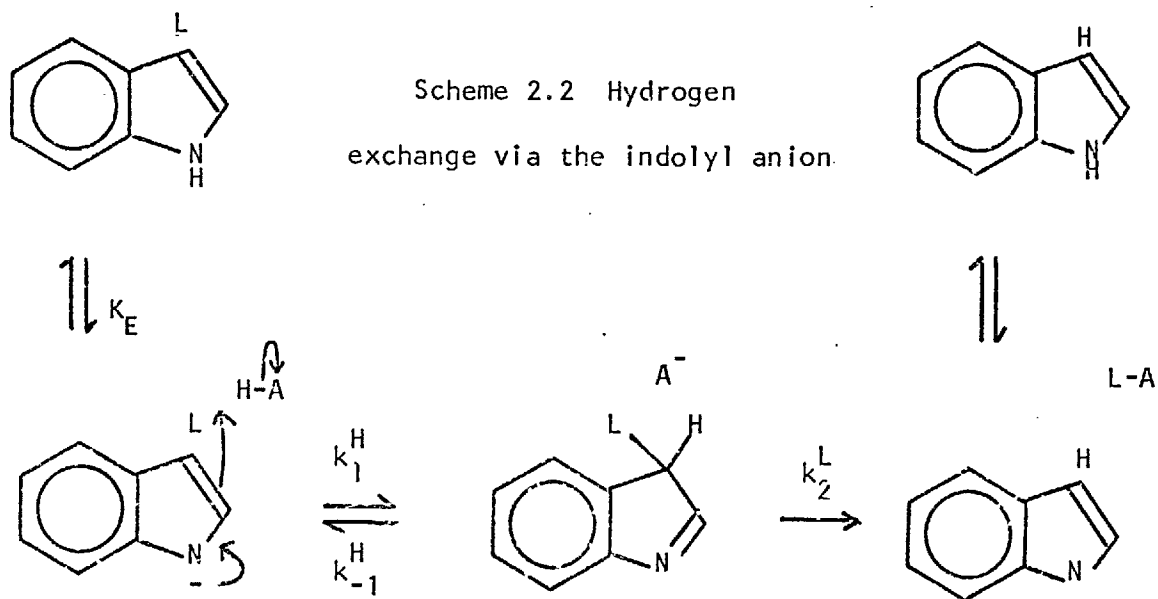
from the equilibrium constant for protonation) is always sufficiently small that the steady state approximation can be used, leading to the following expression for the rate of loss of label.

$$\begin{aligned}
 -d[L]/dt &= k_{bi}^{-L} \cdot [InL] \cdot [HA] & 2.1^* \\
 &= k_o^{-L} \cdot [InL].
 \end{aligned}$$

$$\text{where } k_{bi}^{-L} = k_1^H / [1 + k_{-1}^H / k_2^L] \quad 2.2$$

The observation of general acid catalysis^{35b} and the isolation of the protonated intermediates⁴⁶ strongly supports this mechanism.

In strongly basic solutions, another exchange pathway becomes important (Scheme 2.2)^{35a}.



* The neutral 3-labelled indole is represented by the generic symbol *InL*

In this case the intermediate 3H indolenines have been isolated only for one substrate (2-ethoxy- 3H indolenine) and are known to be normally unstable. The concentration is likely to be low, and a steady state treatment gives

$$-d[L]/dt = k_{bi}^{-L} \cdot [InL] \cdot [B] \cdot K_E/K_{BH} \quad 2.3$$

$$= k_2^{-L} \cdot [InL] \cdot [B] \quad 2.4$$

$$= k_o^{-L} \cdot [InL]$$

where k_{bi}^{-L} is defined by equation 2.2, and K_E and K_{BH} are defined by equations 2.5 and 2.6

$$K_E = [In^-] \cdot [H^+] / [InH] \quad 2.5$$

$$K_{BH} = [H^+] / [B] \cdot [BH^+] \quad 2.6$$

Exchange *via* the indolyl anion is often referred to as the base catalysed pathway, though this is only a kinetic manifestation of acid catalysis. Equation 2.3 only applies when the fraction of ionised indole is less than 1%, which was generally the case for the substrates studied.

In a buffer solution, containing both an acid BH^+ and a base B, catalysed hydrogen exchange can proceed *via* both the acid and base pathways, and the observed rate is the sum of all these (Equ. 2.7)

$$rate = k_{bi}^{-L} \cdot [BH] + k_{bi}^{-L} \cdot [H_3O^+] + k_2^{-L} [B] + k_2^{-L} [OH^-] \quad 2.7$$

Rearranging equation 2.7 one obtains

$$\text{rate} = [\text{BH}] \cdot \left(k_{bi}^{-L} + k_2^{-L} \cdot \frac{[\text{B}]}{[\text{BH}]} \right) + k_{bi}^{-L} [\text{H}_3\text{O}^+] + k_2^{-L} [\text{OH}^-] \quad 2.8$$

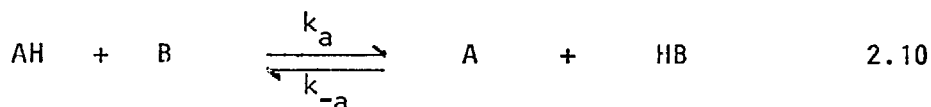
By carrying out runs at a constant buffer ratio, but differing concentration, the hydronium and hydroxyl rates will be constant and a plot of equation 2.8 leads to an intercept with the value $k_2^{-L} [\text{OH}^-] + k_{bi}^{-L} [\text{H}_3\text{O}^+]$ which can be verified independently and a slope equal to

$$\text{slope} = k_{bi}^{-L} + k_2^{-L} \cdot [\text{B}]/[\text{BH}^+] \quad 2.9$$

Use of several buffer ratios enables equation 2.9 to be plotted and the constants k_{bi}^{-L} and k_2^{-L} to be evaluated. This treatment was found to hold very well for the variety of indoles previously studied³⁵.

2.1.2 The Brønsted Relationship.

For hydrogen transfer between an acid and a base (equ. 2.10)



the rate constant k_a is related to the strength of the acid AH (given by the dissociation constant K_a) by

$$k_a = G_a \cdot K_a^\alpha \quad 2.11$$

The exponent α is normally evaluated from the logarithmic form of equ. 2.11

$$\log k_a = -\alpha \text{p}K_a + \text{const.} \quad 2.12$$

Consideration of the reverse step in equation 2.10 leads to a similar relation for k_{-a} , the base catalysed hydrogen transfer.

$$\log k_{-a} = -\beta pK_a + \text{const.} \quad 2.13$$

It can also be shown that $\alpha + \beta = 1$. In aromatic hydrogen exchange, only k_{bi}^{-L} (equ. 2.1) can be evaluated, but since k_{-1}/k_2 (equ. 2.2) represents an almost constant isotope effect, k_{bi}^{-L} is linearly related to k_1 and application of equation 2.12 gives

$$\log k_1^L \approx \log k_{bi}^{-L} + 1.3$$

$$\text{and } \log k_{bi}^{-L} = -\alpha pK_a - 1.3 + \text{const.}$$

A similar treatment is used for the base catalysed pathway, but with the inclusion of the appropriate constant K_E or K_{BH} (Equ. 2.3), depending on whether the catalysing base or indole is kept constant.

Application of these relationships to hydrogen exchange of indoles showed that for the acid catalysed pathway^{35,47} α varied systematically between about 0.4 - 0.7. Though exact interpretation of these parameters can be fraught with difficulties¹¹ this was taken as an approximate indication of a symmetrical transition state. In contrast, the base catalysed pathway for 2-methylindole gave an α of about 0.9, showing a greater degree of asymmetry in the transition state of this reaction. Thus an important difference in the symmetries of the two pathways was detected, and this had considerable bearing on the kinetic isotope effects.

2.1.3 Primary kinetic isotope effects.

Any single exchange rate for indoles is defined by three parameters

(equ. 2.2) and evaluation of isotopic rate ratios of necessity requires certain approximations. Two methods have been used previously, the simplest was employed initially by Kresge⁴⁸ and used subsequently by Challis and Millar³⁵. No correction was made for secondary isotope effects, and more importantly, the calculated value of \underline{r} , the Swain-Schaad exponent⁴², was assumed to be 1.442 . A modification by Kresge⁴⁹ takes secondary isotope effects into consideration, but still makes assumptions concerning the value of \underline{r} .

The experimental isotope effects for indoles were found to be invariant³⁵ and if the Westheimer theory is correct, in conflict with the results obtained from the Brønsted correlations.

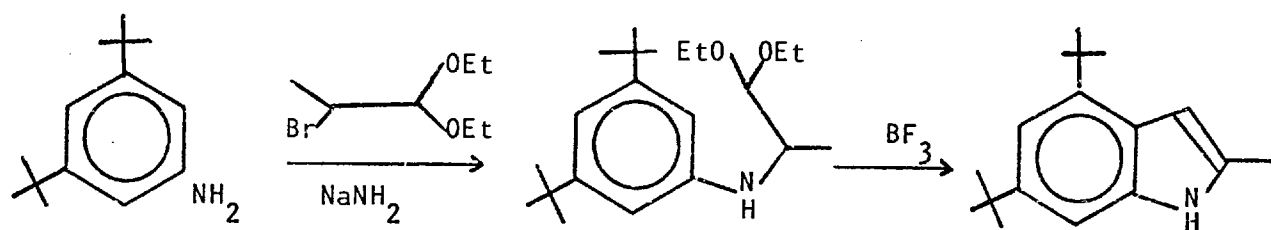
It is apparent that a further index of transition state symmetry is required, since doubt has been cast on the validity of Brønsted exponents and uncertainties in the method of obtaining isotope effects for aromatic hydrogen exchange must be resolved.

2.1.4 Synthesis of the substrates.

A general review of the synthesis of indoles is given by Sundberg⁵⁰. From the point of view of preparing 4-t-butyl indoles, it was thought desirable to incorporate the butyl groups at an early stage. With this in mind the *m*-t butylaniline nucleus was potentially more amenable than either hydrazines (Fischer Synthesis) or *o*- nitrobenzyl ketones (Reissert Synthesis) . The separation of isomeric forms was eliminated by using the symmetric 3,5-di-t butylaniline and for this reason all butylindoles (and also indolinones, chapter 5) have present a 6- t butyl group.

The Bischler - Chastrette Synthesis⁵¹

2-Methyl-4,6-di *t* butylindole (DBMI) was prepared by the route shown in Scheme 2.3

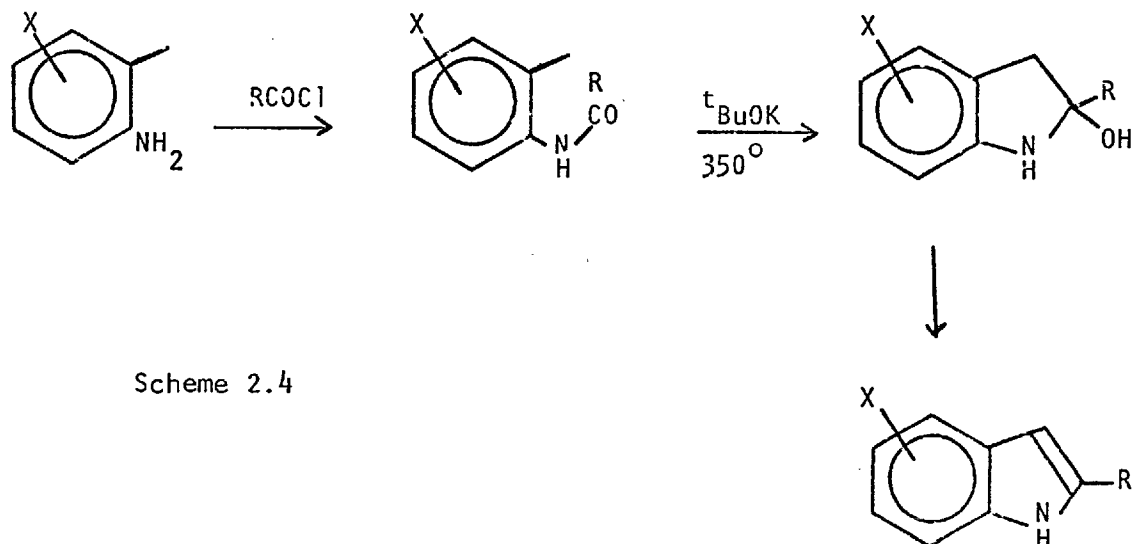


Scheme 2.3

Lewis acids conventionally used for such cyclisations do not work, and carefully controlled conditions with boron trifluoride as catalyst gave only a poor yield of the indole. Extension to give 2- *t* butyl substituents was not considered feasible by this method.

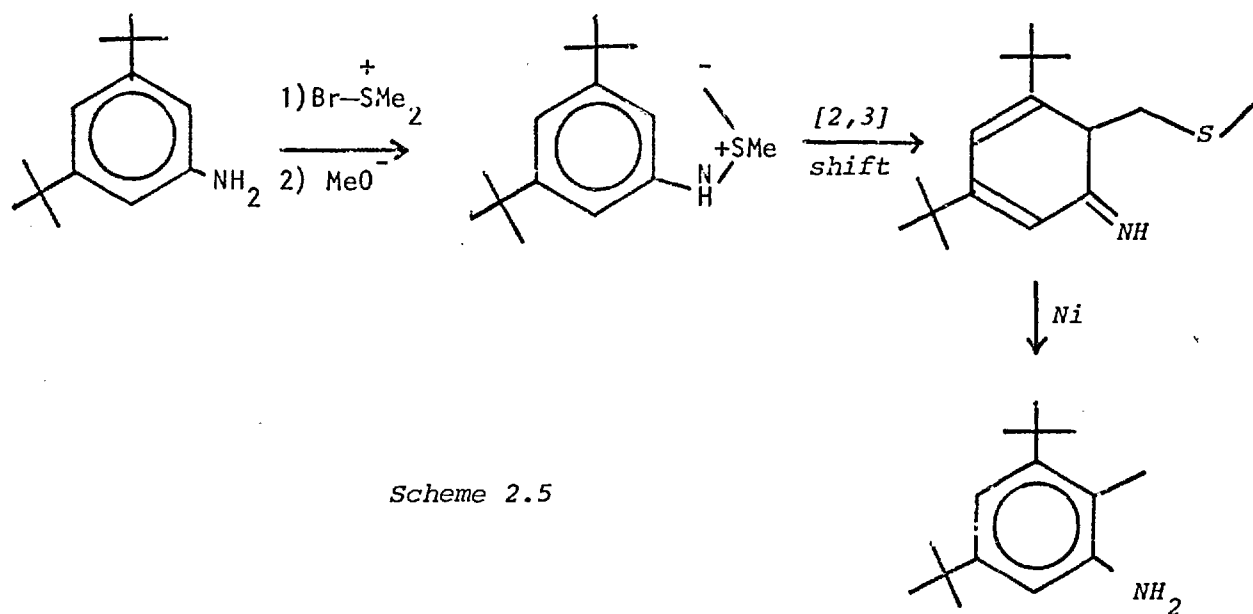
The Madelung Synthesis⁵²

This base catalysed method was found to be well suited for the synthesis of indoles containing acid sensitive groups such as *t* butyl (Scheme 2.4).



Scheme 2.4

The ortho methyl group was introduced using the method of Gassman⁵³
(Scheme 2.5).



Both 2-methyl-4,6-di-t-butylindole (DBMI) and 2,4,6-tri-t-butylindole (TBI) were prepared in moderate yield by this method.

R E S U L T S

2.2 GENERAL ACID AND BASE CATALYSED PROTODETRITIATION OF 2-METHYL INDOLE IN AQUEOUS BUFFERS.

Rate constants for catalysed detritiation of 3-³H₁ 2-methylindole by diethylamine (Table 2.1), piperidine (Table 2.2), 2,2,2-trifluoroethanol (Table 2.3) and 2,6-dimethylpiperidine (Table 2.4) were measured in the manner previously described³⁵. All quoted pK_a values were obtained from the collection by Perrin⁵⁴, except trifluoroethanol which was measured from the pH of the buffers. Catalytic rate constants were evaluated as described in section (2.1.1) and are collected in Table 2.7

Several weaker bases such as pyridine were also studied, principally since pyridines as a class were not studied previously for 2-methyl indole. Pyridine itself, pK_a²⁵ = 5.25, by analogy with acetic acid (pK_a²⁵ = 4.65) was assumed to induce no appreciable base catalysis, and the rate constants are calculated using only one buffer ratio (Table 2.5): 2,6-Dimethylpyridine was studied at two buffer ratios (Table 2.6). The magnitude of the rate constants, particularly k₂^{-T}, may be affected by the presence of traces (ca 1%) of other pyridines which were not removed by purification, and the values given are probably the upper limit. Collected data are given in Table 2.7

TABLE 2.1 Protodetrition of 2-Methylindole-3- $^3\text{H}_1$ in aqueous diethylamine buffers. $\text{pK}_a^{25} = 11.09$. $T = 25^\circ$.

$[\text{BH}^+]/[\text{B}] = 1, I = 0.1 \quad \text{pH} = 11.09 \pm 0.03$

$[\text{BH}^+] / \text{M.}$	$10^6 k_o^{-T} / \text{s}^{-1}$	Run
0.05	8.29	138
0.0388	7.50	139
0.0188	4.20	140
0.0028	2.18	141

$[\text{BH}^+] / [\text{B}] = 10, I = 0.1, \text{pH} = 10.09 \pm 0.02$

0.091	1.65	146
0.064	1.26	147
0.036	0.729	148
0.009	0.217	149

$$k_{bi}^{-T} + k_2^{-T} = 1.29 \times 10^{-4} \text{ s}^{-1} \cdot \text{M}^{-1}.$$

$$k_{bi}^{-T} + 0.1k_2^{-T} = 0.158 \times 10^{-4} \text{ s}^{-1} \cdot \text{M}^{-1}.$$

TABLE 2.2 Protodetrition of 2-Methylindole 3-³H₁ in aqueous piperidine buffers. pK_a²⁵ = 11.08, T = 25°.

<i>[BH⁺]/ [B] = 1, I = 0.1 pH = 11.10 ± 0.1</i>		
<i>[BH⁺ + B]</i>	<i>10⁶ k_o^{-T}/s⁻¹</i>	<i>Run</i>
0.1	12.6	133
0.0766	10.0	128
0.0376	5.6	129
0.0176	3.2	130
0.0056	1.4	132
<i>[BH⁺]/[B] = 11. Added phenol = 0.05 M. [PhOH]/[PhO⁻] = 1</i>		
0.0	11.2	134
0.01	12.0	135
0.03	11.9	136
0.05	11.9	137

$$k_{bi}^{-T} + 0.09 k_2^{-T} = 0.1 \times 10^{-4} s^{-1} . M^{-1} .$$

$$k_{bi}^{-T} + k_2^{-T} = 2.4 \times 10^{-4} s^{-1} . M^{-1} .$$

TABLE 2.3 Protodetritiation of 2-Methylindole 3-³H₁ in aqueous 2,2,2 trifluoroethanol buffers at 25^oC.

$$pK_a^{25} = 12.22 \pm 0.03$$

$$[B^-]/[BH] = 0.108, \quad I = 0.2 \quad \text{with NaCl.}$$

[BH]	$10^5 k_o^{-T} / s^{-1}$.	Run
0.452	2.23	261
0.226	1.19	258
0.091	0.530	259
0.036	0.283	260
$[B^-]/[BH] = 0.523$		
0.312	7.96	262
0.164	4.52	263
0.065	2.16	264
0.028	1.17	265
$[B^-]/[BH] = 1.04$		
0.123	7.00	266
0.049	3.51	267
0.020	2.08	268

$$k_{bi}^{-T} + 0.108 k_2^{-T} = 0.472 \times 10^{-4} s^{-1} . M^{-1} .$$

$$k_{bi}^{-T} + 0.523 k_2^{-T} = 2.41 \times 10^{-4} s^{-1} . M^{-1} .$$

$$k_{bi}^{-T} + 1.04 k_2^{-T} = 4.76 \times 10^{-4} s^{-1} . M^{-1} .$$

TABLE 2.4 Protodetrition of 2-Methylindole in aqueous 2,6-dimethylpiperidine buffers at 25°C.

pH = 11.82, [B]/[BH⁺] = 4, I = 0.2 with NaCl.

[B]/M.	$10^5 k_o^{-T}/s^{-1}$.	Run
0.80	2.32	386
0.10	0.850	498
0.04	0.457	387
0.0	0.300	*

* Calculated from the hydroxyl catalysed rate

$$k_{bi}^{-T} = 3 \times 10^{-5} s^{-1} .M^{-1}.$$

TABLE 2.5 Protodetrition of 2-Methylindole in aqueous pyridine buffers at 25°C. I = 0.1, pK_a²⁵ = 5.25.

[PyH ⁺]/M.	[Py]/M.	$10^4 k_o^{-T}/s^{-1}$.	Run
0.025	0.1	6.24	425
0.0125	0.06	4.11	426
0.0075	0.03	1.83	427
0.0025	0.01	0.98	428
0.0	0.0	0.55	-
0.0	0.0	0.59	*

* Calculated from the hydronium ion rate given by Millar⁵⁵.

$$k_{bi}^{-T} = 2.3 \times 10^{-2} s^{-1} .M^{-1}.$$

TABLE 2.6 Protodetrition of 2-Methylindole 3-³H₁ in aqueous 2,6-dimethylpyridine buffers at 25°C.
 $pK_a^{25} = 6.75 \pm 0.03$, $I = 0.1$ with NaCl.

$[LuH^+]/M.$	$[Lu]/M.$	$10^5 k_0^{-T}/s^{-1}.$	Run
0.1	0.4	4.64	417
0.06	0.24	3.15	418
0.03	0.12	1.83	419
0.01	0.04	0.849	420
0.0	0.0	0.35	-
0.0	0.0	0.22	*
0.1	0.025	5.58	421
0.06	0.0125	5.05	422
0.03	0.0075	4.37	423
0.01	0.0025	4.08	424
0.0	0.0	3.8	-
0.0	0.0	3.0	*

* Calculated from the hydronium ion rate given by Millar⁵⁵.

$$k_0^{-T} = 1.65 \times 10^{-4} [LuH^+] + 6.5 \times 10^{-5} [Lu]$$

TABLE 2.7 Catalytic rate constants for protodetritiation of 2-Methylindole in aqueous solution at 25°.

Catalyst	pK_a^{25}	$10^6 k_{bi}^{-T}/s^{-1}M^{-1}$	$10^4 k_2^{-T}/s^{-1}M^{-1}$.
Diethylamine	11.09	3	1.26
Piperidine	11.1	≈ 1	2.6
Trifluoroethanol	12.23	< 5	4.5
2,6-dimethyl piperidine	11.2	-*	0.3
Pyridine	5.25	23,000	< 1*
2,6-dimethyl pyridine	6.75	165	0.6

* Assumed negligible.

2.3 PROTODETRITIATION OF 2-METHYLINDOLE IN 50% (w/w) AQUEOUS METHANOL BUFFERS.

Preliminary studies are reported for this mixed solvent, since it became apparent that the solubility of t butyl substituted indoles in water was exceedingly small. 50% (w/w) [\equiv 57.7 (v/v)] Methanol was chosen since some accurate thermodynamic dissociation constants have been reported for this medium by Bates⁵⁶.

Results for acetic acid (Table 2.8) and 2,6-dimethylpyridine (Table 2.9) enable the catalytic constants for the acid catalysed pathway to be calculated, if again it is assumed that the extent of exchange via the base catalysed pathway is negligible (Table 2.27).

The hydronium ion concentration was calculated by measurement of the operational pH and applying the correction given by Bates⁵⁷.

$$\text{pH}_{\text{glass electrode}} = \text{pH}^{\ddagger} + 0.13 \quad \text{for 50\%(w/w) methanol.}$$

It can be seen that the agreement within the two sets of buffers for the hydronium ion terms was fairly good.

$$\begin{aligned} k_{\text{bi}}^{-\text{T}} (\text{H}_3\text{O}^+) &= 29 \text{ s}^{-1} \cdot \text{M}^{-1}. \text{ (acetic acid)} \\ &= 33 \text{ s}^{-1} \cdot \text{M}^{-1}. \text{ (2,6-dimethylpyridine)} \end{aligned}$$

Several studies of stronger bases, including OH^- itself, were also made. Some data for OH^- catalysis of 2-methylindole in 50%(v/v) ethanol is reported in section (2.5), however the bulk of the measurements were carried out in methanol, including catalysis by hydroxide (Table 2.10), piperidine (Table 2.11) and dimethylpiperidine (Table 2.12). The contribution to the rates from the acid catalysed

TABLE 2.8 Protodetritiation of 2-Methylindole 3-³H₁ in 50%(w/w) aqueous methanol/acetic acid buffers.

$[B^-]/[BH] = 4, I = 0.1, pK_a^* = 5.53, pH^* = 6.23 \pm 0.05, T = 25^\circ.$

$[AcOH]/M.$	$10^4 k_o^{-T}/s^{-1}.$	Run
0.020	2.42	282
0.010	1.43	283
0.005	0.749	284
0.002	0.380	285

$$k_o^{-T} = 29 [H_3O^+] + 0.011 [AcOH]$$

TABLE 2.9 Protodetritiation of 2-Methylindole 3-³H₁ in 50%(w/w) aqueous methanol/2,6-dimethylpyridine buffers at 25°C. $pK_a^* = 5.82.$

$[B]/[BH^+] = 4, I = 0.1, pH^* = 6.47 \pm 0.03 .$

$[BH^+] /M.$	$10^5 k_o^{-T}$	Run
0.025	2.41	364
0.0125	1.76	365
0.00625	1.48	366
0.00250	1.24	367
0.0	1.12	-

$$k_o^{-T} = 33 [H_3O^+] + 0.00052 [LuH^+]$$

TABLE 2.10 Protodetrition of 2-Methylindole 3-³H₁ in 50%(w/w) aqueous methanol/sodium hydroxide solutions at 25°C.

[NaOH]/M.	$10^5 k_o^{-T} / s^{-1}$.	Run
0.20	18.6	361
0.10	9.32	437

$$k_2^{-T} = 9.3 \times 10^{-4} s^{-1} . M^{-1} .$$

TABLE 2.11 Potodetrition of 2-Methylindole 3-³H₁ in 50%(w/w) aqueous methanol/piperidine buffers at 25°C. $pK_a^* = 10.71$

$$[B]/[BH^+] = 4, I = 0.2, pH^* = 11.31, [OH^-] = 2.04 \times 10^{-3} M.$$

[B]/M.	$10^5 k_o^{-T} / s^{-1}$	Run
0.76	3.37	374
0.76	3.29	391
0.3	1.57	392
0.1	0.668	393
0.04	0.344	394
0.0	0.20	-
0.0	0.19	*

* Calculated from hydroxyl rate, Table 2.10

TABLE 2.12 Protodetrition of 2-Methylindole 3-³H₁ in
50% (w/w) aqueous methanol/2,6-dimethylpiperidine
buffers at 25°C. $pK_a^* = 10.66$

$$[B]/[BH^+] = 4, I = 0.2, pH^* = 11.26, [OH^-] = 1.82 \times 10^{-3} M.$$

$[B]/M.$	$10^6 k_o/s^{-1}.$	Run
0.64	8.48	382
0.30	5.31	383
0.10	2.95	384
0.04	1.85	385
0.0	1.40	-
0.0	1.69	*

* Calculated from hydroxyl rate, Table 2.10

$$k_2^{-T} = 0.13 \times 10^{-4} s^{-1} M^{-1}.$$

pathway is expected to be several orders of magnitude less than the observed rates, and bimolecular rate constants were calculated neglecting this contribution.

With the high concentrations of amine buffers, curvature in the plot of k_0^{-T} against $[B]$ was noted (Figure 2.6 and 2.7). In these cases the point for the most concentrated buffer was not included in the measurement of the slope, and for this reason the rate constants obtained must be considered only approximate. This problem was overcome to some extent by directly comparing rates for different indoles measured at the same buffer concentration and this is elaborated further in section (2.10). The change in medium (all solutions were prepared as 57.7%(v/v), and this can only be equated to 50%(w/w) if the density of the aqueous solution is 1.0) probably accounts for the observed curvature, though other complications such as the existence of cis and trans isomers of 2,6-dimethylpiperidine may also complicate the situation⁵⁸.

2.4 ACID CATALYSED HYDROGEN EXCHANGE OF 2-METHYL-4,6-DI-t BUTYL INDOLE.

This substrate was studied in a series of acetic acid (Table 2.13) and 2,6-dimethylpyridine (Table 2.14) buffers in a manner analogous to 2-methylindole, with the important difference that the rate of loss of deuterium was measured concomitantly with the rate of loss of tritium (see Chapter 6 for experimental details). The deuterium isotope effects reported were all calculated by the method described in section (2.12.1) and will be discussed in detail later. It is

TABLE 2.13 Concomitant protodetrition and dedeuteriation of 2-Methyl-4,6-di-t-butylindole in 50%(w/w) aqueous methanol/acetic acid buffers. at 25^oC.

$$[B^-]/[BH] = 4, I = 0.1, pK_a^* = 5.53, pH^* = 6.23 \pm 0.05$$

$[AcOH]/M.$	$10^4 k_o^{-T}/s^{-1}.$	$10^4 k_o^{-D}/s^{-1}.$	k_2^H/k_2^D
0.020	5.35	-	-
0.0181	4.97	9.81	5.6
0.0100	3.20	-	-
0.0090	2.82	5.26	5.0
0.0050	1.69	-	-
0.0045	1.58	3.26	6.0
0.0020	0.866	-	-
0.0020	0.874	1.91	6.9

$$k_o^{-T} = 68 [H_3O^+] + 0.025 [AcOH]$$

TABLE 2.14 Concomitant protodetrition and dedeuteriation of 2-Methyl-4,6-di-t butylindole in 50%(w/w) aqueous methanol/2,6-dimethylpyridine buffers.

$$[B]/[BH^+] = 4, I = 0.1, pH^* = 6.47 \pm 0.03, T = 25^\circ C.$$

$[BH^+]/M.$	$10^5 k_O^{-T}/s^{-1}$	$10^5 k_O^{-D}/s^{-1}$	k_2^H/k_2^D
0.025	6.24	14.2	7.5
0.0125	4.78	10.2	6.6
0.00615	3.27	7.34	7.3
0.00250	2.82	6.10	7.1
0.0	2.40	-	-

$$k_O^{-T} = 0.00153 [BH^+] + 70 [H_3O^+]$$

TABLE 2.15 Protodetrition of 3-³H₁ Indoles in 50%(v/v) aqueous ethanol/sodium hydroxide solutions at 25°

$[NaOH(D)]/M.$		1.0	0.4	0.1	0.02
$10^5 k_O^{-T}/s^{-1}$	MI	45.6	21.5	5.86	1.33
$10^5 k_O^{-T}/s^{-1}$	DBMI	9.71	4.59	1.27	0.31
	Ratio MI/DBMI	4.7	4.7	4.6	4.3

worth noting that isotope effects were calculated separately for each run, since the concomitant method of analysing the rates minimises the errors within a run, and not within a series.

2.5 BASE CATALYSED HYDROGEN EXCHANGE OF 2-METHYL-4,6-DI-t BUTYL INDOLE.

The hydroxyl catalysed rates were measured initially in ethanol (Table 2.15) in order to compare the relative rates of exchange with 2-methylindole. Subsequent runs were all carried out in 50%(w/w) methanol. Table 2.16 gives the complete data for hydroxyl catalysed exchange of methylindole in this medium. The final column gives the kinetic deuterium isotope effects calculated by the method described in section (2.12.1) and the results at the foot of the Table refer to the method in section (2.12.3). Similar, but not such extensive, kinetic studies were carried out using 2,6-dimethylpiperidine as the catalysing base (Table 2.17) and piperidine itself (Table 2.18). These results are shown later in Figures 2.5 to 2.7 . The isotope effects in Table 2.17 again refer to the method outlined in section (2.12.1).

2.6 HYDROGEN EXCHANGE OF 2,4,5- TRI-t BUTYLINDOLE.

This indole was isolated as a white glass, and crystallisation from aqueous methanol, dioxan, acetone or t-butanol gave crystals

TABLE 2.16 Hydrogen exchange of 2-methyl-4,6-di^tbutylindole in 50%(w/w) aqueous methanol/NaOH(D) solutions at 25°C.

[NaOH(D)]/M.	$10^5 k_O^{-T}/s^{-1}$	$10^5 k_O^{-D}/s^{-1}$	$10^5 k_O^T/s^{-1}$	$10^5 k_O^D/s^{-1}$	k_2^H/k_2^D	Run
0.10	2.89	-	-	-	-	354
0.20	5.56	-	-	-	-	351
0.20	-	11.6	-	-	6.4	355
0.10	-	5.92	-	-	6.1	356
0.10	-	-	2.50	-	-	403
0.20	-	-	4.94	10.5	-	404
0.20	-	-	4.91	-	-	405
0.20	-	-	4.99	13.0	-	475
0.104	-	-	2.57	6.49	-	476
k_2^{+X}	2.84	5.86	2.48	6.00	6.3	-

$$a = 2.067, a' = 2.165 \quad b = 2.419, b' = 2.883, k_O^{-T}/k_O^T = 1.142$$

$$k_2^H/k_2^D = 6.09 \pm 1.7, \quad k_1^H/k_1^D = 6.47, \quad k_2^H/k_2^T = 14.4 \pm 3.6, \quad k_2^D/k_2^T = 2.36 \pm 0.075.$$

$$r = 1.474 \pm 0.266$$

TABLE 2.17 Hydrogen exchange of 2-Methyl-4,6-di-t butylindole
in 50%(w/w) aqueous methanol/2,6-dimethylpiperidine
buffers at 25°C. $pK_a^* = 10.66$

$$[B]/[BH^+] = 4, I = 0.2, pH^* = 11.26, [OH^-] = 1.82 \times 10^{-4} M.$$

$[B]/M.$	$10^7 k_O^{-T}/s^{-1}.$	$10^7 k_O^{-D}/s^{-1}.$	k_2^H/k_2^D
0.8	6.73	14.1	6.4
0.3	5.89	13.3	7.2
0.1	4.81	10.3	6.7
0.04	3.71	8.15	7.0
0.0	3.6	-	-
0.0	5.2*	-	-

* calculated from the hydroxyl rate, Table 2.16

TABLE 2.18 Protodetrition of 2-Methyl-4,6-di-t butylindole
in 50%(w/w) aqueous methanol/piperidine buffers
at 25°C. $pK_a^* = 10.71$

$$[B]/[BH^+] = 4, I = 0.2, pH^* = 11.31, [OH^-] = 2.04 \times 10^{-3} M.$$

$[B]/M.$	$10^6 k_O^{-T}/s^{-1}.$	Run
0.8	5.43	447
0.3	3.16	448
0.1	1.60	449
0.04	0.931	450
0.0	0.540	*

* Calculated from the hydroxyl rate, Table 2.16

of the approximately 1:1 molecular complex. For this reason deuterium exchange kinetics could not be followed, since the methanol extracted with the indole resulted in the observation of variable deuterium contents. Excellent first order protodetrition kinetics were observed however (Section 6.1.7), and the results for catalysis by acetic acid, 2,6-dimethylpyridine and hydroxide are given in Tables 2.19 to 2.21 respectively. The catalytic rate constants obtained for tributylindole, and also methyldibutylindole and methylindole are summarised in Table 2.27 for acid catalysed exchange and Table 2.28 for base catalysed exchange. Also reported in this latter Table are the hydroxyl catalysed protodetrition rates for several other 2- and 4- substituted indoles.

2.7 PROTONATION OF INDOLES IN ACIDIC MEDIA.

It has been established that indoles protonate on the 3- carbon atom in fairly strong acids, and the equilibrium can be easily followed by observing the U.V. spectral changes⁵⁹. No data is available for the butylindoles, and accordingly the protonation equilibria were measured, in methanol to provide a direct comparison with the kinetic results. All the indoles appeared stable by U.V. and good isobestic points were obtained (Section 6.1.8). The indoles were sufficiently basic that the overlap principle was not used, plots of the ratio $\log [IrH_2^+]/[InH][H_3O^+]$ against $[H_2SO_4]$ proving sufficiently linear for a reliable extrapolation to zero ionic strength to be made. The data are given in Tables 2.22 to 2.24 and were fitted by least squares analysis to a straight line to obtain the Thermodynamic pK value (Table 2.25). The last column in Tables

TABLE 2.19 Protodetrition of 2,4,6- tri t butylindole
in 50%(w/w) aqueous methanol/acetic acid buffers

$[B^-]/[BH] = 5, I = 0.1, pK_a^* = 5.53, pH^* = 6.26 \pm 0.03, T = 25^\circ C.$

$[AcOH]/M.$	$10^5 k_O^{-T} / s^{-1}.$	Run
0.02	19.7	438
0.0107	10.6	439
0.0053	6.04	440
0.0	1.4	-
0.0	2.0	*

* Calculated from the lutidine rate, Table 2.20

$$k_O^{-T} = 38 [H_3O^+] + 0.009 [AcOH]$$

TABLE 2.20 Protodetrition of 2,4,6- tri t butylindole
in 50%(w/w) aqueous methanol/2,6-dimethyl
pyridine buffers at 25°C.

$[B]/[BH^+] = 5, I = 0.1 \text{ with NaCl}, pH^* = 6.54$

$[LuH^+]/M.$	$10^5 k_O^{-T} / s^{-1}.$	Run
0.1	1.80	446
0.025	1.47	435
0.0125	1.34	434
0.00625	1.28	433
0.00250	1.30	432
0.0	1.28	-

$$k_O^{-T} = 38 [H_3O^+] + 0.00006 [LuH^+]$$

TABLE 2.21 Protodetrition of 2,4,6- tri t butylindole in 50%(w/w) aqueous methanol/sodium hydroxide solutions at 25°C.

$[NaOH]/M.$	$10^6 k_0^{-T}/s^{-1}.$	Run
1.0	17.0	429
0.2	3.46	430
0.1	1.74	431

$$k_2^{-T} = 1.74 \times 10^{-5} s^{-1} . M^{-1}.$$

TABLE 2.22 Equilibrium protonation of 2-methylindole in 50%(w/w) aqueous methanol at 25°C.

$$[Indole] = 4 \times 10^{-5} M.$$

$[H_2SO_4]/M.$	$\log [InH_2^+]/[InH][H_3O^+]$	$\log [InH_2^+]/[InH][H_3O^+]$
0.0	-	- 2.66**
1.50	- 1.413	- 1.408
1.75	- 1.232	- 1.200
2.00	- 0.949	- 0.992
2.18	- 0.848	- 0.843
2.51	- 0.549	- 0.569
2.915	- 0.253	- 0.232

** Calculated from the least squares regression line.

TABLE 2.23 Equilibrium protonation of 2-Methyl-4,6-di t butylindole in 50%(w/w) aqueous methanol at 25°C.

$$[\text{Indole}] = 4 \times 10^{-5} \text{M.}$$

$[\text{H}_2\text{SO}_4]/\text{M.}$	$\log[\text{InH}_2^+]/[\text{InH}][\text{H}_3\text{O}^+]$	$\log[\text{InH}_2^+]/[\text{InH}]/[\text{H}_3\text{O}^+]$
0.0	-	- 1.17**
0.4	- 0.937	- 0.948
0.6	- 0.812	- 0.838
0.8	- 0.763	- 0.727
1.0	- 0.610	- 0.619
1.25	- 0.495	- 0.479
1.50	- 0.353	- 0.341
1.73	- 0.211	- 0.214
2.00	- 0.047	- 0.065

TABLE 2.24 Equilibrium protonation of 2,4,6-tri t butyl indole in 50%(w/w) aqueous methanol at 25°C.

$$[\text{Indole}] = 6 \times 10^{-5} \text{M.}$$

$[\text{H}_2\text{SO}_4]/\text{M.}$	$\log[\text{InH}_2^+]/[\text{InH}]/[\text{H}_3\text{O}^+]$	$\log[\text{InH}_2^+]/[\text{InH}]/[\text{H}_3\text{O}^+]$
0.0	-	- 1.96**
1.25	- 1.34	- 1.31
1.50	- 1.13	- 1.18
2.0	- 0.90	- 0.92
2.3	- 0.814	- 0.769
2.63	- 0.638	- 0.597
3.0	- 0.398	- 0.406
3.3	- 0.221	- 0.250

** Calculated from the least squares regression line.

2.22 to 2.24 is the value of the indicator ratio calculated from the regression line. The slopes of these plots (Table 2.25) are considerably different, suggesting the butyl groups may be having a considerable effect on the solvation of the protonated indole.

To test the validity of the extrapolation to zero ionic strength, all the data were also fitted to a polynomial of the form

$$y = a + b.x + c.x^2$$

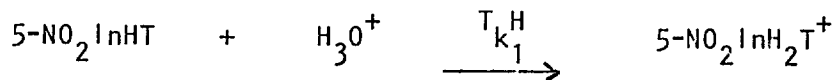
where $x = [H_2SO_4]$. No significant improvement in the fits was obtained and the linear extrapolation is probably reliable.

TABLE 2.25 pK_a values for indoles in 50%(w/w) aqueous methanol at 25°.

<i>Substrate</i>	pK_a^{25}	$\frac{d pK_a}{d[H_2SO_4]}$	<i>Standard error.</i>
Methylindole	-2.66 ± 0.06	0.831 ± 0.027	0.031
Tributylindole	-1.96 ± 0.06	0.518 ± 0.023	0.042
Methyldibutylindole	-1.17 ± 0.02	0.552 ± 0.015	0.022

2.8 ACTIVATION PARAMETERS FOR THE PROTONATION OF INDOLES.

The activation parameters for the acid catalysed reaction



were measured previously by Iqbal⁶⁰ and the parameters for the corresponding reaction via the indolyl anion are reported here for comparison.



Kresge⁶¹ has shown that to a good approximation, the activation parameters obtained from the temperature variation of k_{bi}^{-L} (equation 2.1) correspond to the rate of protonation of the indole to form the Wheland intermediate (k_1^H , equation 2.2). For the anion reaction however (equation 2.3), it is necessary to eliminate the equilibrium constant K_E and this was accomplished by studying the rate of protodetritiation of the indole in sufficiently concentrated sodium hydroxide solutions to completely ionise the substrate. First order rate constants were also divided by the absolute water concentration⁶² in order to obtain the bimolecular rate constant k_{bi}^{-T} . The results are given in Table 2.26 and the data was fitted by least squares to equation 2.14.

$$\ln k_{bi}^{-T}/T = 23.76 + \frac{\Delta S^\ddagger}{R} - \frac{\Delta H^\ddagger}{RT} \quad 2.14$$

TABLE 2.26 Activation parameters for the protodetrutiation of 5-nitroindole 3-³H₁ in aqueous sodium hydroxide solutions. [NaOH] = 4.0 N.

$T/^{\circ}C.$	$10^5 k_o^{-T}/s^{-1}.$	$10^7 k_{bi}^{-T}/s^{-1}.M^{-1}.$
25.0	1.50	4.43
50.0	20.8	48.7
69.5	113.0	268.0

$$\Delta H^{\#} = 75.8 \text{ kJ.mol}^{-1} = 18.1 \text{ kcal.mol}^{-1}.$$

$$\Delta S^{\#} = -113 \text{ J.K}^{-1}.\text{mol}^{-1} = -27 \text{ cal.K}^{-1}.\text{mol}^{-1}.$$

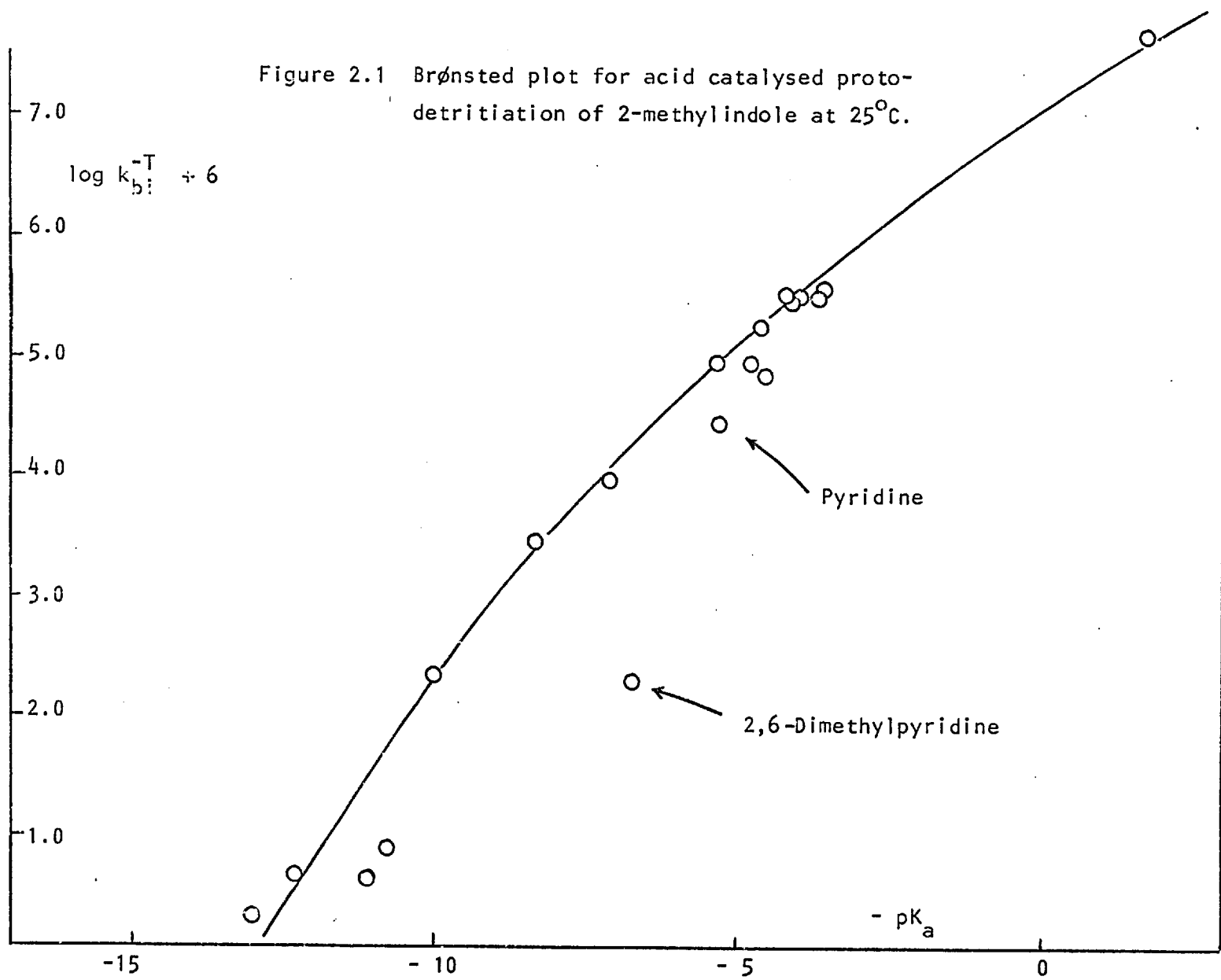
D I S C U S S I O N

2.9.1 RATE CORRELATIONS FOR ACID CATALYSED EXCHANGE IN AQUEOUS SOLUTIONS.

Challis and Long⁴⁷ have shown that protodetrition of 2-methyl indole is general acid catalysed and the Brønsted plot (equation 2.12), incorporating the data determined here is shown (Figure 2.1). The range of the data (15 pK_a units) is sufficiently large to show an appreciable curvature in the plot, the initial slope being about 0.4 and the final slope about 0.63. This does tend to suggest that the Brønsted α is a local constant reflecting the degree of proton transfer, and thus varying as the reactivity of the system changes. An often cited objection to this type of treatment^{11c} is that the gross changes in the structure of the acid catalyst over the wide reactivity range may be responsible for the curvature. In fact, a series of similar plots for other indoles (using the same set of acid catalysts in each case) shows that the α obtained in each case varies with the indole basicity⁶⁰, and suggests that the curvature in Figure 2.1 is not an artifact.

These results can be contrasted with those of Kemp and Casey^{11c} for the elimination of benzisoxazoles. Variation in the reactivity of both the base and substrate gave the same uniform Brønsted exponent, and this may be a direct consequence of the concertedness of this E2 elimination.

Over a limited range of acidity the curvature in the Brønsted plot



is not detectable and the method can be used analytically to predict relative rates of reaction. It is apparent, for example, that 2,6-dimethylpyridine deviates considerably from the plot. This cannot be due to a major change in the catalyst structure¹¹ since pyridine itself deviates very little. Similar behaviour was found by Zollinger⁶³, who found that the removal of the proton from the Wheland intermediate in diazocoupling by 2,6-dimethylpyridine was a factor of ten slower than expected. Several other examples are known³⁸, particularly for ionisation of ketones⁶⁴ where a factor of seven for acetone and twenty four in the rate of ionisation of pinacolone was observed. It appears however that this type of behaviour is unusual in A-S_E2 reactions⁴⁴. The implications of this result are discussed later (section 2.11.3).

2.9.2 ACID CATALYSED HYDROGEN EXCHANGE IN AQUEOUS METHANOL SOLUTIONS.

The arguments in the previous section can also be applied to methanolic solutions, and it becomes apparent from the collected data (Table 2.27) that 2,6-dimethylpyridine is about 25 times less effective as a catalyst than acetic acid, which has a similar basicity in this solvent. It has also been demonstrated^{35,60} that the rate of exchange with a specific catalysing acid increases with the basicity of the indole substrate, with an α of from 0.4 to 0.7 and it seems reasonable to expect this relationship to hold for methanolic solutions. The basicities of the three indoles studied were measured (Table 2.25) and it can be seen that the rate of catalysis by acetic acid (Figure 2.2) and hydronium ion (Figures 2.2 and 2.3, intercept values) follow this rule. This is also true for catalysis by the conjugate acid of 2,6-dimethylpyridine (Figure 2.3) with the one exception of

Figure 2.2 Acid catalysed protodetritiation of indoles in 50%(w/w) aqueous methanol/acetic acid buffers.

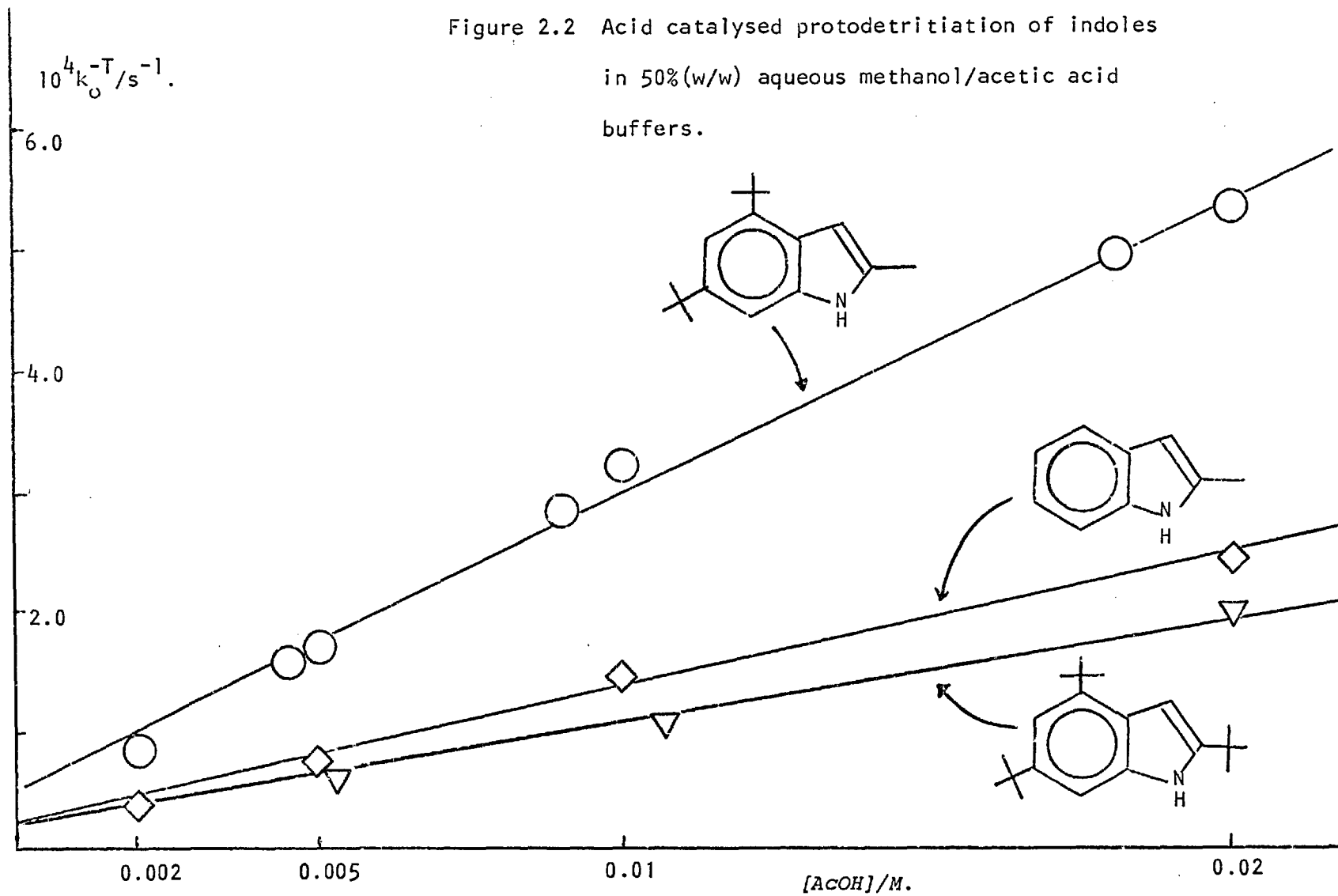
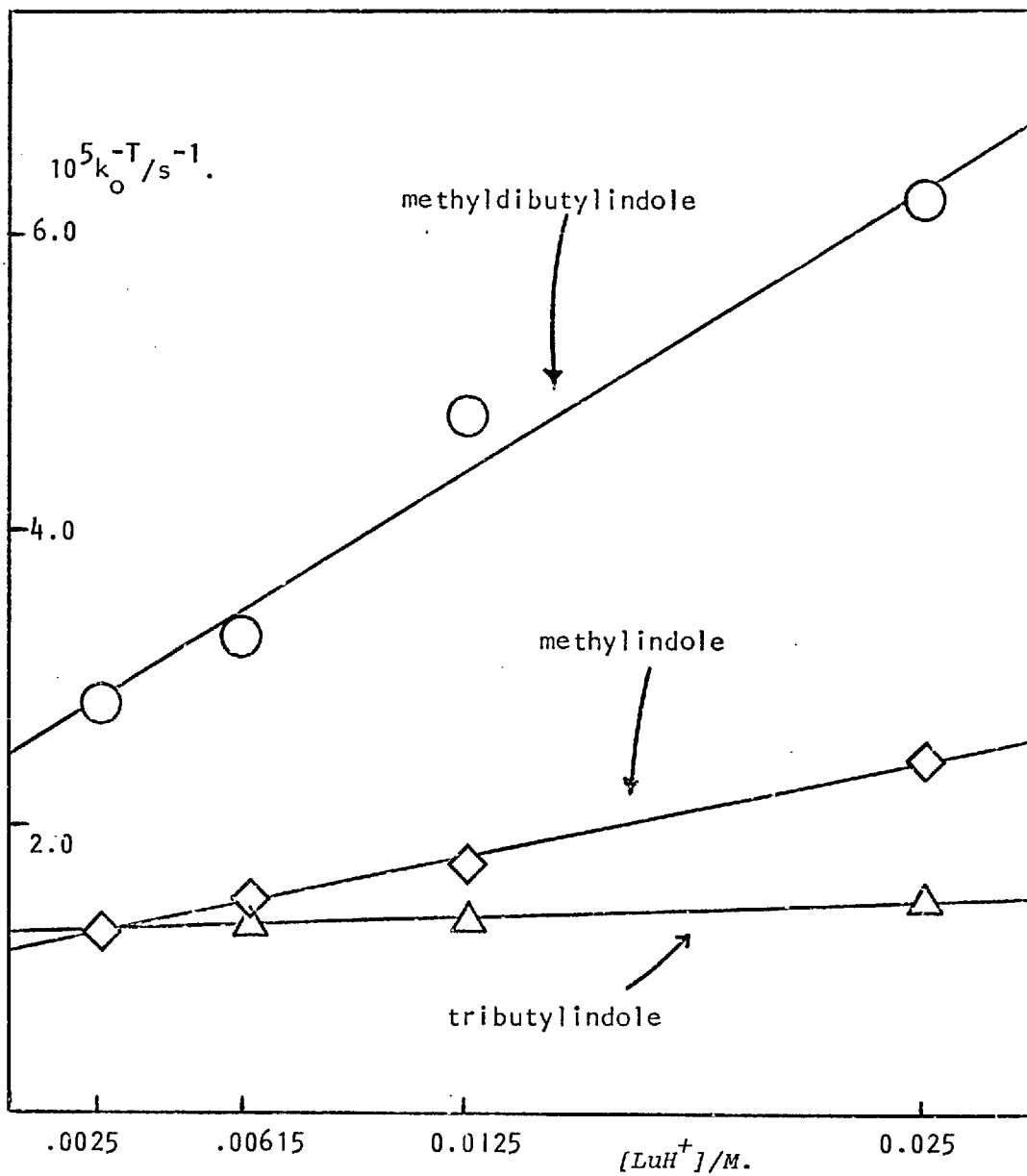


Figure 2.3 Acid catalysed protodetritiation of indoles in 50%(w/w) aqueous methanol/2,6-dimethylpyridine buffers.



the rate for tributylindole, which is about ten times slower in comparison with methylindole/2,6-dimethylpyridine and about 200 times slower than methylindole/acetic acid. The important point to note is that the anomalous effect of the lutidine is not increased on reaction with methyldibutylindole and the steric effects (with the one exception above) are a result of steric hindrance on the catalysing acid and not on the indole.

TABLE 2.27 Catalytic rate constants for the protodetritiation of indoles in 50% (w/w) aqueous methanol buffers at 25°C.

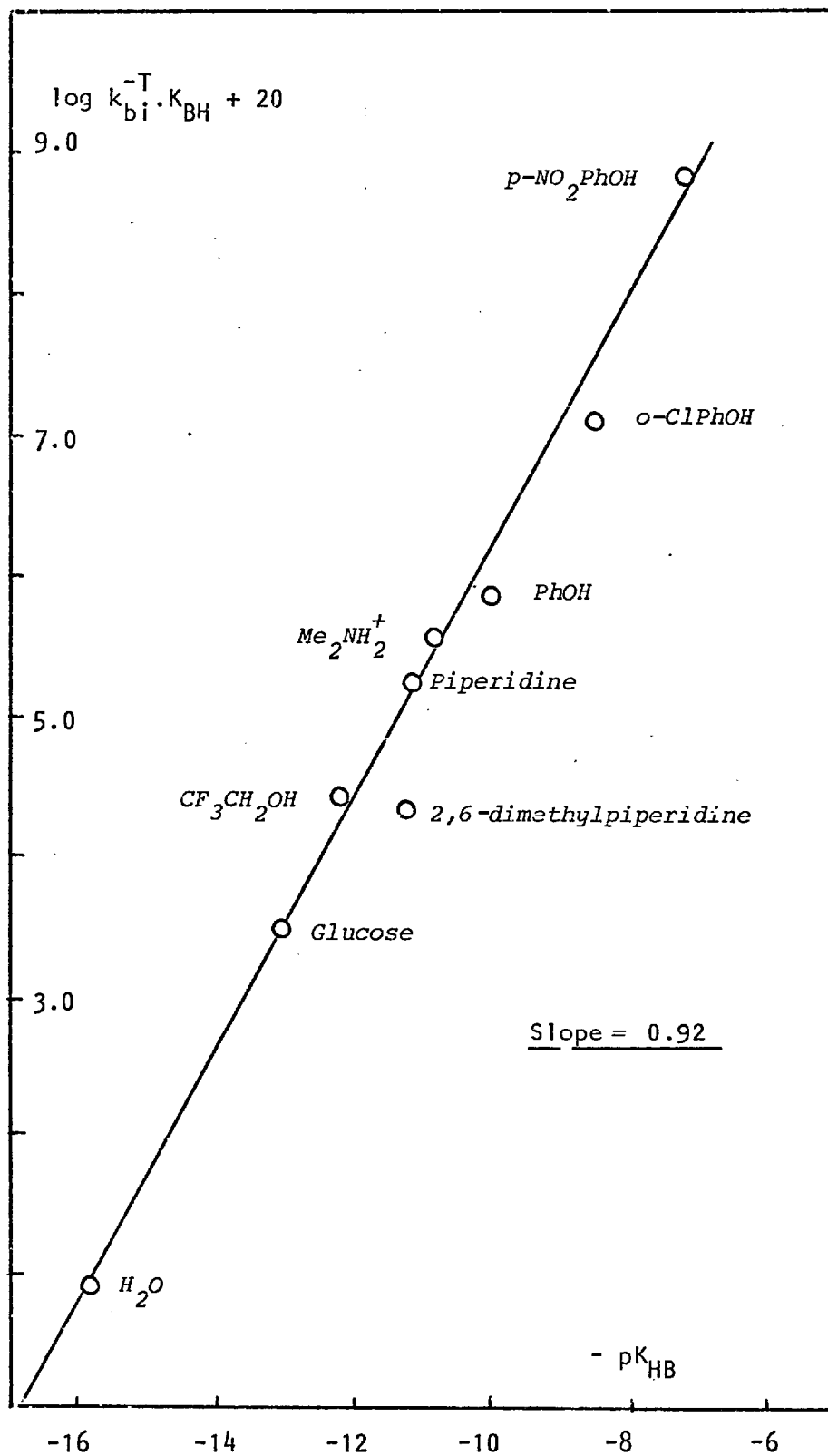
Indole	pK_a	$k_{bi}^{-T}/s^{-1}.M^{-1}$.		
		H_3O^+	AcOH	2,6 LuH ⁺
DBMI	- 1.17	70	0.025	0.00153
TBI	- 1.96	38	0.009	0.00006
MI	- 2.66	33	0.011	0.00052

2.10 RATE CORRELATIONS FOR BASE CATALYSED EXCHANGE

2.10.1 AQUEOUS SOLUTIONS.

The base catalysed protodetritiation of 2-methylindole was measured for several catalysts previously⁴⁷ and the Brønsted plot from

Figure 2.4 Brønsted plot for 'base' catalysed hydrogen exchange of 2-methylindole at 25°C.



equation 2.3 is given in Figure 2.4 . Two catalysts deviate from this plot, particularly 2, 6-dimethylpiperidine which catalyses the exchange about 6-7 times more slowly than expected. This factor is smaller than that for 2,6-dimethylpyridine and the difference in the catalyst structure and hybridisation, as well as the transition state symmetry, probably accounts for this (Section 2.11.3). Moreover, steric effects of a similar magnitude have been found for the protodetrition of 1,4-dicyano-2-butene⁶⁵, factors of about 4 and 9 being observed for 2,6-dimethyl and 2,2,6,6-tetramethylpiperidines respectively. Since the proton is more hindered in these reactions ($\alpha = 0.05$ against 0.92 for the indole reaction) it seems that a direct comparison with the pyridines cannot really be made.

Challis and Millar³⁵ have also shown that the rate of reaction of indolyl anions with a specific acid (H_2O) increases with the basicity of the 3-position. There is no available parameter which directly measures this basicity, but a good correlation (with α about 0.5) was found with the pK_a for protonation of the neutral substrate. Thus k_{bi}^{-L} (equation 2.3) truly reflects the electrophilic nature of the attack by water on the indolyl anion. One can use this information to predict the relative rates of hydroxyl catalysed exchange from the pK_a values.

2.10.2 AQUEOUS METHANOLIC SOLUTIONS.

The exchange rates of indolyl anions with a specific acid are determined not only by k_{bi}^{-L} but also by K_E (equation 2.3)

and consequently the relative variation of K_E within the series of indoles has to be determined. More particularly, we need to know the effect of t butyl groups in the 2, 4, and 6 positions of the indole, and results by Yagil⁶⁶ using a variety of substituents (2-CO₂⁻, 6-MeO, 4-Me) suggest that K_E is insensitive to electron donating groups. All these indoles ionise only in very concentrated sodium hydroxide solutions and consequently long extrapolations are required to dilute ' kinetic ' conditions. Such extrapolations are particularly undesirable with butylindoles, since the overlap technique cannot be used (section 2.7) and moreover, the necessary concentration of sodium hydroxide cannot be achieved in 50%(w/w) methanol. Since these equilibrium constants are not directly accessible, a series of model compounds were used.

Ridd has reported that 3-(p-nitrophenylazo)indoles ionise readily in dilute base (0.01 N NaOH)⁶⁷ with a large spectral shift. Accordingly a number of these derivatives were prepared and the pK_E values determined (Table 6.6) in 54%(w/w) aqueous methanol and dilute ' kinetic ' conditions.

The results show that a 5- nitro substituent has only slightly less effect on the pK_E of these derivatives (- 1.3) as on indoles themselves (≈ 2)⁶⁶ in a different solvent, and it seems that these compounds are adequate models. The results enabled the following increments to be deduced.

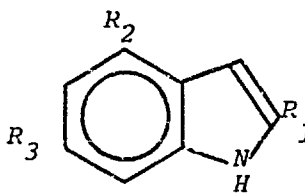
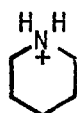
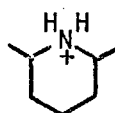
4,6- dibutyl	+	0.27
2- <u>t</u> butyl	+	0.33
4- methyl	+	0.12

This enables the pK_E for 2-butyl-4-methylindole to be predicted as 12.57 and the observed value of 12.60 is in good agreement. The pK_E of the 2,4,6-tributylindole derivative could not be measured with any confidence, since demethylation of the 2-t butyl group appears to occur during preparation and further, this indole is the only one which shows any steric effect ($> 10^3$) for diazocoupling (Section 3.6.3), possibly invalidating the use of the azo derivative as a model compound. The increments deduced previously enable the pK_E to be predicted as 12.71, which is the value subsequently used.

The protodetritionation of methylindole, methyldibutylindole and tributylindole by hydroxide (Figure 2.5), piperidine (Figure 2.6) and particularly 2,6-dimethylpiperidine (Figure 2.7) does not give linear plots, and the most deviant point was not considered in obtaining a value for the slope (k_2^{-T}). These values were corrected for K_{BH} by use of equation 2.3 and are summarised in Table 2.28. If a value for K_E for 2-methylindole of about 10^{-17} is used⁶⁶, the catalytic rate constant for piperidine catalysis becomes; $k_{bi}^{-T} = 88$. The value obtained for exchange via the neutral indole (Table 2.7) of $< 10^{-5}$ enables the difference in reactivity of the neutral indole and the conjugate base to be estimated as greater than 10^7 , similar to the estimate obtained from diazocoupling (Section 3.2.2). This tends to suggest that the interpretation of the mechanism of exchange is substantially correct.

The values of $k_{bi}^{-T} \cdot K_E$ in Table 2.28 have to be corrected not only for K_E but also for changes in the basicity of the indole if comparisons are to be made. The results of Challis and Millar^{35a} suggest that the relative order of rate constants found for the

TABLE 2.28 Catalytic rate constants for protodetrinitiation of indolyl anions in 50%(w/w) aqueous methanol buffers at 25°C.

	$10^{17} k_{bi}^{-T} \cdot K_E / s^{-1}$.		
			H ₂ O
$R_1=Me, R_2=R_3=tBu^{**}$	18	1.5	0.00723
$R_1=R_2=R_3=tBu$	-	-	0.000425
$R_1=R_2=Me, R_3=H$	-	-	0.0246
$R_1=Me, R_2=R_3=H$	88	26	0.0233
$R_1=tBu, R_2=Me, R_3=H$	-	-	0.00343
$R_1=tBu, R_2=R_3=H$	-	-	0.00440
K_{BH}	2×10^{-11}	2×10^{-11}	4×10^{-16}

** Indoles are arranged in decreasing order of basicity.

Figure 2.5 Base catalysed protodetritiation of indoles in 50%(w/w) aqueous methanol/ sodium hydroxide solutions at 25°C.

The slopes have the value 1.0 ± 0.05

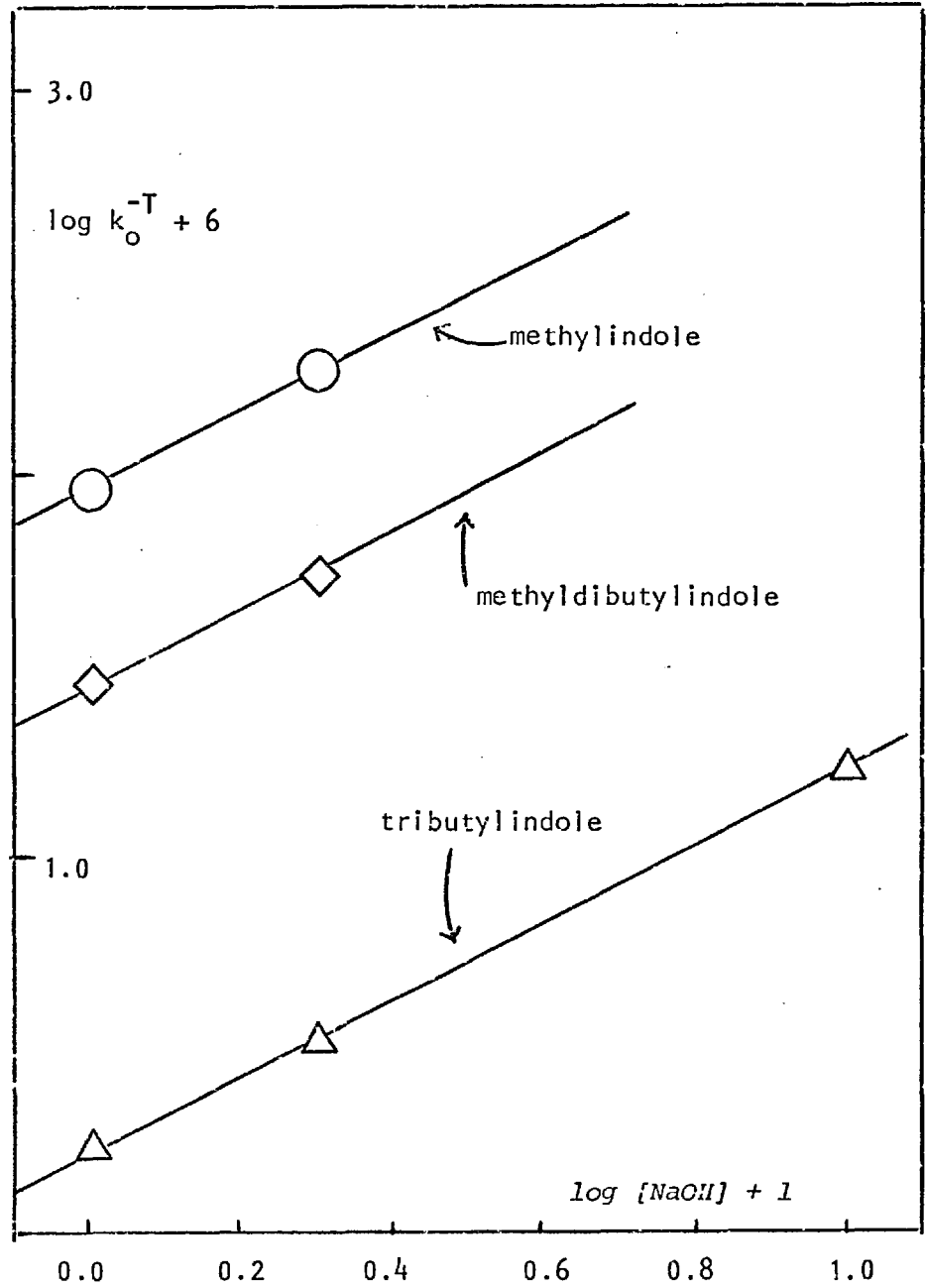


Figure 2.6 Base catalysed protodetrition of indoles in 50%(w/w) aqueous methanol/piperidine buffers at 25°C.

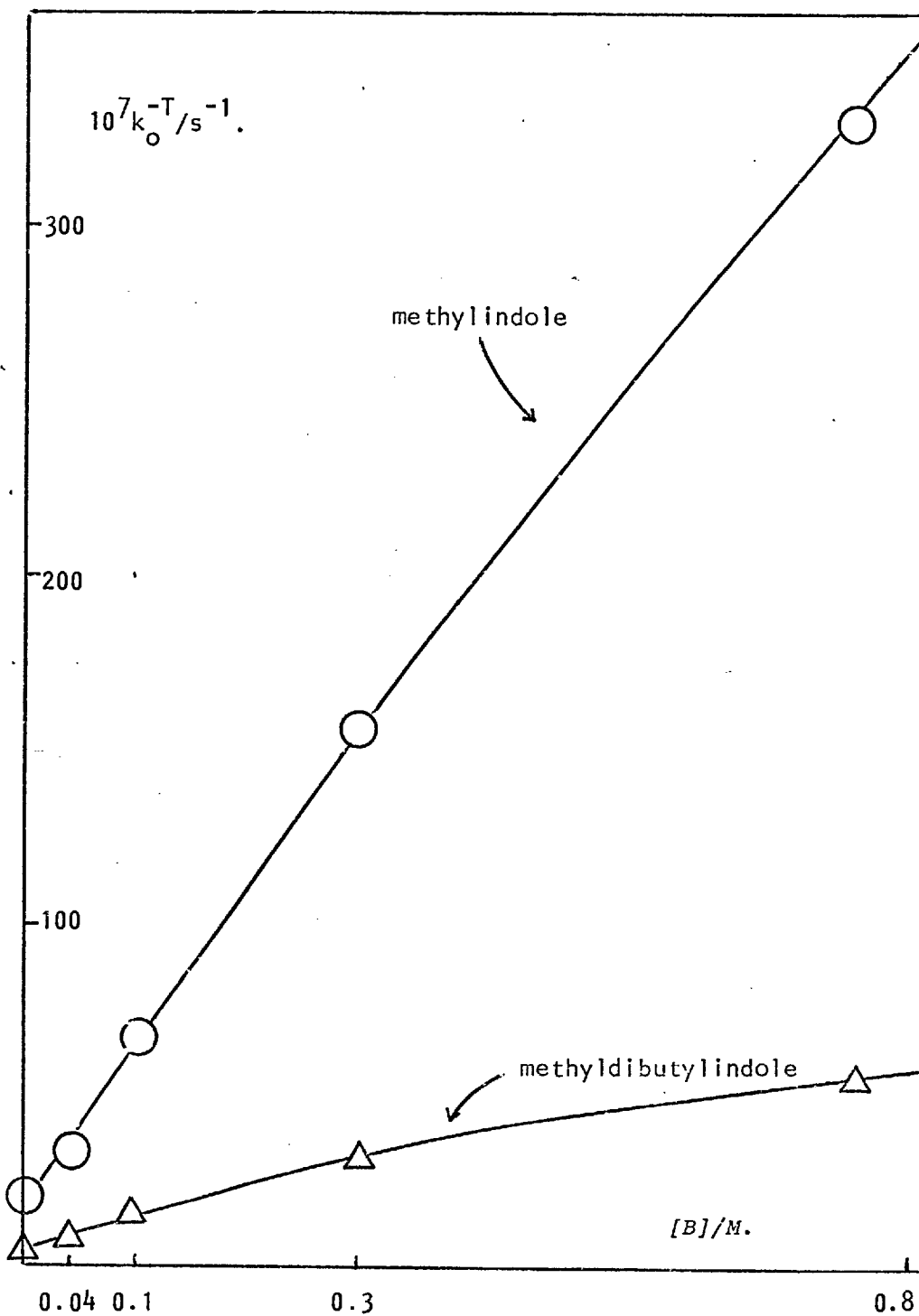
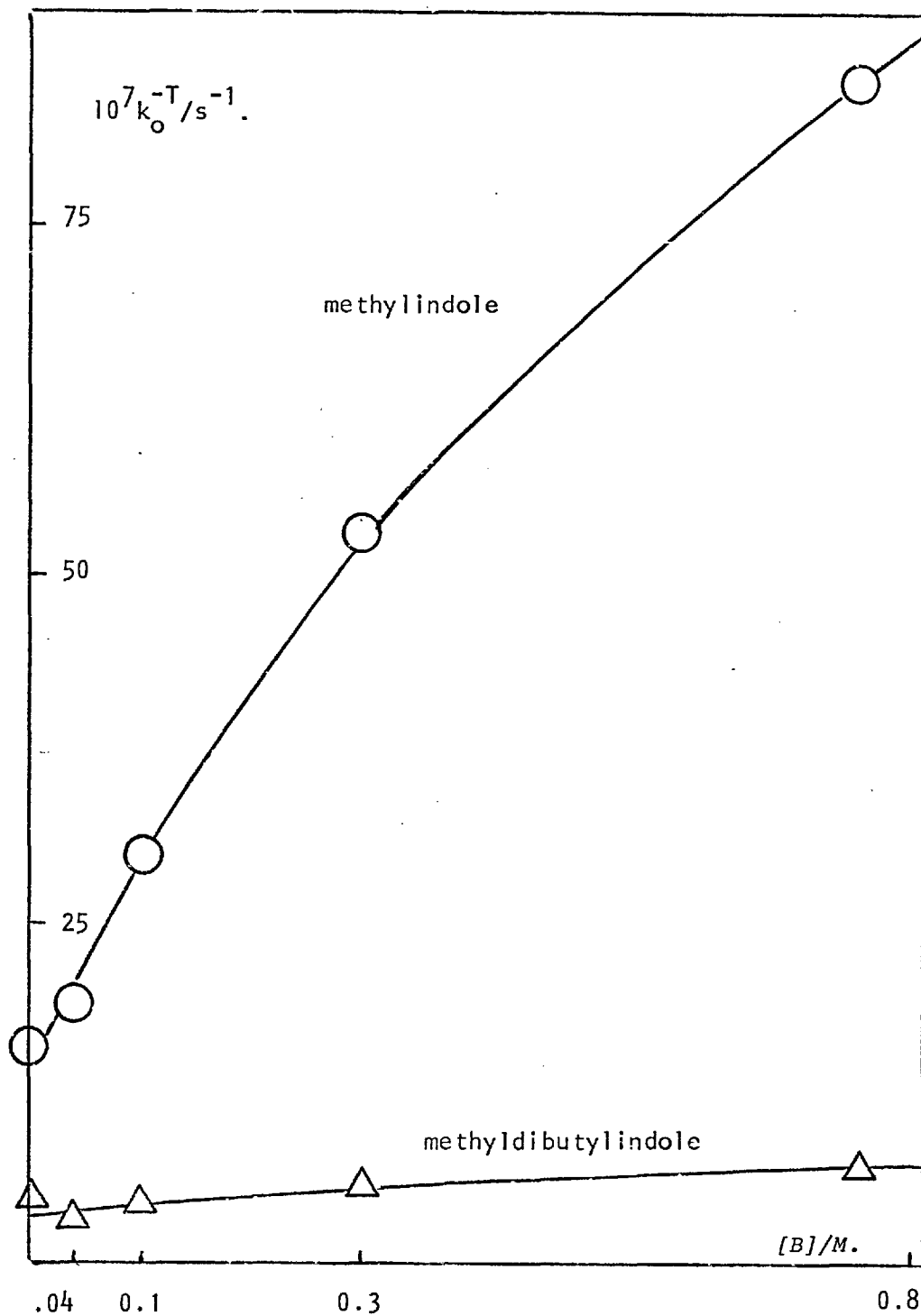
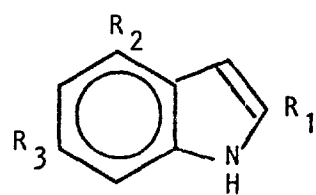
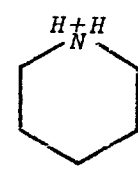
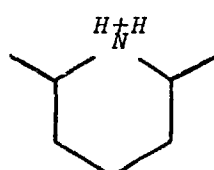


Figure 2.7 Base catalysed protodetrition of indoles in 50%(w/w) aqueous methanol/2,6-dimethyl piperidine buffers at 25°C.



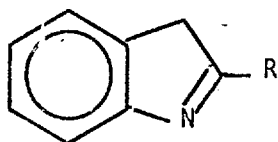
acid catalysed exchange (Table 2.27) ought to be mirrored in the base catalysed exchange. The rate constants in Table 2.28 were corrected for K_E using the relative values obtained from the 3-(p-nitrophenylazo) indole, and for the basicity using the relative values of the hydronium ion catalysed exchange. The difference between the rates calculated in this manner and the observed rates (Table 2.29) are greater than unity in several cases and it is apparent that there are several differences from the acid catalysed pathway. Firstly, the water rate for tributyl indole is about 16 times slower than expected- whereas the hydronium ion acid catalysed rate is normal. Secondly, a bulky group in the 4- position increases the steric effect for 2,6-dimethylpiperidine catalysis, whereas no such effect was observed for 2,6-dimethylpyridine. The interpretation of these results is discussed in the next section.

TABLE 2.29 Steric effects for protodetrition of indolyl anions in 50%(w/w) aqueous methanol buffers at 25°C.

	$\sim 10^{17} K_E$	Catalysing acid		H ₂ O
				
$R_1=Me, R_2=R_3=tBu$	0.54	5	59	3.5
$R_1=R_2=R_3=tBu$	0.25	-	-	16.5
$R_1=R_2=Me, R_3=H$	0.76	-	-	1.0
$R_1=Me, R_2=R_3=H$	1.0	1.0	3.4	1.0
$R_1=tBu, R_2=Me, R_3=H$	0.33	-	-	2.2
$R_1=tBu, R_2=R_3=H$	0.47	-	-	2.0

2.11 THE NATURE OF THE TRANSITION STATE.

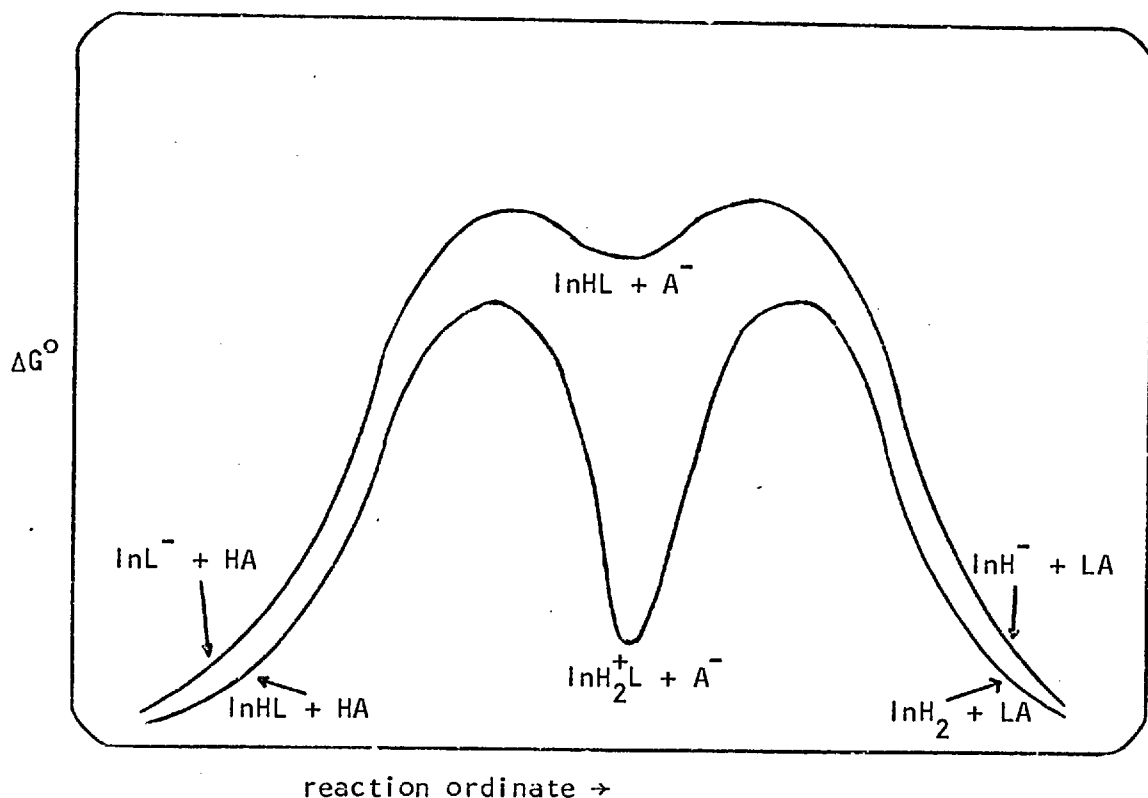
Any model of the transition state must rationalise the *peri* interactions observed for exchange via the indolyl anion. One gains some idea from the high Brønsted α for this reaction, which suggests the transition state is very product like, with the proton almost completely transferred. An alternative argument could be based on a consideration of the relative energy of the intermediate and reactants. This intermediate is in fact the indolenine tautomer of indole



and it is known from n.m.r. studies in solution that this tautomer must be unstable with respect to the indole form. The stability of the indolenine tautomer is increased if the group R is electron donating, yet with $R = \text{SEt}$ the indole form still predominates⁶⁸ and only when $R = \text{OEt}$ does the percentage of indolenine roughly equal that of the indole⁶⁹. The high energy of this intermediate indolenine, coupled with the high Brønsted α tends to confirm that the transition state and intermediate are similar in energy (Figure 2.8).

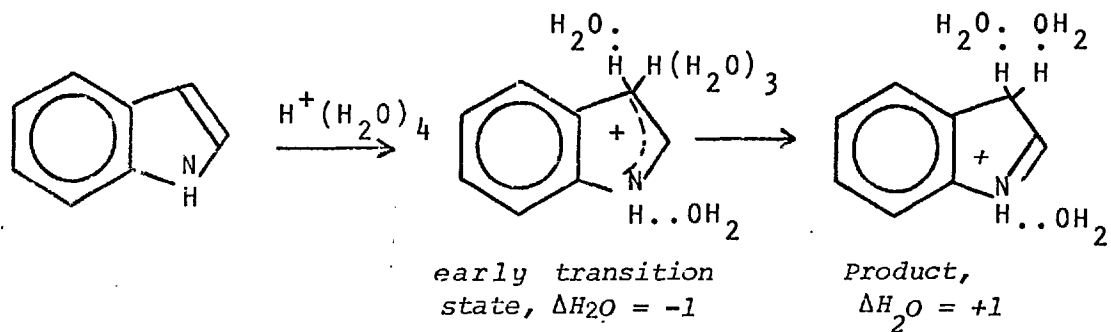
In contrast, the intermediate species for exchange via the neutral indole are indolium salts. These species are stable both as solids (Section 6.1.3) and in solution (Section 6.1.8). This fact, coupled with an intermediate value for the Brønsted α , tends to suggest that the energies of the transition state and product are not similar (Figure 2.8).

Figure 2.8 The reaction pathway for hydrogen exchange of indoles.



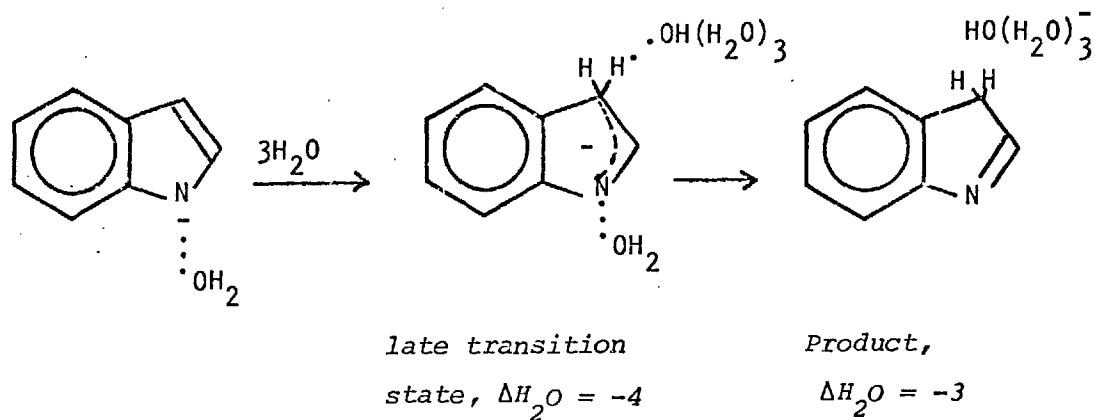
A further indication of the properties of the transition state, albeit one open to several interpretations, comes from the activation parameters for the neutral molecule and conjugate base reactions. Possible solvation patterns for the two reactions are outlined in Scheme 2.6. It can be seen that the small negative entropy of activation for the neutral molecule reaction is more suited to an early transition state than a late one, using an approximate rule of thumb that loss of a water molecule is equivalent to -10 e.u. The larger negative entropy for the anion reaction on this basis corresponds to a product like transition state. These are very qualitative conclusions and serve only to support a general pattern.

Scheme 2.6 Transition state solvation for the indole hydrogen exchange reaction.



$$\Delta H^\ddagger = 18.5 \text{ kcal.mol}^{-1}.$$

$$\Delta S^\ddagger = -9.1 \text{ cal.K}^{-1}.\text{mol}^{-1}.$$

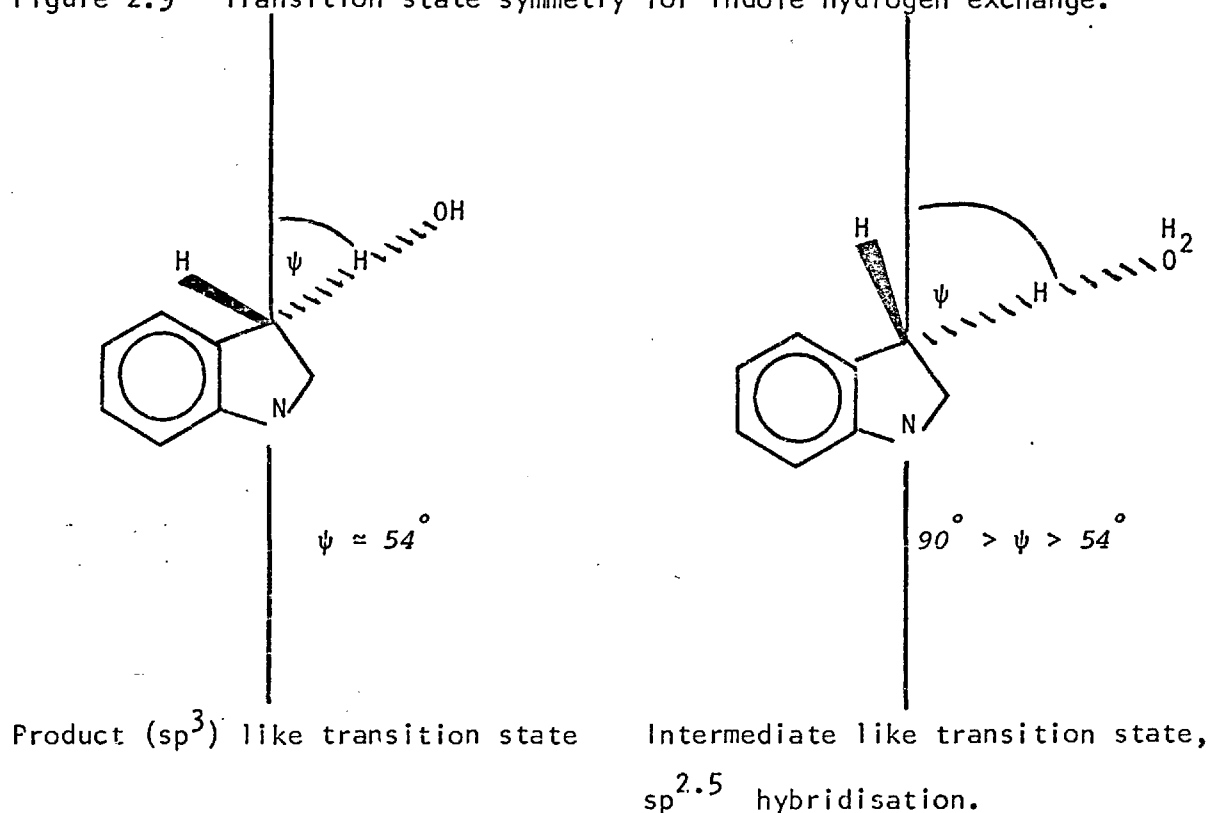


$$\Delta H^\ddagger = 18.1 \text{ kcal.mol}^{-1}.$$

$$\Delta S^\ddagger = -27 \text{ cal.K}^{-1}.\text{mol}^{-1}.$$

Having established the extent of proton transfer in the transition states, one can now consider the changes in bond hybridisation that occur. Protonation of indoles results in a change of hybridisation from sp^2 to sp^3 at the 3-carbon atom, and consequently the extent of proton transfer and the hybridisation are closely related (Figure 2.9).

Figure 2.9 Transition state symmetry for indole hydrogen exchange.

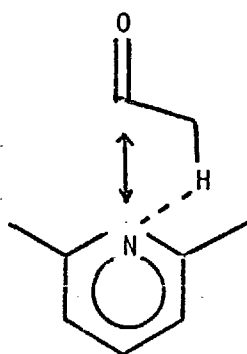


It can be seen from this figure that the smaller the angle ψ , the greater will be the peri interactions with a 4- or 2- substituent on the nucleus. This is the case for the indolyl anion reaction, with the result that substrate induced steric effects are observed.

This argument can be inverted to account for steric effects induced by the catalysing acid. The relatively early transition state for

2,6-dimethylpyridine acid catalysis means the hydrogen will still interact strongly with the ortho methyl groups, raising the energy of the transition state and inducing a steric effect. Gold⁶⁴ has suggested that one of the reasons for the large steric effects observed for this base in the ionisation of ketones is that overlap is possible between the π orbitals of the carbonyl group and the aromatic nitrogen. This fixed conformation results in an unfavourable interaction between the methyl groups and the transferring proton (Figure 2.10).

Figure 2.10



The fixed geometry of the indoles prevents this conformation from being adopted, but it is still possible that some π electron interactions may occur. For a late transition state, the proton is further away from the donating acid and will interact less with any substituents on the acid. The small steric effects obtained with 2,6 dimethyl piperidine could be explained on this simple basis, though as mentioned previously the steric interactions of this aliphatic base are not very well understood⁶⁵.

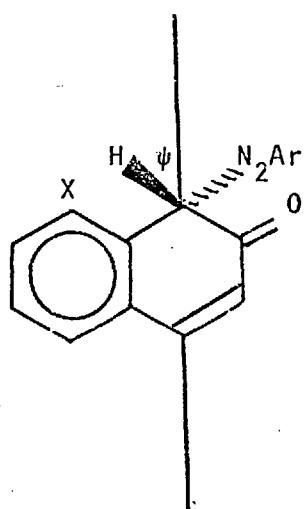
One can argue then, merely from a consideration of bond angles

that as the transition state for a proton transfer from an acid to a base becomes later, the steric influence of the acid will decrease and that of the base will increase.

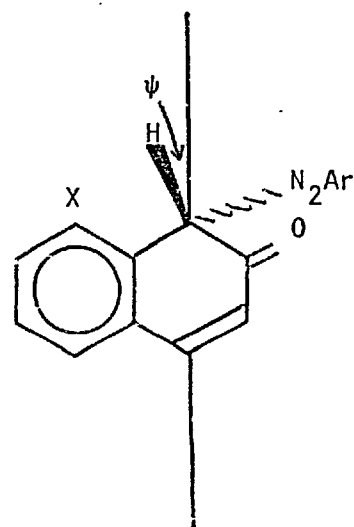
Another possibility which must be considered is that the overall dimensions of the transition state change. On this basis, one has to postulate a tight transition state for the indolyl anion reaction, and a 'loose' one for the neutral molecule reaction. This approach does leave several questions unanswered, such as the relative steric influence of 2,6-dimethylpyridine and piperidine.

These results for hydrogen exchange can be compared with the conclusions arrived at by Zollinger⁷⁰ from a study of diazocoupling reactions (Figure 2.11).

Figure 2.11 The symmetry of the σ intermediates in diazocoupling.



X = H, symmetric
 σ complex.

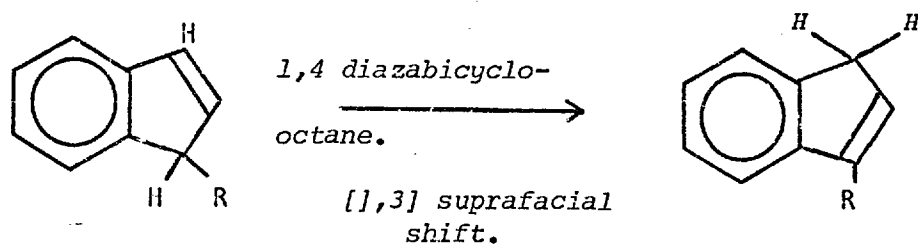


X = Bulky group,
asymmetric σ complex.

The steric interactions between the diazo group and the substituent X resulted in the diazo group moving out of the plane of the molecule, and bringing the hydrogen nearer to X. As a consequence a steric effect was observed for removal of the proton by a base. Thus, decrease in the angle ψ , resulting in steric effects, is common to both hydrogen exchange of indoles and diazocoupling of naphthols- but for different reasons.

Another reaction which appears to show this effect is the rearrangement of substituted indenenes⁷¹ (Figure 2.12) .

Figure 2.12 Rearrangement of 1- alkylindenenes.



The mechanism appears to involve a [1,3] suprafacial hydrogen transfer (via an ion pair intermediate ?) to give the more stable 3-alkylindene. The proton transfer is slow (as shown by a large deuterium isotope effect) and the rate was found to increase in the series $R = \text{Me}, \text{PhCH}_2, \text{Ph}_2\text{CH}$ but to decrease (> 30 fold) for $R = \text{Ph}_3\text{C}$. Though this is a real steric effect, it is not easy to

to interpret it in terms of transition state symmetry, due to the conformational complexity of the triphenylmethyl group.

2:11.1 CONCLUSIONS.

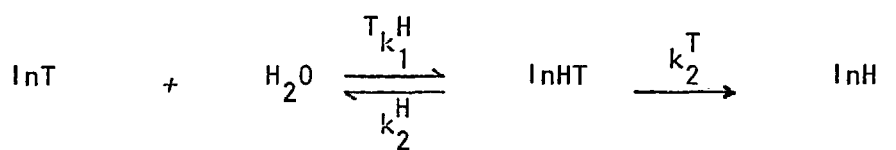
Several different methods have been used to show that the transition state for the hydrogen transfer reactions of indole and its conjugate base differ considerably in symmetry. One of these methods involved the observation of steric effects and it is suggested here that these can be used as a new index of transition state symmetry.

2.12 KINETIC ISOTOPE EFFECTS FOR AROMATIC HYDROGEN EXCHANGE.

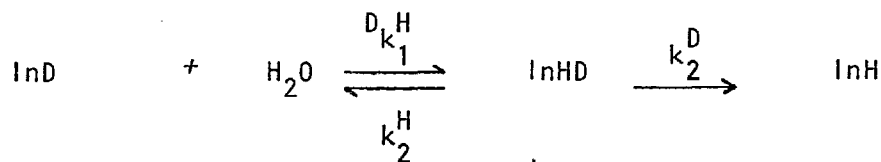
Four hydrogen exchange systems can be envisaged as being practical (Scheme 2.7), two involving loss of D and T to H₂O and two loss of T and H to D₂O. Two further permutations, loss of H and D to T₂O, are equilibrium processes and the kinetic analysis becomes too complex. There follows a brief elaboration of the methods used by Kresge^{48,49} and also a new method which involves no assumptions concerning the value of the Swain-Schaad exponent r. Since all isotopic rates were measured in pairs for the same solution it follows that the ratio of the observed first order rate constants equals the ratio of bimolecular constants (Equation 2.1).

$$k_o^{-L}/k_o^{-L'} = k_{bi}^{-L}/k_{bi}^{-L'}$$

Scheme 2.7 Possible hydrogen exchange systems for indoles.

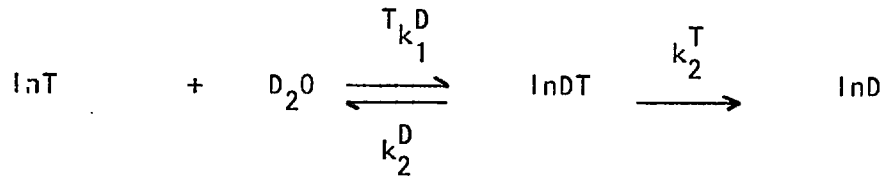


$$k_{bi}^{-\text{T}} = \frac{k_1^{\text{T,H}}}{1 + k_2^{\text{H}}/k_2^{\text{T}}} \quad 2.15$$

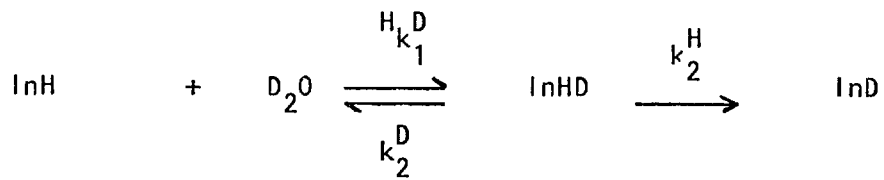


$$k_{bi}^{-\text{D}} = \frac{k_1^{\text{D,H}}}{1 + k_2^{\text{H}}/k_2^{\text{D}}} \quad 2.16$$

Scheme 2.7 Contd.



$$k_{bi}^T = \frac{k_1^T}{1 + k_2^D/k_2^T} \quad 2.17$$



$$k_{bi}^D = \frac{k_1^H}{1 + k_2^D/k_2^H} \quad 2.18$$

2.12.1 EVALUATION NEGLECTING SECONDARY ISOTOPE EFFECTS.

This method, used extensively by Challis³⁵, requires two approximations.

$$k_{k_1}^{T,H} = k_{k_1}^{D,H} \quad 2.19$$

$$(k_2^H/k_2^D)^{1.442} = k_2^H/k_2^T \quad 2.20$$

One defines the experimental ratio

$$k_o^{-D}/k_o^{-T} = k_{bi}^{-D}/k_{bi}^{-T} = a \quad 2.21$$

and the isotope effects

$$k_2^H/k_2^T = x \quad 2.22$$

$$k_2^H/k_2^D = y \quad 2.23$$

Dividing equation 2.16 by 2.15 one obtains

$$a = \frac{1 + y^{1.442}}{1 + y} \quad 2.24$$

In practice, equation 2.24 was solved for Y by the 'BFI' method of constructing by computer a matrix of values for a for all reasonable values of y, ranging from 1.0 to 50.0 in subdivisions of 0.1 . Equation 2.24 was also solved by rearranging to 2.25

$$y^{1.442} - a.y - a + 1 = 0 \quad 2.25$$

and solving by the Newtonian iteration method.

2.12.2 EVALUATION USING A THEORETICAL VALUE FOR THE SWAIN-SCHAAD EXPONENT⁴⁹.

Several slightly more sophisticated approximations are made.

$$\frac{D_{k_1}}{T_{k_1}} = \frac{H_{k_1} \cdot D_{k_1}}{T_{k_1} \cdot H_{k_1}} \quad 2.26$$

$$\left(\frac{H_{k_1}}{D_{k_1}} \right)^r = \frac{H_{k_1}}{T_{k_1}} \quad 2.27$$

Equation 2.27 implies that the Swain-Schaad relationship holds for secondary isotope effects. One defines \underline{a} , \underline{x} and y by equations 2.21, 2.22 and 2.23 and also

$$b = \frac{k_{bi}^D}{k_{bi}^T} = \frac{k_o^D}{k_o^T} \quad 2.28$$

Then

$$a = \frac{D, H}{T, H} k_1 \cdot \frac{1 + x}{1 + y} \quad 2.29$$

$$b = \frac{H, D}{T, D} k_1 \cdot \frac{1 + x/y}{1 + 1/y} \quad 2.30$$

It follows from equations 2.26 and 2.27 that

$$\frac{D, H}{T, H} k_1 = \left(\frac{H, D}{T, D} k_1 \right)^{r-1/r} \quad 2.31$$

and also replacing \underline{x} by $y^{1.442}$ and eliminating from equations 2.29 and 2.30 one obtains

$$\frac{a^{r/(r-1)}}{b} = \frac{\left(\frac{1 + y^r}{1 + y} \right)^{r/(r-1)}}{\frac{1 + y^{r-1}}{1 + 1/y}} \quad 2.32$$

This equation was solved by generating a matrix of values for $a^{r/(r-1)}/b$ for values of y from 1.0 to 50.0 in increments of 0.1; and generating one matrix each for values of r from 1.142 to 1.642 in increments of 0.05 .

2.12.3 EVALUATION ASSUMING EXPERIMENTAL VALUES FOR THE SECONDARY ISOTOPE EFFECTS.

In this treatment, the secondary isotope effects k_1^D/k_1^H and k_1^H/k_1^T were assumed to have the values evaluated by Kresge⁴⁹. Kresge evaluated these by assuming $r = 1.442$, and since this method is in fact designed to *evaluate* r , the argument could be accused of being cyclic. The justification put forward here is that secondary isotope effects in A-S_E2 reactions are probably fairly independent of the value taken for r , and moreover are probably not greatly influenced by tunnelling or transition state symmetry.

The data given by Kresge gives the following secondary isotope effects

$$k_1^D/k_1^H = 1.1751$$

$$k_1^H/k_1^T = 1.0476$$

and equations 2.29 and 2.30 therefore become

$$a' = a \cdot 1.0476 = \frac{1 + x}{1 + y} \quad 2.33$$

$$b' = b \cdot 1.1751 = \frac{1 + x/y}{1 + 1/y} \quad 2.34$$

solving for x and y we obtain

$$y = k_2^H/k_2^D = \frac{a' - 1 - b'}{b' - 1 - a'} \quad 2.35$$

$$x = k_2^H/k_2^T = \frac{1 - a' - b'}{b' - 1 - a'} \quad 2.36$$

$$w = k_2^D/k_2^T = \frac{1 - a' - b'}{a' - 1 - b'} \quad 2.37$$

where w has now been defined as the deuterium/tritium isotope effect.

From equations 2.15 and 2.17 one obtains

$$\frac{T_{k_1^H} / T_{k_1^D}}{k_o^T} = \frac{1 + x}{1 + x/y} \cdot \frac{k_o^{-T}}{k_o^T} \quad 2.38$$

and finally

$$r = \frac{\log x}{\log y} \quad 2.39$$

To test the accuracy of this new method, a complete error analysis was carried out. For a function $y = f(a,b)$ the propagation of error from \underline{a} and \underline{b} to y is given by

$$\sigma_y^2 = (\partial y / \partial a)^2 \sigma_a^2 + (\partial y / \partial b)^2 \sigma_b^2 \quad 2.40$$

where $\sigma_{a,b}$ & σ_y are the standard errors of a, b & y . Defining a, b and y as previously, it follows directly from equation 2.40 that

$$\sigma_y = \frac{2}{(b^1 - 1 - a^1)^2} (\sigma_{a^1}^2 + \sigma_{b^1}^2)^{\frac{1}{2}} \quad 2.41$$

$$\sigma_x = \frac{2}{(b^1 - 1 - a^1)^2} ([1 - b^1]^2 \cdot \sigma_{a^1}^2 + a^1 \cdot \sigma_{b^1}^2)^{\frac{1}{2}} \quad 2.42$$

$$\sigma_w = \frac{2}{(1 + b^1 - a^1)^2} (b^1 \cdot \sigma_{a^1}^2 + [1 - a^1]^2 \cdot \sigma_{b^1}^2)^{\frac{1}{2}} \quad 2.43$$

$$\sigma_r^2 = \frac{\sigma_x^2}{x^2 \cdot (\ln y)^2} + \frac{\sigma_y^2 \cdot (\ln x)^2}{y^2 \cdot (\ln y)^4} \quad 2.44$$

By assuming that $\sigma_a \approx \sigma_b$ and also taking the results given in Table 2.16 as typical values for \underline{a} and \underline{b} , equations 2.41 to 2.44 reduce to approximate forms

$$\sigma_y \approx 35 \sigma_{a/b} \quad 2.45$$

$$\sigma_x \approx 73 \sigma_{a/b} \quad 2.46$$

$$\sigma_w \approx 2 \sigma_{a/b} \quad 2.47$$

The error analysis was normally carried out using the rigorous equations 2.41 to 2.44 .

2.12.4 THE MAGNITUDE OF PRIMARY ISOTOPE EFFECTS FOR INDOLES.

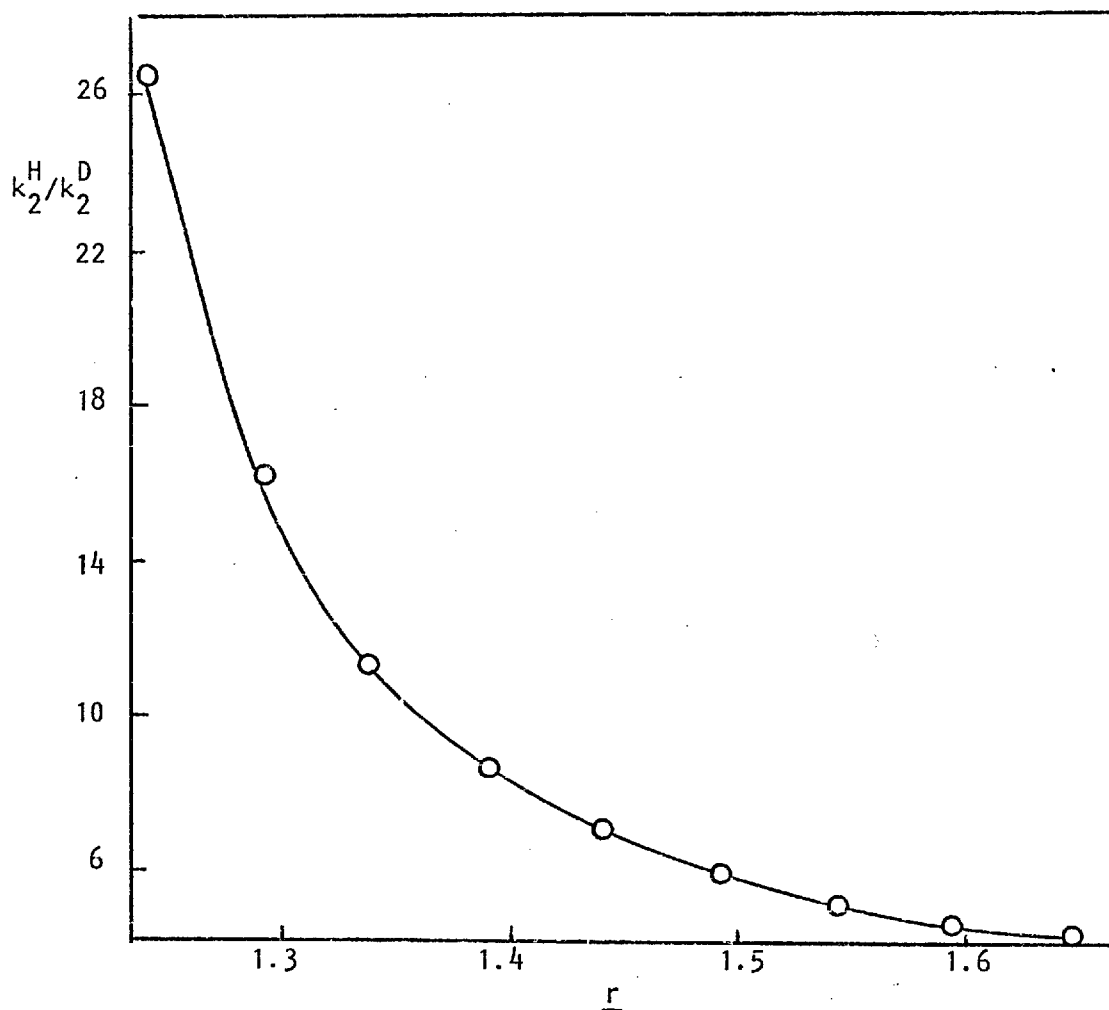
The experimental ratio k_o^{-D}/k_o^{-T} was measured for acetic acid and 2,6-dimethylpyridine (acid catalysed), and hydroxyl and 2,6-dimethylpiperidine (base catalysed) exchange of methylidibutyl indole (Tables 2.13, 2.14, 2.16, 2.17 respectively). The deuterium isotope effects were all evaluated by the method in Section 2.12.1 . For base catalysed reactions, a change in solvent from H_2O to D_2O results in a solvent isotope effect on the equilibrium constants that define the exchange rate (equation 2.3). The solvent ratio then becomes

$$\frac{k_o^{-T}}{k_o^T} = \frac{k_{bi}^{-T}}{k_{bi}^T} \cdot \frac{K_E(H_2O)}{K_E(D_2O)} \cdot \frac{K_{BD}}{K_{BH}} \quad 2.48$$

For catalysis by water, since K_E ($\sim 10^{-17}$) and K_{H_2O} ($\sim 10^{-16}$) are about equal, the solvent isotope effect may be expected to cancel and the ratio of k_o^{-L} will still represent the ratio of k_{bi}^{-L} . This approximation is probably still reasonably valid for dimethyl piperidine catalysis.

The primary deuterium isotope effects are all within the range 5.0 - 7.5, with a random distribution within these limits and it can be seen that changes in transition state symmetry and even the incidence of steric hindrance (where proton tunnelling should be particularly favourable) does not appreciably alter the magnitude of the isotope effect. This is in line with the similar observations made by Challis and Millar³⁵ for a range of substituted indoles.

The question arises whether this is a valid conclusion, or whether this invariance is some artifact specific to aromatic hydrogen exchange. One serious objection is that the value of the Swain-Schaad exponent is assumed to be constant and though Lewis⁴⁰ has shown that this constant is not affected by tunnelling in nitroalkane ionisation, this remains to be proved for aromatic hydrogen exchange. It is possible that \underline{r} may be reduced in magnitude by tunnelling⁴¹ and the serious implications of this will be illustrated by adopting the sophisticated method of analysis used by Kresge⁴⁹ to study the effect of variation in \underline{r} (Figure 2.13).

Figure 2.13 Variation in the isotope effect with the exponent \underline{r} 

The values given in Table 2.16 for \underline{a} and \underline{b} were used, and for a normal value for \underline{r} of 1.442, $k_2^H/k_2^D = 7.0$ which is very close to the range of values obtained by the simpler method. It can be seen from the figure that when a low value for \underline{r} is used a high value for the isotope effect is obtained and either (or both) of these observations would normally be cited as compelling evidence for tunnelling. Consequently this method of analysis can still lead to ambiguous values for the primary deuterium isotope effect.

Evidently an approach is needed where no *a priori* assumptions concerning \underline{r} are made, and this can only be done by assuming that secondary isotope effects are independent of tunnelling effects.

The results for hydroxyl catalysed exchange of methyldibutylindole were analysed by the method described in Section 2.12.3 (Table 2.16). An error of $\sigma_a = \pm 0.03$ and also $\sigma_b = \pm 0.06$ was used to obtain the following values.

$$k_2^H/k_2^D = 6.09 \pm 1.7 \text{ (28\%)}$$

$$k_2^D/k_2^T = 2.36 \pm 0.075 \text{ (3\%)}$$

$$k_2^H/k_2^T = 14.4 \pm 3.6 \text{ (25\%)}$$

$$\underline{r} = 1.474 \pm 0.266 \text{ (18\%)}$$

One first notes that again the deuterium isotope effect is within the range 5.0 - 7.5 observed for this indole, making use of the simplified calculational method, and this is a direct consequence of the value for \underline{r} being close to the Swain-Schaad value of 1.442 . The error in the value for the deuterium isotope effect is large, but it still allows us to say with some certainty that gross tunnelling effects such as are observed with nitroalkanes^{21,40} do not occur in this system. The large error in \underline{r} precludes any similar conclusions concerning this parameter. One can say that if \underline{r} is influenced by tunnelling effects it will not be possible to detect this in aromatic hydrogen exchange.

It is worth speculating whether an improvement in the accuracy of the data would lead to a meaningful value for \underline{r} . The reported data of Kresge⁴⁹ are analysed below as an example.

$$\begin{aligned} \text{Kresge gives } a' &= \frac{1.384 \pm 0.008}{0.620 \pm 0.005} \times 1.0476 \\ b' &= \frac{2.79 \pm 0.10}{1.048 \pm 0.002} \times 1.1751 \end{aligned}$$

Using equation 2.40 for the propagation of error in a quotient;

$$a' = 2.338 \pm 0.023, \quad b' = 3.128 \pm 0.013$$

and from these we obtain

$$y = 8.5 \pm 1.2$$

$$w = 2.50 \pm 0.04$$

$$x = 21.3 \pm 2.3$$

$$r = 1.428 \pm 0.108$$

It appears that even with highly accurate data, \underline{r} still has error limits which encompass the entire range normally allowable ($1.33 < \underline{r} < 1.55$)⁴¹.

More remarkable is that the error in k_2^D/k_2^T is about ten times less than the other isotopic rate ratios, and this is a direct consequence of $1 + b' - a'$ (equation 2.43) being many times larger than $b' - 1 - a'$ (equation 2.41). The conclusion is that if isotope effects are to be evaluated for an A-S_E2 reaction, the deuterium/tritium ratio should be selected. Whether this is significantly changed by tunnelling remains to be proven. It appears nevertheless that the value obtained for hydroxyl catalysed exchange of methyldibutylindole (2.36) is very close to the expected value of 2.26 - 2.34 as calculated from force constant data³¹, which further confirms the conclusion that tunnelling appears not to be important in these reactions.

2.12.5 CONCLUSIONS.

Accurate primary isotope effects are very difficult to obtain

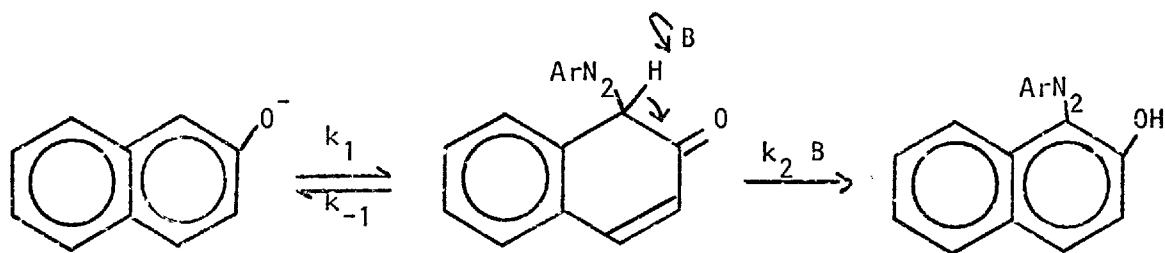
for aromatic $A-S_E2$ reactions without making several assumptions and approximations, which are most likely to be invalidated by tunnelling phenomena. The experimental isotope effects were found to be constant over a wide range of reactivity, and were not influenced by changes in transition state symmetry or steric effects in the hydrogen transfer. It is probable that any variation in the magnitude of isotope effects in aromatic hydrogen transfer reactions must be a result of tunnelling, and aromatic $A-S_E2$ reactions are not well suited to test this hypothesis since changes in the Swain-Schaad exponent ρ will offset any resultant changes in the isotope effects. The available results suggest that gross tunnelling effects as a result of steric hindrance in the transition state do not occur for indoles, and this may be a direct result of the very asymmetric potential barrier in this reaction, which does not favour tunnelling⁸ (see also section 5.9).

CHAPTER III

THE REACTION OF ARYLDIAZONIUM IONS WITH INDOLES

3.1 INTRODUCTION.

Aryl diazonium ions are mildly electrophilic reagents that substitute activated aromatic compounds. The mechanism of these reactions is well known - particularly as a result of the work of Zollinger⁶³, who established that coupling to naphthols occurs via an A-S_E2 mechanism (Scheme 3.1).



Scheme 3.1 A-S_E2 mechanism for diazocoupling.

The concentration of the intermediate σ complex was assumed to

constant and low, and application of steady state kinetics gives equation 3.1 .

$$- d[ArN_2^+]/dt = k_{bi}^{-L} [ArN_2^+]. [Substrate]$$

$$\text{where } k_{bi}^{-L} = k_1 / (1 + k_{-1}/k_2[B]) \quad 3.1$$

Zollinger in 1955⁶³ demonstrated that certain hindered naphthol sulphonic acids exhibit large primary deuterium isotope effects, which suggested that the ratio $k_{-1}/k_2[B]$ was larger than unity. If this is the case then equation 3.1 reduces to equation 3.2 .

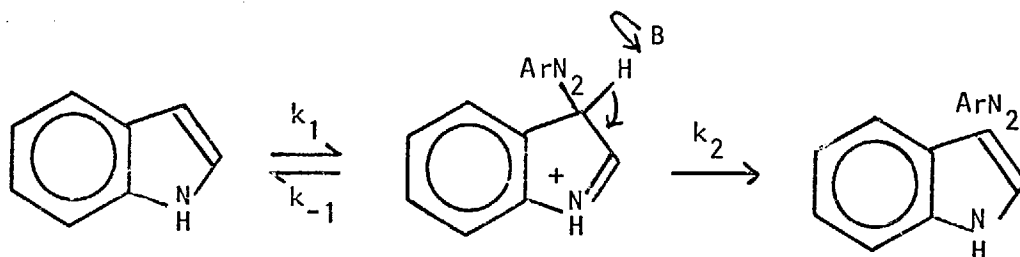
$$\text{Rate} = \frac{k_1 k_2}{k_{-1}} [ArN_2^+]. [Substrate]. [Base]. \quad 3.2$$

The rate is directly proportional to k_2 and a full isotope effect should be expected. This equation also involves the base concentration, and Zollinger was in fact able to observe general base catalysis, evaluating the value of k_{-1}/k_2 by suitable treatment of the data according to equation 3.1 .

Reactions such as nitrosation⁷² have shown that electrophilic substitution of indoles is fairly analogous to naphthols, and the general mechanism is expected to be similar (Scheme 3.2).

There has been one initial study of this reaction by Ridd⁶⁷. Only a reactive diazonium ion such as the p-nitro derivative gave good yields and simple first order kinetics on reaction with indole, and then only over a limited range of pH. Less reactive diazonium

Scheme 3.2 Diazocoupling of indoles.



ions gave low yields of the azoproduct and the kinetics exhibited induction periods. There have been recent reports that a 2-3 migration on the indole nucleus can occur, particularly with alkyl groups such as PhCH_2 ^{73a} and the diazo group itself,^{73b,c} which may account for the complex kinetic behaviour observed by Ridd⁶⁷. A further complication is that indoles with no 2- substituent are known to undergo an acid catalysed dimerisation and trimerisation reaction⁵⁰. Both these problems should be solved by substituting the 2- position of the indole and accordingly 2-methylindole was selected as a suitable substrate.

Interest in these reactions lies in the deuterium isotope effects. Zollinger³⁶ has reported an initial study of some naphthol sulphonic acids where variation in the magnitude of the isotope effect was observed with the strength of the base (equation 3.2), and indoles appear a suitable system to study this phenomenon further. Ridd⁶⁷ however, has reported an isotope effect of unity for indole itself and further verification of the coupling mechanism is evidently required in order to rationalise this result.

RESULTS

3.2 REACTION OF ARYLDIAZONIUM IONS WITH 2-METHYLINDOLE.

Reaction of 2-methylindole (MI) and p-methylbenzenediazonium chloride or tetrafluoroborate in dilute (kinetic) or more concentrated preparative solutions gave only one major product which was characterised as the 3-substituted azo compound. At pH > 4 this product could be estimated by U.V. spectroscopy at 380 nm, whereas at pH < 3 the azo indole exists as the N-protonated conjugate acid ($\lambda_{\text{max}} \approx 440 \text{ nm}$) and indeed when prepared in an aprotic medium the solid salt is isolated.

Comparison of the U.V. extinction coefficient with that of a purified sample showed that coupling is quantitative (>95%) between pH \sim -1 to 7 in 20% (v/v) dioxan at 25°C. At a higher pH however the yield with the p-methylbenzenediazonium ion dropped to about 50%. There has been a recent report that diazocoupling may partially proceed by a homolytic pathway^{74a} and indoles are known to be particularly prone to radical oxidation reactions^{74b,c}. Zollinger⁷⁵ has shown that electron withdrawing substituents such as p-nitro on the diazonium ion promote the homolytic pathway, particularly in the presence of a base such as pyridine and accordingly one may expect electron donating substituents to decrease homolysis. This was observed in practice, when use of p-methoxybenzenediazonium salts gave improved yields ($\sim 80\%$) up to about pH 11, and these salts were used at this pH.

3.2.1 VERIFICATION OF RATE ORDER.

The A-S_E2 mechanism requires that the rate of coupling at constant pH follows equation 3.3.

$$d[\text{Product}]/dt = \bar{k}_{bi} \cdot (\text{Indole}) \cdot [\text{ArN}_2^+] \quad 3.3^{**}$$

In the region pH 1-7, (Indole) = [InH] and $\bar{k}_{bi} = k_{bi}$ (equation 3.1).

Pseudo first order rate constants were obtained for the coupling, using a constant excess of indole, when equation 3.4 applies.

$$\text{Rate} = k_o [\text{ArN}_2^+] \quad 3.4$$

And from equation 3.3,

$$\bar{k}_{bi} = k_o / (\text{Indole}) \quad 3.5$$

Results are presented in Table 3.1 which show that \bar{k}_{bi} is constant for a range of indole concentration and the intercept is effectively zero (Figure 3.1). One run was carried out using equimolar concentrations of both substrates and the rate constant obtained agreed well with the

** *Stoichiometric reactant concentrations are denoted by terms in round brackets and actual concentrations by terms in the usual square brackets. Differences in the two concentrations are significant for the indoles because of prototropic equilibria, the various substrate species being denoted by InH, InH₂⁺ and In⁻ for the neutral species, its conjugate acid and base respectively, with (Indole) representing the concentration of all three. Rate coefficients dependent on the stoichiometric concentration are denoted with a superscript bar.*

TABLE 3.1 Diazodeprotonation of 2-methylindole in 20%(v/v) aqueous dioxan at 27.5°C.

Initial $[p\text{MeArN}_2^+\text{Cl}^-] = 10^{-4}\text{M}$. $[\text{KH phthalate}] = 0.04$, $\text{pH} = 3.5 \pm .3$

$10^3 [\text{InH}]/\text{M}$.	$10^3 k_o/s^{-1}$.	$\bar{k}_{bi}/s^{-1} \cdot \text{M}^{-1}$.
5.5	11.5	2.09
4.0	8.16	2.08
3.0	6.45	2.14
2.0	4.20	2.10
1.4	3.03	2.16
0.5	0.97	1.95
0.25 ^a	0.52	2.08
0.1 ^b	-	1.9
1.0 ^c	1.58	1.58
0.1 ^d	-	1.55

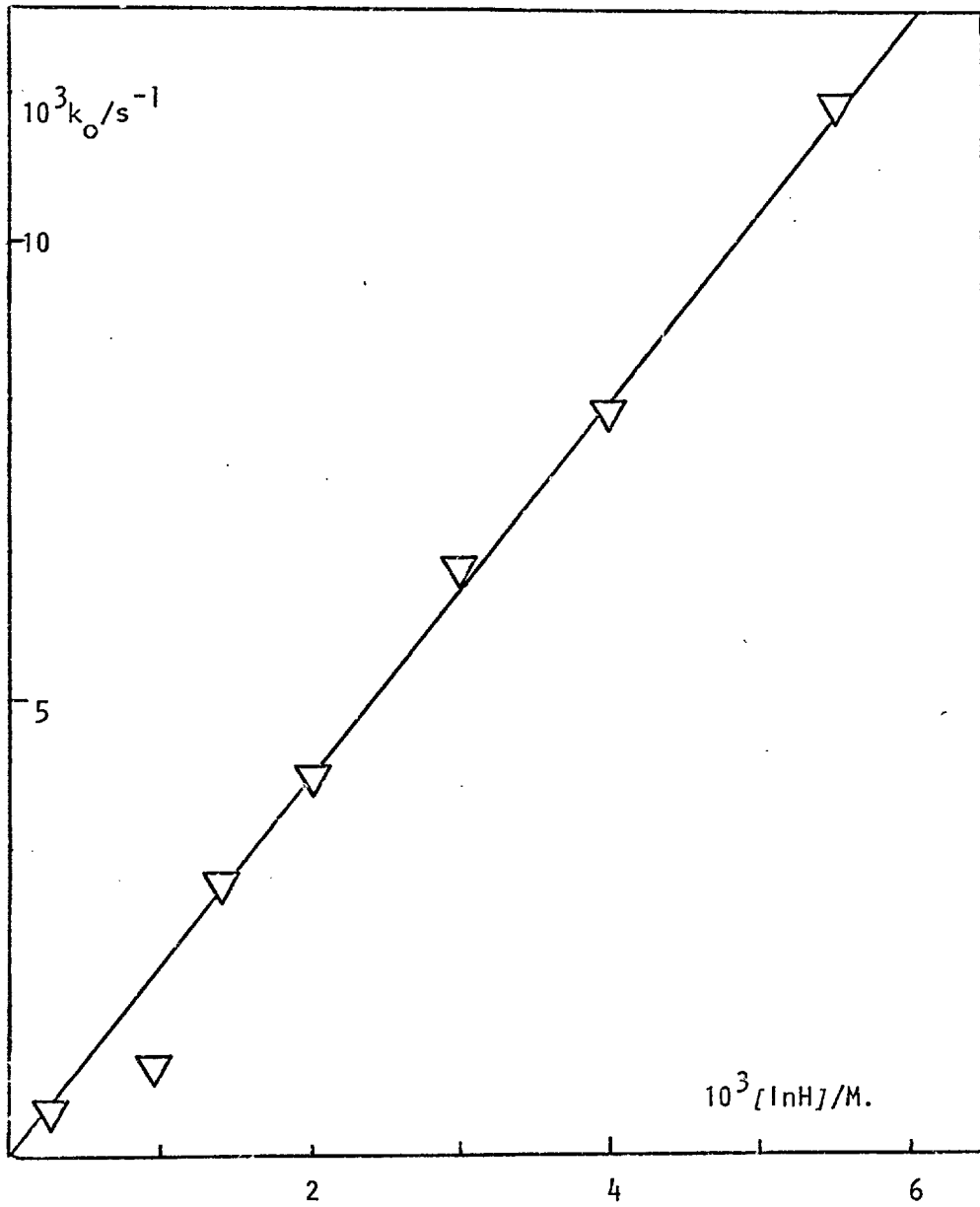
^a $[p\text{-MeArN}_2^+\text{Cl}^-] = 2.5 \times 10^{-5}$

^b Equimolar concentrations

^c Followed by R-salt method, 0% dioxan

^d Equimolar concentration, R-salt method, 0% dioxan.

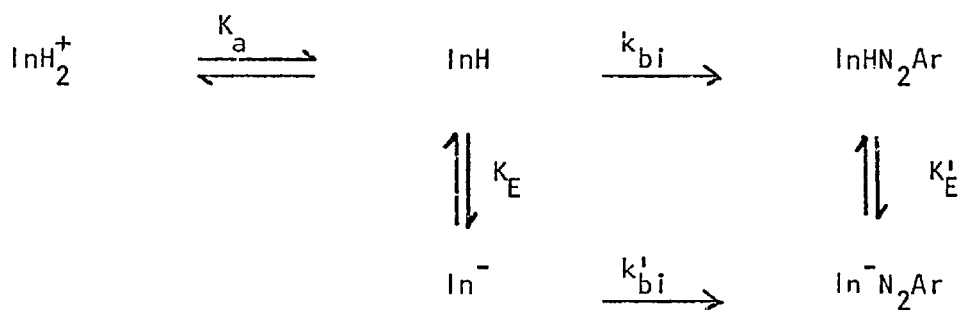
Figure 3.1 Diazodeprotonation of 2-methylindole in 20%(v/v) dioxan at 27.5°C.



previous determinations. Though the majority of the kinetics were followed by monitoring the appearance of product, several runs were carried out by measuring the concentration of diazonium ion by coupling with 'R-salt'. Aqueous solutions were used, since there was no need to promote the solubility of the product, and the results suggest there is only a small effect on changing the solvent (Table 3.1).

3.2.2 ACIDITY DEPENDENCE OF THE COUPLING RATE.

Because 2-methylindole is both a weak base ($pK_a = -0.3$)⁵⁹ and a weak acid ($pK_E = 16.95$)⁶⁶ it was expected that \bar{k}_{bi} would be acidity dependent. Further, both the neutral indole and its conjugate base, but not the conjugate acid, would be expected to react with diazonium ions under the appropriate conditions. The potential pathways to product, allowing for prototropic equilibria, are given in Scheme 3.3.



Scheme 3.3 Prototropic equilibria in diazocoupling.

Equation 3.6 relates the stoichiometric rate constant \bar{k}_{bi} to the molecular rate constant for reaction via the neutral molecule (k_{bi}) and the indole anion (k'_{bi}).

$$\bar{k}_{bi} = \frac{k_{bi} + k'_{bi} (K_E/[H^+])}{[H^+]/K_a + 1 + K_E/[H^+]} \quad 3.6$$

The relevant constants of equation 3.6 have to be evaluated under limiting conditions. At pH < 9, reaction via the indole anion is negligible since $[H^+] \gg K_E$ and equation 3.6 reduces to equation 3.7 .

$$[H_3O^+] = \frac{k_{bi}}{\bar{k}_{bi}} \cdot K_a - K_a \quad 3.7$$

The rate of coupling was measured at high acidity (Table 3.2) and a plot of $[H_3O^+]$ against $1/\bar{k}_{bi}$ (Figure 3.2) gives a straight line, which curves at high acidity since $[H_3O^+]$ no longer represents the effective acidity of the medium and an h_1 function needs to be used⁵⁹. The value obtained for the pK_a of the indole was - 0.14 at an ionic strength of 2.0 , which compares well with the value reported by Hinman and Lang (- 0.3, $I=0.0$ in H_2O)⁵⁹.

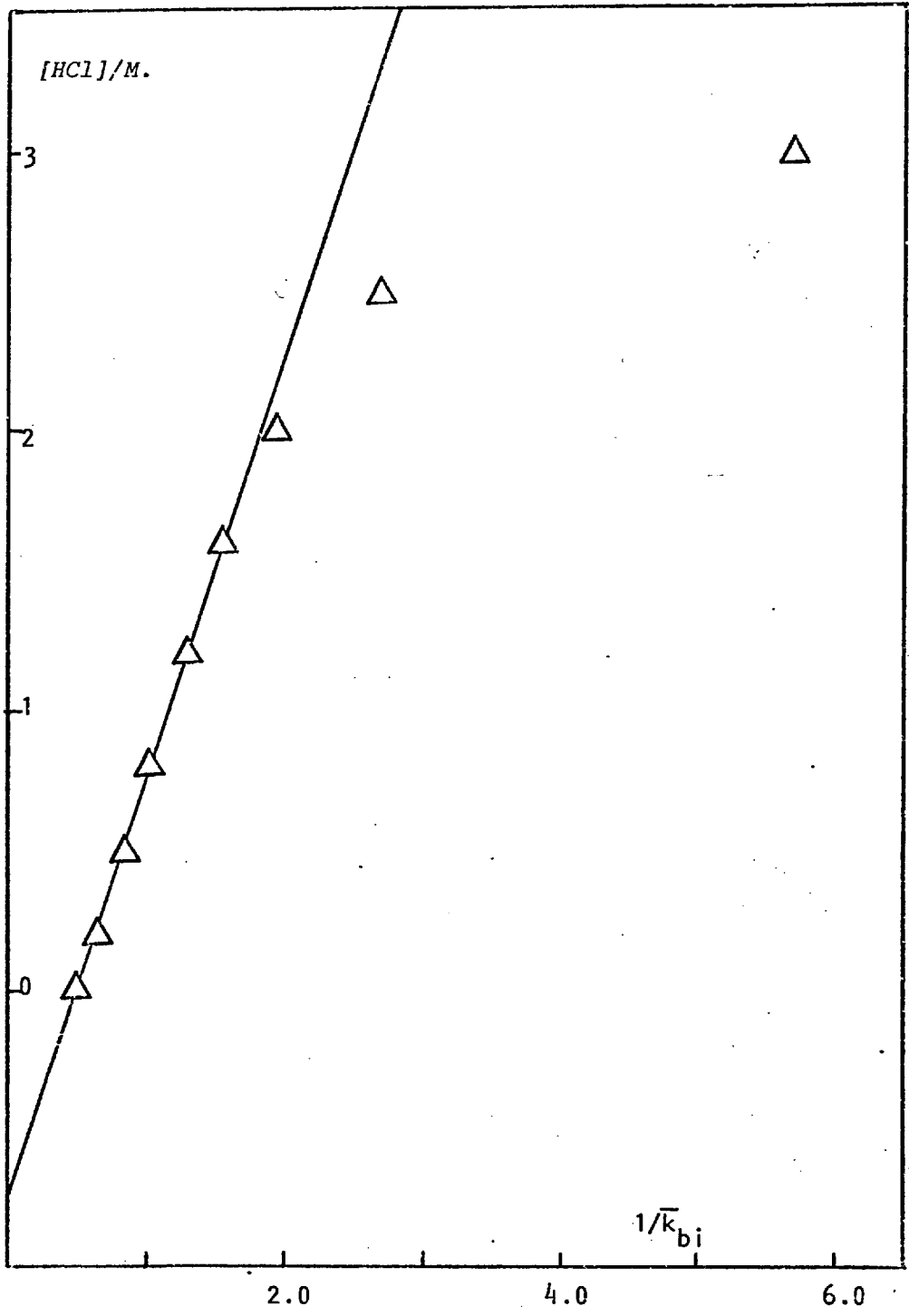
In mildly alkaline solution ($12 > \text{pH} > 9$) reaction via the indolyl anion becomes important, despite its low concentration. Here, $K_E \ll [H_3O^+]$ and $K_a \gg [H_3O^+]$ and equation 3.6 reduces to

TABLE 3.2 Diazodeprotonation of 2-methylindole in acidic solutions at 25°C and $I = 2.0$.

Initial $[p\text{-MeArN}_2^+] = 10^{-4} M$. $[\text{Indole}] = 1.5 \times 10^{-3} M$.

$\bar{k}_{di}/s^{-1} \cdot M^{-1}$	$1/\bar{k}_{di}$	$[\text{HCl}]/M$
2.0	0.50	0.0
1.54	0.65	0.2
1.16	0.86	0.5
0.98	1.02	0.8
0.75	1.33	1.2
0.65	1.54	1.6
0.52	1.95	2.0
0.49	2.04	2.25
0.37	2.70	2.5
0.18	5.66	3.0

Figure 3.2 Acidity dependence on the rate of diazodeprotonation of 2-methylindole at 25°C.



$$\bar{k}_{bi} = k_{bi} + k'_{bi} \cdot K_E / [H_3O^+] \quad 3.8$$

The study of rates in this region was possible only with p-methoxy benzenediazonium salts, and results for 2-methylindole are shown in Table 3.3 and Figure 3.3. The slope enables the product $k'_{bi} \cdot K_E$ to be evaluated as $\sim 7 \times 10^{-10} \text{ s}^{-1}$. An approximate value for K_E is 10^{-17} , which strictly was determined in purely aqueous solution⁶⁶ for indole itself, and we have assumed here that the effect of a 2-methyl group will be small.^{35a} This leads to a value of $\sim 7 \times 10^7 \text{ s}^{-1} \text{ M}^{-1}$ for k'_{bi} and the ratio $k'_{bi}/k_{bi} \sim 2 \times 10^8$, which compares well with about 10^8 found for the naphtholate/naphthol ratio⁷⁶ and about 10^7 for aromatic hydrogen exchange (Section 2.10.2). This high value for k'_{bi} is only about 100 fold less than for a diffusion controlled reaction.

There are precedents for this type of acidity dependence. For example, mono- and di-alkyl-N-anilines show a similar decrease in the rate of coupling as they become protonated,⁷⁷ and the coupling to 2-amino-5-hydroxy naphthol over a wide range of acidity gave a rate profile similar to that observed for indoles, coupling of the neutral and anionic species only occurring⁷⁸. No isotope effect for any of these reactions has been reported.

It should be noted that the pH of the reaction medium could not be raised much above about 12 since benzene diazohydroxide and diazotate are formed in this region at a detectable rate.⁷⁹

TABLE 3.3 Diazodeprotonation of 2-methylindole in 20%(v/v) dioxan at high pH and 25°C.

Initial $[p\text{-MeOArN}_2^+] = 10^{-4}M$. $[\text{Indole}] = 10^{-3}M$. $[\text{Borate}] = 0.02M$.

pH_{obs}	$10^{-10}/[H_3O^+]/M^{-1}$.	$\bar{k}_{bi}/s^{-1}.M^{-1}$.
3.2	0	0.38
9.05	0.11	1.26
9.65	0.45	3.35
9.81	0.645	5.56
10.20	1.59	11.6

$$k'_{bi} \cdot K_E = 7 \times 10^{-10} s^{-1}.$$

TABLE 3.4 Activation parameters for diazodeprotonation of 2-methylindole in aqueous solutions.

Initial $[p\text{-MeArN}_2^+] = 10^{-4}M$. $[\text{Indole}] = 10^{-3}M$. $pH = 3.0 \pm 0.05$

$T/^\circ C$.	$\bar{k}_{bi}/s^{-1}.M^{-1}$.
0	0.365
5	0.508
10	0.679
17.5	1.05
25	1.54
30	2.15
35.4	3.22

Figure 3.3 The rate of diazodeprotonation of 2-methylindole with p-methoxybenzenediazonium ion at high pH.

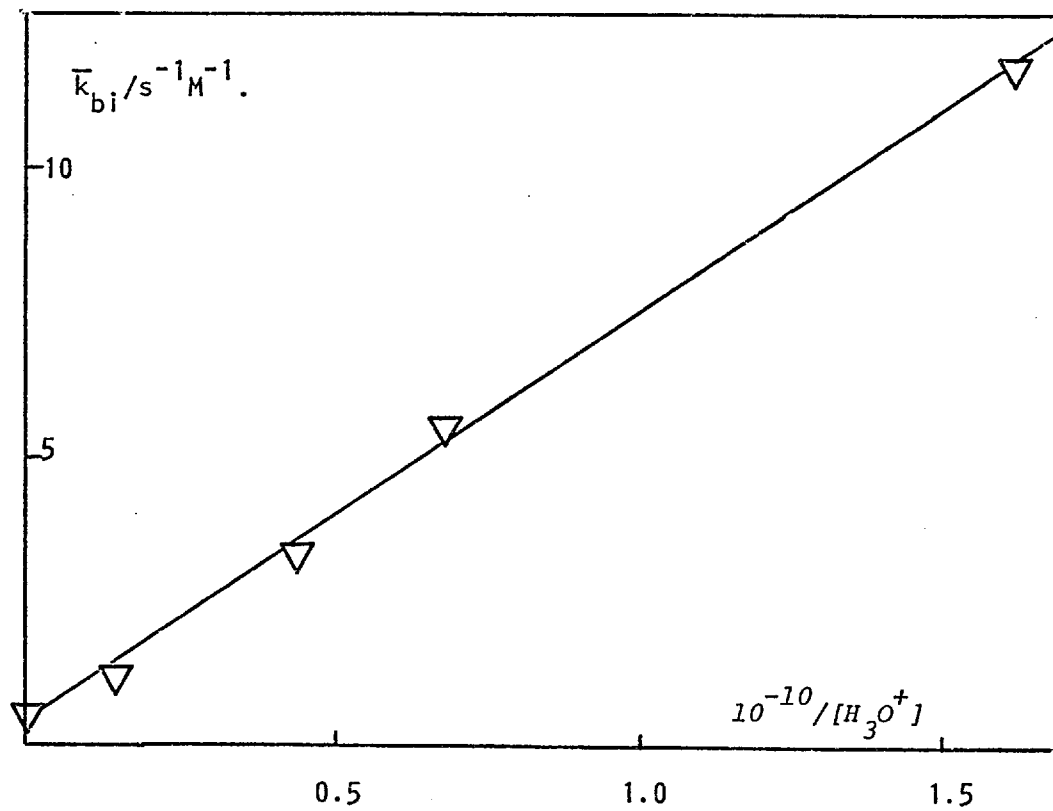
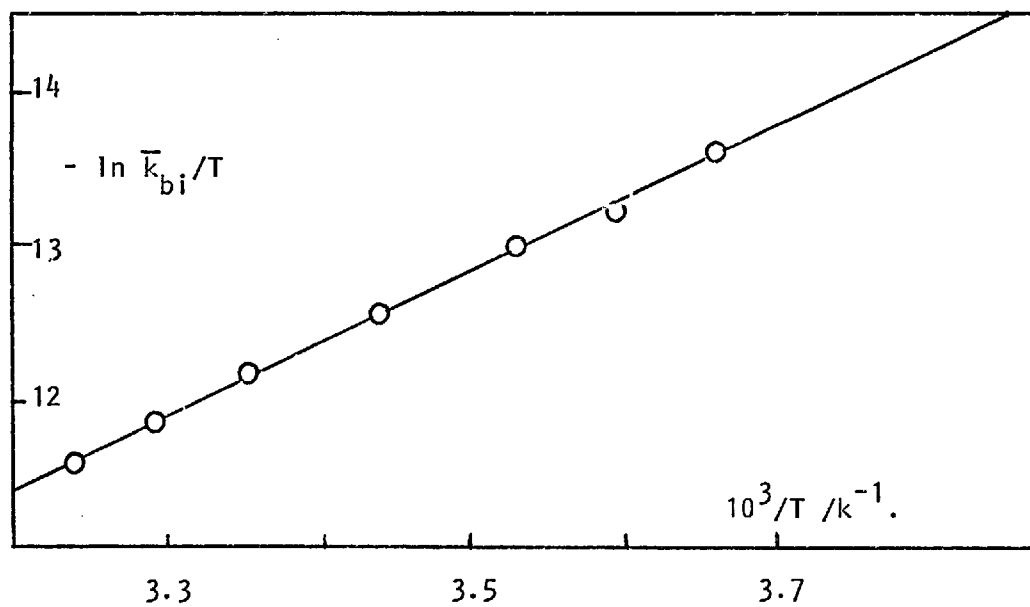


Figure 3.4 Temperature dependence of the rate of diazodeprotonation of 2-methylindole.



3.2.3 DEUTERIUM ISOTOPE EFFECTS.

The two rate constants k_{bi}^{-D} and $k_{bi}^{\prime-D}$ were evaluated for 2-methyl indole in the manner described in the previous section. Isotopic rate ratios for coupling of the neutral indole (k_{bi}^{-H}/k_{bi}^{-D}) and the anion ($k_{bi}^{\prime-H}/k_{bi}^{\prime-D}$) were both found to be 1.0 ± 0.2 , showing the same behaviour as indole⁶⁷. Also the ratio (k_{bi}^{-H}/k_{bi}^{-T}) was evaluated by simultaneously monitoring the rate of coupling by U.V. (to give k_{bi}^{-H}) and the rate of loss of tritium from the 3-position (which gives k_{bi}^{-T} when the rate of general acid/base catalysed detritiation is subtracted). This ratio agreed with the deuterium isotope effect, being 0.96 ± 0.1 (section 6.2.4).

3.2.4 ACTIVATION PARAMETERS.

The isotope effects of unity suggest that $k_{-1}/k_2[B] < 1$ (equation 3.1) and consequently $\bar{k}_{bi} = k_1$. The bimolecular rate constant was measured at several different temperatures, at pH 3 when $\bar{k}_{bi} = k_{bi} = k_1$ (Table 3.4). The data was plotted according to equation 3.9 and a straight line was obtained (Figure 3.4) from which the activation parameters were obtained.

$$\ln k_{bi}/T = 23.76 + \frac{\Delta S^\ddagger}{R} - \frac{\Delta H^\ddagger}{RT} \quad 3.9$$

$$\Delta H^\ddagger = 9.1 \text{ kcal.mol}^{-1}.$$

$$\Delta S^\ddagger = -33 \text{ cal.K}^{-1}.\text{mol}^{-1}.$$

3.2.5 LINEAR FREE ENERGY RELATIONSHIPS.

The rate of coupling is influenced by the reactivity of both the indole and the electrophile. Whereas little experimental results have been reported for the former⁸⁰, there are several examples of the latter in the literature^{76,77} for substrates such as methylaniline.

Coupling to 2-methylindole using a variety of substituted diazonium ions is summarised in Table 3.5. Application of the Hammett relationship (equation 3.10) using σ_p^+ for the substituent constant

$$\log \frac{k_{bi}(X)}{k_{bi}(H)} = \rho \cdot \sigma_p^+ \quad 3.10$$

gives the value $\rho = 3.3$ (Figure 3.5). This compares with $\rho = 4.0$ obtained by Sterba for coupling to N-methylaniline^{77a}. N- coupling also occurs for this substrate, with the same reaction constant but at a rate about 20 times greater than C- coupling. This was ascribed to the greater kinetic basicity of the amino group, and the slowness of the acid catalysed decomposition of the N- coupled triazine. At low pH triazine formation is reversible and the thermodynamically more stable C- product is formed.

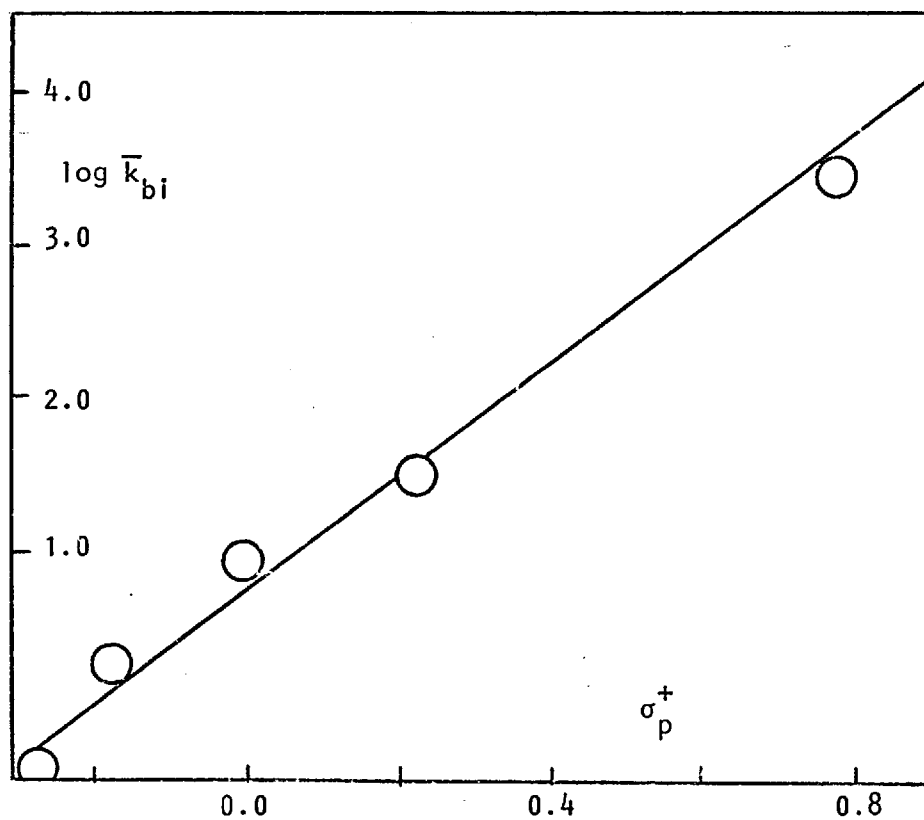
The 3- position in indoles is considerably more basic than the nitrogen, which is not the case for methylaniline and for neutral indoles at least N- coupling is probably not significant. This is confirmed by the observation that the rate of 3-³H₁ loss is equal to the rate of azoindole product formation (assuming the N- triazine would have a similar U.V. spectrum). If appreciable N- product were formed, then 3-³H₁ loss would be slower than the U.V. coupling rate. Slow N- coupling followed by a fast [1,3] sigmatropic

TABLE 3.5 The rate of coupling of 2-methylindole with p-substituted benzenediazonium ions in 20%(v/v) aqueous dioxan at 25°C.

<i>Substituent</i>	$\bar{k}_{bi}/s^{-1}.M^{-1}$	σ_p^+
MeO	0.37	- 0.27
Me	1.8	- 0.17
H	9.2	0.0
Cl	31	0.23
NO ₂ ^a	2700	0.78

^a Extrapolated to 25°C from 3°C using the activation parameters in Table 3.4

Figure 3.5 Hammett σ_p plot for the reaction of 2-methylindole with p-substituted benzenediazonium ions.



rearrangement would be ruled out on symmetry grounds and the dissociative mechanism⁷¹ is equivalent to direct C- coupling.

Coupling via the indolyl anion would favour a greater extent of N- coupling due to the greater nitrogen basicity and the greater stability of the triazine. Product analysis (tlc + U.V.) failed to detect any N- coupled product and it seems likely that only a small percentage of the reaction goes through N- coupling. Subsequent homolysis of the N-N bond would explain the poor yields observed at high pH^{73,75}.

3.3 DIAZOCOUPLING IN APROTIC SOLVENTS.

As discussed previously, to observe a deuterium isotope effect the ratio $k_{-1}/k_2[B] > 1$. This can be accomplished by either increasing k_{-1} or decreasing either k_2 or $[B]$. The base in this case is evidently water and one can reduce its concentration by using aprotic solvents.

Precedent for using such solvents was established by Messmer⁸¹ and Zollinger⁸². Zollinger reported coupling to dimethylaniline in numerous aprotic solvents, but was concerned mainly with the influence of solvent on the reaction rate. No verification of rate order was made and isotope effects were not studied. Messmer⁸¹, in a communication which has never been elaborated on, stated that in nitrobenzene several anilines and naphthylamines exhibit 3rd order kinetics when coupling with p-methylbenzenediazonium salts. In all but one case (m-toluidine) primary deuterium isotope effects were

observed. Third order kinetics would arise if the aniline itself were the base that removes the proton from the σ intermediate (equation 3.12).

$$\text{Thus rate} = \frac{k_1 [\text{Aniline}] \cdot [\text{ArN}_2^+]}{1 + k_{-1}/k_2 [\text{Aniline}]} \quad 3.11$$

If $k_{-1}/k_2 [\text{Aniline}] > 1$ then

$$\text{rate} = \frac{k_1 \cdot k_2}{k_{-1}} [\text{Aniline}]^2 [\text{ArN}_2^+] \quad 3.12$$

Since the rate in equation 3.12 is directly proportional to k_2 this implies that deuterium isotope effects must be observed. The lack of an isotope effect for *m*-toluidine does not conform with this.

To increase the probability of observing an isotope effect the hindered 2-t butyl-4-methylindole was studied in acetonitrile, nitromethane and nitrobenzene (Table 3.6). This should have the effect not only of decreasing H_2O , but also k_2 through steric hindrance to removal of the proton. Reasonable yields were obtained in these solvents, but the reactions gave only moderate first order plots. The results are sufficiently accurate to show that third order kinetics are not obtained, the order in the indole being unity.

Deuterium isotope effects were measured in acetonitrile and nitrobenzene, however difficulty was experienced with hydrogen exchange between the solvent and substrate. The relatively acidic medium ($\sim 10^{-4} \text{M HBF}_4$) and traces of residual water not removed by purification ($\sim 10^{-2} \text{M}$, 0.02% w/w) means the rate of hydrogen exchange is of the same order as diazocoupling. Increasing the indole concentration increases the latter without increasing the former and small isotope

TABLE 3.6 Diazocoupling of 2-t-butyl-4-methylindole in aprotic solvents at 25°C.

Initial $[p\text{-MeArN}_2^+] = 10^{-4} M$. Followed at 470 nm.

Solvent	$10^2 [\text{Indole}]/M$.	$\bar{k}_{bi}/s^{-1} \cdot M^{-1}$.
Acetonitrile	0.4	0.15
	1.2	0.16
	2.0	0.16
	4.0	0.18
Nitromethane	0.6	0.12
	0.6*	0.12
	1.0	0.18
	2.0	0.13
	4.0	0.13
	4.0*	0.076
Nitrobenzene	4.0	0.14
	4.0*	0.06
Water	-	0.68

* Rate for 3-²H₁ indole.

were then observed. The isotope effect for coupling in aqueous solution was found to be 1.0 (Table 3.7). This result does suggest that water acts as a fairly efficient base in protic media.

3.4 COUPLING TO STERICALLY HINDERED INDOLES.

The 4- position in indoles is equivalent to the peri (8) position in naphthols, where introduction of bulky groups has led to the observation of steric effects⁷⁰. Indoles have the further advantage that a bulky group in the 2-position can be introduced. The effect of sterically hindering the removal of the proton by introducing bulky 2- and 4- substituents was therefore investigated.

Another approach, which involved using sterically hindered diazonium ions was eliminated when instant loss of nitrogen was observed on attempted diazotisation of 2,6-diethylaniline⁸³. The results for two indoles are given in Table 3.7. Several points are worth emphasizing.

- a) Replacement of 2-methyl by 2-^tbutyl slows the rate of diazo-coupling by about 2. This is slightly greater than the value for protodetritiation of these two substrates (1.2)⁵⁵ which is a result of the greater selectivity of the diazonium ion as an electrophile⁸⁰. In both cases the rate difference is due to the greater basicity of 2-methylindole⁵⁵.
- b) Addition of a 4-methyl group to 2-^tbutylindole has no significant effect on the rate of coupling. One might expect a 4-methyl substituent to increase the basicity of the indole only slightly and the observed rates are consistent with there being no steric effect.
- c) The deuterium isotope effect for both indoles was found to be 1.0 ± 0.2 .

TABLE 3.7 Diazocoupling of hindered indoles in aqueous solutions at 25°C.

Initial $[ArN_2^+] = 10^{-4} M$. (Indole) = $10^{-3} M$. pH = 4.0 ± 0.6

Indole	Method	% dioxan	$\bar{k}_{bi}/s^{-1} \cdot M^{-1}$
2-Bu ^t	376nm	20	0.750
2-Bu ^t	376nm	20	0.792
2-Bu ^t	R-Salt	8	0.811
2-Bu ^t	380nm	20	0.188 ^a
2-Bu ^t -3- ² H ₁	376nm	20	0.790
2-Bu ^t -3- ² H ₁	376nm	20	0.823
2-Bu ^t -4-Me	384nm	40	0.737 ^b
2-Bu ^t -4-Me	384nm	40	0.677
2-Bu ^t -4-Me-3- ² H ₁	384nm	40	0.651
2-Bu ^t -4-Me-3- ² H ₁	384nm	40	0.683

^a Using $p-MeOArN_2^+$, all the other runs refer to $p-MeArN_2^+$.

^b (Indole) = $2 \times 10^{-3} M$.

3.5 REACTION OF ARYLDIAZONIUM IONS WITH 2-METHYL-4,6-DI-t BUTYL INDOLE.

The kinetic form of the reaction with methyldibutylindole was verified by coupling under pseudo first order conditions with an excess of either the indole or the diazonium ion (Table 3.8). Yields of azo-product were normally better than 90% irrespective of the relative reactant concentrations. With excess indole this behaviour prevailed up to about pH 11, whereas excess diazonium ion induced rapid autocatalytic decomposition of the product above pH 9. The second order rate constants obtained by either method are in reasonable agreement and the forward rate (k_1 , equation 3.1), after correction for the value of the denominator in equation 3.1, (section 3.6.1) is a factor of 12 greater than the rate for 2-methylindole. This is due entirely to the increased basicity of the molecule (Table 2.25).

3.5.1 ACIDITY DEPENDENCE OF THE COUPLING RATE.

The rate of coupling over a range of acidity was studied in manner analogous to 2-methylindole. The data obtained in acidic solution fit equation 3.7 fairly well (Figure 3.6), however the pK_a obtained from the slope (+ 0.6) and from the intercept (+ 0.1) do not agree very well. This is probably because protonation of this butylindole does not follow the usual indole acidity function of Hinman and Lang⁵⁹. These kinetic results, summarised in Table 3.9, do show qualitatively that methyldibutylindole is more basic than methylindole itself.

TABLE 3.8 Kinetic rate order for diazodeprotonation of 2-methyl-4,6-di-t butylindole in 40%(v/v) aqueous dioxan at pH 4 and 25°C.

$10^5 [\text{Indole}]/M.$	$10^5 [p\text{-MeOArN}_2^+]/M.$	$10^3 k_o/s^{-1}$	$\bar{k}_{bi}/s^{-1} \cdot M^{-1}$
40	4	1.33	3.3
40	4	1.28	3.2
80	4	2.46	3.1
4	35	1.19	3.4
4	70	2.28	3.3
4	140	4.51	3.2
100*	10	.36	.36

*Rate for 2-methylindole.

Figure 3.6 Diazodeprotonation of 2-methyl-4,6-di^tbutylindole in 4%(v/v) aqueous dioxan/sulphuric acid solutions.

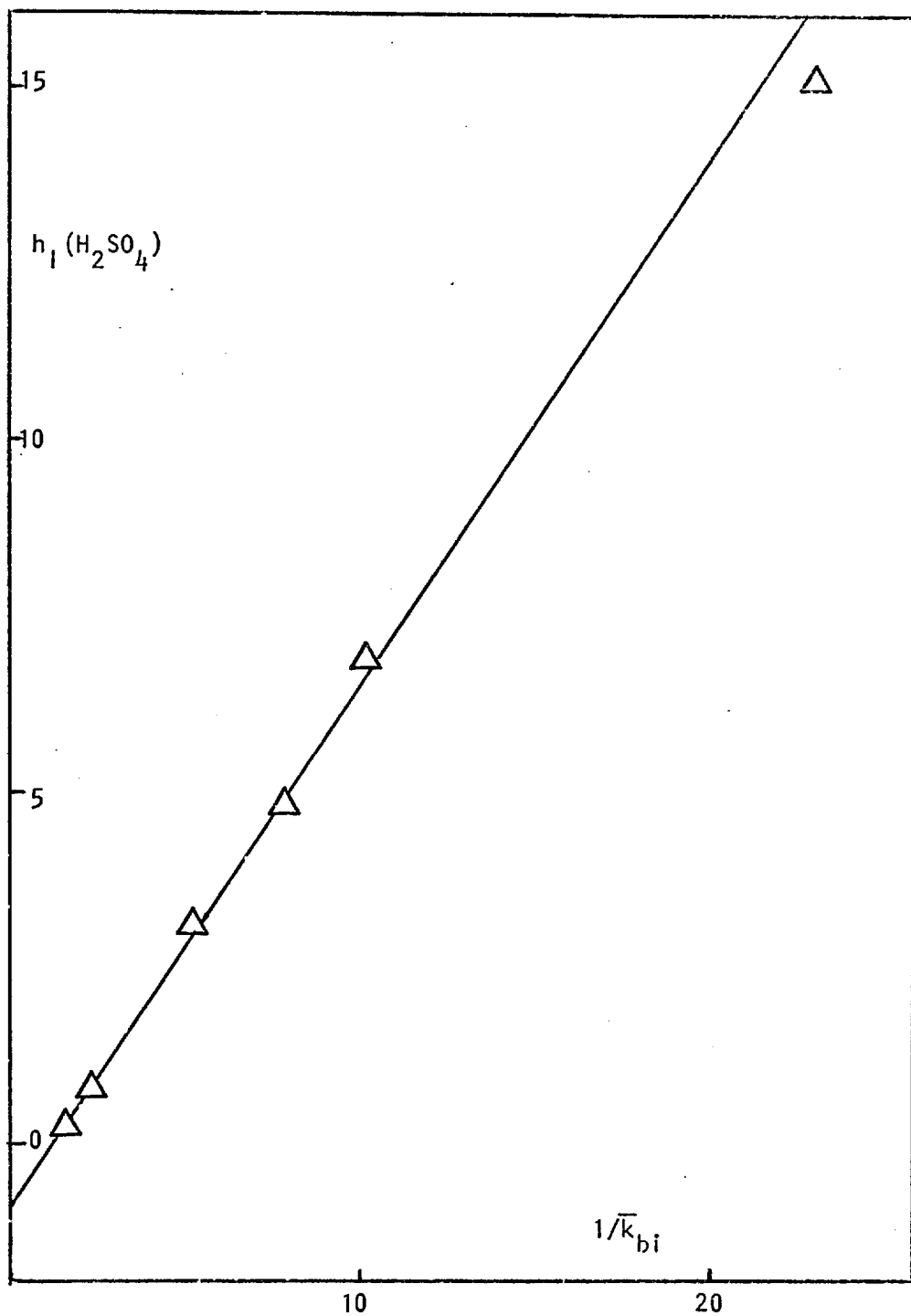


TABLE 3.9 Diazodeprotonation of 2-methyl-4,6-di-t butyl indole in acidic 4%(v/v) aqueous dioxan solutions at 25°C.

Initial [Indole] = 4×10^{-6} M. [pMeOArN₂⁺] = 10^{-2} M. Followed at 525nm.

$\bar{k}_{bi}/s^{-1}.M^{-1}$.	$1/\bar{k}_{bi}$	[H ₂ SO ₄]/M.	h_I^*
3.1 ^{††}	0.0	0.0	0.0
0.667	1.5	0.2	0.219
0.415	2.41	0.5	0.83
0.193	5.18	1.0	3.09
0.127	7.87	1.25	4.79
0.0959	10.4	1.5	6.92
0.0436	22.9	2.0	15.1

* From reference 59.

†† Reaction rate in 40% (v/v) dioxan, followed at 401 nm.

In dilute tetraborate buffers the rate of diazocoupling increases, and the kinetics were found to fit equation 3.8 fairly well (Figure 3.7). A direct comparison between these results and those for 2-methyl indole is not possible since the insolubility of the product necessitated a change in solvent from 20% to 40% v/v dioxan. The working pH values measured by a glass electrode are reasonably equivalent in these two solvents⁸⁴ and one need only consider the change in the ionisation constant K_E .

Results for methyldibutylindole and also the $3\text{-}^2\text{H}_1$ substrate are given in Table 3.10. The parameters obtained from equation 3.8 were evaluated as

$$\bar{k}_{bi}^{-H} = 3.1 + \frac{5.9 \times 10^{-10}}{[H_3O^+]}$$

$$\bar{k}_{bi}^{-D} = 1.5 + \frac{3.6 \times 10^{-10}}{[H_3O^+]}$$

3.5.2 KINETIC ISOTOPE EFFECTS.

The results above show that for reaction via the neutral indole species the deuterium isotope effect is

$$k_{bi}^{-H}/k_{bi}^{-D} = 2.1$$

This value must be corrected for the isotopic purity of the indole (equation 3.13).

$$y = \frac{y_0 \cdot \Omega}{1 - y_0(1 - \Omega)} \quad 3.13$$

where y is the deuterium isotope effect, y_0 the observed value and Ω the fraction of deuterium in the substrate. This leads to the value

Figure 3.7 Diazocoupling of 2-methyl-4,6-di ^tbutylindole in 40%(v/v) aqueous dioxan/tetraborate buffers.

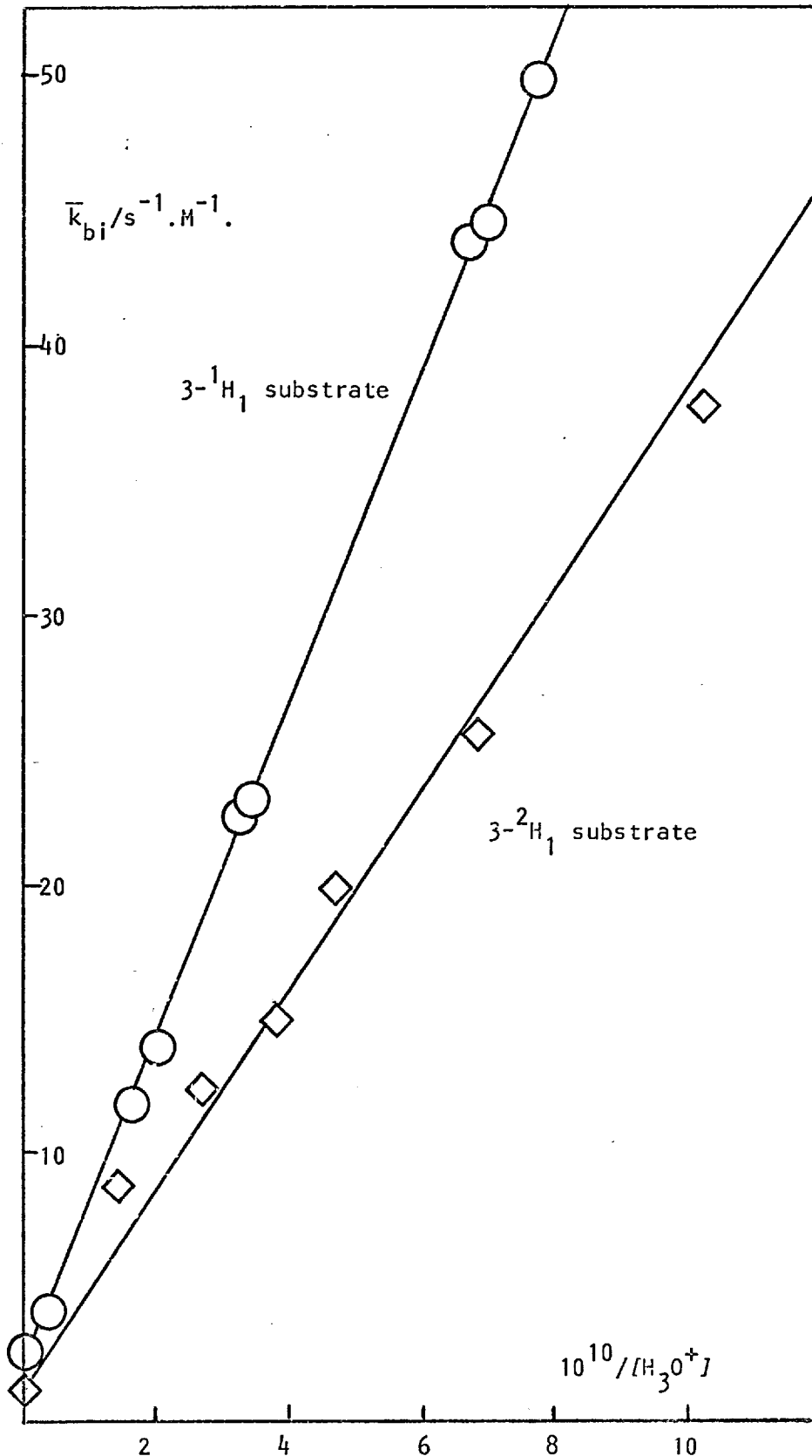


TABLE 3.10 Diazocoupling of 2-methyl-4,6-di^tbutylindole
in 40%(v/v) aqueous dioxan/tetraborate
buffer solutions at 25°C.

Initial $[p\text{-MeOArN}_2^+] = 4 \times 10^{-5} \text{M}$. $[\text{Indole}] = 4 \times 10^{-4} \text{M}$. $[\text{Borate}] = 0.01$.

pH_{obs}	$10^{10}/[\text{H}_3\text{O}^+]$	$\bar{k}_{\text{DI}}/s^{-1} \cdot \text{M}^{-1}$
4.0	0	3.1
9.460	0.29	4.1
10.210	1.62	11.7
10.305	2.02	13.9
10.505	3.19	22.8
10.535	3.42	23.2
10.825	6.67	40.4
10.843	6.94	44.5
10.885	7.69	50.0
7.2 **	0	1.48
10.265	1.36	8.82
10.422	2.65	12.3
10.574	3.75	15.0
10.675	4.74	19.8
10.833	6.80	26.2
11.010	10.2	38.0

** Results for 3-²H₁ substrate.

$$k_{bi}^{-H}/k_{bi}^{-D} = 2.6 \pm 0.3$$

The tritium isotope effect was measured by following the rate of loss of tritium and rate of appearance of product simultaneously. The detailed kinetic results are given in Chapter 6 (Table 6.11).

$$k_{bi}^{-T}/k_{bi}^{-D} = 5.1 \pm 0.3$$

The deuterium isotope effect for reaction via the indolyl anion was obtained from the relative slopes of Figure 3.7 .

$$k_{bi}'^{-H} \cdot K_E / k_{bi}'^{-D} \cdot K_E = 1.67$$

K_E is subject only to a secondary deuterium isotope effect resulting from labelling in the 3-position and is effectively unity. Correction for isotopic purity yields

$$k_{bi}'^{-H}/k_{bi}'^{-D} = 2.0 \pm 0.2$$

Two points arise concerning these values. It is possible that in the case of the indolyl anion reaction some base catalysis by OH^- occurs, similar to the behaviour that is thought to prevail in aprotic media (equation 3.12). The contribution must be small, since the expected second order term in $[OH^-]$ is not in fact observed. It is also interesting to note that though observation of a tritium isotope effect could be explained by initial fast N-coupling followed by (5 fold) slower C- coupling, this is totally ruled out by the observation of a deuterium isotope effect greater than unity- since N-coupling would not be affected by remote isotopic substitution.

DISCUSSION.

3.6.1 THE SWAIN-SCHAAD RELATIONSHIP.

Since both the deuterium and tritium isotope effects are available for methyldibutylindole, the Swain-Schaad exponent \underline{r} can be evaluated.⁴²

$$k_{bi}^{-H}/k_{bi}^{-D} = 2.6, \quad k_{bi}^{-H}/k_{bi}^{-T} = 5.1$$

$$\log (k_{bi}^{-H}/k_{bi}^{-T}) / \log (k_{bi}^{-H}/k_{bi}^{-D}) = 1.71$$

This value is outside the limits set for \underline{r} of $1.33 < r < 1.55$ and is moreover in the wrong direction from the value expected if tunnelling occurs⁴¹. This may be a consequence of the fact that k_{bi} is in fact a composite constant (equation 3.1).

$$k_{bi}^{-H} = k_1 / (1 + k_{-1}/k_2^H[B]) \quad 3.1$$

Similar expressions hold for k_{bi}^{-D} and k_{bi}^{-T} and it should be the constant k_2^L which obeys the Swain-Schaad rule (equation 3.14).

$$\log (k_2^H/k_2^T) = 1.442 \log (k_2^H/k_2^D) \quad 3.14$$

Solving equations 3.1 and 3.14 with the known data one obtains

$$k_2^H/k_2^D = 7, \quad k_2^H/k_2^T = 18, \quad k_{-1}/k_2^H[H_2O] = 0.31$$

This treatment gives isotope effects similar in magnitude to those reported by Zollinger⁶³ and a reasonable value for $k_{-1}/k_2^H[B]$. Since however the experimental isotope effects are only accurate to about $\pm 5\%$, this leads to considerable errors in the values evaluated above, and this treatment is only carried out to show that if $k_{-1}/k_2[B] < 10$ then experimental isotope effects may be grossly deviant from the true values.

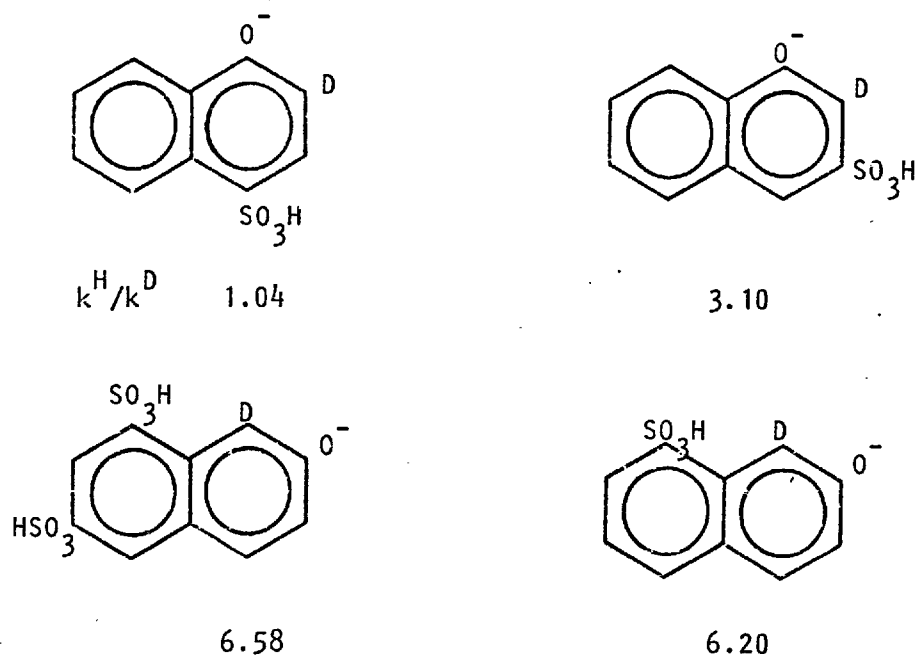
The method adopted by Zollinger^{63,70}, whereby k_{-1}/k_2 is evaluated from the slope of the base catalysis plot, does not suffer from this defect. Such a method was not possible in this case since the rate can only be enhanced 30% by reducing the denominator in equation 3.1 to unity.

3.6.2 DEUTERIUM ISOTOPE EFFECTS IN DIAZOCOUPILING.

The similarity between the present results obtained for indoles and the early work of Zollinger on naphthols is striking⁶³. It is worth considering in detail the main points that emerge from the naphthol work.

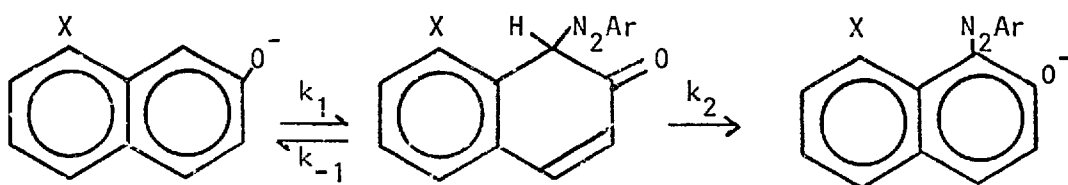
Isotope effects measured for various naphthol sulphonic acids (Scheme 3.4) suggest that only when substantial peri- interactions occur do the isotope effects exceed unity. Base catalysis by pyridine was observed only in those cases where an isotope effect larger than unity was measured, and suitable treatment of the data enabled the ratio $k_{-1}/k_2 [Py]$ to be obtained. The results for various pyridines gave the following values.

Scheme 3.4 Diazocoupling to substituted naphthol sulphonic acids.



	Pyridine	2-methylpyridine	2,6-dimethylpyridine
k_{-1}/k_2	0.77	1.54	5

Taking the increased basicity of the lutidine into account, Zollinger showed that the value for 2-methylpyridine was 3 times too high and that for 2,6-dimethylpyridine was about 10 times too high. This enabled Zollinger to suggest that the proton transfer was subject to a steric effect, probably the first such example in an $A-S_E2$ reaction⁴⁴. Further work on 8-substituted naphthols (Scheme 3.5)



Scheme 3.5 X = Cl, Br, I, Ph, Me, Et, ⁱPr.

showed that in the case of X = Ph, a sterically induced isotope effect of 2.7 is observed. Zollinger has never reported an isotope effect for 2-naphthol itself, but his statement certainly implies it is unity. With the other substituents, base catalysis by pyridine was noted (implying a slow proton transfer) and the ratio k_{-1}/k_2 evaluated (Table 3.11)⁷⁰.

TABLE 3.11 Rate constants for diazocoupling of 8-substituted 2-naphthols.⁷⁰

X	$10^6 k_1/\text{min}^{-1} \cdot R_f/\text{nm} \cdot ^*$	$10^2 k_{-1}/k_2$	$pK_{\text{naphthoate}}$
Cl	0.37	0.65	8.96
Br	0.63	0.47	8.94
I	0.99	0.31	8.98
Me	5.0	0.29	9.42
Et	8.8	0.26	9.54
<i>i</i> Pr	10.7	0.23	9.52

*

R_f , the free radius, is defined as in Figure 3.8

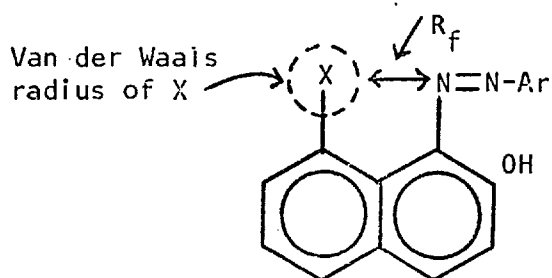


Figure 3.8

As the steric interaction increases, so does the ratio k_{-1}/k_2 , and this cannot be explained by the apparent basicity of the leaving proton if the pK_a for ionisation of the O-H is at all a reliable guide. Zollinger concluded that the proton transfer was sterically hindered. None of these groups appears to be as effective as SO_3H , for which the ratio $k_{-1}/k_2 \approx 1$, compared with ~ 0.01 for these alkyl groups, and solvation may be playing a major role in this effect. For example, coupling to the hindered 1,3,5 trimethoxybenzene shows tritium and deuterium isotope effects of unity⁸⁵ and this substrate is obviously insufficiently hindered.

The rate of electrophilic attack of the diazonium ion on the nucleophile has far reaching ramifications. Zollinger⁷⁰ found that k_1 increased in accord with the reactivity parameter of the 8-substituent (σ_m^+) and so was not subject to a steric effect. The Law of microscopic reversibility then requires that the reverse step (k_{-1}) also be free of steric restraint. Since the stability of the intermediate σ complex should in principle affect both k_{-1} and k_2 equally, the basicity of the nucleophile should not affect the ratio k_{-1}/k_2 . The variation observed in this ratio was therefore interpreted in terms of a steric effect on k_2 only, bolstering the observation of the hindered proton removal observed with 2,6-dimethyl pyridine.

The results for indoles tend to confirm this line of argument. Indolyl anions are perhaps 8 pK units more basic than naphtholates and the neutral indole is 8 pK units less basic, implying that the stability of the intermediate complex is considerably different in each case. In spite of this in all three cases $k_{-1}/k_2 < 1$ if the

site of attack is not hindered, suggesting that both k_{-1} and k_2 are influenced equally by the large change in σ complex stability (Figure 3.9). For methyldibutylindole it appears that for the neutral species k_1 is not hindered. Thus k_1 is about 12 times greater than for 2-methylindole which is in accord with the increased basicity. For the anion, the product $k_{bi}^1 \cdot K_E$ is the same for both 2-methylindole and methyldibutylindole. If the correction for K_E established previously (Section 2.10.2) is assumed valid for 20-40% dioxan then it seems that dibutylmethylindole reacts with diazonium ions about twice as fast via the indolyl anion as does methylindole. Bearing in mind the differences in solvents it is probable that if a steric effect exists for the k_1 step it is less than about 5 . It was shown in section 3.5.2 that the results for hindered indoles are consistent with an increase in the ratio k_{-1}/k_2 . Since k_1 (and hence k_{-1}) is not hindered we see that in indoles as well as naphthols, the proton transfer from the Wheland intermediate is subject to steric effects.

3.6.3 THE NATURE OF THE TRANSITION STATE.

Zollinger has rationalised his results for hindered naphthols in terms of an asymmetric intermediate σ complex (Figure 3.10).⁷⁰

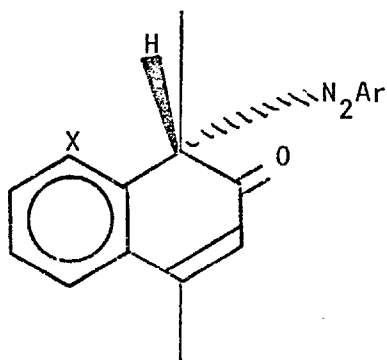


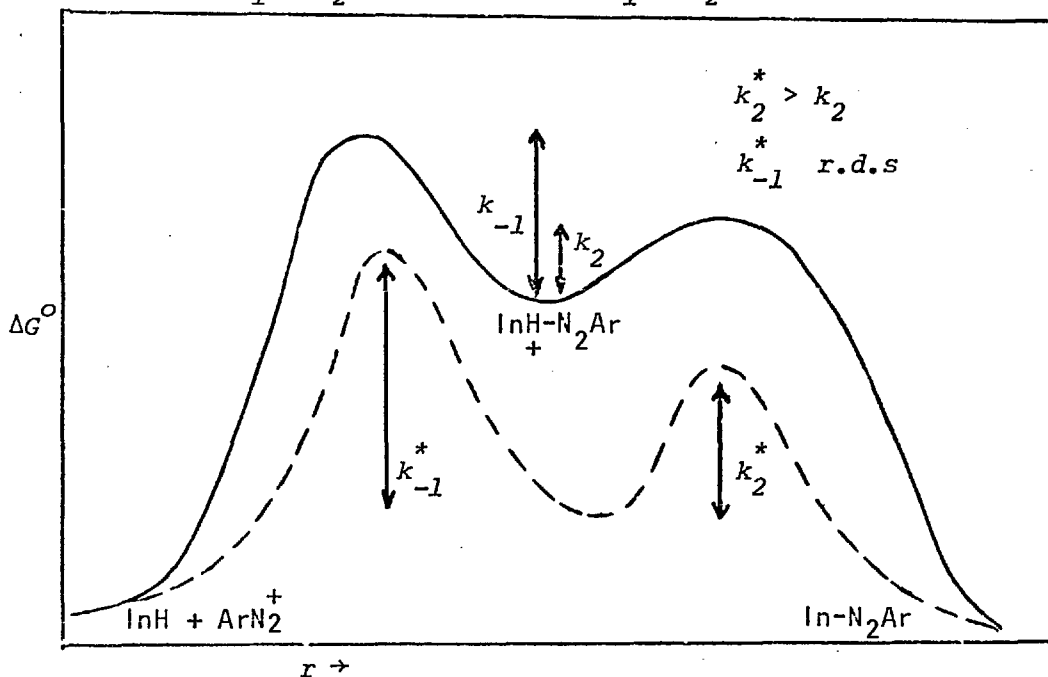
Figure 3.10 Asymmetric σ complex for diazocoupling to hindered naphthols

Figure 3.9 Free energy diagrams for diazocoupling.

— represents a substrate less basic than ----

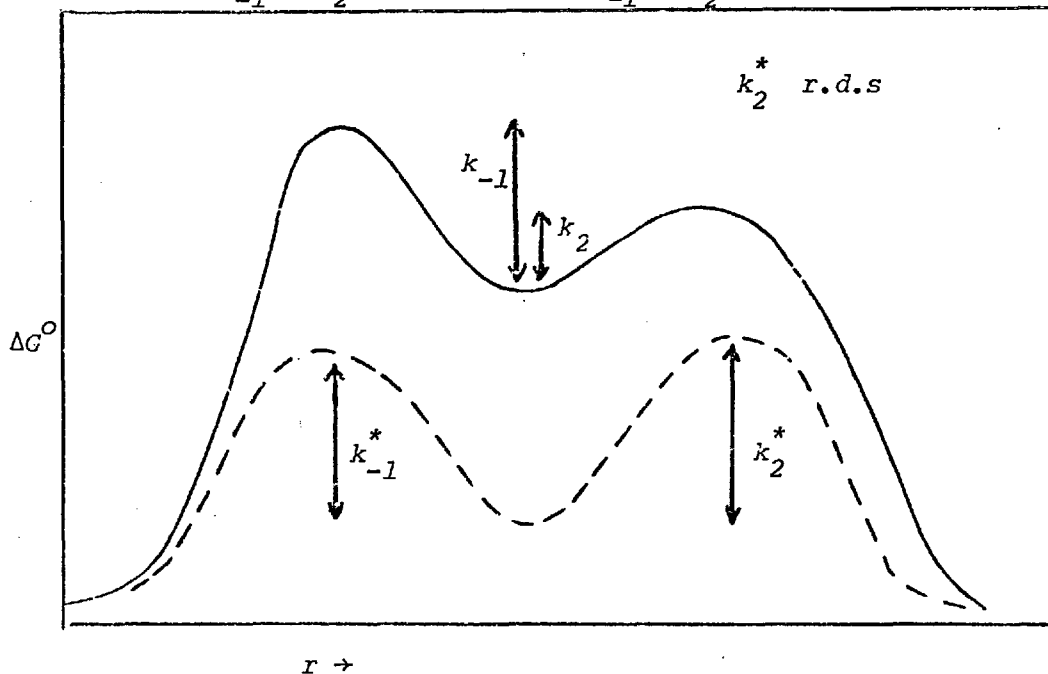
a) No steric effect on hydrogen transfer.

$$\frac{\Delta G_{k_{-1}}}{\Delta G_{k_2}} \approx \frac{\Delta G_{k_{-1}}^*}{\Delta G_{k_2}^*}$$



b) A steric effect on hydrogen transfer of the more basic species.

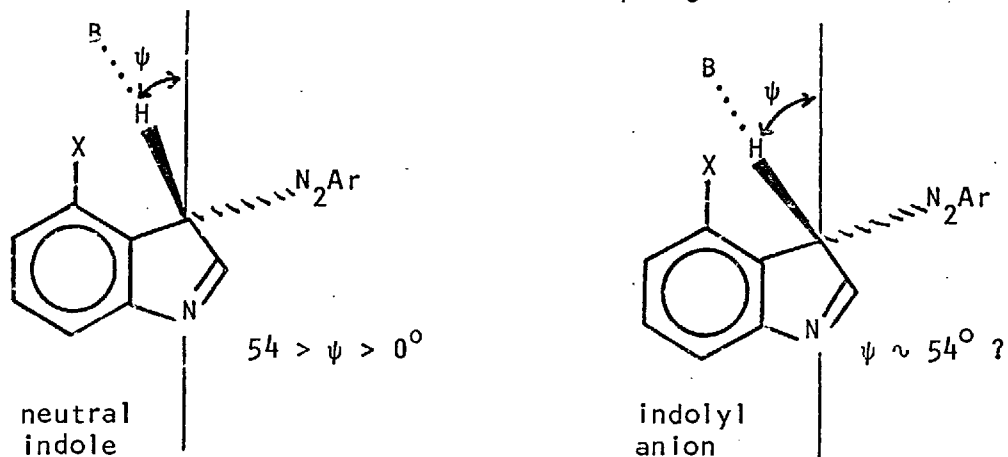
$$\frac{\Delta G_{k_{-1}}}{\Delta G_{k_2}} > \frac{\Delta G_{k_{-1}}^*}{\Delta G_{k_2}^*}$$



The transition state for the forward step must resemble a π complex even more than the intermediate does, and thus it is not surprising that there is little interaction between the incoming electrophile and the group X. If the transition state for the hydrogen transfer is early (sp^3 like) or even more product (sp^2) like it is evident that there will be considerable interactions between the group X and the incoming base.

It was shown in Chapter 2 that the addition of the electrophilic proton to indoles went through a symmetric transition state for the neutral molecule and a product like transition state for the indolyl anion. The corollary to this is that proton removal from the intermediates is very reactant like for the indolyl anion and again symmetric for the neutral molecule. These differences in symmetry are reduced when one considers the asymmetric intermediate in diazocoupling (Figure 3.11). Comparison with Figure 2.9 suggests that for diazocoupling the angle ψ might be less than 54° in both cases, explaining why both the neutral molecule and the conjugate base reactions show a steric effect for proton transfer.

Figure 3.11 Transition states for diazocoupling of Indoles.



It seems then that in indole hydrogen exchange reactions alone, changes in a remote substituent (NH *vis a vis* N⁻) are sufficient to change the transition state symmetries. In diazocoupling a proximate substituent (-N₂Ar) also alters the symmetry of the transition states.

Further sterically hindering the indole eventually affects the rate of attack of electrophile. This was observed in hydrogen exchange with 2,4,6-tributylindole/2,6-dimethylpyridine and when the electrophile is a benzenediazonium ion an even greater effect ($>10^3$) is observed. This is a conservative estimate of the steric effect, since the products of the reaction include dealkylated azoindoles as well as the tributylazoindole. There is no doubt that if accurate kinetics had been measurable a large deuterium isotope effect would have been found.

Finally it should be mentioned that the concept of remote and proximate steric effects in aromatic substitution reactions may have a wider applicability. For example Farrell and Mason^{86a} observed an isotope effect of 2.6 for *ortho* bromination of dimethylaniline and 1.0 for *para* bromination. A similar effect was found for iodination^{86b}. These are probably both proximate steric effects and it remains to be seen whether remote steric effects can be found.

CHAPTER IV

DECARBOXYLATION OF INDOLE 3- CARBOXYLIC ACIDS.

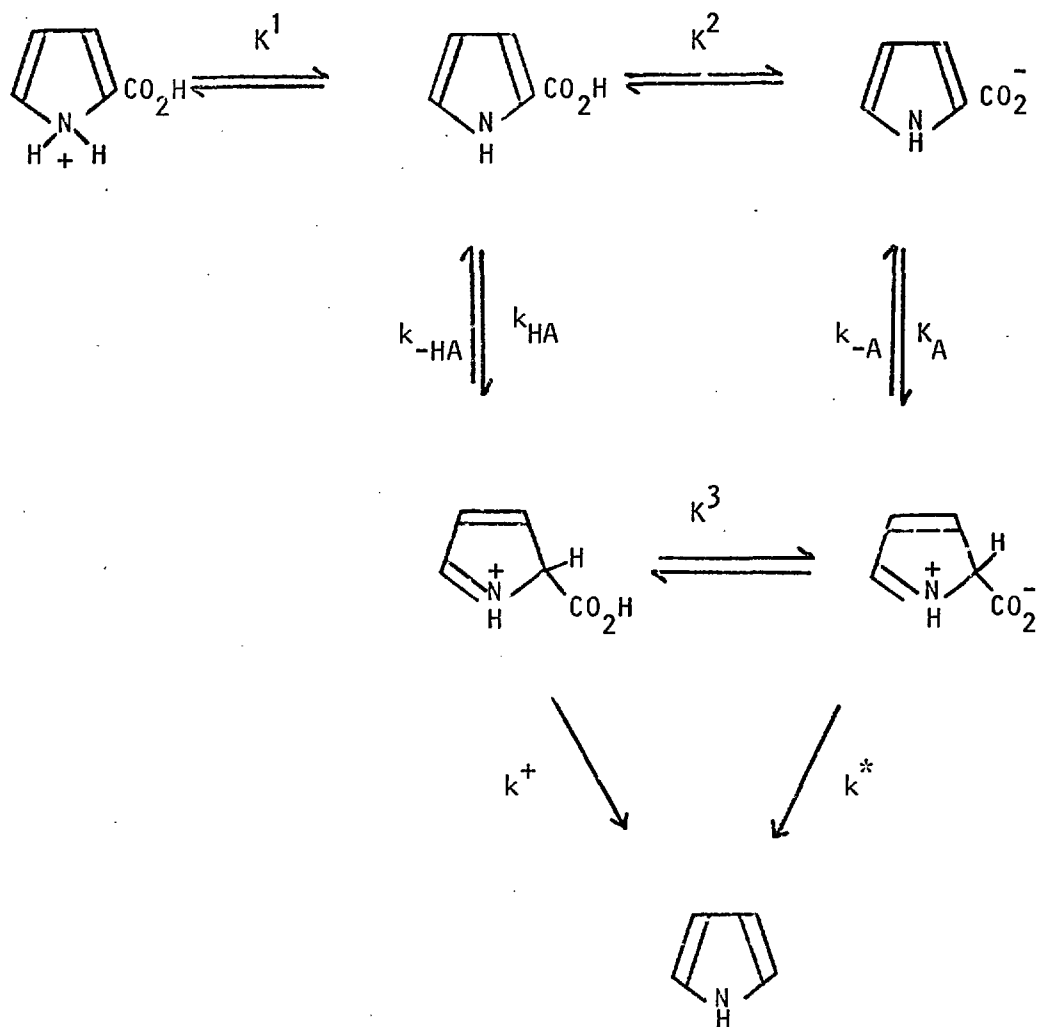
4.1 INTRODUCTION.

The mechanism of acid catalysed aromatic decarboxylation has been established from studies on a variety of different compounds. Of particular importance has been the observation that the proton transfer under certain conditions can be rate limiting, and this system is therefore potentially useful in studying hydrogen isotope effects.

Willi⁸⁷ studied anthranilic acid and established that at high pH (~ 4.7) proton transfer was rate limiting but in more acidic media the C-C bond breaking became slow. This was further confirmed by studies on 2,4-dihydroxybenzoic acid which clearly showed the transition in rate determining steps⁸⁸. Zielinski⁸⁹ confirmed that the C-C cleavage becomes slow by observing a ¹³C isotope effect of 1.0105 for protodecarboxylation of anthranilic acid and also pyridine mono and dicarboxylic acids. A complementary study of the isotope rate ratios was carried out by Noyce⁹⁰ who showed that in dilute sulphuric acid the decarboxylation of p-methoxy β methylcinnamic acid gave a primary deuterium isotope effect of about 3, reducing to 1.7 in strong acid due to the change in the slow step.

The most complete studies were first carried out by Long⁹¹, who observed both $^{12}\text{C}/^{13}\text{C}$ and $^1\text{H}/^2\text{H}$ isotope effects in the decarboxylation of azulene carboxylic acids according to acidity and Dunn⁹², who studied a variety of compounds. The behaviour of pyrrole-2-carboxylic acid in particular was closely analogous to the azulene reaction and essentially the same mechanism was postulated by both Long and Dunn to account for the results (Scheme 4.1)

Scheme 4.1 Acid catalysed protodecarboxylation of pyrrole 2-carboxylic acid.



When the concentration of the intermediates is assumed low, application of steady state theory gives equation 4.1

$$k_{O}^{-CO_2} = \frac{k_A \cdot K^2 + k_{HA} [H^+]}{1 + \frac{[H^+]}{K^1} + \frac{K^2}{[H^+]}} \cdot \frac{k^* \cdot K^3 + k^+ \cdot [H^+]}{K^3 (k^* + k_{-A}) + [H^+] (k^+ + k_{-HA})}$$

4.1

The ^{13}C isotope effects enabled several simplifications to be made. At low $[H^+]$, no ^{13}C effect is observed and so $k^* \gg k_{-A}$. At high $[H^+]$ virtually a maximum ^{13}C effect is found which suggests that $k_{-HA} \gg k^+$. Related to these approximations is the inequality $k^* \cdot K^3 \gg k^+ \cdot [H^+]$. The experimental evidence tends to confirm that the protonated carboxylic acid does not decarboxylate *per se*, but ionises first to give the zwitter ion. If the acidity of the medium is such that $K^2/[H^+] \ll 1$, then equation 4.1 reduces to equation 4.2.

$$k_{O}^{-CO_2} = \frac{k_A \cdot K^2 + k_{HA} [H^+]}{1 + \frac{k_{-HA} \cdot [H^+]}{K^3 \cdot k^*}} \quad 4.2$$

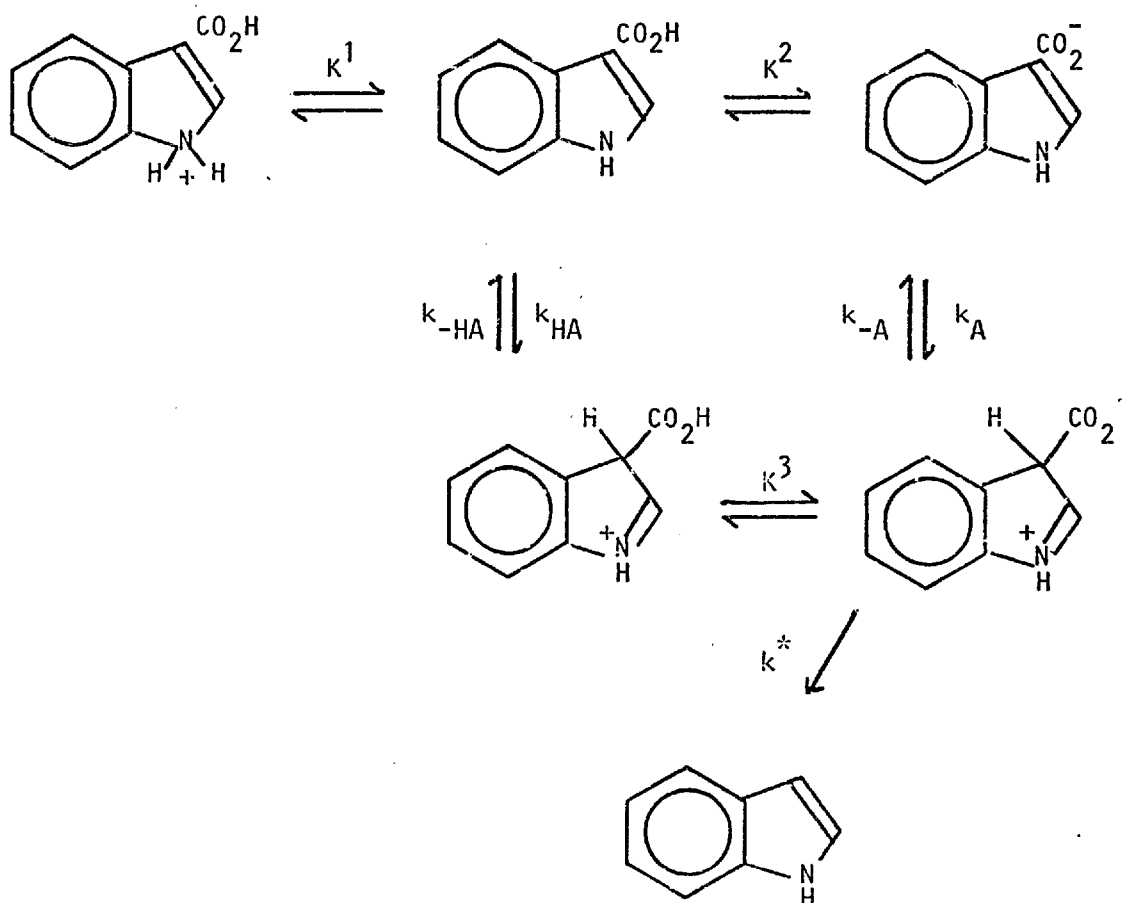
Equation 4.2 has been found to fit experimental decarboxylation kinetics for a variety of substrates. Willi⁸⁸ has analysed data for dihydroxybenzoic acid in terms of the parameterised form of equation 4.2.

$$k_o^{-CO_2} = \frac{a + b.h_o}{1 + c.h_o} \quad 4.3$$

where h_o represents the acidity function for the substrate used. If the value for b is compared in the two acids H^+ and D^+ , then a direct estimate of the isotope effect can be made. The results for azulene-1-carboxylic acid⁹¹ fit equation 4.3 using both H_2O and D_2O as solvents and a value for the ratio k_{HA}/k_{DA} is reported. The extensive investigations of Dunn⁹² also verify the general form of equation 4.3 .

From the limited data available for decarboxylation of indole carboxylic acids in acidic solutions⁹³ and also according to Powers⁹⁴, it seems probable that decarboxylation occurs by a similar mechanism (Scheme 4.2)

Scheme 4.2 Protodecarboxylation of indole-3-carboxylic acid.



4.1.1 STATISTICAL ANALYSIS OF DATA.

For a moderately dilute acid solution maintained at a constant ionic strength, equation 4.3 can be replaced with equation 4.4,

$$k_o^{-CO_2} = \frac{a + b.[H_3O^+]}{1 + c.[H_3O^+]} \quad 4.4$$

Two methods have been used previously to analyse data in terms of this equation. At very low $[H_3O^+]$, $c.[H_3O^+] \ll 1$ and equation 4.4 reduces to

$$k_o^{-CO_2} = a + b.[H_3O^+] \quad 4.5$$

At relatively high $[H_3O^+]$, $b.[H_3O^+] \gg a$ and equation 4.4, with some rearrangement reduces to equation 4.6 .

$$k_o^{-CO_2}/[H_3O^+] = b - c.k_o^{-CO_2} \quad 4.6$$

Both Long⁹¹ and Dunn⁹² have used a combination of equations 4.5 and 4.6 to evaluate the constants in equation 4.4, however in this work a statistical analysis of equation 4.4 using a rigorous weighted non-linear least squares regression method was used (section 7.2) and the method was applied to the data of Dunn for pyrrole^{92b} (Table 4.1) and the data for azulene^{91b} (Table 4.2). An excellent comparison with the literature analyses was found and standard error estimates are available as a bonus. Figure 4.1 illustrates how accurately equation 4.4 fits the decarboxylation data.

TABLE 4.1 PROTODECARBOXYLATION OF PYRROLE-2-CARBOXYLIC ACID IN WATER AT 50°C. I = 1.0

$[H_3O^+]/M.$	$10^4 k_o^{-CO_2}/s^{-1}.$	$k_o^{-CO_2}(Calc)$	Weight
0.0	-	0.272	
0.00039	0.28	0.281	192
0.00118	0.321	0.298	189
0.00219	0.345	0.321	188
0.00646	0.422	0.414	181
0.0151	0.601	0.603	163
0.0309	0.913	0.942	127
0.0479	1.23	1.30	96
0.1019	2.42	2.39	37
0.1603	3.48	3.48	19
0.2495	4.90	5.02	10
0.3606	6.99	6.74	5.1
0.3990	7.20	7.28	4.8
0.4656	8.41	8.18	3.5
0.6592	10.5	10.5	2.2
0.8337	12.6	12.2	1.6
1.45	16.8	16.8	0.9
2.49	20.8	21.3	0.6

$a = 2.722 \pm 0.075 \times 10^{-5} s^{-1} (\text{Lit.}^{92b} 2.9 \times 10^{-5})$
 $b = 2.229 \pm 0.032 \times 10^{-3} s^{-1} M^{-1} (\text{Lit. } 2.2 \times 10^{-3}).$
 $c = 0.648 \pm 0.029 M^{-1}. (\text{Lit. } 0.58)$

TABLE 4.2 Protodecarboxylation of Azulene-1-carboxylic acid in water at 25°C. $I = 1.0$

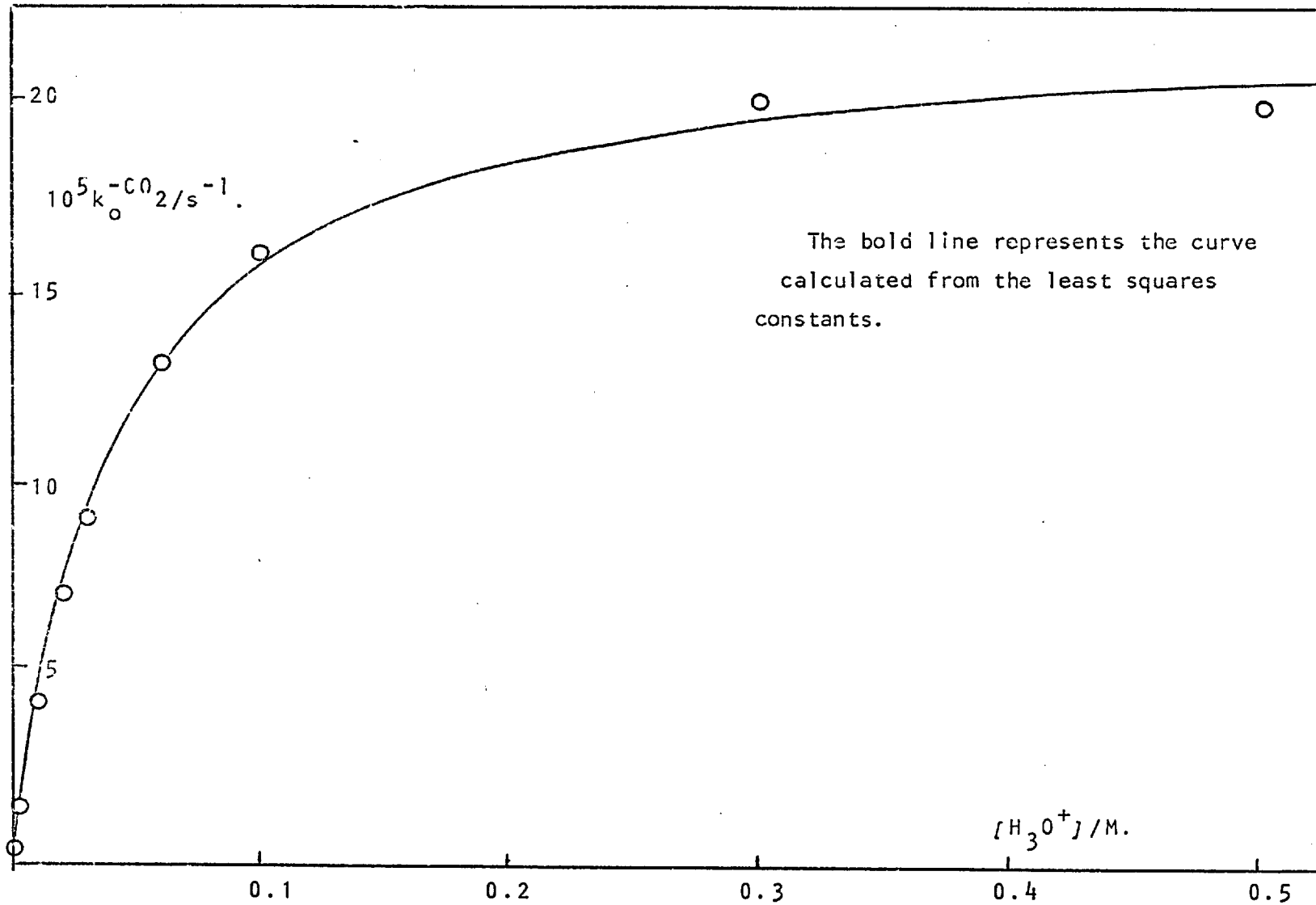
$[H_3O^+]/M.$	$10^5 k_o^{-CO_2}/s^{-1}.$	$k_o^{-CO_2}$ (Calc)	Weight
0.00102	0.575	0.474	3.8
0.00296	1.57	1.43	4.5
0.0100	4.33	4.28	7.7
0.0200	7.08	7.20	12.6
0.0300	9.11	9.29	15.2
0.0600	13.12	13.09	13.6
0.1000	16.05	15.64	9.5
0.0300	19.83	19.42	6.4
0.5000	19.76	20.40	6.4

$$a = -6.3 \pm 36 \times 10^{-7} s^{-1} \text{ (Lit. } ^{91b} \text{ -)}$$

$$b = 5.39 \pm 0.32 \times 10^{-3} s^{-1} M^{-1}. \text{ (Lit. } 5.3 \times 10^{-3} \text{).}$$

$$c = 24.4 \pm 1.7 M^{-1}. \text{ (Lit. } 26.3 \text{).}$$

Figure 4.1 Protodecarboxylation of azulene-1-carboxylic acid in Water at 25°C.



4.1.2 THE KINETIC METHOD.

The methods used previously by Long⁹¹, Dunn⁹², Willi⁸⁸ and others centered extensively on monitoring the U.V. spectrum of the reaction solution. For indoles it was found that the U.V. spectrum of reactant and product were almost identical and this method could not be used.

It was decided to measure reaction rates by radiotracer methods using ¹⁴C labelled indoles. These compounds were synthesised (as described in the experimental section) from ¹⁴CO₂ and the corresponding 3-indolylmagnesium iodide^{95,96}. Care was taken not to monitor reaction rates before all the N- carboxylic acid which is also produced by this method had decarboxylated.

RESULTS

4.2 INDOLE-3-CARBOXYLIC ACID.

4.2.1 THE RATE OF DECARBOXYLATION AT LOW pH.

Good first order plots for the protodecarboxylation were obtained in all cases for up to 98% reaction, and the pseudo first order rate constants were fitted to equation 4.4 (Table 4.3). The range of acidity covered in this set of results means that $K^2/[H^+] \ll 1$, since Melzer⁹⁶ has estimated the pK^2 to be about 5.5 - 6.0 and the lowest acidity employed here had a pH of about 3.6 . Thus equation 4.4 should represent closely the kinetic form predicted from the mechanism and indeed the results appear to fit very well (Figure 4.2).

An analogous series of runs was carried out in D_2O (containing at least 98% d) as solvent, using as the acid a solution of HCl gas in D_2O . The isotopic rate ratios were evaluated to be

$$k_{HA}/k_{DA} = 2.72 \pm 0.085$$

$$\frac{K_A \cdot K^2 (H_2O)}{K_A \cdot K^2 (D_2O)} = 2.56 \pm 0.53$$

$$\frac{k_{-A}/K^3 \cdot k^* (H_2O)}{k_{-A}/K^3 \cdot k^* (D_2O)} = 2.24 \pm 0.090$$

The standard errors were obtained from the expression for the propagation of errors (equation 4.7)

TABLE 4.3 Protodecarboxylation of indole-3-carboxylic acid in water at 25°C. $I = 1.0$ maintained with NaCl.

$[H_3O^+]$	$10^6 k_o^{-CO_2}/s^{-1}$	$10^6 k_o^{-CO_2}(Calc)$	Weight
0.0003	0.685	0.703	52
0.0016	1.18	1.26	5.8
0.00731	3.47	3.38	8.5
0.0089	4.06	3.90	9.3
0.0146	5.50	5.54	12.3
0.0273	8.53	8.31	16.0
0.0467	10.7	11.1	16.9
0.0636	12.6	12.8	13.8
0.1030	15.6	15.2	10.1
0.1070	15.5	15.4	10.2
0.1770	17.4	17.5	8.2
0.2460	18.4	18.6	7.4
1.000	21.2	21.1	5.6

$$a = 5.71 \pm 1.0 \times 10^{-7} s^{-1}.$$

$$b = 4.54 \pm 0.13 \times 10^{-4} s^{-1} \cdot M^{-1}.$$

$$c = 20.5 \pm 0.76 M^{-1}.$$

TABLE 4.4 Deuteriodecarboxylation of indole-3-carboxylic acid in deuterium oxide at 25°C. $I = 1.0$ maintained with NaCl.

$[D_3O^+]/M.$	$10^6 k_o^{-CO_2}/s^{-1}.$	$10^6 k_o^{-CO_2}(Calc)$	Weight.
0.00001*	0.220	0.225	36
0.0047	0.966	0.965	4.3
0.0159	2.52	2.51	5.5
0.0257	3.64	3.65	5.9
0.0447	5.57	5.45	5.2
0.0696	7.11	7.22	4.1
0.1100	9.10	9.24	2.9
0.255	12.8	12.8	1.5
1.035	16.6	16.5	0.9

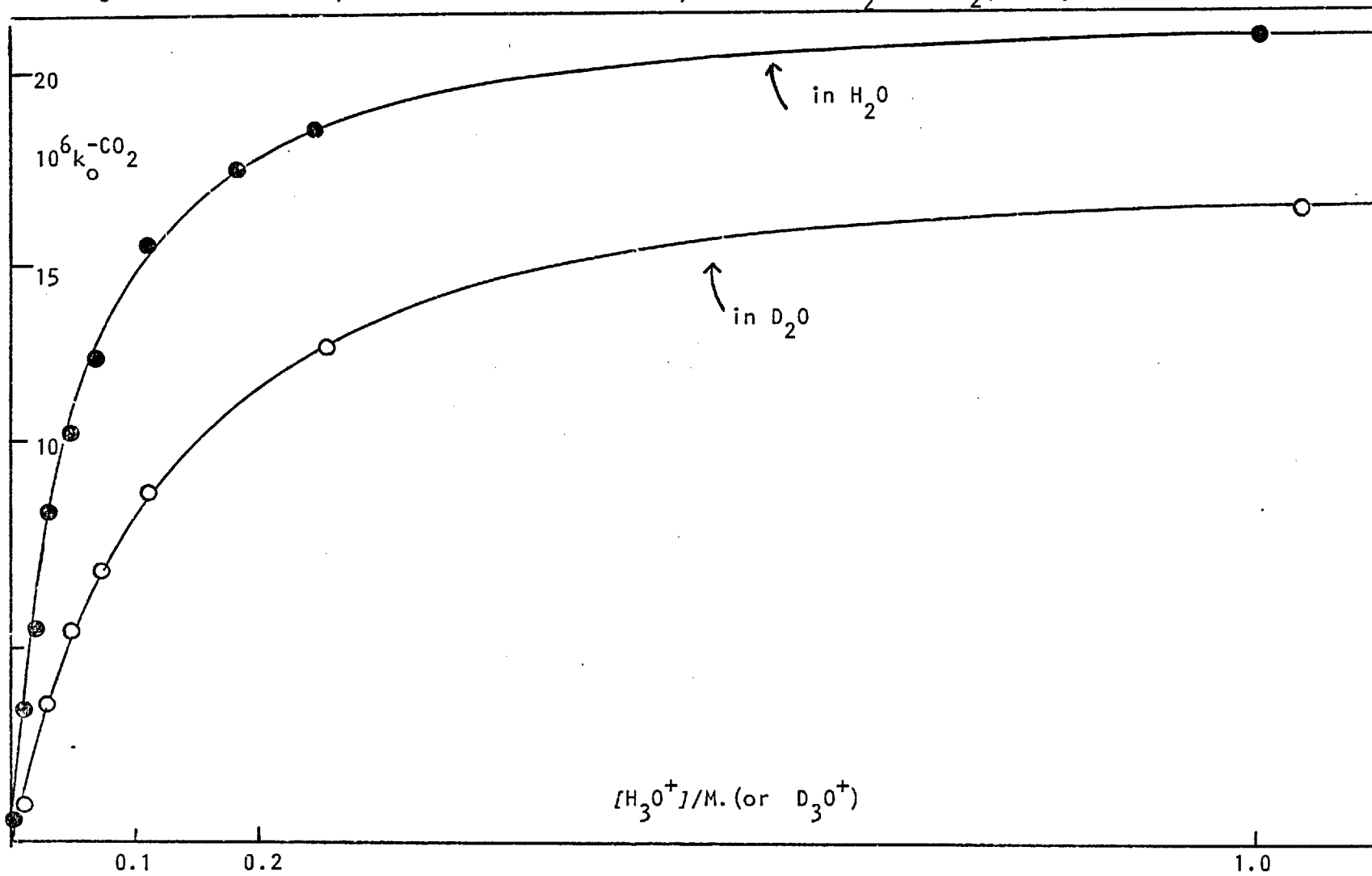
* Measured in a dilute phthalate buffer.

$$a = 2.23 \pm 0.25 \times 10^{-7} s^{-1}.$$

$$b = 1.667 \pm 0.023 \times 10^{-4} s^{-1} \cdot M^{-1}.$$

$$c = 9.16 \pm 0.20 M^{-1}.$$

Figure 4.2 Decarboxylation of Indole-3-carboxylic acid in H_2O and D_2O at $25^\circ C$.



$$\sigma_{x/y}^2 = \sigma_{x/y}^2 + \sigma_y^2 \cdot x^2/y^4 \quad 4.7$$

4.2.2 THE RATE OF DECARBOXYLATION AT HIGH pH.

When the pH of the solution is such that an appreciable fraction of the carboxylic acid is ionised to the carboxylate anion, equation 4.1 reduces to

$$k_o^{-CO_2} = \frac{k_A \cdot K^2}{1 + K^2/[H_3O^+]} \quad 4.8$$

This arises since $k_{HA}[H^+] \approx 0$, $k^* > k_{-A}$ and $k_{-HA}/k^*K^3 \approx 0$.

In this region it may also be possible to detect general acid catalysis, and a general equation for such catalysis would be

$$k_o^{-CO_2} = \frac{a' + b'[HA]}{1 + c'[HA]} \quad 4.9$$

It is no longer certain that the coefficients a', b' and c' have the same meaning as previously. This is partly because the inequality $k^* > k_{-A}$ need no longer hold, as k_{-A} will certainly be increased as a consequence of the stronger base present. In order to verify equation 4.8 the kinetics of decarboxylation were carried out in a series of buffers of constant pH and extrapolated to zero buffer concentration to exclude the effect of the general acid catalysis observed (Table 4.5). By using a value for $k_A \cdot K^2$ of 2.82×10^{-5} at 60° (Table 4.7) a value for K^2 was obtained by substituting in equation 4.8 (Table 4.6).

TABLE 4.5 Decarboxylation of indole-3-carboxylic acid
in aqueous pyridine buffers at 60°C. $l = 1.0$

$[PyH^+]/M.$	pH_{Obs}^{60}	$10^5 k_O^{-CO_2}/s^{-1}.$
0.8	4.81	1.99
0.3	4.83	1.76
0.06	4.83	1.27
0.0	-	1.2
0.01	5.84	0.352
0.006	5.88	0.297
0.003	5.88	0.253
0.0	-	0.21
0.017	5.58	0.591
0.010	5.60	0.468
0.005	5.63	0.369
0.0	-	0.32

TABLE 4.6 Evaluation of the equilibrium constant K^2 .
at 60°C.

$10^5 k_O^{-CO_2}/s^{-1}.$	$10^5 [H_3O^+]$	$10^5 K^2/M.*$
1.2	1.5	2.0
0.32	0.26	1.6
0.21	0.13	2.0

* Evaluated from equation 4.8

The value obtained for pK^2 was 4.7 at 60°C. Melzer⁹⁶ has measured this constant at 25° in 95% and 50% ethanol, and a very approximate extrapolation to the conditions used here suggest that $pK^2 \sim 5$. This is certainly of the same order of magnitude as the kinetic value obtained here and tends to support this treatment.

4.2.3 ACTIVATION PARAMETERS.

The rate of protodecarboxylation was measured at 60° (Table 4.7). The values obtained for k_{HA} at two different temperatures were

$$k_{HA}^{25} = 4.54 \times 10^{-4} \text{ s}^{-1} \text{ M}^{-1}.$$

$$k_{HA}^{60} = 174.5 \times 10^{-4} \text{ s}^{-1} \text{ M}^{-1}.$$

The activation parameters were obtained from these two temperatures.

$$\Delta H^{\#} = 83.6 \text{ kJ.mol}^{-1}. \text{ (} 20 \text{ kcal.mol}^{-1} \text{.)}$$

$$\Delta S^{\#} = -28 \text{ J.K}^{-1} \text{ mol}^{-1}. \text{ (} -7 \text{ cal.K}^{-1} \text{ .mol}^{-1} \text{.)}$$

Both the enthalpy and entropy of activation are similar to the parameters obtained previously for the protonation of indoles themselves⁶⁰.

TABLE 4.7 Protodecarboxylation of Indole-3-carboxylic acid at 60°C. $I = 1.0$

$[H_3O^+]/M.$	$10^4 k_o^{-CO_2}/s^{-1}$	$10^4 k_o^{-CO_2} (Calc)$	Weight
0.00017*	0.311	0.312	338
0.0122	2.24	2.21	44.0
0.0208	3.28	3.37	48.3
0.0378	5.46	5.33	44.2
0.0627	7.63	7.57	34.0
0.0950	9.50	9.74	25.4
0.157	12.5	12.5	15.7
0.241	15.1	14.8	10.9
0.991	20.0	20.1	6.3

* Measured in a phthalate buffer.

$$a = 283 \pm 41 \times 10^{-7} s^{-1}.$$

$$b = 174.5 \pm 3.4 \times 10^{-4} s^{-1} \cdot M^{-1}.$$

$$c = 7.7 \pm 0.25 M^{-1}.$$

4.3 2-METHYLINDOLE-3-CARBOXYLIC ACID.

The rate constants for decarboxylation in H₂O (Table 4.8) and D₂O (Table 4.9) were all obtained by the radiotracer method used previously for indolecarboxylic acid itself. The isotopic rate ratios were evaluated as

$$k_{HA}/k_{DA} = 2.35 \pm 0.069$$

$$\frac{k_{-A}/K^3 \cdot k^*(H_2O)}{k_{-A}/K^3 \cdot k^*(D_2O)} = 2.15 \pm 0.077$$

The errors in the quantity $K^2 \cdot k_A$ were very large and consequently the solvent isotope effect for this constant is probably fairly meaningless. Discussion of these values is deferred till later.

4.4 5-CHLOROINDOLE-3-CARBOXYLIC ACID.

The decarboxylation kinetics were observed to be first order over more than 90% reaction and the results in H₂O (Table 4.10) and D₂O (Table 4.11) fit equation 4.4 very well (Figure 4.4). The isotopic rate ratios were

$$k_{HA}/k_{DA} = 2.23 \pm 0.11$$

$$\frac{k_{-A}/K^3 k^*(H_2O)}{k_{-A}/K^3 k^*(D_2O)} = 2.00 \pm 0.13$$

The ratio for $K^2 \cdot k_A$ is again very inaccurate. These results will be discussed later.

TABLE 4.8 Protodecarboxylation of 2-methylindole-3-carboxylic acid at 25°C. I = 1.0

$[H_3O^+]/M.$	$10^4 k_o^{-CO_2}/s^{-1}.$	$10^4 k_o^{-CO_2}(Calc).$	Weight.
0.000063 ^a	0.284	0.288	16.4
0.000063 ^b	0.290	0.288	16.4
0.0043	2.81	2.94	3.9
0.0074	4.39	4.31	6.4
0.0119	5.95	5.77	11.2
0.0171	6.85	6.98	17.3
0.0275	8.47	8.56	23.7
0.0382	9.73	9.56	22.9
0.0492	10.2	10.3	22.5
0.0748	11.2	11.2	19.6
0.0994	11.8	11.8	17.9
0.2503	12.8	12.9	15.3
0.5044	13.4	13.3	13.9
0.9750	13.5	13.5	13.7

^a Extrapolated from acetate buffers to zero buffer concentration.

^b Extrapolated from pyridine buffers to zero buffer concentration.

$$a = 239 \pm 72 \times 10^{-7} s^{-1}.$$

$$b = 800 \pm 16 \times 10^{-4} s^{-1} \cdot M^{-1}.$$

$$c = 58.2 \pm 1.3 M^{-1}.$$

TABLE 4.9 Deuteriodecarboxylation of 2-methylindole-3-carboxylic acid at 25°C. $I = 1.0$

$[D_3O^+]/M.$	$10^4 k_o^{-CO_2}/s^{-1}$	$10^4 k_o^{-CO_2} (Calc)$	Weight.
0.000012*	0.077	0.028	8.7
0.0051	1.33	1.54	1.4
0.0056	1.54	1.67	1.5
0.0138	3.40	3.43	2.7
0.0226	4.71	4.78	3.9
0.0384	6.51	6.41	4.2
0.0422	6.69	6.71	4.3
0.0526	7.41	7.38	4.0
0.0752	8.39	8.42	3.4
0.0959	9.22	9.07	2.9
0.255	10.8	11.0	2.1
0.970	12.1	12.1	1.7

* Measured in a dilute phthalate buffer.

$$a = 24 \pm 58 \times 10^{-7} s^{-1}.$$

$$b = 340 \pm 7.3 \times 10^{-4} s^{-1} \cdot M^{-1}.$$

$$c = 27.1 \pm 0.76 M^{-1}.$$

Figure 4.3 Decarboxylation of 2-methylindole-3-carboxylic acid in H₂O and D₂O at 25°C.

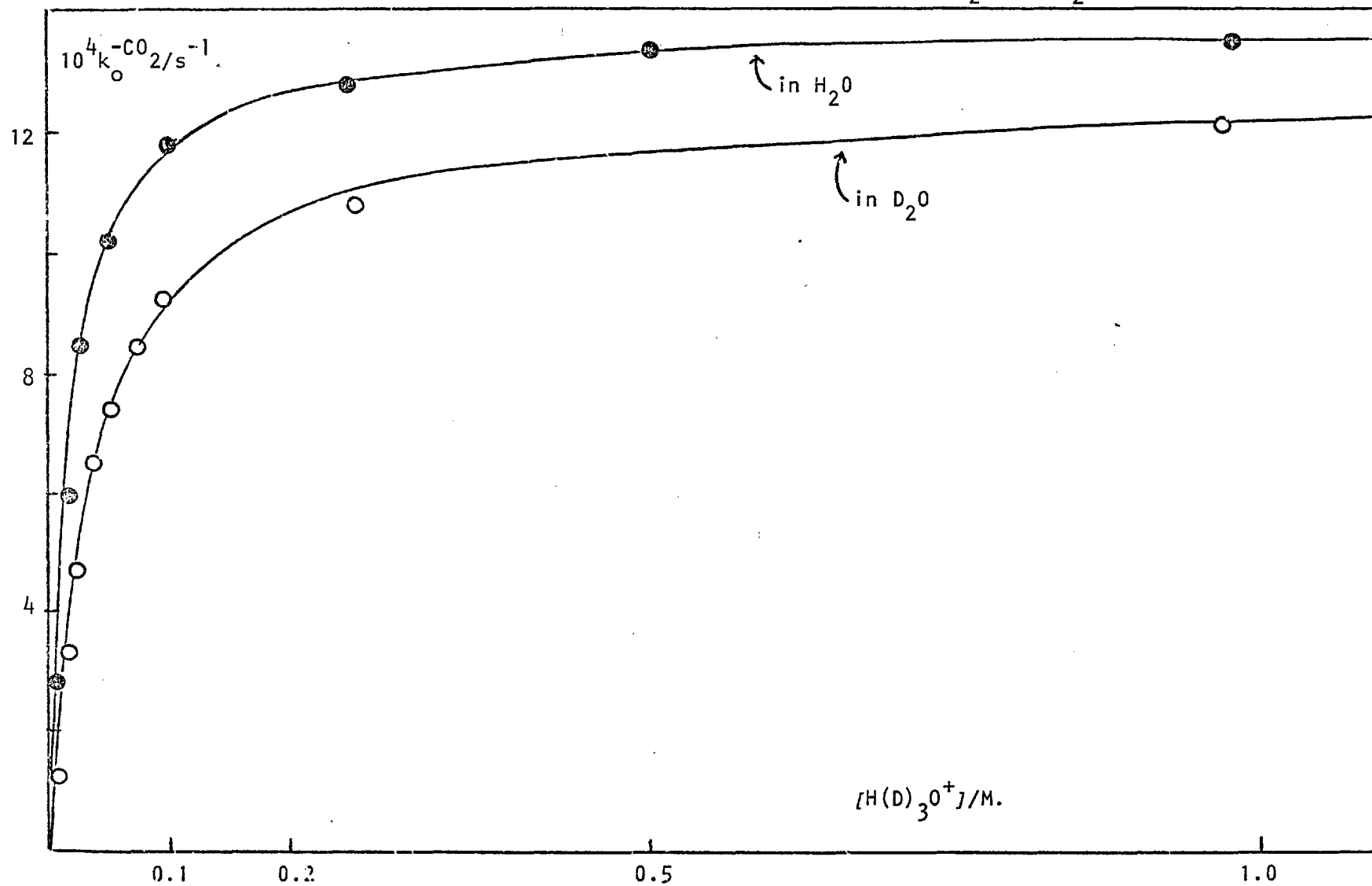


TABLE 4.10 Protodecarboxylation of 5-chloroindole-3-carboxylic acid at 25°C. $I = 1.0$

$[H_3O^+]/M.$	$10^6 k_o^{-CO_2}/s^{-1}.$	$10^6 k_o^{-CO_2} (Calc)$	Weight.
0.0198	2.05	2.04	13.9
0.0394	3.24	3.25	14.7
0.0598	4.12	4.13	12.3
0.0750	4.63	4.63	10.6
0.1001	5.29	5.26	8.6
0.1986	6.62	6.63	5.7
0.4012	7.69	7.65	4.2
0.6019	8.00	8.07	3.9
0.7993	8.23	8.29	3.7
1.000	8.51	8.43	3.5

$$a = 1.80 \pm 0.64 \times 10^{-7} s^{-1}.$$

$$b = 1.216 \pm 0.026 \times 10^{-4} s^{-1} \cdot M^{-1}.$$

$$c = 13.45 \pm 0.33 M^{-1}.$$

TABLE 4.11 Deuteriodecarboxylation of 5-chloroindole-3-carboxylic acid at 25°C. I = 1.0

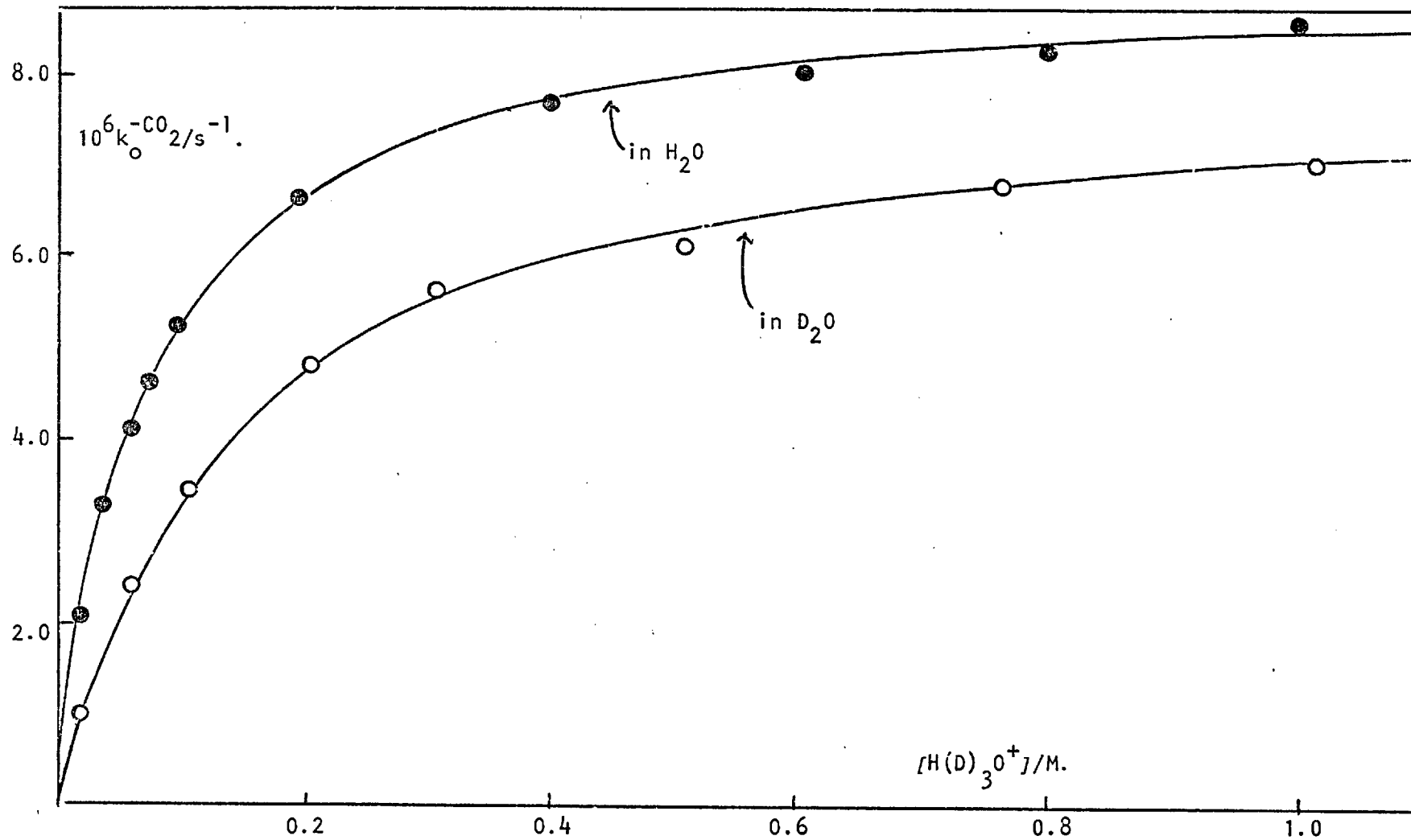
$[D_3O^+]/M.$	$10^6 k_o^{-CO_2}/s^{-1}$	$10^6 k_o^{-CO_2}$ (Calc)	Weight.
0.0205	0.995	0.974	4.6
0.0610	2.29	2.35	3.5
0.1090	3.44	3.42	2.0
0.2070	4.78	4.71	1.1
0.3080	5.58	5.46	0.8
0.507	6.16	6.26	0.66
0.761	6.79	6.78	0.54
1.016	7.01	7.07	0.51

$$a = -0.08 \pm 0.78 \times 10^{-7} s^{-1}.$$

$$b = 0.545 \pm 0.025 \times 10^{-4} s^{-1} \cdot M^{-1}.$$

$$c = 6.72 \pm 0.39 M^{-1}.$$

Figure 4.4 Decarboxylation of 5-chloroindole-3-carboxylic acid in H_2O and D_2O at 25°C .

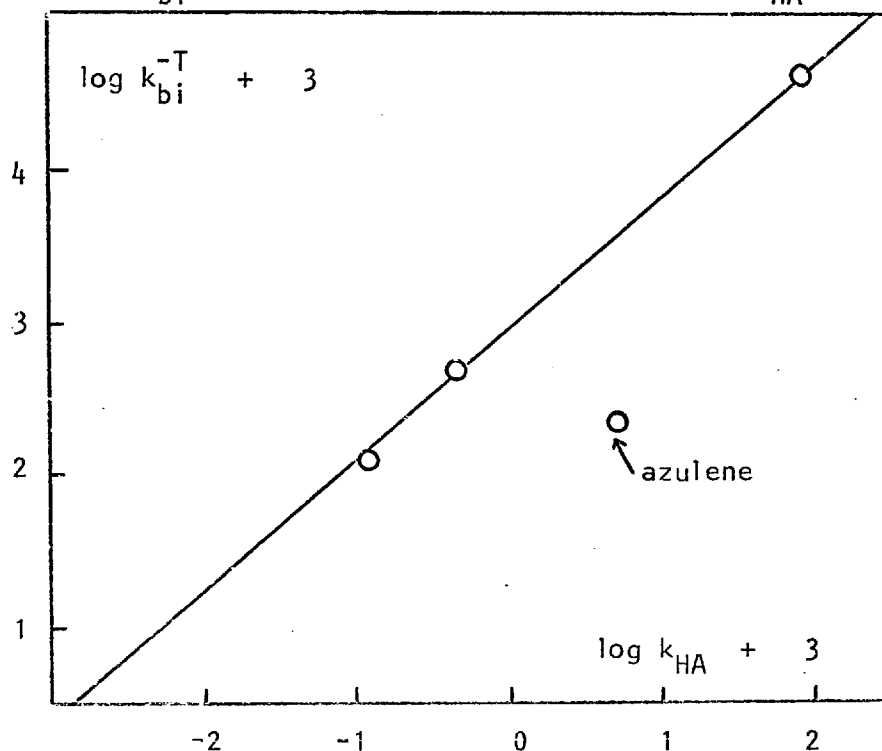


DISCUSSION

4.5 THE RATE EQUATION FOR DECARBOXYLATION.

The complexity of the full rate expression (equation 4.1) for the decarboxylation of indole carboxylic acids (Scheme 4.2) makes it necessary to take great care in interpreting the values of the parameters obtained. Of particular importance is whether k_{HA} accurately represents the rate of proton transfer to the aromatic nucleus. To test this the protonation rates for indoles themselves³⁵ were correlated with the parameters k_{HA} obtained for protonation of the carboxylic acids (Figure 4.5). A good straight line was obtained with three points, with a slope of 0.88 and this tends to confirm that k_{HA} reflects to a reasonable degree the rate of protonation of indole carboxylic acids.

Figure 4.5 Correlation between the rate of protonation of Indoles (k_{bi}^{-T}) and Indole-3-carboxylic acids (k_{HA}).



It is interesting to note that the data for azulene⁹¹ do not correlate very well with the points for indoles, the reasons for this not being very clear.

The rate constant k_{HA} must also be considered within the context of the full rate equation. When the carboxylic acid group is not ionised this can be shown to reduce to equation 4.10

$$k_o^{-CO_2} = a + b.[H^+]. \frac{k^*.K^3}{K^3(k^* + k_{-A}) + k_{-HA}[H^+]} \quad 4.10$$

Normally the assumption $k^* \gg k_{-A}$ is justified by the lack of a carbon isotope effect at low acidities^{92b}. Under this condition the equation reduces to

$$k_o^{-CO_2} = (a + b.[H^+]) / (1 + k_{-HA}[H^+] / K^3.k^*) \quad 4.11$$

and when $[H^+] \approx 0$ it can be seen that $k_o^{-CO_2}$ does not depend on the rate of C-C cleavage. Conversely, if $k^* \ll k_{-A}$ equation 4.10 reduces to

$$k_o^{-CO_2} = (a + b.[H^+]). \frac{k^*/k_{-A}}{1 + k_{-HA}[H^+] / K^3.k_{-A}} \quad 4.12$$

and when $[H^+] \approx 0$,

$$k_o^{-CO_2} = (a + b.[H^+]). (k^*/k_{-A}) \quad 4.13$$

and a full $^{13}C/^{12}C$ isotope effect of about 1.04 would be expected.

The relative magnitudes of k^* and k_{-A} also influence the primary deuterium solvent isotope effect, which is the ratio of the coefficients $b(\text{H}_2\text{O})/b(\text{D}_2\text{O})$ in equations 4.10 to 4.13. Thus this ratio is not affected if equation 4.11 applies, however if $k^* \ll k_{-A}$ then equation 4.12 applies and the solvent isotope effect is

$$b(\text{H}_2\text{O})/b(\text{D}_2\text{O}) = \frac{k_{\text{HA}} \cdot k_{-A}^{\text{D}}}{k_{\text{DA}} \cdot k_{-A}^{\text{H}}} \quad 4.14$$

where we have assumed that k^* is solvent independent. It is expected that $k_{-A}^{\text{H}} / k_{-A}^{\text{D}} \sim 7$ and consequently the evaluated isotope effect would be up to 7 times too small.

The conclusion to be drawn from the preceding argument is that the magnitude of the primary deuterium isotope effect may be altered if the equality $k^* \geq 10 k_{-A}$ does not hold.

Though information on this point would be obtained from measurement of the carbon isotope effects, an alternative approach is possible: If $k^* \ll k_{-A}$, the coefficient of $[\text{H}^+]$ in the denominator of equation 4.10 becomes

$$c = \frac{k_{-HA}}{k^* \cdot K^3} \quad 4.15$$

where c represents the evaluated parameter (equation 4.4). The solvent isotope effect on this parameter is

$$c(\text{H}_2\text{O})/c(\text{D}_2\text{O}) = \frac{k_{-HA} \cdot K^3(\text{D}_2\text{O})}{k_{-DA} \cdot K^3(\text{H}_2\text{O})} \quad 4.16$$

and since k_{-HA}/k_{-DA} may be expected to be about 7, whereas the solvent isotope effect on the equilibrium constant is normally

about 3^{97} , this leads to an overall ratio

$$c(\text{H}_2\text{O})/c(\text{D}_2\text{O}) = 2.3$$

which compares well with the values of 2.15 and 2.22 found for 2-methylindole and indolecarboxylic acids.

If $k^* \ll k_{-A}$, $c = k_{-HA}/k_{-A} \cdot K^3$ and so

$$c(\text{H}_2\text{O})/c(\text{D}_2\text{O}) = \frac{k_{-HA}}{k_{-DA}} \frac{k_{-A} K^3(\text{D}_2\text{O})}{k_{-A} K^3(\text{H}_2\text{O})} \quad 4.17$$

Both rate ratios may be expected to give deuterium isotope effects of about 7, and the equilibrium constant one of about 3^{97} , leading to an overall solvent isotope effect of

$$c(\text{H}_2\text{O})/c(\text{D}_2\text{O}) = 0.33$$

This suggests that as the inequality $k^* \gg k_{-A}$ reverses, the solvent isotope effect on the evaluated parameter c changes from 2.3 to 0.3. In practice, only the value for 5-chloroindole carboxylic acid has the slightly low value of 2.0, which suggests the approximate equality $k^* = 5k_{-A}$. This has two ramifications. It increases the observed primary deuterium isotope effect from about 2.23 to 2.6, bringing it into line with the other results. Also predicted is a small carbon isotope effect of about 1.007 (assuming a full value of 1.04) for the ratio b ($^{13}\text{C}/^{12}\text{C}$). It is interesting to speculate that the electron withdrawing substituents on the indole tend to preferentially weaken the C-H bond rather than the C-C bond, thus bringing the postulated equality between k^* and k_{-A} about.

4.6 THE MAGNITUDE OF THE DEUTERIUM ISOTOPE EFFECTS.

Only in the case of indole carboxylic acid was it possible to obtain a reasonably accurate value for the product $k_A \cdot K^2$. The solvent isotope effect was found to be 2.56 for this parameter. Since the solvent isotope effect on K^2 alone should be about 3, together with an isotope effect of not more than about 3.6 for the rate constant⁹⁸ it can be seen that the experimental value is about 3-4 times too low. One possible explanation is that this parameter reflects the extent of the homolytic decarboxylation which occurs in the reaction, being effectively the decarboxylation rate at zero hydronium ion concentration. Homolytic decarboxylation would not be expected to show a solvent isotope effect and if about 30% of the reaction goes by this pathway at low acidity the isotope effect for the product $k_A \cdot K^2$ would be reduced considerably in magnitude. The behaviour of this indole at high pH (Section 4.2.2) precludes the homolytic rate from being much higher than this value.

The primary deuterium isotope effect for the protonation of the indole carboxylic acids, and also some data for indoles themselves have been summarised in Table 4.12 . The low values for the isotope effects are expected for catalysis by the hydronium ion, arising from a secondary solvent isotope effect⁹⁸ and the maximum predicted classical value is about 3.6 . The observed values vary from about 61% to 76% of this value- and included in this range is the value obtained by Long for azulene-1-carboxylic acid and

TABLE 4.12 Deuterium solvent isotope effects for the protonation of aromatic substrates at 25°C.

Substrate	$k_{H_3O^+}/k_{D_3O^+}$	$k_{bi}(H_3O^+)/s^{-1}M^{-1}$
Indole, 3-CO ₂	2.72	0.454
.. 3-CO ₂ , 2-Me	2.35	80.0
.. 3-CO ₂ , 5-Cl	2.23	0.122
.. 3-H, 2-Me	2.59	41,000
.. 5-CN	2.60	5.27
Azulene, 1-CO ₂	2.5	5.39
.. 1-H	-	181
Indole 1-H	-	500
.. 5-Cl	-	118

the two solvent isotope effects obtained for 2-methylindole by Challis and Millar^{35b} and 5-cyanoindole by Iqbal⁶⁰.

The values are constant over a range of reactivity of 10^5 which again tends to suggest that primary isotope effects are insensitive to changes in reactivity, and as a result, transition state symmetry. Also, large changes in the reacting system, caused by the introduction of a 3-carboxy substituent, do not appear to significantly influence the isotope effects. It did not prove possible to study the

transition states further by utilising steric effects, since the corresponding 4-^tbutylindolecarboxylic acids could not be synthesised. Nevertheless the general conclusions concerning isotope effects and transition state symmetry seem substantiated by the results for indole carboxylic acids.

CHAPTER V

HYDROGEN EXCHANGE OF 2-INDOLINONES

5.1 INTRODUCTION.

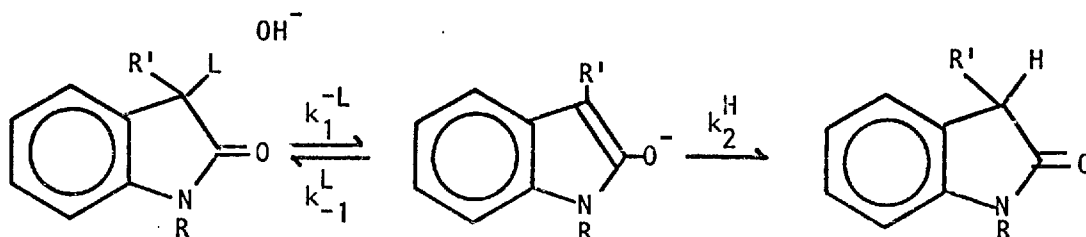
Indolinones are formally the 2-hydroxy derivatives of indoles, though in solution they exist almost entirely in the keto form (Scheme 5.1). This is probably true of the solid too, where i.r. shows only a small amount of absorption attributable to the enol form.



Scheme 5.1 Indole-Indolinone tautomerism.

Little work has been done on hydrogen exchange of these compounds, though it is known that N-methylindolinone (or N-methyloxindole) exchanges the 3- protons on reflux with $\text{Na}_2\text{CO}_3/\text{D}_2\text{O}$ ⁹⁹. This suggests a close similarity to α -keto compounds, for which a considerable bulk of work has been reported and the exchange mechanism well established³⁸. By analogy, indolinones are expected to undergo base catalysed hydrogen exchange by the route shown in Scheme 5.2 .

Scheme 5.2 The hydrogen exchange mechanism for Indolinones.

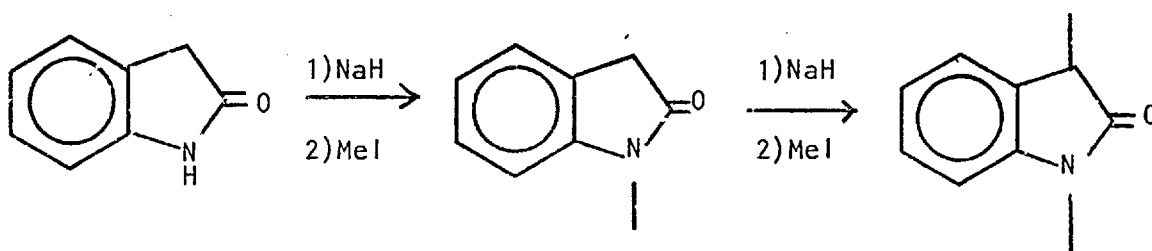


For actual study, N-methylindolinones were used to prevent possible complications arising from ionisation of the N-H hydrogen. Further, problems due to secondary isotope effects were reduced by using 3-alkylated substrates wherever possible.

5.1.1 SYNTHESIS OF SUBSTRATES.

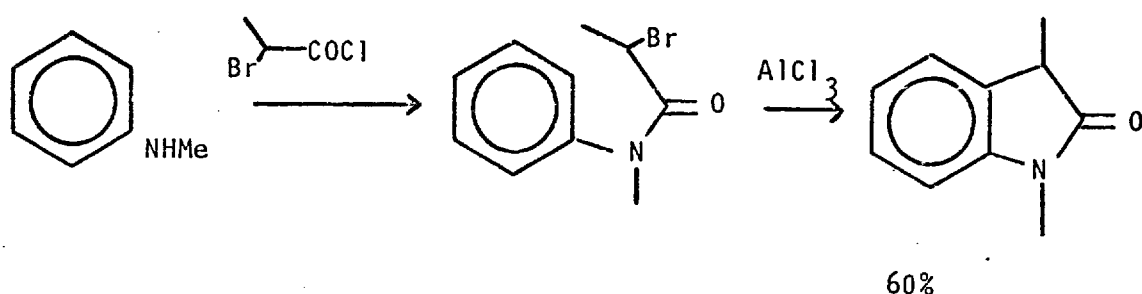
Alkylated indolinones are often obtained by alkylation of the parent indolinone¹⁰⁰, which can be achieved sequentially by using sodium hydride (Scheme 5.3).

Scheme 5.3 The sequential alkylation of Indolinones.



All three alkylated products are obtained in practice, and subsequent purification is difficult. A specific route to the 1,3-dimethylindolinone has been reported by Julian¹⁰¹ (Scheme 5.4).

Scheme 5.4 The Julian¹⁰¹ Synthesis of Indolinones.

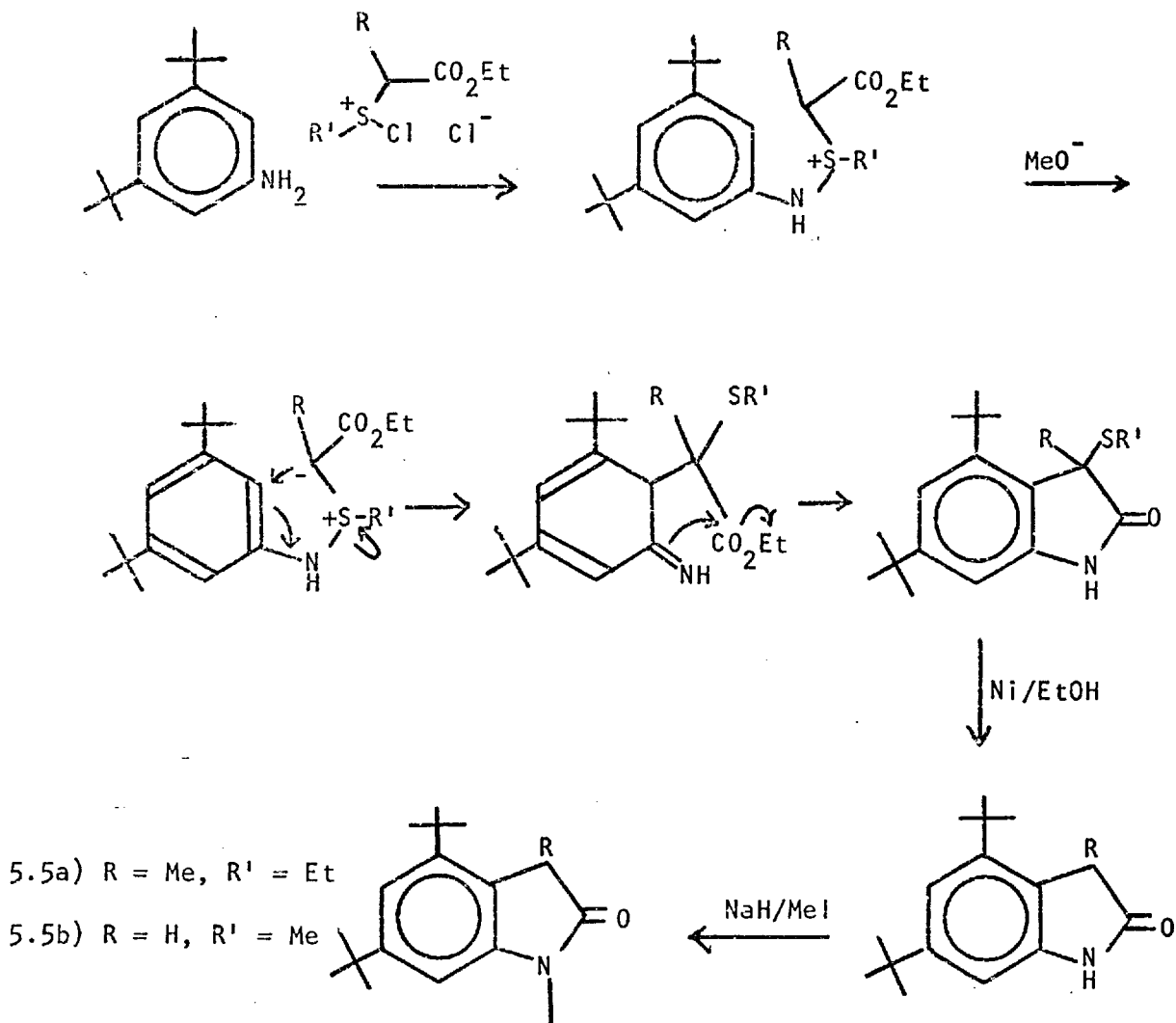


^t-Butyl substituted Indolinones.

The most available precursor to 1- and 1,3- methyl-4-^tbutyl indolinones was considered to be 3,5-dibutylaniline. The Julian method was first tried, but no Lewis acid was found that could effect cyclisation of the intermediate α -bromoacetanilide. The recently reported Gassman synthesis⁵³ was tried next (Scheme 5.5). In the case of Scheme 5.5a, cyclisation did not occur, the intermediate azasulphonium ylide not undergoing the normally rapid and facile [2,3] sigmatropic rearrangement. The butylindolinone was finally prepared by the route in Scheme 5.5b. N-Methylation was achieved using NaH/Mel in pentane, and the second methyl group introduced by changing the solvent to toluene. No

trialkyl products were formed in appreciable quantities, compared with the very facile trialkylation of indolinone itself.

Scheme 5.5 The Gassman⁵³ Synthesis of Indolinones.



5.1.2 EXCHANGE RATES BY TRITIUM OR DEUTERIUM ANALYSIS.

For the exchange mechanism shown in Scheme 5.2, the steady state derivation gives

$$-d[L]/dt = \frac{k_1^{-L} [HO^-] \cdot [Substrate]}{1 + \frac{k_1^L}{k_2^H}} \quad 5.1$$

For loss of L = T,D to H₂O, the internal return (k_{-1}^L) is negligible and equation 5.1 reduces to equation 5.2 .

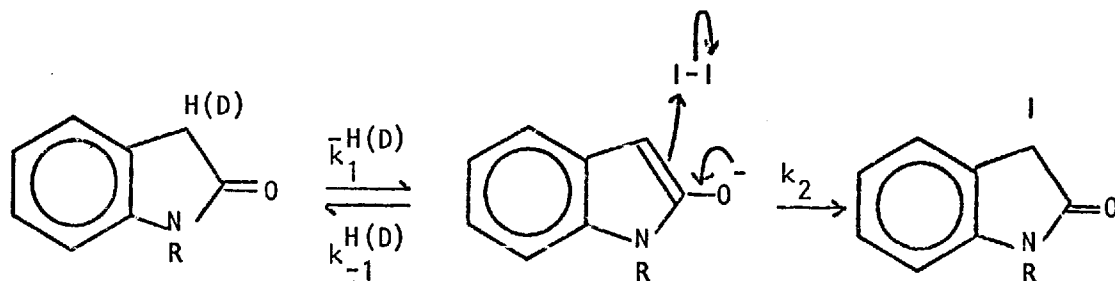
$$\begin{aligned}
 - d[L]/dt &= k_1^{-L} \cdot [HO^-] \cdot [3\text{-}^X H_1 \text{ substrate}] & 5.2 \\
 &= k_o^{-L} \cdot [3\text{-}^X H_1 \text{ substrate}]
 \end{aligned}$$

For loss of L = H to D₂O, the denominator of equation 5.1 is slightly greater than unity and a small correction has to be applied. It can be show that both equations 5.1 and 5.2 are approximate forms of a more rigorous expression derived for exchange of such systems by Long¹⁰².

5.1.3 PROTON AND DEUTERIUM EXCHANGE RATES BY HALOGENATION.

Not all the substrates could be studied by direct (mass spectrometric) deuterium estimation and several alternatives exist. Potentially an attractive method is following the rate of racemisation of an optically active indolinone, however this could only be used with compounds which have Chiral centres. Of more general application is the halogenation method. This, in its various forms, has been discussed in numerous papers by Bell¹⁷ and a survey is given by Jones³⁸. The most common variation, and the method used here, involves trapping out the intermediate enolate anion formed by ionisation with iodine (Scheme 5.6).

Scheme 5.6 The iodination of Indolinones.



$$-d[I_2]/dt = \frac{\bar{k}_1^H \cdot [OH^-] \cdot [Indolinone]}{1 + k_{-1}^H/k_2 [I_2]} \quad 5.3$$

Several experimental conditions are imposed.

a) $[I^-] \gg [I_2]$ Since the equilibrium constant (equation 5.4)

$$[I_3^-]/[I^-] \cdot [I_2] = 715^{(Ref. 17)} \quad 5.4$$

is so large the iodide liberated during the course of the reaction will not affect the fraction of total iodine present as I₂. It follows that

$$d[I_2]/dt = d[I_3^-]/dt \quad 5.5$$

b) $[Indolinone] \gg [I_2]$ and the indolinone concentration is constant throughout. Equation 5.3 then reduces to

$$-d[I_3^-]/dt = \frac{{}^*k_1^H}{1 + k_{-1}^H/k_2^* [I_3^-]} \quad 5.6$$

where ${}^*k_1^H = \bar{k}_1^H \cdot [OH^-] \cdot [Indolinone]$ and $k_2^* = k_2/715 [I^-]$

Integration of equation 5.6 gives

$$[I_3^-] = k_1^H \cdot t - \frac{k_{-1}}{k_2} \cdot \ln[I_3^-] + \text{const} \quad 5.7$$

Equation 5.7 reaches two limits, depending on the value of $k_{-1}/k_2^*[I_3^-]$. If this is less than unity, then

$$\Delta[I_3^-]/\Delta t = k_1^H \quad 5.8$$

This zero order form is normally observed in these reactions³⁸ and suggests that reprotonation of the enolate anion is slow. If $k_{-1}/k_2^*[I_3^-] \gg 1$, then

$$\ln[I_3^-] = \frac{k_1^H \cdot k_2^*}{k_{-1}} t + \text{const} \quad 5.9$$

and consequently if reprotonation of the enolate is fast compared with iodination, a first order dependence in $[I_3^-]$ should be observed. Such a kinetic form is indeed observed for the ionisation of phenylacetylene¹⁰³. If the kinetic form is neither of these extremes, then the integrated form of equation 5.6 has to be used. This intermediate behaviour has been observed for acid catalysed iodination of acetone¹⁰⁴ and the base catalysed halogenation of ortho-hydroxy acetophenone¹⁰⁵.

Both proton and deuterium ionisation rates can be measured by this method, though certain ramifications arise out of the reprotonation of the enolate. Since this occurs from the H₂O solvent, the value obtained for k_{-1}/k_2^* should be independent of the original isotopic composition of the substrate, and this is open to

experimental verification. Secondly, care must be taken to adjust the experimental conditions such that this reprotonation does not dilute the isotopic purity of the substrate excessively.

It can be seen then that indolinones are a potentially useful system for probing the properties of isotope effects, without the inherent disadvantages associated with hydrogen exchanges of indoles themselves.

RESULTS

5.2 TRITIUM EXCHANGE OF 1,3-DIMETHYLINDOLIN-2-ONE.

Aqueous solutions of 50%(w/w) methanol were used throughout, in order to provide a comparison with the results for indoles. Hydrogen exchange was found to be of a convenient order between pH 8-10 for this indolinone and normally a dilute (0.01 M) sodium tetraborate buffer was used to maintain the pH. Comparison with results in dilute sodium hydroxide solutions suggests the contribution to the rate from general base catalysis by the borate will be small.

Excellent first order protodetrutiation kinetics were observed, for at least 98% reaction and the rate was found to be catalysed by OH^- (Table 5.1). A plot of $k_{\text{O}}^{-\text{T}}$ (equation 5.2) against the hydroxide concentration was found to pass through zero (Figure 5.1), suggesting no contribution at this pH from any acid catalysed pathway.

5.3 PROTIUM AND DEUTERIUM EXCHANGE OF 1,3-DIMETHYLINDOLIN-2-ONE.

Iodination was studied using an excess (> 14 fold) of the indolinone over the initial iodine concentration. A curved plot of $[I_3^-]$ against time was obtained, whereas zero order kinetics require a linear plot. When plotted in first order form (equation 5.9) a

TABLE 5.1 Protodetrition of 1,3-dimethylindolinone in 50%(w/w) aqueous methanol/tetraborate buffers. T = 25°C, I = 0.13 maintained with KI.

pH_m	$10^5 k_o^{-T}/s^{-1}$.	$k_I^{-T}/s^{-1} \cdot M^{-1}$.	Run
9.040	1.31	1.19	467
8.920	0.991	1.19	468
8.724	0.631	1.19	469
8.227	0.223	1.23	470

Note. pH_m represents the measured pH. The effective pa_H^* = $pH_m - 0.13$ (Ref. 57) but this was consistently not applied to facilitate comparison of rates.

Figure 5.1 Protodetrition of 1,3-dimethylindolinone in 50%(w/w) methanol/tetraborate buffers.

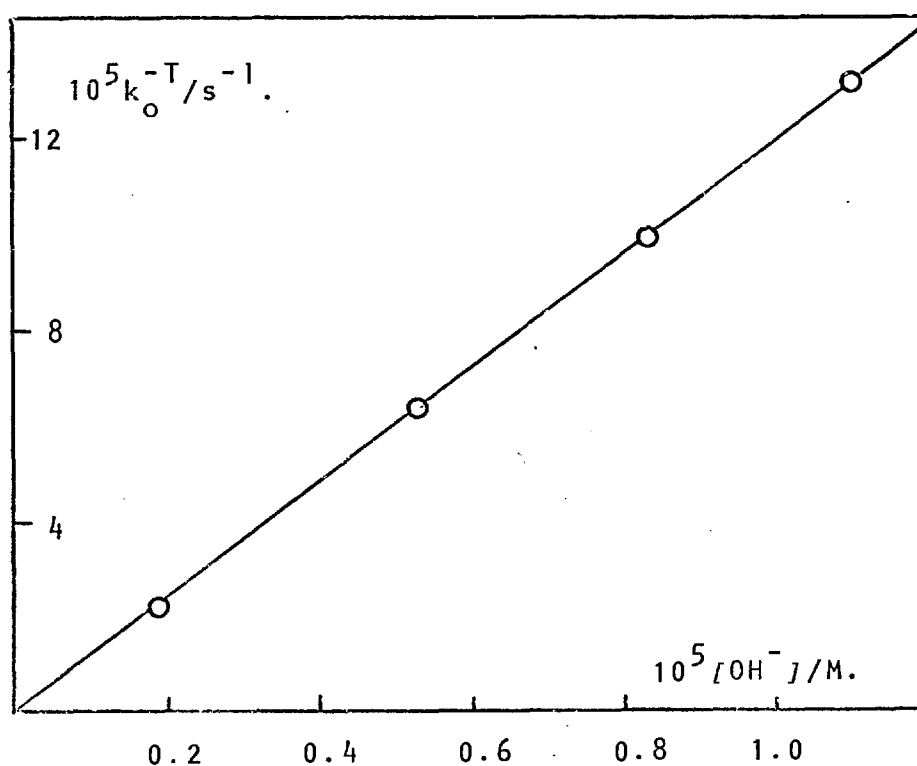
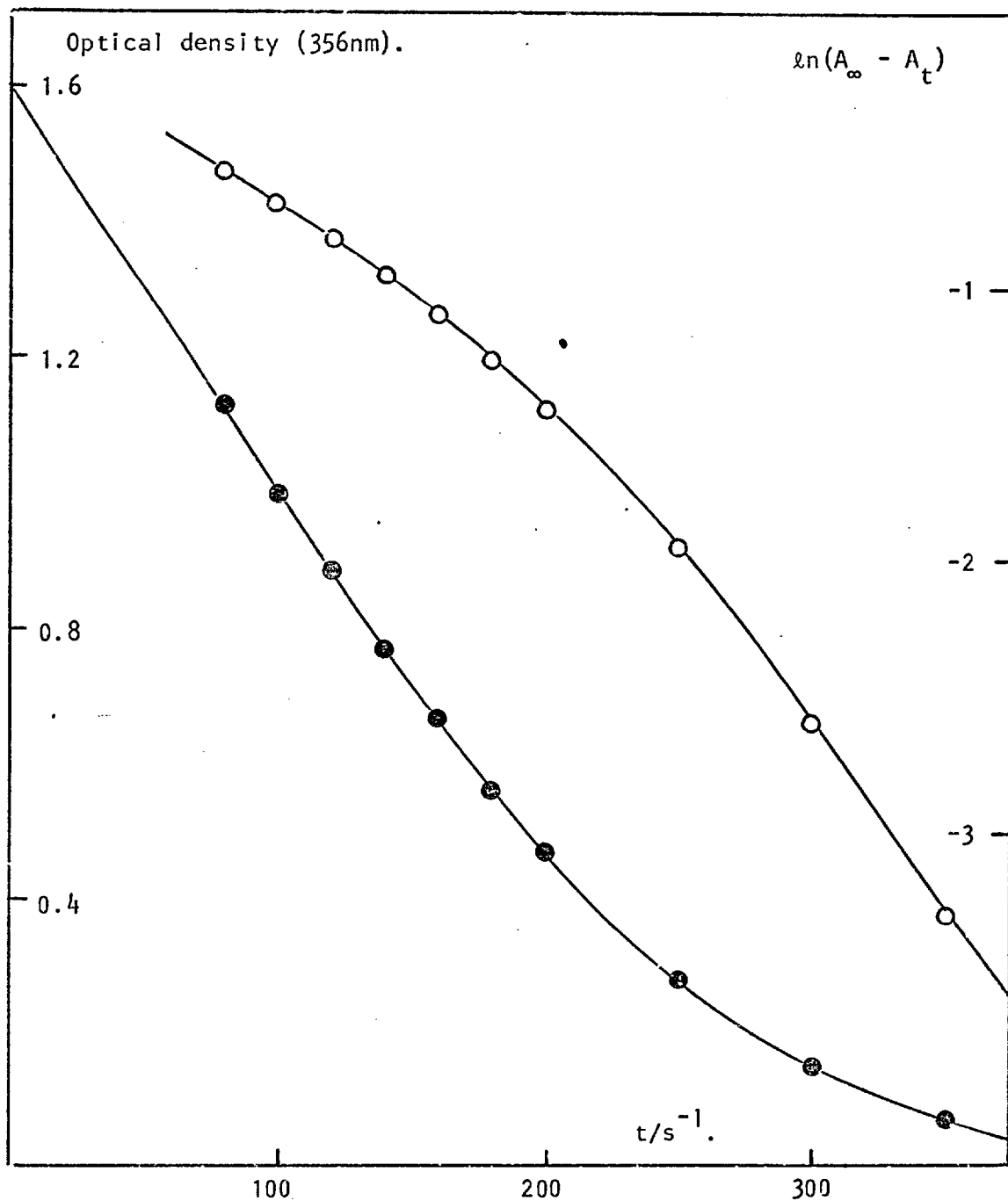


Figure 5.2 Iodideprotonation of 1,3-dimethylindolinone at pH_m 9.118 and 25°C . $[\text{Indolinone}] = 2 \times 10^{-3}\text{M}$. $[\text{I}_2]_{\text{initial}} = 6 \times 10^{-5}\text{M}$. $[\text{I}^-] = 0.1$ Run 445.



⊗ 'Zero order plot'. The solid line is that calculated using equ. 5.7

○ 'First order plot'. Plotted according to equ. 5.9

curve is also obtained (Figure 5.2). This kinetic form was completely reproducible, and was not changed on using a sample of zone refined dimethylindolinone. The initial slope of the zero order plot (Figure 5.2) gave a value for the protium exchange rate which was in approximate agreement with the established tritium exchange rate and accordingly the data was treated using equation 5.7 . As can be seen from the figure equation 5.7 gives an excellent statistical fit to the data (see section 6.4.5 for a further discussion) which tends to suggest that for this indolinone reprotonation is fairly fast compared with iodination.

An important fact to emerge is that the value obtained for $^*k_1^H$ from equation 5.7 ($37.2 \times 10^{-8} \text{ M.s}^{-1}$) is more than 50% greater than the initial slope of the zero order plot ($25.0 \times 10^{-8} \text{ M.s}^{-1}$). This suggests that taking the initial slope of even a slightly curved 'zero order' plot may only give an approximate value for the rate constant. Some reported literature rate constants may therefore be of questionable accuracy.

Variation of the indolinone concentration and also the pH_m leads to the same value for \bar{k}_1^H and also k_{-1}/k_2^* (Table 5.2) which further justifies the treatment adopted here. It can also be seen that the initial iodine concentration does not affect these values, as expected. The sole contribution to the exchange rate appears from the hydroxyl catalysis as shown by a plot of $^*k_1^H$ against the hydroxide concentration (Figure 5.3), which has a least squares intercept of zero.

$$\text{slope} = k_1^{-H} = 13.74 \pm 0.20 \text{ s}^{-1} \cdot \text{M}^{-1}$$

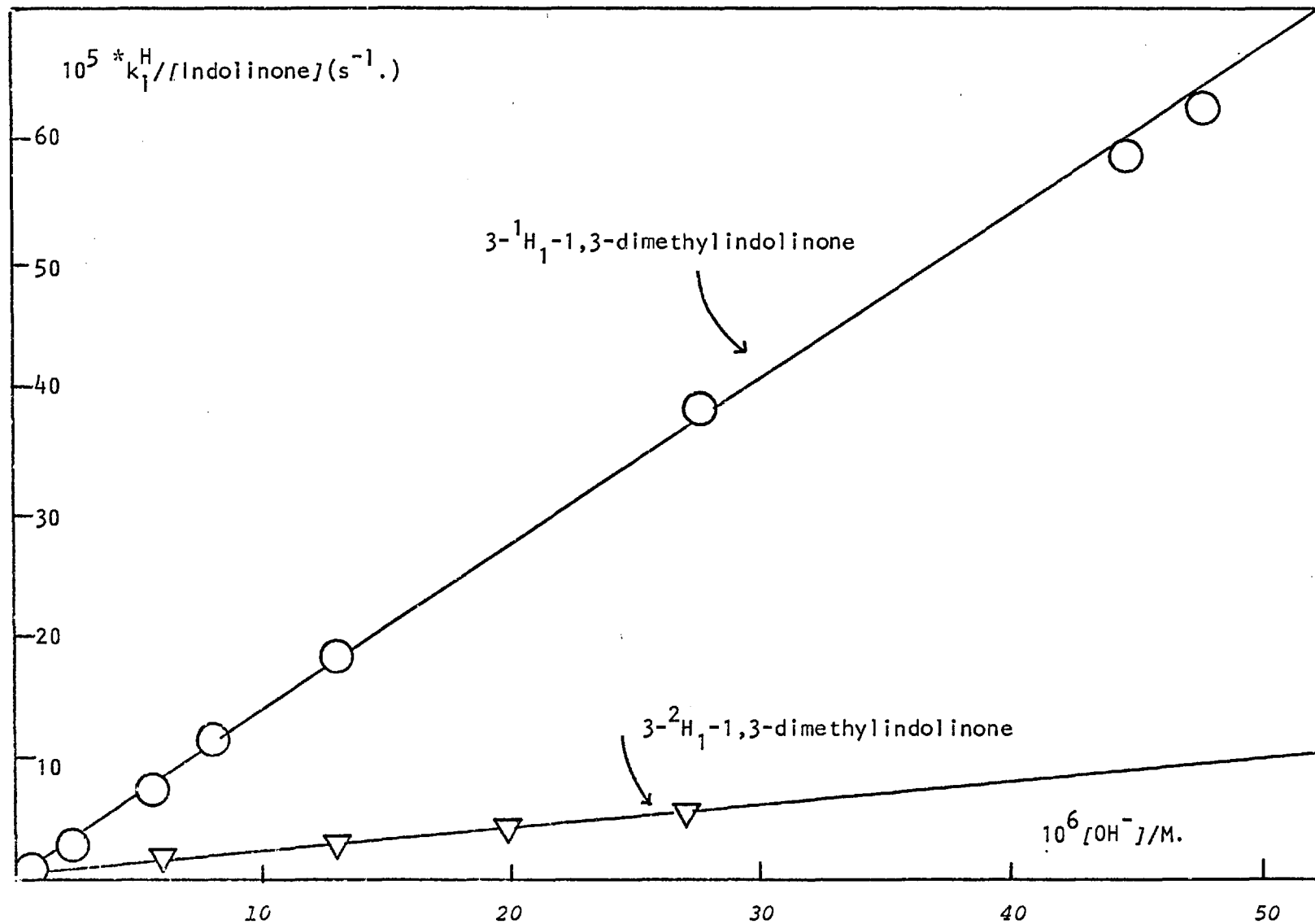
$$\text{Intercept} = -0.006 \pm 0.005 \times 10^{-4}$$

TABLE 5.2 Iododeprotonation of 1,3-dimethylindolinone in 50%(w/w) aqueous methanol/tetraborate buffers at 25°C. $[I^-] = 0.12M$. $[I_2]_{initial} = 6 \times 10^{-5}M$.

pH_m	$10^6 [OH^-] [Indolinone]$	10^3	$10^5 k_{-1}/k_2^*$	$10^8 * k_1^H / M.s^{-1}$	$k_1^{-H} / s^{-1} M^{-1}$
7.910	0.813	10	2.08	10.8	13.34
8.350	2.24	5	2.18	15.5	13.84
8.360	2.30	10	1.96	29.0	12.61
8.582	3.82	5	1.94	25.2	13.19
8.750	5.62	2	2.14	14.9	13.26
8.903	8.00	2	2.26	22.8	14.25
9.108	12.8	2	2.01	35.9	14.06
9.108	12.8	2	2.01	37.8	14.77
9.115*	13.0	2	2.23	32.3	12.40
9.118	13.1	1	2.07	18.0	13.74
9.118	13.1	2	2.29	37.2	14.20
9.437	27.4	1	2.28	38.1	13.90
9.648	44.5	1	2.16	58.4	13.12
9.672	47.0	1	2.19	62.2	13.23
Mean			<u>2.12</u>		<u>13.67</u>

* $[I_2]_{initial} = 2 \times 10^{-4}M$, followed at 390 nm.

Figure 5.3 Protium and deuterium exchange rates of 1,3-dimethylindolinone by iodination.



It was found that 1,3-dimethylindolinone could be easily deuteriated, and n.m.r. established the site of exchange as the 3-position. The rate of ionisation was measured by the iodination method (Table 5.3) and it should be noted that the value for k_{-1}/k_2^* was identical to that obtained previously, suggesting that it is indeed a fast reprotonation that causes the departure from zero order iodination kinetics. The magnitude of the primary deuterium isotope effect corroborates the proposed mechanism; this result will be discussed in detail later.

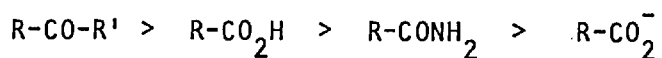
TABLE 5.3 Iododeuteriation of 1,3-dimethylindolinone in 50% (w/w) aqueous methanol/tetraborate buffers at 25°C. $[I^-] = 0.12M$, $[I_2]_{initial} = 6 \times 10^{-5}M$.

pH_m	$10^6 [OH^-]$	$10^2 [Indolinone]$	$10^5 k_{-1}/k_2^*$	$10^8 *k_1^D/M.s^{-1}$	$k_1^{-D}/s^{-1}M^{-1}$
8.050	1.12	2	3.65	5.09	2.27
8.800	6.31	1	2.14	15.2	2.41
9.072	11.8	1	2.13	26.6	2.25
9.075	11.9	1	2.38	28.3	2.38
9.118	13.1	1	2.08	28.6	2.18
9.303	20.1	1	2.51	41.0	2.04
9.432	27.0	0.5	2.06	31.9	2.35
Mean			<u>2.23</u>		<u>2.27</u>

DISCUSSION

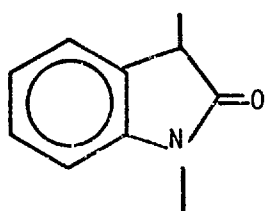
5.4 THE EXCHANGE KINETICS OF 1,3-DIMETHYLINDOLINONE.

The results of the previous section suggest that the hydroxyl catalysed ionisation of indolinones proceeds by a mechanism totally analogous to the well established ionisation of carbonyl and nitro compounds. Since formally indolinones are amides, a comparison of the reactivity of this group with other acidifying substituents can be made.¹⁰⁶



Given below are some literature rate constants for the ionisation of various carbon acids.

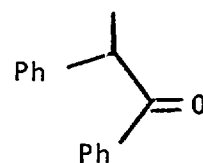
Scheme 5.7 The ionisation rate constants for various carbon acids.



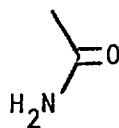
$k_1^{-H}/s^{-1} \cdot M^{-1}$ 14



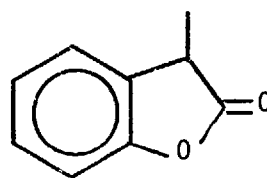
0.167 (Ref. 107)



0.0251 (Ref. 108)



$\sim 10^{-5}$ (Ref. 106)



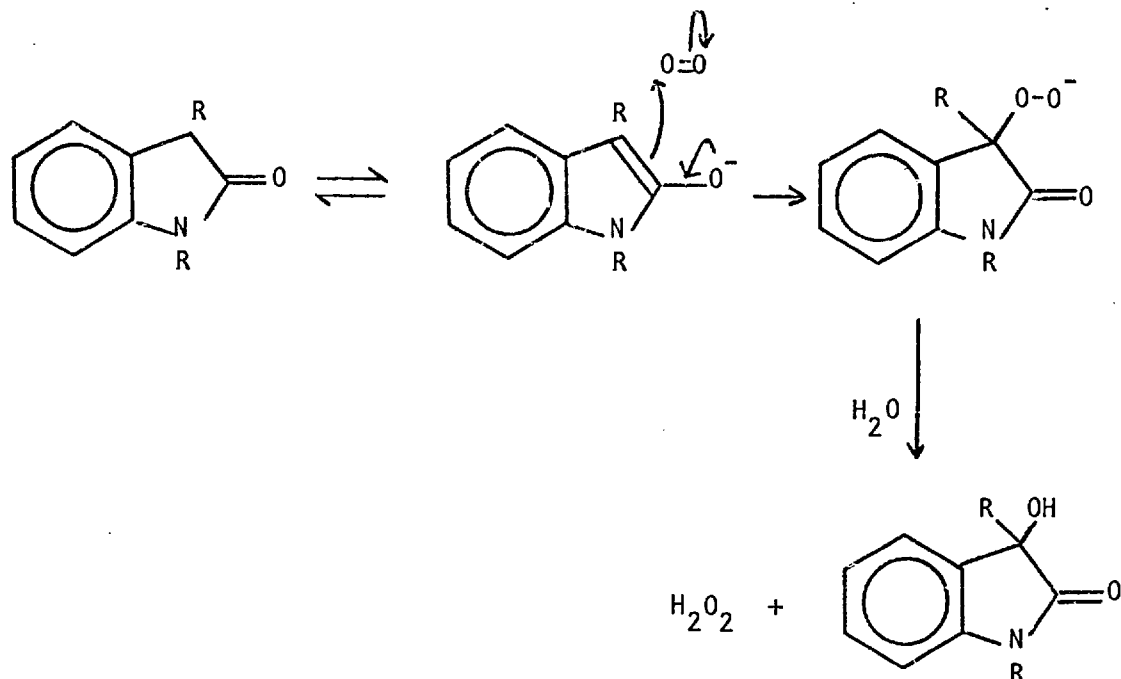
?

Remarkably, the indolinones are perhaps 10^6 kinetically more acidic than acetamide, a fact which qualitatively has been known a long time^{50b}. Further, reprotonation of the enolate anion approaches the rate of nucleophilic attack on molecular iodine, behaviour which is unusual for carbonyl compounds¹⁰⁵. The rapid ionisation can be rationalised in terms of the stability of the enolate ion, which can conjugate with the aromatic ring and which should be reflected in the pK_E for ionisation. Measurement of the ionisation ratio by U.V. was complicated by rapid air oxidation (Section 5.4.1) but a crude estimate was obtained by the method used previously for indoles themselves (Section 2.10.2). Reaction of N-methyl indolinone with p-nitrobenzenediazonium tetrafluoroborate yields what appears to be 3H-3-(p-nitrophenylazo)-N-methylindolin-2-one or a tautomer. This species ionises (apparently slowly, $k_1^{-H} \sim 0.16 \text{ s}^{-1} \cdot \text{M}^{-1}$.) with a pK_E about equal to 5-nitro-3-(p-nitrophenylazo)-2-methylindole, suggesting that N-methylindolinone has an acidity about the same as 5-nitroindole (~ 14.7). This compares with a pK_E of about 22 for acetone and perhaps 16-17 for a cyclic ketone such as cyclopentanone³⁸.

5.4.1 THE ACCURACY OF IONISATION RATES BY IODINATION. AIR OXIDATION.

Tertiary ketones are particularly prone to air oxidation and the consequences of this are not always considered. Gold^{22a} has discussed this problem several times in detail. Indolinones are not exceptional, absorbing molecular oxygen in basic solutions only^{50b}. (Scheme 5.8).

Scheme 5.8 The air oxidation of indolinones.



The α -keto alcohol ($R = \text{Me}$) was indeed isolated by passing oxygen through a solution of dimethylindolinone in sodium methoxide/methanol/ether, and was first discovered by Julian¹⁰⁹ using essentially the same method.

Since oxidation is subsequent to ionisation, this has no effect on deuterium exchange rates. Only if oxygen competes effectively with water for the enolate ion will deuterium exchange followed by mass spectrometry be affected. The consequence, curved first order rate plots, were only observed once (over only the last 10% of exchange) and the initial slope was taken (Section 5.6).

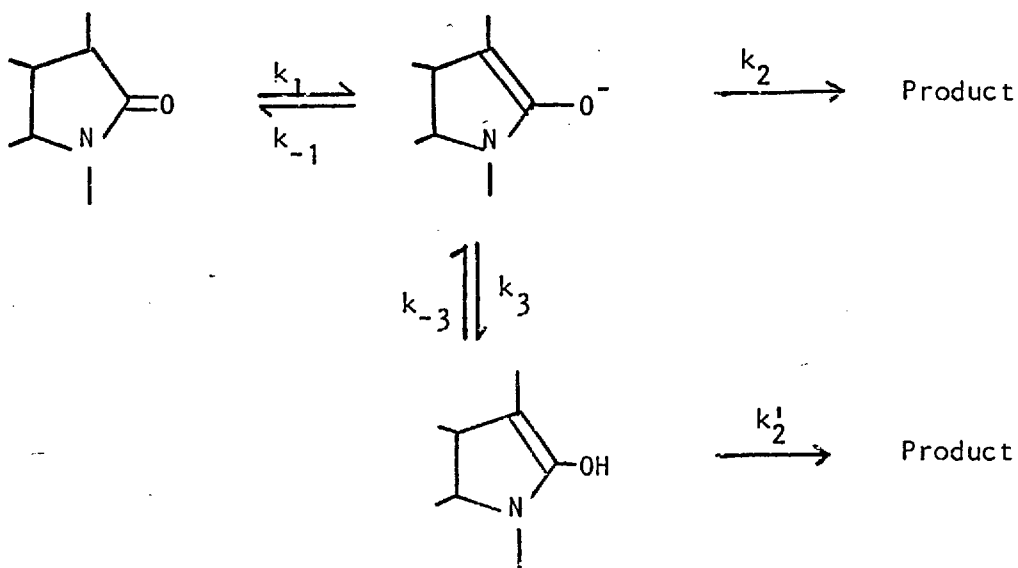
Iodination kinetics are more complex, since though the alcohol does not liberate iodine, the intermediate hydroperoxide does^{22a}. It was found however that only a stock solution of dimethylindolinone which had been kept at $\text{pH} \sim 10$ for at least a day liberated molecular iodine from potassium iodide before consuming it again. As a precaution all solutions were degassed before use, nevertheless it

may be that only a slight amount of oxidation perturbs the kinetics of iodination appreciably.

5.4.2 IODINATION THROUGH THE NEUTRAL ENOL INTERMEDIATE.

The iodination of enols is a well studied reaction¹⁰⁴, and the consequences of an accumulation of intermediate enol (2-hydroxy indole) were studied here (Scheme 5.9).

Scheme 5.9 Reaction of the neutral enol with iodine.



Assuming steady state conditions for the enol and enolate ion;

$$-d[I_2]/dt = \frac{k_1 [\text{Indolinone}] [\text{OH}] \left\{ 1 + k_2' \left(\frac{[I_2]}{k_{-3}} + \frac{k_3}{k_{-3} k_2} \right) \right\}}{1 + \frac{k_{-1}}{k_2} [I_2] + k_2' \left(\frac{k_{-1}}{k_2 k_{-3}} + \frac{k_3}{k_{-3} k_2} + \frac{[I_2]}{k_{-3}} \right)}$$

If $k_2' = 0$ then the equation reduces to the normal form. Proton transfer from oxygen is normally fast and hence $k_{-3} \sim 10^8$ and since $[I_2] = 10^{-5}$ the terms $[I_2]/k_{-3}$ and $k_{-1}/k_2 k_{-3}$ can be ignored.

Equation 5.10 now reduces to

$$-d[I_2]/dt = \frac{k_1 [\text{Indolinone}] [OH^-]}{1 + k_{-1}/k_2 [I_2] \left\{ 1 + \frac{k_2' k_3}{k_{-3} k_2} \right\}} \quad 5.11$$

This result suggests that according to Scheme 5.9, the rate constant k_1 will not be influenced by any reaction via the neutral enol.

5.4.3 THE ISOTOPIC PURITY OF THE SUBSTRATE.

When deuterium exchange is followed by iodination, high isotopic purity is necessary, nevertheless in practice 1-2% H remain. A certain amount of H is also introduced if the reprotonation of enolate ion is fairly fast. This last error is probably minimised for indolinones since the analytical analysis of the data tends to extrapolate to zero time, when the original isotopic purity of the substrate is still intact. The isotopic impurity can be corrected for by using equation 3.13

$$y = \frac{y_0 \cdot \Omega}{1 - y_0 (1 - \Omega)} \quad 3.13$$

but neglect of this term can have an appreciable effect on evaluated parameters, such as the Swain-Schaad exponent r (Section 3.6.1).

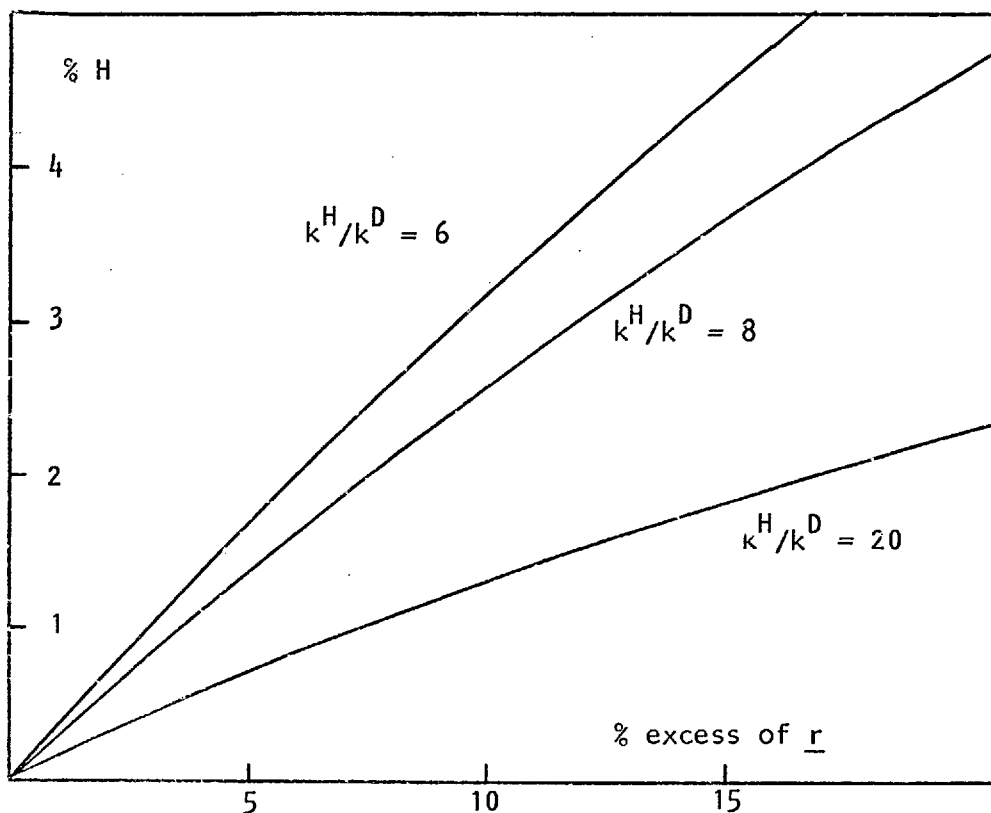
As a preamble to the next section, it is worth considering the effect of a small protium content on Swain-Schaad exponents calculated from rate constants measured by the iodination method

(Figure 5.4). Application of equation 3.13 gives the following approximate rule,

$$\% \text{ error in } \underline{r} = 0.4\gamma \cdot \Omega \quad (\Omega > 96\%)$$

and the results are shown in Figure 5.4 . It can be seen that only 1% H content, if not corrected for, can give a value for \underline{r} which is 3%, or $1.442 + 0.044$ too high. Much literature data, particularly early work, may be prone to this error⁴⁰.

Figure 5.4 The error in the Swain-Schaad exponent as a function of the isotopic purity.



5.5 KINETIC ISOTOPE EFFECTS FOR 1,3-DIMETHYLINDOLINONE.

The rate constants reported previously give the following isotope effects.

$$k_1^{-H} = 13.74 \pm 0.2 \quad k_1^{-D} = 2.15 \pm 0.06 \quad (\text{Corrected for } 1\% \text{ H}) \quad k_1^{-T} = 1.19 \pm .03$$

$$k_1^{-H}/k_1^{-D} = 6.36 \pm 0.21 \quad k_1^{-H}/k_1^{-T} = 11.48 \pm 0.34$$

$$k_1^{-D}/k_1^{-T} = 1.81 \pm 0.06 \quad r = 1.32 \pm 0.06$$

The ratio k_1^{-D}/k_1^{-T} was measured by two different techniques and is low in magnitude compared with a value of 2.35 obtained for indoles (Section 2.12.4), 2.20 obtained from butylindolinones (Section 5.7) and between 2.26 and 2.34 calculated from force constants³¹. This suggests that the errors previously mooted for iodination rates may be as high as 20%. A further error that can be introduced is that both iodination rates are directly dependent on the value taken for the extinction coefficient of the tri-iodide ion, though this is unlikely to be as high as 20%.

Another interpretation could be the formation of a hydrate or hemiketal by the indolinone^{38g,110} which would only affect the kinetics of iodination. Such a hydrate would be the long sought tetrahedral intermediate in amide hydrolysis¹¹¹, but no corroborative evidence for such a species was found.

If a value of 2.20 for k_1^{-D}/k_1^{-T} (Section 5.7) is taken, the isotope effects can be corrected to give

$$k_1^{-H}/k_1^{-D} = 6.36$$

$$k_1^{-H}/k_1^{-T} = 14.0$$

$$k_1^{-D}/k_1^{-T} = 2.20$$

$$r = 1.43$$

This revised value for the Swain-Schaad exponent is now consistent with the calculated value⁴² and the experimental values obtained for indoles (1.47) and butylindolinones (1.38).

Since the deuterium isotope effect was obtained by a consistent method, errors in the method probably cancel out and the ratio is probably reliable. The question arises whether the curvature observed in the zero order iodination kinetics is due to the errors mentioned above or whether the interpretation of fast internal reprotonation is correct. The reproducibility of the ratio k_{-1}/k_2^* , its independence of pH, isotopic composition of substrate, substrate concentration or initial iodine concentration seems to argue for the internal return mechanism, though it is not clear why this occurs for indolinones and not for a more basic species such as acetone for example.

It seems nevertheless that the numerous complications that arise when the iodination method is used result in some uncertainties in the primary deuterium isotope effects so obtained. The next section will deal with the results for substrates where this method did not have to be used.

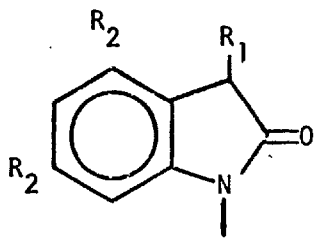
5.6 HYDROGEN EXCHANGE OF 4-^tBUTYLINDOLINONES. RESULTS.

Analogy with the substituted indoles previously studied suggested that the hydrogen exchange of 4-^tbutylindolinones may be subject to steric effects, and for this reason a series of these compounds were studied.

The protodetrition of these compounds was studied initially, in order to establish the electronic effects of the various substituents. Two indolinones were used which had no 3-alkyl substituent, but since the mole fraction of the label present is very small it is unlikely that two tritium atoms will be incorporated in the same molecule- which means that secondary isotope effects can be neglected.

The protodetrition of N-methylindolinone and N-methyl-4,6-di-^tbutylindolinone both gave excellent first order plots, and both were subject to base catalysis by OH^- (Table 5.4). The ratio of the two rates established that the electronic effect of the ^tbutyl groups slows the rate by a maximum of 4.7, it may be smaller due to a small steric effect (~ 2 by analogy with indoles) but we have no means of detecting this. One can show this result to be approximately correct by considering the results for indoles. Methyl-dibutylindole is 1.5 pK_a units more basic than methylindole and forms a protonated σ complex about 3 times faster, hence one expects proton loss to be about 10 times slower ($\log 30 = 1.5$) and this agrees with the factor of 4.7 observed for indolinones.

TABLE 5.4 Protodetrition of substituted N-methyl indolinones in 50%(w/w) aqueous methanol buffers at 25°C. [NaCl] = 0.1, [Borate] = 0.01M.

	pH_m	$10^5 k_o^{-T} / s^{-1}$	$k_1^{-T} / s^{-1} M^{-1}$	Run
$R_1 = R_2 = H$	9.020 ^a	4.97	4.74	487
$R_1 = R_2 = H$	9.475	15.4	5.16	489
$R_1 = H, R_2 = Bu^t$	9.020	1.11	1.06	488
$R_1 = H, R_2 = Bu^t$	9.480	3.13	1.04	491
$R_1 = Me, R_2 = H$	9.570	4.66	1.25 ^b	490, 442
$R_1 = Me, R_2 = Bu^t$	12.151 ^c	10.9	0.0077	495, 496
$R_1 = Me, R_2 = Bu^t$	12.350 ^d	15.9	0.0071	497

^a For 50% methanol, $pH_m = pa_H^* + 0.13$. For comparative purposes this correction need not be applied.

^b Cf Table 5.1, where KI was used to maintain ionic strength.

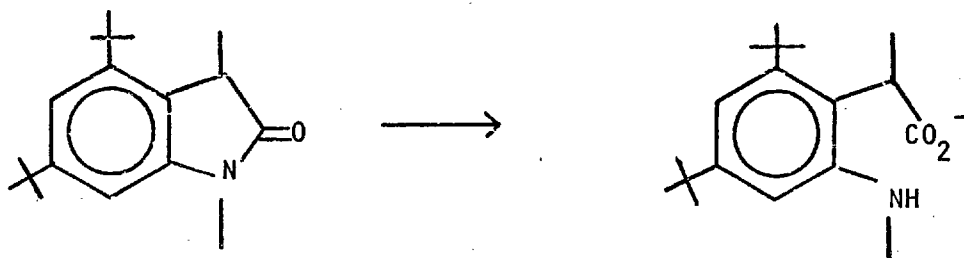
^c Using 0.01 N NaOH, the rate was extremely slow at pH 9.5

^d Using 0.015 N NaOH.

Examination of 1,3-dimethylindolinone and 1,3-dimethyl-4,6-di-^tbutylindolinone was also made, where secondary isotope effects are no longer a problem (Table 5.4). Protodetrition gave excellent first order plots, which tends to confirm that the rate of exchange of only one species is being followed. The exchange kinetics of dimethyldibutylindolinone were found to be very slow in borate buffers and accordingly dilute sodium hydroxide solutions were used, where again hydroxide catalysis was observed.

The extreme slowness of the rate could be accounted for by rapid hydrolysis to the acyclic amino acid (Scheme 5.10).

Scheme 5.10 Hydrolysis reaction of indolinones.



That this was not so was confirmed when the deuterium exchange kinetics were measured by a mass spectral method, similar to that used previously for indoles. The deuterium rates were of the same order as the tritium rates, which rules out the above intermediate.

5.7 ISOTOPE EFFECTS FOR 1,3-DIMETHYL-4,6-DI-^tBUTYLINDOLINONE:

The ratio k_1^{-D}/k_1^{-T} was obtained in protic solvents by measuring

the simultaneous loss of tritium and deuterium for the indolinone (Table 5.5). Though this ratio should reflect whether any tunnelling occurs in this system^{31,40}, it was thought desirable to measure the rate of protium exchange, since this is most susceptible to tunnelling effects. A mass spectral method was again adopted to measure k_1^{-H} .

By using deuteriated solvents, the rate of deuterium uptake by the indolinone, equal to the protium loss, is given by

$$-d[3-^1H_1 \text{ Indolinone}]/dt = \frac{k_1^{-H}}{1 + \frac{k_{-1}^H [H_2O]}{k_2^D [D_2O]}} \quad 5.12$$

If $[H_2O]/[D_2O] = 0.005$ and $k_{-1}^H/k_2^D \sim 7$, the denominator becomes 1.035 and with this correction applied one can obtain k_1^{-H} . A correction must also be applied for the solvent isotope effects introduced by employing deuteriated solvents as a medium.

For purely aqueous solutions, the ratio $k_1^{-H}(OD^-)/k_1^{-H}(OH^-)$ is typically about 1.2- 1.4^{38f}. For methanol, Gold finds $k_1^{-H}(MeOD)/k_1^{-H}(MeOH) \approx 2.3$ ¹¹² and consequently some intermediate value can be expected for the 50% methanolic solutions used here. It should also be noted in passing that a 57.7%(v/v) solution of MeOH in H₂O contains the same mole fraction of methanol as a 57.7% (v/v) solution of MeOD in D₂O (as a result of density changes) and consequently no change in solvent composition results. The solvent isotope effect was evaluated in practice by measuring the simultaneous loss of protium and tritium to the solvent and assuming that

$$k_1^{-H}/k_1^{-T} (D_2O) \approx k_1^{-H}/k_1^{-T} (H_2O)$$

TABLE 5.5 Hydrogen exchange of 1,3-dimethyl-4,6-di^tbutylindolinone in 50%(w/w) MeOH(D)/NaOH(D) solutions at 25°C. I = 0.11 maintained with NaCl.

[NaOH(D)]/M.	$10^4 k_o^{-T}/s^{-1}$	$10^4 k_o^{-D}/s^{-1}$	$10^4 k_o^T/s^{-1}$	$10^4 k_o^D/s^{-1}$	k_1^{-D}/k_1^{-T}	k_1^{-H}/k_1^{-T}	Run
0.015	1.59	3.43	-	-	2.16	-	497
0.010	1.10	2.45	-	-	2.23	-	496
0.005	-	-	0.893	15.4	-	17.9	500

$$k_1^{-D}/k_1^{-T} = 2.20 \pm 0.05 \quad k_1^{-H}/k_1^{-T} = 17.9 \pm 0.204 \quad k_1^{-H}/k_1^{-D} = 8.11 \pm 0.20$$

$$k_1^{-T}(D_2O)/k_1^{-T}(H_2O) = 1.62 \quad r = 1.377 \pm 0.017$$

This assumption was also made in solving the indole hydrogen exchange data and is made here for purposes of comparison, but it may not be entirely accurate. Gold and Grist^{22b} cite results which suggest that for aqueous solutions, $k^H/k^D(\text{H}_2\text{O}) \approx 1.04 k^H/k^D(\text{D}_2\text{O})$; and in methanol $k^H/k^D(\text{MeOH}) \approx 1.07 k^H/k^D(\text{MeOD})$, catalysed by HO^- and MeO^- respectively. A similar ratio appears to prevail for catalysis by 2,6-dimethylpyridine^{22a}.

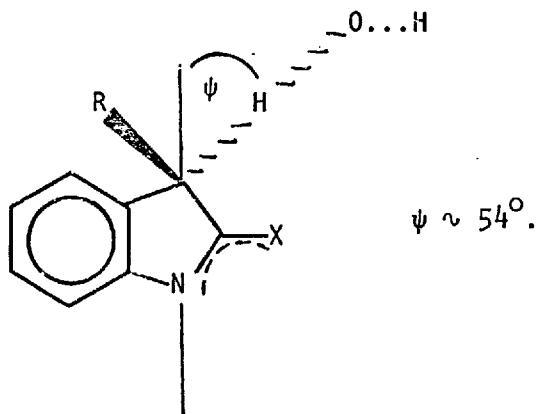
The secondary solvent isotope effect is seen from Table 5.5 to be about 1.6 (for loss of tritium) which is in accord with the results of Gold.

5.8 HYDROGEN EXCHANGE OF 4-^tBUTYLINDOLINONES. STERIC EFFECTS AND TRANSITION STATE SYMMETRY.

The rate of protodetrition of 1-methylindolinone (Table 5.4) is reduced by 4.7 when ^tbutyl groups are introduced in the 4,6 positions, whereas analogous treatment of 1,3-dimethylindolinone results in a rate reduction of about 170. One can conclude that a minimum steric effect of about 37 is observed for the ionisation of 1,3-dimethyl-4,6-dibutylindolinone by hydroxide, which is larger than steric effects observed for hydroxyl catalysed exchange of butylindoles. These steric effects in fact refer to deprotonation of the indolinones and protonation of the indoles, however the Law of Microscopic Reversibility suggests that the transition states for either reaction should be identical for the same substrate, and consequently the two steric effects can be compared.

The observation of similar rate reductions in two such closely related systems suggests the transition states for hydrogen transfer are fairly similar, with a considerable amount of sp^3 character for the substrate C-H bond (Figure 5.5). This results in considerable interactions with the 4-substituent, and will be increased for the 3-alkyl indolinones by the alkyl group moving out of the plane of the ring, decreasing the angle ψ and increasing the steric effect still further, in a manner closely similar to the postulated transition state for diazocoupling (Section 3.6.3). Such close comparisons are possible between indoles and indolinones since the two systems differ only in the position of the π system, in one case endocyclic and in the other exocyclic, and since we postulate an early

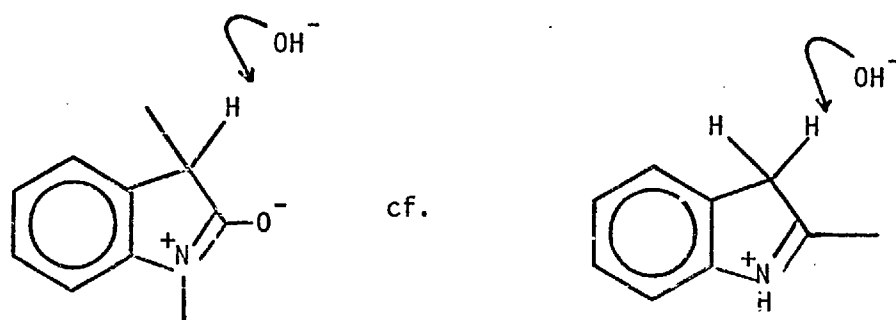
Figure 5.5 An sp^3 like transition state for hydrogen exchange of indolinones and indolyl anions.



transition state these π electrons will not be greatly involved anyway.

The predictions concerning the transition state symmetry of the indolinone hydrogen transfer reaction which were arrived at by considering the observed steric effects can be verified in two ways. If the structure for indolinones is indeed best represented by the keto form and not the dipolar species in Figure 5.6, then the Brønsted β for general base catalysis should have a low (reactant like) value. It should not be as low as the value for indoles (0.08) since the energies of the indolinone and enolate anion are more similar than the corresponding indolenine and indolyl anion (Figure 2.8). One can see that the dipolar species represented in Figure 5.6 on this basis should have a more product like transition state, which resembles that in the exchange mechanism of the neutral indole and not the indolyl anion.

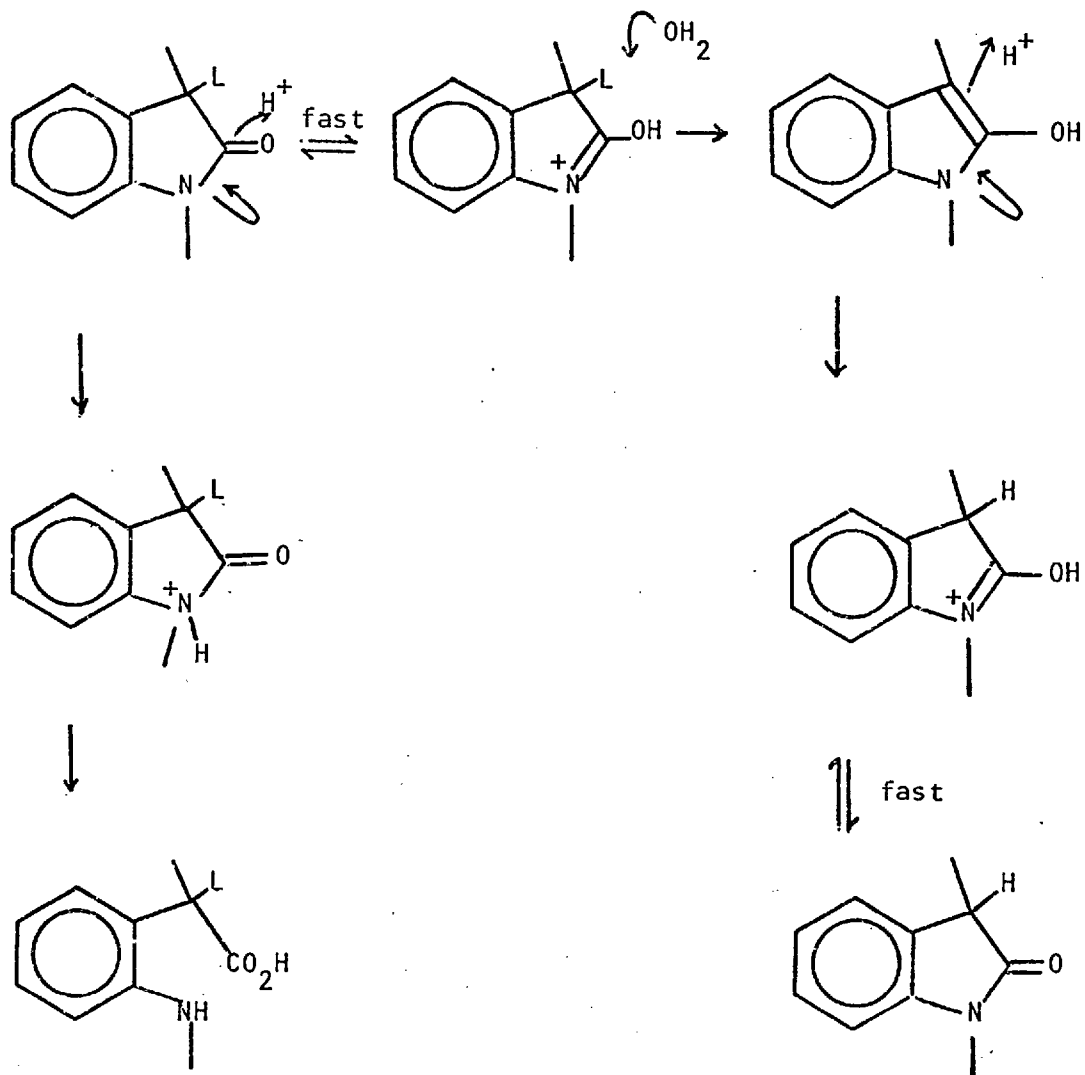
Figure 5.6 Dipolar representation of indolinones.



Consideration of the Brønsted exponents alone could be misleading, especially since the reactivity of indolinones may be considerably different from the indoles studied previously. The problem could be overcome, as it was for indoles, by comparing results for exchange via base and acid catalysed routes. One of several possible acid catalysed exchange mechanisms for indolinones is given in Scheme 5.11. A serious complication to the study of the acid catalysed exchange is the possibility of N-protonation leading to ring cleavage; effectively we have to consider the relative rates of exchange and hydrolysis. For acetamide in NaOH, this ratio is about 30:1¹⁰⁶ but since NH is a better leaving group than N⁻ the ratio would probably be lower in acidic solutions. Indolinones are exceptional, in that O protonation retains the conjugated π system, whereas N protonation interrupts it and on this argument alone the hydrolysis reaction may well be negligible compared with exchange.

A direct comparison of the Brønsted exponents for the acid and

Scheme 5.11 A possible acid catalysed mechanism for hydrogen exchange of 1,3-dimethylindolinone.



base catalysed pathways would now verify whether the base catalysed pathway is indeed more reactant like in the transition state than the acid catalysed pathway. One can also predict on this argument that steric effects caused by substituents on the indolinone should be smaller for the acid catalysed pathway than for the base catalysed route. They should not vanish completely, since the effect of the 3-alkyl group would be to make the transition states for both pathways

more reactant like, and more susceptible to steric interactions with 4-indolinone substituents.

It can be concluded that though observation of steric effects for the base catalysed hydrogen exchange of indolinones suggests a transition state similar to that for base catalysed exchange of indoles, further work on the acid catalysed exchange of indolinones is needed to verify this.

5.9 THE MAGNITUDE OF ISOTOPE EFFECTS FOR HYDROGEN EXCHANGE OF INDOLINONES.

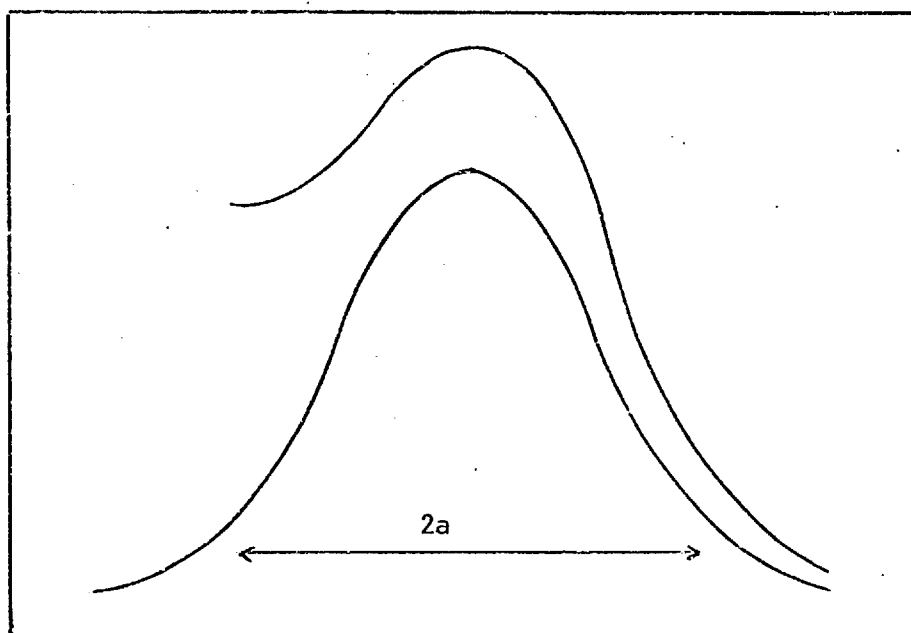
The isotope effects obtained by the mass spectral method for dimethyldibutylindolinone are considered more reliable than those obtained by iodination, since oxidation and the possibility of reversible hydration is now less of a problem. Isotopic rate ratios obtained for indolinones are also directly comparable with those obtained for indoles, since they refer to the same step, namely deprotonation of the σ complex (cf Figure 5.6). This is to be contrasted with the protodetrition rates, which refer to different steps.

The primary isotope effects for dimethyldibutylindolinone (8.1) and dimethylindolinone (6.4) are very similar to the value for methyl dibutylindole (6.1). These values seem not to depend on whether the transition state is sterically hindered or asymmetric, and this certainly does not verify the postulate by Westheimer¹.

It appears then that for a transition state where only a carbon

hydrogen bond is being broken, isotope effects do not necessarily give any indication of the symmetry of the transfer, and moreover that factors in addition to steric hindrance are responsible for proton tunnelling. It is worth speculating why proton tunnelling does not seem to occur for such hindered reactions as the ionisation of dimethyldibutylindolinone. This may well be a direct result of the highly asymmetric transition states in these reactions giving a large value for the width of the assumed parabolic energy barrier at the base³⁷ (Figure 5.7).

Figure 5.7 The symmetries of potential energy barriers for different transition states.



The value of $2a$ has been computed to be about 12.5 - 16 nm for reactions without tunnelling and to decrease to 11- 10 nm when tunnelling occurs. These values are calculated for symmetric barriers

and a consequence of the asymmetry may be to increase the value of $2a$. Certainly for a reasonably symmetric transition state such as that found in the system 2-nitropropane/2,4,6-collidine the isotope effect is about 4 times larger than normal⁴⁰, whereas a system where the proton transfer may be more asymmetric (diethylketone/2,6-lutidine) the isotope effect is only about 1.5 times larger than expected^{22a}.

This argument predicts that acid catalysed exchange of indoles and indolinones may be more subject to tunnelling since the transition states are more symmetric, however in most cases studied evidently insufficient steric hindrance was induced to bring the value of $2a$ down to the dimensions of a proton ($\lambda \sim 10-12\text{nm}$). Only in one case (2,6-lutidine/2,4,6-tributylindole) was an unambiguous steric effect observed, but no isotope effects could be measured.

Since tunnelling evidently makes no major contributions to these exchange reactions it is not surprising that little variation in isotope effects is observed with transition state symmetry; particularly as Bell argues⁸ that changes in transition state vibrational and bending frequencies have little effect on isotope effects and that only tunnelling is responsible. This conclusion is in direct contrast to those of More O'Ferrall^{5,6} and Westheimer¹ and suggests that great care must be taken in interpreting isotope effects in terms of transition state symmetry.

P A R T T H R E E

THE EXPERIMENTAL DETAILS

CHAPTER VI

Melting points were determined on a Kofler hot-stage apparatus. Infra-red spectra were recorded as mulls (nujol or 'Kel-F' grease) or liquid films. Nmr spectra were measured for solutions in carbon tetrachloride or $^2\text{H}_1$ -chloroform (except where stated otherwise) with tetramethylsilane as internal reference.

pH measurements were made at 25°C on a Radiometer 26pH meter, using G202B glass electrodes calibrated with standard aqueous buffers. Sodium ion corrections were made when necessary.

Radioactive assay was made on a Beckman LS200 scintillation counter, with at least 10^5 counts being registered for each sample.

6.1 HYDROGEN EXCHANGE OF INDOLES.

6.1.1 PREPARATION AND PURIFICATION OF SUBSTRATES.

2-Methylindole (BDH) and 2-^tbutylindole¹¹³ were purified by sublimation, m.p. 57-8° (Lit.¹¹⁴, 59-60°) and 72-3° (Lit.¹¹³, 73-4°) respectively.

2-^tButyl-4-methylindole.

2,3-Dimethylaniline was treated with trimethylacetyl chloride in benzene to give the anilide in 90% yield, m.p. 123° (Sublimed). Found C, 75.90; H, 9.27; N, 7.01%. C₁₃H₁₉NO requires C, 76.05; H, 9.32; N, 6.82%.

Fusion with potassium ^tbutoxide⁵² gave on workup 2-^tbutyl-4-methylindole (60%), m.p. 86° (Sublimed).

ν_{\max} 3390, 1589, 1540, 790, 771, 698 cm⁻¹.

δ 1.33 (9H, s), 2.52 (3H, s), 6.27 (1H, d), 7.0 (3H, m).

Found C, 83.43; H, 9.18; N, 7.52%. C₁₃H₁₇N requires C, 83.37; H, 9.14; N, 7.47%.

2,4-Dimethylindole was prepared in a similar fashion from 2,3-dimethylaniline and acetyl chloride, b.p. 102°/0.2mm (Lit.⁵²94-96°/< 1mm).

2-Methyl-4,6-di^tbutylindole (Scheme 2.3).

3,5-Di^tbutylbenzoic acid was prepared from 3,5-di^tbutyltoluene by the method of Wepster¹¹⁵ and converted to 3,5-di^tbutylaniline by

treatment with sodium azide in sulphuric acid¹¹⁶. This product had a characteristic AB₂ type nmr spectrum with J_{AB} 1.6Hz.

Found C, 81.95; H, 11.13; N, 6.64%. Calculated for C₁₄H₂₃N:
C, 81.88; H, 11.28; N, 6.82%.

The aniline (80g) in dried dimethoxyethane (250ml) was refluxed with freshly prepared sodamide (15g) till evolution of ammonia ceased, at which point 2-bromo-1,1-diethylacetal⁵¹ (70g) was added in small portions. After refluxing for one hour the solvent was removed and excess water added. Ether extraction followed by fractional vacuum distillation gave 2-(3,5-di^tbutylphenylamino)-1,1-diethylacetal (30g), b.p. 122-130°/0.4 mm.

m/e 335 (M⁺), 232 (Ar-NH=CH-Me).

The acetal (20g) was slowly dissolved in boron trifluoride saturated benzene (200ml) and further boron trifluoride was passed in with cooling to resaturate the solution. After 4 hours at 20° excess triethylamine was added and the solution filtered and washed with water. Removal of the solvent gave a thick oily residue which was purified by chromatography on an alumina column eluted with pet. ether/dichloromethane (10:90) to give 2-methyl-4,6-di^tbutylindole (15%) as the first eluted fraction, m.p. (hexane) 172-3°.

ν_{\max} 3370, 1617, 1548, 849, 784, 755 cm⁻¹.

δ 1.35, 1.45 (18H, d), 2.37 (3H, s), 6.27 (1H, m), 6.97 (2H, s), 7.4 (1H, br, exchanges with D₂O).

λ_{\max} , nm (log ϵ) 223 (4.53), 272 (3.95).

m/e 243 (M⁺), 229 (M⁺ - 15).

Found C, 83.67; H, 10.25; N, 5.84%. $C_{17}H_{26}N$ requires C, 83.89; H, 10.35; N, 5.75%.

2-Methyl-4,6-di^tbutylindole (Scheme 2.5).⁵³.

Bromine (8g) was added to dimethyl sulphide (3.2g) in dichloromethane (40 ml) at -46° (chlorobenzene/ N_2 cooling bath) with no precautions taken to exclude moisture. A yellow crystalline precipitate of the bromosulphonium bromide salt was formed. 3,5-Di^tbutylaniline (10g) and triethylamine (5g) in dichloromethane (10 ml) were added dropwise, during the course of which the yellow salt dissolved and white crystals of triethylammonium bromide were deposited. After two hours at -46° a solution of sodium (2.5g) in methanol (15 ml) was added, resulting in the production of a white precipitate of sodium bromide. After 8 hours at 20° the rearrangement was essentially complete and the solution was shaken with water, the solvent separated and evaporated to give a yellow oil (12g, 95%) which crystallised on standing.

δ 1.30 (9H, s), 1.47 (9H, s), 2.13 (3H, s), 4.12 (4H, br), 6.53, 6.83 (2H, dd, J_{AB} 2 Hz).

m/e 265 (M^+), 218 ($M^+ - CH_3S^{\cdot}$).

Raney nickel (prepared from 210g of 50% Ni/Al alloy¹¹⁷) was stirred with a solution of the 2-methylthiomethyl-3,5-di^tbutylaniline (32g) in ethanol (150 ml) at 70° for 1 hour. Filtration and evaporation of the solvent gave an oil which on distillation gave 2-methyl-3,5-di^tbutylaniline (66%), b.p. $126^{\circ}/2.7$ mm.

δ 1.25, 1.38 (18H, d), 2.17 (3H, s), 3.27 (2H, s), 6.43, 6.75 (2H, dd, J_{AB} 2Hz).

m/e 219 (M^+), 204 ($M^+ - 15$).

Found C, 81.95; H, 11.41; N, 6.19%. $C_{15}H_{25}N$ requires C, 82.12; H, 11.48; N, 6.38%.

2-Methyl-3,5-di^tbutylaniline (2g) (Scheme 2.4) in ether (20 ml) and triethylamine (1g) was mixed with acetyl chloride (1.2g) in ether. After one hour the ether was washed with 0.01N HCl and the solvent removed to give the acetyl derivative (90%).

m/e 261 (M^+), 246 ($M^+ - 15$).

The acetyl derivative was cyclised by potassium ^tbutoxide at 360° to give⁵² a melt which was boiled up with water. Ether extraction followed by crystallisation from hexane gave 2-methyl-4,6-di^tbutyl indole (30%), m.p. 176°. The physical data were identical to that previously obtained.

2,4,6-Tri^tbutylindole (Scheme 2.4).

2-Methyl-3,5-di^tbutylaniline was acylated with trimethylacetyl chloride in ether to give the anilide (97%), m.p. (ether) 215°.

m/e 303 (M^+).

Fusion with potassium ^tbutoxide⁵² at 350° gave on cooling a solid which was treated with water, giving brown crystals of the 1:1 ^tbutanol complex. These were dried and sublimed very slowly at 70° to give a colourless glass (25%), pure by nmr and tlc.

ν_{max} 3450, 3310, 2960, 2870, 1645, 1600, 1370, 800 cm^{-1} .

δ 1.30, 1.35, 1.48 (27H, t), 6.25 (1H, d, J 2Hz), 6.95 (1H, d, J 2Hz), 7.72 (1H, s, exchanges with D_2O).

m/e 285 (M^+), 270 ($M^+ - 15$).

Found C, 84.12; H, 10.97; N, 4.76%. $C_{20}H_{31}N$ requires C, 84.14; H, 10.94; N, 4.90%.

Purification of reagents.¹¹⁸

All buffer solutions were made up in distilled water. Piperidine was distilled from calcium hydride, b.p. 105-106°/760 mm. 2,6-Dimethyl piperidine was similarly treated, b.p. 128-9°/760 mm. 2,2,2-Trifluoro ethanol was distilled from anhydrous sodium carbonate, b.p. 74-5°/760 mm. 2,6-Dimethylpyridine (100g) and boron trifluoride etherate (4g) were fractionated, b.p. 143°/760 mm¹¹⁹ and the purity checked by nmr. The amine hydrochlorides of piperidine, 2,6-dimethylpiperidine, and diethylamine were crystallised from methanol and stored over P_2O_5 before use¹¹⁸.

Sodium chloride, pyridine, acetic acid and methanol were all AnalaR grade and were used as such. Methanol- d_1 (>99.5%, Aldrich) was used as supplied. BDH volumetric solutions of standard HCl and NaOH were used, the latter were normally checked by titration with the former prior to use.

6.1.2 LABELLED INDOLES.

a) Acid catalysed labelling was found unsatisfactory for some indoles, particularly 2-^tbutylindoles and the following method was generally adopted for deuteration.

The indole (~500mg) was dissolved in a solution of sodium (~500mg) in methanol- d_1 (10ml) and allowed to stand overnight. Evaporation

of the methanol at reduced pressure and addition of D₂O generally precipitated the required product which was filtered and dried. In some cases the precipitate was extracted into ether and the extract washed, dried and evaporated. Both the site of substitution and the deuterium content were estimated by nmr, which showed >80% d in the 3-position. Purification was achieved by sublimation where possible.

b) Tritiation was accomplished by the same method, using the indole (~500mg) in MeOH(10ml) containing sodium or potassium (~500mg) and THO (1ml, 20 mCi/ml) . Removal of the methanol and addition of water gave the required crystalline indole.

6.1.3 CHARACTERISATION OF PROTONATED INDOLES.

The solid salts were isolated from 2-methylindole and their properties recorded. Nmr spectra of all the indole salts were obtained by preparing the salt *in situ* using 10% H₂SO₄ in trifluoroacetic acid as solvent. The spectra are summarised in Table 6.1 .

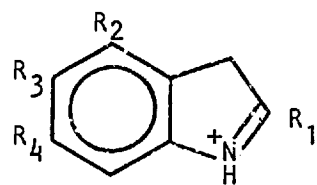
2-Methylindolium hydrogen sulphate.

A modification of the method of Hinman and Whipple⁴⁶ was used. A solution of 2-methylindole in ether (1 eq) was added to H₂SO₄ in ether (1.05 eq) and the precipitated white solid filtered off and washed with ether.

ν_{\max} (KBr disk) 3260br, 1640, 1610, 1585, 760, 709, 401 cm⁻¹.

Found S, 14.15%. C₉H₁₁NSO₄ requires S, 13.98%.

TABLE 6.1 Pmr spectra of protonated indoles in ~ 10% H₂SO₄/CF₃CO₂H at about 35°C.



	δ Butyl	δ Methyl	δ Methylene	δ Aromatic
$R_1=Me, R_2=R_3=R_4=H$	-	3.05	4.49	7.70
$R_1=Me, R_2=R_4=H, R_3=Cl$	-	3.02	4.50	7.66
$R_1=Me, R_2=R_4=H, R_3=NO_2$	-	3.19	4.80	8.03 (1H,dd) 8.6 (2H,dd).
$R_1=tBu, R_2=R_3=R_4=H$	1.67	-	4.55	7.72
$R_1=R_2=Me, R_3=R_4=H$	-	3.05, 2.47	4.37	7.5
$R_1=tBu, R_2=Me, R_3=R_4=H$	1.68	2.51	4.44	7.56
$R_1=Me, R_2=R_4=tBu, R_3=H$	1.43, 1.51	3.00	4.57	7.61, 7.83 (2H,dd, J1.6)
$R_1=R_2=R_4=tBu, R_3=H$	1.43, 1.51, 1.68	-	4.62	7.72, 7.85 (2H,dd, J1.6)

2-Methylindolium tetrafluoroborate

Boron trifluoride etherate was distilled over CaH_2 , b.p. $80^\circ/40$ mm. and added (2g) to anhydrous hydrogen fluoride (5ml) and ether (10ml) in a plastic bottle at 0°C . 2-Methylindole (3g) in ether (10ml) was then added slowly and the solid obtained filtered off and washed with ether, m.p. $151-154^\circ\text{d}$.

λ_{max} (KBr-F) 3140, 3060, 2930, 2915, 1638, 1618, 1592, 1475 cm^{-1} .

Found C, 49.34; H, 4.65; N, 6.19%. $\text{C}_9\text{H}_{10}\text{NBF}_4$ requires C, 49.36; H, 4.60; N, 6.39%.

6.1.4 CALCULATION OF BUFFER RATIOS.

For most buffers where $[\text{OH}^-] < 10^{-4}\text{M}$, equation 6.1 was used.

$$\text{pH} = \text{pK}_a - \log \frac{[\text{BH}^+]}{[\text{B}]} \quad 6.1$$

In the case of the amine buffers and particularly trifluoroethanol, the more complete equation was used.

$$\text{pH} = \text{pK}_a - \log \frac{[\text{BH}^+] + [\text{OH}^-]}{[\text{B}] - [\text{OH}^-]} \quad 6.2$$

In practice, the required buffer ratio was used to calculate the pH from equation 6.1, and this value converted to $[\text{OH}^-]$. A stock solution was made up of the species BH, of concentration equivalent to the total $[\text{BH} + \text{B}]$ required and more standard NaOH added in an amount calculated from equation 6.3.

$$\text{Hydroxide added} = \frac{[\text{BH}]_{\text{total}}}{1 + y} + [\text{OH}^-]_{\text{pH}} \quad 6.3$$

where y is the required buffer ratio $[\text{BH}]/[\text{B}]$.

6.1.5 MEASUREMENT OF DETRITIATION RATES.

For aqueous solutions the method of Challis and Millar³⁵ was used. Ionic strength was maintained by addition of the appropriate amount of sodium chloride. The pH of the solutions was measured using a meter calibrated with standard potassium hydrogen phthalate, sodium tetraborate or calcium hydroxide solutions⁵⁷; the pH within a series of buffers normally agreed to ± 0.01 units but if small deviations occurred adjustment was made with HCl or NaOH.

When high concentrations of amines were present in the reaction solution, aliquots (10 ml) were extracted with xylene (15 ml) and sufficient 1M. acetic acid to give a pH of about 7 in the aqueous phase. Scintillation solution (*Diphenyloxazole (10g) and 1,4-bis [2-(4-methyl-5-phenyloxazolyl)] benzene (0.25g) in xylene (1 l)*) was added (5 ml) and the mixture assayed by scintillation counting.

Where trifluoroethanol or aqueous methanolic solutions were employed, tritium in the form R-OH was carried over into the xylene extract and to remove this air was bubbled through for about 5-15 minutes until a constant count was obtained.

Runs in aqueous methanol were initiated by adding the substrate ($\sim 1\text{mg}$) in methanol (0.7 ml) to a 100 ml flask containing the buffer

and methanol (57.0 ml) and making up the volume to 100 ml. The usual extraction procedure was then followed, the extracts always being flushed with air to remove MeOT.

6.1.6 MEASUREMENT OF DEUTERIUM EXCHANGE RATES.

a) DEDEUTERIATION.

The rate of dedeuteriation of 3-²H₁ methylidibutylindole was followed by a mass spectral method, which will be described in full here.

The buffer solution was added in the required amount for 100 ml of solution and methanol (57 ml) added. The run was initiated when a solution of the 3-²H₁ indole (≈82%^d, 5 mg) and 3-³H₁ indole (1 mg) in methanol (0.7 ml) was added. Periodic aliquots (8 x 3 ml) were withdrawn for tritium assay as described previously and (8 x ≈6-8 ml) for deuterium assay. The latter were shaken vigorously with 2,2,4-trimethylpentane (≈2 ml) and a mixture of KHCO₃:NaCl (4:1, ≈300 mg) for about 30 seconds. After the octane had separated it was transferred to a specimen tube of 2 ml capacity and the octane removed slowly by evaporation in an evacuated vacuum dessicator. After at least 24 hours the sample was analysed by mass spectrometry.

b) DEUTERIATION.

A procedure analogous to the one above was followed. The reaction solution was made up with methanol-d₁ and D₂O and initiated by adding 3-¹H₁ indole (≈5mg) and 3-³H₁ indole (≈1mg). The sampling technique

was the same as before for tritium assay. For deuterium assay the aliquots (8 x ~6-8ml) were shaken with NaCl (300mg) and octane (~2ml). After two minutes the separated octane was transferred to a stoppered test tube containing 0.1 N NaOH (10 ml) and shaken for exactly two minutes. The octane was transferred to a specimen tube and treated as before.

c) DEUTERIUM ASSAY BY MASS SPECTROMETRY.

Methyldibutylindole gives a strong parent ion at m/e 243, with a natural isotopic abundance calculated for $C_{17}H_{25}N$ as 120

$$M^+ = 100\%, \quad M+1 = 18.9\%, \quad M+2 = 1.7\%.$$

This was verified for several samples and subsequently always assumed.

In following dedeuteriation kinetics, it was established that all N-D content of the indole was normally removed in the first 30 seconds of reaction and consequently only assay for d_1 content was made (Equation 6.4), where R is the ratio of peak heights $M+1/M$.

$$\%d_1 = \frac{100(R - 0.189)}{1 + (R - 0.189)} \quad 6.4$$

Equation 6.4 takes no account of the M-1 peak, found to be 3.5% of M and when this is considered, the $\%d_1$ is increased by a fairly uniform factor of about 1.03. This factor will therefore not affect the rate constants obtained.

For deuteriation runs, uptake of both C-D and N-D occurred. Due

to the extreme lability of the latter it was removed prior to assay by shaking the octane with 0.1 N NaOH as described above. Both d_1 and d_2 were obtained from equation 6.5, where R is the ratio

$$\begin{aligned} \% d_1 &= \frac{100(1.007R - 0.189)}{0.830 + 0.783R + S} \\ \% d_2 &= \frac{100(S - 0.189R + 0.011)}{0.830 + 0.783R + S} \end{aligned} \tag{6.5}$$

$M+1/M$ and S is $M+2/M$. A correction for the $M-1$ peak has been included. The d_2 abundance was normally found to be $<0.5\%$ and the much more convenient equation 6.4 was normally used.

Mass spectra were run on an AEI MS 9 spectrometer using a direct dry probe inlet technique, a probe temperature of 140° and an ionising voltage of 70 e.v. At this voltage most of the ion current is carried by the M^+ and $M-15$ peaks, and since the latter arises from fragmentation of the t butylgroups no isotopic partitioning should occur. For each sample six scans, using an expanded trace scale, were made over the molecular ion region and a background trace included. Variable deuterium content was normally the result of insufficient sample drying, a wet sample probe or sample cross contamination. To minimise the latter all eight or nine samples submitted were run in sequence (decreasing $\%d_1$) using the same instrument settings and the batch completed in a day.

d) ACCURACY OF THE DEUTERIUM ASSAY.

Variation in $\%d_1$ within the six scans was generally $\pm 0.2-0.4 \%d_1$. A similar value is obtained by assuming an absolute error in peak

heights of ± 0.02 cm and propagating this error to $\%d_1$ using equation 6.6 .

$$\sigma_{d_1} = 100 \sigma_M \cdot \frac{(M+1)^2 + M^2)^{\frac{1}{2}}}{(M+1 + 0.812M)^2} \quad 6.6$$

For a peak height of typically 2-5 cm and $\sigma_M = 0.02$, $\sigma_{d_1} = 0.3-0.5 \%d_1$

Samples with deviations greater than 3σ ($>1.5\%d_1$) were reanalysed or rejected.

Examples of all the kinetic methods are given in Tables 6.2 to 6.5 . Table 6.2 illustrates protodetrition by trifluoroethanol in aqueous solution, Table 6.3 the simultaneous protodetrition and protodeuteriation of methyldibutylindole in 2,6-dimethylpyridine buffers, Table 6.4 the simultaneous deuteriodetrition and deuteriodeprotonation of methyldibutylindole in sodium deuterioxide solutions and Table 6.5 the protodetrition of tributylindole.

6.1.7 ANALYSIS OF THE KINETIC DATA.

Normally replacement of a label (^3H) by solvent H_2O was found to be quantitative after about ten half lives and equation 6.7 was used.

$$\log (\text{cpm}_t - \text{cpm}_\infty) = - \frac{1}{2.3026} k_o^{-L} \cdot t + b \quad 6.7$$

In all cases cpm_∞ was normally checked once for a particular batch of labelled substrate and normally did not exceed the natural background

count for tritium (~ 40 cpm) by more than about 10-40 cpm, depending on the initial count. This background was then assumed for all subsequent runs. Excellent first order kinetics were obtained, in some cases for up to 99.8% reaction.

Dedeuteriation runs were treated as in equation 6.7, replacing cpm by $\%d_1$, where d_∞ was found to be effectively 0 for methyl dibutylindole.

Deuteriation runs were analysed using equation 6.8 .

$$\log (\%d_\infty - \%d_t) = -\frac{1}{2.3026} k_o^D \cdot t + b \quad 6.8$$

Though the reaction solutions invariably contained $>99\%$ d, as shown by the HOD and ^{13}C satellite nmr peaks, $\%d_\infty$ was more typically 87-95%. This may be a consequence of having to remove N-D before analysis by shaking with 0.1 N NaOH, and in the process removing some C-D. Care was taken to shake all the samples for the same time, and such errors should not affect the first order rate constant obtained.

A non-linear least squares analysis of equation 6.7 was also carried out using a relative error weighting scheme (section 7.1). Standard errors in the rate constants were normally $<2\%$, and the calculated infinity was normally close to the observed value.

A similar treatment of deuterium exchange rates was used with an absolute error weighting (section 6.1.6) . Analysis by this method gives a standard error for the variable $\%d$ of 0.4-1.0 $\%d$,

and this external error is indeed comparable with the internal error of about 0.5%. Deuteriation rates gave slightly higher errors (<1.5%) which suggests introduction of errors in the manipulation techniques. Since d_{∞} is well defined (especially for dedeuteriation, where $d_{\infty} = 0$) use of equation 6.7 or 6.8 is satisfactory-since the one degree of freedom less reduces the standard errors. If d_{∞} is allowed to float (Section 7.1) the error in its evaluation is about 0.8-3.0%, which is in excess of the uncertainty in the experimental value and no advantage is gained from using this treatment.

Standard errors in deuterium exchange rate constants were typically about 3%, and probably represent an improvement on the⁵⁵ infra-red method of analysis.

TABLE 6.2 Protodetrition of 2-methylindole in
2,2,2-Trifluoroethanol buffers at 25°C.

$[BH + B^-] = 0.25M$. $[B^-]/[BH] = 1.04$ Run 266

<i>Time/min.</i>	<i>cpm</i>	<i>cpm(Calc)</i>	<i>%reaction</i>
0	46,856	46,925	0
49	37,803	37,959	19.3
104	30,187	29,927	35.6
202	19,831	19,609	57.7
296	12,766	13,092	72.8
413	8,049	7,944	82.8
753	1,947	1,948	95.9
∞	0	175 ± 90	100

$$k_0^{-T} = 7.05 \pm 0.11 \times 10^{-5} s^{-1}.$$

TABLE 6.3 Simultaneous protodetrition and dedeuteriation of methyldibutylindole in 50%(w/w) aqueous methanol/2,6-dimethylpyridine buffer at 25°C.

$[BH^+] = 0.0062$, $pH^* = 6.47$, $I = 0.1$, Run 370

- T			- D		
Time/min.	cpm	cpm(Calc)	Time/min.	%d ₁	%d ₁ (Calc).
1	6157	6177	0	56.6	56.4
72	5419	5357	30	48.7	49.4
160	4509	4490	82	39.6	39.2
240	3758	3825	140	31.3	30.3
443	2566	2549	223	19.9	21.0
740	1410	1412	200	15.0	14.9
1357	430	425	310	11.2	11.4
1405	385	389	467	7.3	7.0
∞	0	26 ± 16	∞	0	- 0.2 ± 1.7

$$k_o^{-T} = 3.27 \pm 0.05 \times 10^{-5} s^{-1} \quad k_o^{-D} = 7.34 \pm 0.49 \times 10^{-5} s^{-1}.$$

TABLE 6.4 Simultaneous deuteriodeprotonation and deuterio-detrification of methyldibutylindole in 50%(w/w) aqueous methanol-d₁/sodium deuterioxide solutions at 25°C.

[NaOD] = 0.104 N, Run 476

- T			+ D		
Time/min	cpm	cpm(Calc).	Time/min.	%d ₁	
0	36,961	36,830	-2	0	
110	30,999	31,107	20	9.6	
304	23,151	23,104	60	22.7	
490	17,332	17,383	120	39.7	
730	12,048	12,058	280	66.3	
1350	4,758	4,743	360	71.4	
1670	2,961	2,965	488	80.7	
			563	85.7	
			728	89.5	
∞	301	183 ± 41	∞	94.7	92.6 ± 1.8 (calc)

$$k_o^T = 2.573 \pm 0.013 \times 10^{-5} s^{-1}.$$

$$k_o^D = 6.49 \pm 0.3 \times 10^{-5} s^{-1}.$$

(fixed %d_∞)

$$k_o^D = 7.09 \pm 0.5 \times 10^{-5} s^{-1}$$

(floated %d_∞)

TABLE 6.5 Protodetrition of 2,4,6-tri^tbutylindole in 50% (w/w) aqueous methanol/sodium hydroxide at 25°C.

[NaOH] = 0.2N, Run 430

<i>Time/min.</i>	<i>cpm</i>	<i>cpm(Calc).</i>	<i>% Reaction.</i>
0	68,244	68,446	0
1350	51,632	51,662	24
2760	38,444	38,530	44
4320	28,380	27,878	59
5895	19,922	20,134	71
9990	8,708	8,727	87
12945	4,858	4,852	93
∞	66	333 ± 181	100

$$k_o^{-T} = 3.50 \pm 0.05 \times 10^{-6} \text{ s}^{-1}.$$

6.1.8 MEASUREMENT OF THE pK_a FOR PROTONATION OF INDOLES.

The method used previously by Hinman and Lang⁵⁹ was employed. The U.V. spectra of 2-methylindole, 2-methyl-4,6-di^tbutylindole and 2,4,6-tri^tbutylindole were recorded between 210 and 290nm for a series of sulphuric acid/50%(w/w) methanol solutions and $4 \times 10^{-5}M$. indole. The spectrum of each solution was recorded at least three times to check that the spectrum did not vary with time. The ratio $[BH]/[B]$ was evaluated at about 222 nm, where the absorption difference was a maximum. The pK_a was evaluated using equation 6.9

$$pK_a = \log [BH^+]/[B] - \log [H^+] \quad 6.9$$

and extrapolated to $C_{H_2SO_4} = 0$. Good isobestic points were obtained (at about 235 and 248 nm) which confirm only two absorbing species (Figure 6.1).

6.1.9 MEASUREMENT OF THE pK_E FOR THE IONISATION OF 3-(p-NITRO-PHENYLAZO) INDOLES.

The substrates, in the form of the tetrafluoroborate salts, were all prepared from the indole and p-nitrobenzenediazonium tetrafluoroborate as described in Section 6.2.2 . Ionisation ratios were measured at the absorption maximum of the anion and the pK_E evaluated from equation 6.10

$$pK_E = 14 + \log [OH^-] - \log [In^-]/[InH] \quad 6.10$$

Excellent isobestic points were obtained in all cases (Figure 6.2). Physical data are recorded in Table 6.6 for the compounds studied.

Figure 6.1 U.V spectra of 2-methyl-4,6-di^tbutylindole in 50% (w/w) methanol/sulphuric acid solutions.

[Indole] $\approx 4 \times 10^{-5}$ M.

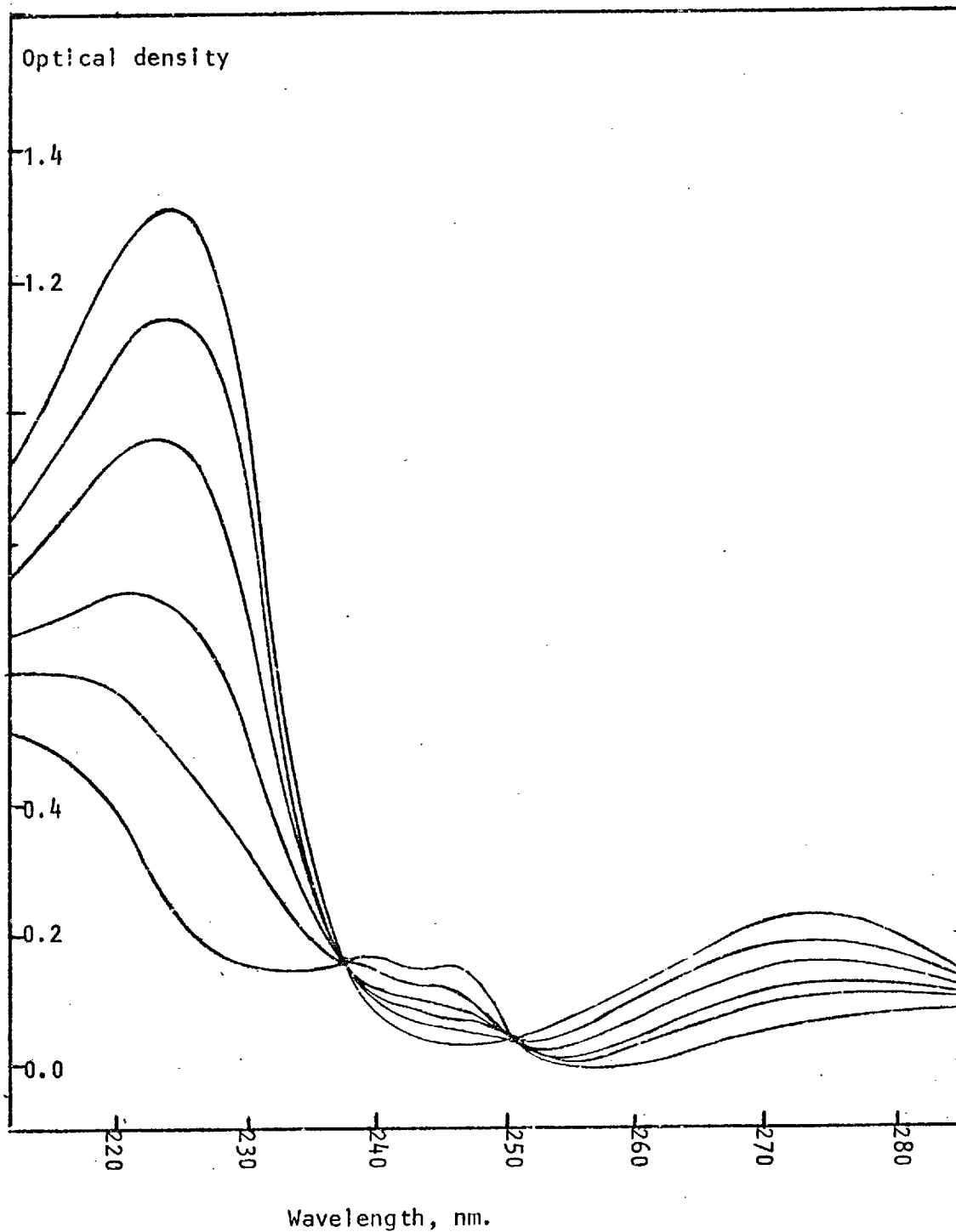


Figure 6.2 U.V. spectra of 2-^tbutyl-3-(p-nitrophenylazo)-4-methylindole in 54%(w/w) aqueous methanol/sodium hydroxide solutions at 25°C.

$$[\text{Indole}] = 1.97 \times 10^{-5} \text{ M.}$$

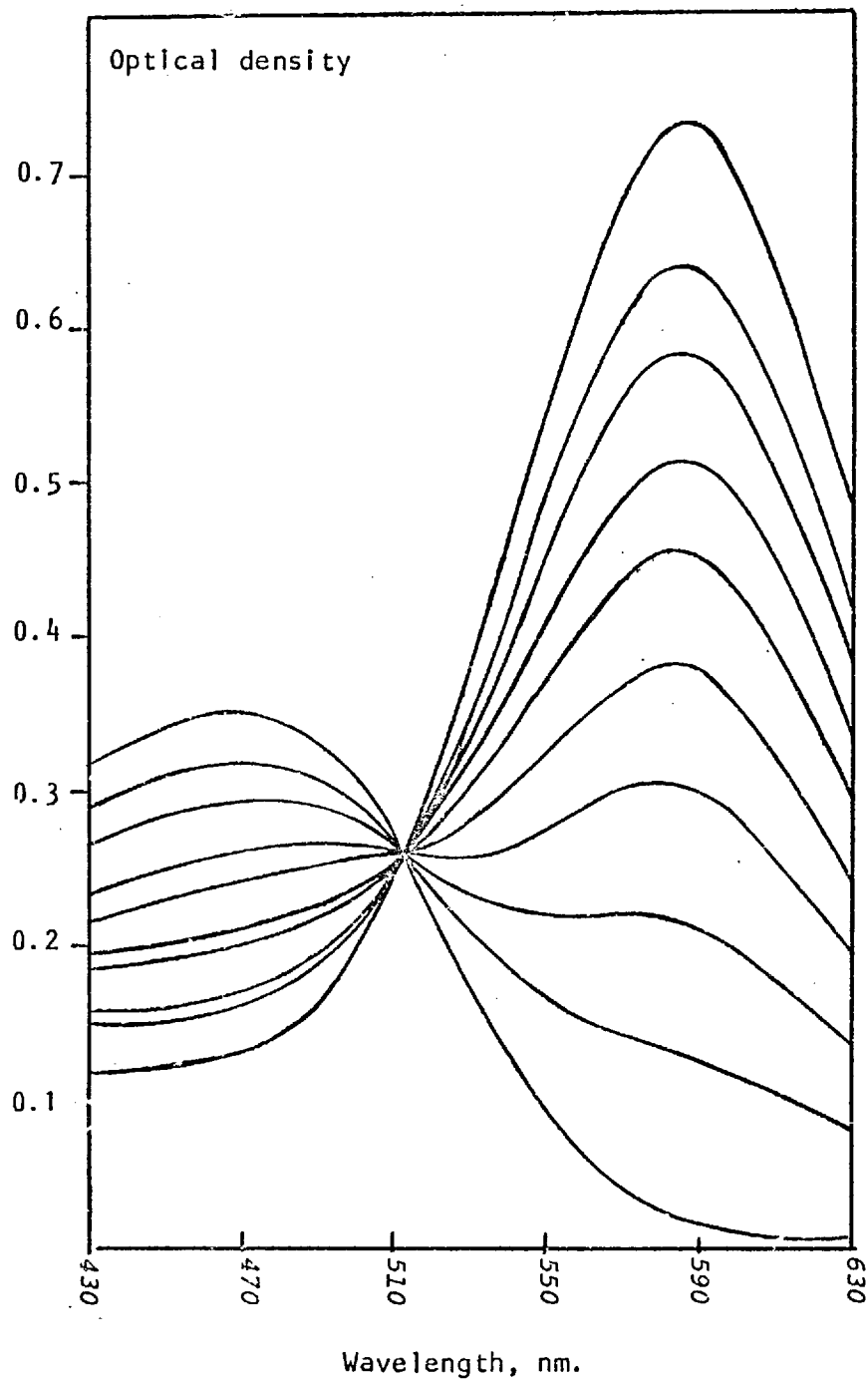
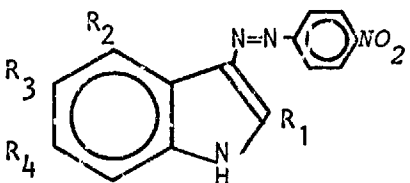


TABLE 6.6 Physical data for 3-(p-nitrophenylazo)indoles in 54%(w/w) aqueous methanol at 25°C.

	<i>m/e</i>	$\lambda_{\text{max}}^{\text{InH}^-}/\text{nm}$	$\lambda_{\text{max}}^{\text{In}^-}/\text{nm}$	$10^{-4} \epsilon_{\text{max}}^{\text{In}^-}/\text{M}^{-1} \text{cm}^{-1}$	$\text{pK}_{\text{E}}^{25}$
$R_1 = \text{Me}, R_2 = R_4 = \text{H}, R_3 = \text{NO}_2$	325	419	537	3.69	10.81
$R_1 = \text{Me}, R_2 = R_4 = \text{H}, R_3 = \text{Cl}$	314	420	536	4.44	11.71
$R_1 = \text{Me}, R_2 = R_3 = R_4 = \text{H}$	280	442	545	4.15	12.11
$R_1 = R_2 = \text{Me}, R_3 = R_4 = \text{H}$	294	466	573	4.20	12.23
$R_1 = {}^t\text{Bu}, R_2 = R_3 = R_4 = \text{H}$	322	-	559	4.13	12.44
$R_1 = {}^t\text{Bu}, R_2 = \text{Me}, R_3 = R_4 = \text{H}$	336	470	584	3.80	12.60
$R_1 = \text{Me}, R_2 = R_4 = {}^t\text{Bu}, R_3 = \text{H}$	392	490	595	4.11	12.38
$R_1 = \text{OH}, R_2 = R_3 = R_4 = \text{H}, N\text{-Me}$	296	419	540	-	~10.9

6.2 REACTION OF ARYLDIAZONIUM IONS WITH INDOLES.

6.2.1 PREPARATION AND PURIFICATION OF SUBSTRATES.

Indoles and labelled indoles were prepared as in section 6.1.1 and 6.1.2 .

Solutions of diazonium ions were prepared by either a) diazotising a standard solution of amine¹²¹, prepared from reagent grade material purified by sublimation or b) from the solid diazonium tetrafluoroborate, prepared according to Sukigara¹²² and crystallised several times from acetone by addition of hexane. Concentrations of all solutions were checked by measuring the optical density at about 280nm and the two methods were found to agree closely.

Dioxan was passed down a fresh alumina column before use to remove peroxides. Nitromethane was treated similarly and distilled, b.p. 100-1^o/760 mm. Acetonitrile was treated with calcium hydride to remove water and distilled over P₂O₅, b.p. 80.6^o/760 mm. Deuterium oxide was reagent grade (99.7%d) and was checked for isotopic purity by nmr comparison with samples of known purity. Aqueous buffers were prepared from AnalaR materials.

6.2.2 PREPARATION OF PRODUCTS.

Reaction products were prepared by dissolving the indole (1.1 equiv) in acetone and adding a solution of the aryldiazonium fluoroborate (1 equiv) in acetone. After 20 minutes hexane was slowly added to precipitate the tetrafluoroborate salt of the azoindole. Absence of 3H protons in the nmr spectrum confirmed the site of the substitution as the 3- position in all cases. Physical constants are given in

Table 6.7 and analytical data in Table 6.8 .

No pure product was isolated with 2,4,6-tri^tbutylindole, but the mass spectrum of the reaction mixture showed a very small peak at m/e 403 (<0.03% of the base peak at 270) corresponding to the 3-p-tolylazo product. The azoindoles normally generated strong molecular ions.

6.2.3 MEASUREMENT OF DIAZOCOUPLING RATES.

a) U.V. assay of product.

The rates of diazocoupling at pH > 3.5 were normally measured by U.V. assay of the reaction at the absorption maximum of the product (λ_{\max} 377-401 nm). Coupling in acidic solutions was followed at the absorption maximum of the protonated product¹²³. For example the conjugate acid of 2-methyl-3-(p-tolylazo)indole has a pK_a of 3.0 ± 0.2 and λ_{\max} 445 nm and the conjugate acid of 2-methyl-3-(p-methoxyphenylazo)-4,6-di^tbutylindole had λ_{\max} 525 nm.

Measurements were made directly on the reaction solution in a spectrophotometer cell, contained in a thermostatted cell holder at $25^{\circ} \pm 0.2$. Control experiments established the decomposition of the diazonium ions under the conditions used for coupling, this was normally negligible compared to the rate of coupling but was corrected for when necessary.

The optical density of the final reaction solution generally agreed to within 15% of the calculated value obtained from the extinction coefficient of the purified product. Reaction solutions more than about one hour old showed some decomposition of product.

TABLE 6.7 Physical data for 3-arylazoindole tetrafluoroborate salts.

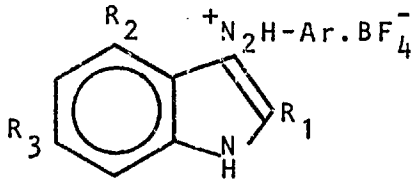
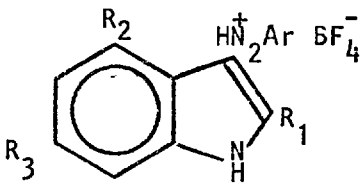
	m/e M^+	$\nu_{\max}/\text{cm}^{-1}$	Nmr/δ	λ_{\max}/nm (log ϵ)
$Ar = p\text{-MePh}, R_1 = \text{Me},$	249	3220, 1603, 1550,	2.37(3H,s), 2.77(3H,s),	282 (4.02)
$R_2 = R_3 = \text{H}$		830, 760, 750.	7.2-7.8(7H,m), 8.42 (1H,m), 11.7(2H,br)	377 (4.34)
$Ar = p\text{-MePh}, R_1 = \text{tBu},$	305	-	1.75(9H,s), 2.47(3H,s), 2.83(3H,s), 7.32-7.80 (7H,m).	-
$R_2 = \text{Me}, R_3 = \text{H}$				
$Ar = p\text{-MePh}, R_1 = \text{Me},$	361	3300, 1630, 1608,	1.35, 1.57(18H,d), 2.34	289 (4.14)
$R_2 = R_3 = \text{tBu}$		1062, 878, 809.	(3H,s), 2.65(3H,s), 7.18 (2H,s), 7.2-7.7(2H,dd, J8.2Hz)	401 (4.19)
$Ar = p\text{-MeOPh}, R_1 = \text{Me},$	377	3270, 1601, 1060,	1.34, 1.55(18H,d), 2.61	289 (4.16)
$R_2 = R_3 = \text{tBu}$		875, 840.	(3H,s), 3.78(3H,s), 6.98- 7.72(4H,dd, J9Hz), 7.14(2H,s).	401 (4.22)

TABLE 6.8 Analytical data for 3-arylazindoles.

		%C	%H	%N
<i>Ar</i> = <i>p</i> -MePh, <i>R</i> ₁ = Me,	Found	57.08	4.94	12.27
<i>R</i> ₂ = <i>R</i> ₃ = H, C ₁₆ H ₁₆ N ₃ BF ₄	requires	57.00	4.78	12.46
<i>Ar</i> = <i>p</i> -MePh, <i>R</i> ₁ = ^t Bu, <i>R</i> ₃ = H,	Found	61.04	6.22	10.86
<i>R</i> ₂ = Me, C ₂₀ H ₂₄ N ₃ BF ₄	requires	61.08	6.15	10.68
<i>Ar</i> = <i>p</i> -MePh, <i>R</i> ₁ = Me,	Found	64.44	7.18	9.41
<i>R</i> ₂ = <i>R</i> ₃ = ^t Bu, C ₂₄ H ₃₂ N ₃ BF ₄	requires	64.15	7.17	9.35
<i>Ar</i> = <i>p</i> -MeOPh, <i>R</i> ₁ = Me,	Found	61.90	6.96	8.95
<i>R</i> ₂ = <i>R</i> ₃ = ^t Bu, C ₂₄ H ₃₂ N ₃ OBF ₄	requires	61.96	6.93	9.02
<i>Ar</i> = <i>p</i> -NO ₂ Ph, <i>R</i> ₁ = Me,	Found	57.41	6.03	11.66
<i>R</i> ₂ = <i>R</i> ₃ = ^t Bu, C ₂₃ H ₂₉ N ₄ O ₂ BF ₄	requires	57.51	6.09	11.66

121

b) U.V. assay of reactant.

In those runs where the concentration of the indole exceeded the diazonium ion concentration, it was possible to quench aliquots of the reaction solution (8 x 2ml) in 5% 2-naphthol-3,6-disulphonic acid in saturated borax (5ml) ('R-Salt'). The naphthol azo product formed almost instantly ($t_{\frac{1}{2}} \sim 1$ sec) and was estimated by U.V. at about 498 nm. Rate constants obtained by this method agreed fairly well with method a), to within 5%.

c) Measurement of Diazodetritiation rates.

Measurement of simultaneous azo-coupling and detritiation rates was carried out in several cases and the conditions employed will be discussed in detail here. At least a tenfold excess of diazonium ion over indole was used in order to completely remove tritium from the indole and the runs were carried out at a carefully adjusted pH such that radical induced decompositions which occur at $\text{pH} \sim 10$ were minimised and also so that solvent catalysed protodetritiation was very slow with respect to diazocoupling. The optimum pH was about 7.3 to 7.8 .

The run was initiated by adding the requisite amount of $3\text{-}^3\text{H}_1$ labelled indole ($\sim 1\text{mg}/100\text{ml}$ reaction solution) to the solution, dissolved in a small amount of dioxan, and transferring an aliquot to the spectrophotometer cell. Aliquots of the remaining solution (10ml) were quenched by shaking with xylene (15ml) for one minute, which effectively extracted only the indole into the xylene.

After about 15 minutes 10ml of the xylene layer was taken and scintillation solution (Section 6.1.5) (5ml) was added. Air was passed through for about 15 minutes to remove excess tritium in the form of THO and to clear the solution, before it was counted in a scintillation counter. The latter was calibrated beforehand for the extensive quenching induced by the azoindole product formed by constructing a quenching curve using authentic coupled product.

Blank experiments in the absence of diazonium ion determined the amount of general acid/base catalysed protodetrition.

d) Measurement of diazodeuteriation rates.

In cases where diazodeuteriation was followed using $3\text{-}^2\text{H}_1$ labelled indoles in H_2O , control experiments carried out using $3\text{-}^3\text{H}_1$ indole established that the amount of exchange with solvent during the duration of the run was negligible. In cases where this was not so D_2O was employed as a solvent.

6.2.4 TREATMENT OF KINETIC DATA.

a) Pseudo first order conditions.

For a bimolecular reaction $\text{A} + \text{B} \xrightarrow{k_{bi}} \text{C}$, the rate is given by

$$d[\text{C}]/dt = -d[\text{A}]/dt = -d[\text{B}]/dt = k_{bi}[\text{A}].[B] \quad 6.11$$

and if the concentration of one of the reactants is considerably greater than the other, such that it remains constant, one obtains for indoles

$$\frac{d[\text{Product}]}{dt} = \frac{-d[\text{ArN}_2^+]}{dt} = k_o [\text{ArN}_2^+]; \quad (\text{Indole}) \gg [\text{ArN}_2^+] \quad 6.12a$$

$$= k_o (\text{Indole}); \quad [\text{ArN}_2^+] \gg (\text{Indole}) \quad 6.12b$$

The concentration terms are defined as previously elaborated (Section 3.2.1). Integration of equation 6.12 yields

$$\ln (a - x) = -k_o t + b; \quad a > x \quad 6.13a$$

$$\ln (x - a) = -k_o t + b; \quad x > a \quad 6.13b$$

where a and x (in 6.13a) are proportional to the final and transient (at time t) concentrations of the product or (in 6.13b) of a reactant. Equation 6.13 is normally plotted as such, which has the disadvantage of introducing large errors if the value for a is uncertain, particularly a problem if the product is unstable and a cannot be accurately measured. This was overcome by expressing equation 6.13 in the form

$$x = a - e^{(-k_o t + b)} \quad 6.14a$$

$$x = a + e^{(-k_o t + b)} \quad 6.14b$$

and solving these expressions by a non-linear least squares regression method (Section 7.1) for a and k_o , using as input values of x and t , and evaluating standard errors as well. Agreement of the observed value for a with that calculated is normally taken as an indication of good first order kinetics¹²⁵. Only for comparatively slow reactions

was this not the case for indoles.

Weighting of data.

The standard plot of equation 6.13 has the effect of assigning a relative (or percentage) error in the variable \underline{x} . This type of error is normally found in tritium assay, where samples are counted to a specified % accuracy (normally about 0.7%) and analysis using equation 6.14 was carried out using a weight of $W_i = 1/(\text{cpm})^2$. Optical density measurements probably have an absolute experimental error of about $\pm 0.002 A$ (limited by the specifications of the instrument) and analysis in terms of equation 6.14 was accomplished with $W_i = 1$.

In Tables 6.9 to 6.11 are typical examples of the analysis of first order data for various systems, including three methods for following the rate of coupling of 2-methylindole and two for methyl dibutylindole. The rate constants (where comparable) agree to within 6% and are within their respective 69% confidence limits.

b) Second order conditions.

Several runs were carried out using equimolar concentrations (equation 6.15).

$$1/(b-x) - 1/b = \bar{k}_{bi} \cdot t \quad 6.15$$

where (b-x) represents the concentration of either component at time t and b is the initial concentration. Good agreement was obtained with

the pseudo first order method.

c) Accuracy of the rate constants.

The precision of a rate constant is reflected in the external variance, derived from the precision of the data used to define it. Errors were generally $\pm 4\%$ or less in the rate constant, approaching a limit of $\pm 0.6\%$ determined by the spectrophotometric accuracy of ± 0.001 A. The accuracy of the rate constants was lower, being subject to such errors as a variation in temperature, solvent composition, substrate concentrations and pH, and is reflected in the agreement obtained when two different methods are used to obtain the same rate constant. This was estimated as about $\pm 6\%$.

TABLE 6.9 Diazdeprotonation of 2-methylindole in aqueous solution at pH 3.25 and 25°C. 'R-Salt' method.

Initial $[p\text{-MeArN}_2^+] = 10^{-4} \text{ M}$. $[\text{Indole}] = 10^{-3} \text{ M}$. Run 64

Time/s	Optical density(498nm)	O.D. (Calc).
0	-	0.371
30	0.351	0.355
60	0.342	0.340
120	0.316	0.311
180	0.283	0.285
240	0.264	0.262
300	0.240	0.240
360	0.218	0.221
480	0.187	0.186
600	0.157	0.158
900	0.106	0.106
1200	0.073	0.073
∞	0.018	0.017 \pm 0.007

$$k_o = 1.535 \pm 0.059 \times 10^{-3} \text{ s}^{-1}.$$

TABLE 6.10 Simultaneous diazodeprotonation and diazodetrition of 2-methylindole in 40%(v/v) aqueous dioxan/sodium hydrogen phosphate solution (pH 7.81) at 25°C.

$[p\text{-MeOArN}_2^+] = 5 \times 10^{-3} \text{ M}$, $[\text{Indole}] \sim 4 \times 10^{-5} \text{ M}$. Run 308.

Time/min.	Diazodeprotonation		Diazodetrition	
	O.D. (380nm)	O.D. (Calc)	cpm	cpm(Calc)
0	0.089	0.087	8162	8231
1	0.140	0.143		
2	0.195	0.195		
3	0.242	0.242	6272	6267
4	0.286	0.285		
6	0.361	0.361	4815	4774
8	0.425	0.425		
10	0.479	0.478	3341	3325
12	0.525	0.523		
14	0.562	0.561	2309	2319
18	0.621	0.619	1643	1621
22	0.660	0.660	1113	1137
28			679	674
∞	0.750	0.757 \pm .004	40	40 \pm 28

$$k_o = 1.46 \pm 0.02 \times 10^{-3} \text{ s}^{-1}$$

$$k_o^H/k_o^T = 0.97$$

$$k_o = 1.523 \pm 0.023 \times 10^{-3} \text{ s}^{-1}$$

$$k_o(\text{blank}) = 0.02 \times 10^{-3} \text{ s}^{-1}$$

TABLE 6.11 Simultaneous diazodeprotonation and diazodetrition of 2-methyl-4,6-di^tbutylindole in 40%(v/v) aqueous dioxan/sodium hydrogen phosphate solution (pH 7.37) at 25°C.

$[p\text{-MeOArN}_2^+] = 1.5 \times 10^{-3} \text{ M}$. Initial [Indole] $\sim 4 \times 10^{-5} \text{ M}$. Run 310

Time/s	Diazodeprotonation		Diazodetrition	
	O.D. (401nm)	O.D. (Calc)	cpm	cpm(Calc).
0			12081	11532
60	0.347	0.346		
80	0.417	0.416		
100	0.477	0.479		
120	0.534	0.536		
140	0.586	0.587		
180			9307	9616
200	0.715	0.713		
220	0.748	0.747		
260	0.808	0.806		
300	0.854	0.854		
340	0.893	0.893		
360			7688	8025
420	0.952	0.951		
600			6519	6318
840			5013	4987
1200			3523	3520
1800			2016	2018
2400			1211	1212
∞	1.080	$1.067 \pm .003$	30	278 ± 142

$$k_o = 5.086 \pm 0.047 \times 10^{-3} \text{ s}^{-1}.$$

$$k_o = 1.007 \pm 0.055 \times 10^{-3} \text{ s}^{-1}.$$

$$k_o(\text{blank}) = 0.006 \times 10^{-3} \text{ s}^{-1}.$$

6.3 DECARBOXYLATION OF INDOLE-3-CARBOXYLIC ACIDS.

6.3.1 PREPARATION OF ^{14}C LABELLED CARBOXYLIC ACIDS.

The following method was used to prepare the 3-carboxylic acids of 5-chloroindole, 2-methylindole and indole itself.

^{14}C -Barium carbonate (360mg, 1.5 mmole, $\sim 100\mu\text{Ci } ^{14}\text{C}$) was placed in a small three necked flask, one neck of which was attached to a vacuum line. Sulphuric acid (5ml) was added slowly from a dropping funnel and the $^{14}\text{CO}_2$ generated was frozen out in a 500ml receiving bulb. A solution of methylmagnesium iodide was prepared by refluxing dry magnesium (72mg, 3 mmole) and iodomethane (430mg, 3 mmole) in ether (2.5ml) for 45 minutes and adding the indole (3 mmole) in ether (15ml) slowly to give the indolyl magnesium iodide. After 45 minutes further refluxing two layers normally separated out and these were dispersed by rapid stirring before a nitrogen bath was applied. The flask containing the frozen solution was attached to the vacuum line and evacuated. The labelled carbon dioxide was condensed into this flask by further cooling with nitrogen and when transfer was complete the flask was sealed and detached. The flask was shaken when the ether solution liquefied and on attaining room temperature 5N HCl (5ml) was stirred in and the ether layer separated, washed and shaken with 2N NaOH (15ml). The aqueous phase was then poured into 10 N HCl (15ml) at 0° and the precipitate collected and dried at 45° for several hours. Yield: 180mg, 75%.

The acid as prepared contained significant amounts of N-CO_2^{95}

which was removed by heating the solid to not more than about 70^o for about 6 hours.

In certain cases insufficient carboxylic acid was formed to be precipitated from solution and purification was achieved by sequential extraction of the acid into NaOH from ether, and from the NaOH into HCl in ether. In either case a stock solution of the acid in dilute sodium hydroxide solution was prepared for use in kinetic runs.

6.3.2 MEASUREMENT OF DECARBOXYLATION RATES IN H₂O

A typical run will be described in detail here. In a 100 ml volumetric flask was added a measured amount of standard HCl solution (or buffer solution of known pH) followed by the appropriate amount of 2.5 N sodium chloride solution to make the ionic strength up to 1.0 . The run was initiated by adding 1 ml of the sodium indole carboxylate solution to the contents of the flask, previously equilibrated at the reaction temperature. The first reading was taken after an estimated 20% of reaction had occurred, in order to ensure no remaining N- carboxylic acid remained (the N- acid decarboxylates about 20 times as fast as the C-). Aliquots (8 x 10ml) were withdrawn at intervals and shaken with 15 ml of a mixture of xylene and ethyl acetate (4:1 v/v) for at least a minute. After allowing the organic layer to separate for 15 minutes a sample (10ml) was removed, scintillation solution (5ml) added (Section 6.1.5) and air bubbled through for 15 minutes to clear the solution and remove excess carbon dioxide. The initial count of samples prepared in this manner ranged from 2,000 to about 20,000 cpm. Infinity values were generally measured

for each stock indole carboxylate solution and were < 200 cpm, more often 45-70 cpm. Having established this value it was generally assumed for the other runs using the stock solution.

After each run had terminated the reaction solution was titrated against standardised sodium hydroxide, using bromophenol blue as indicator, to determine the acidity. For reactions carried out at 60° volumetric corrections for the expansion of the solvent were made.

6.3.3 MEASUREMENT OF DECARBOXYLATION RATES IN D₂O.

These runs were essentially scaled down to 25 ml total volume, or in the case of very dilute acidic solutions 50 ml to facilitate the titration with sodium hydroxide. Aliquots (9 x 2 ml) were removed and quenched as previously. A stock solution of DCI was prepared by dissolving HCl gas in D₂O and normally the deuterium content of the final solution was better than 98%*d*. Buffers (ie potassium hydrogen phthalate) and also sodium chloride used to maintain the ionic strength were added as weighed out solids.

6.3.4 TREATMENT OF KINETIC DATA.

Pseudo first order conditions are obeyed in this reaction and rate constants were evaluated from equation 6.16 .

$$\log (\text{cpm}_t - \text{cpm}_\infty) = - k_o t + b \quad 6.16$$

though occasional use of equation 6.14 was made.

Excellent first order plots were obtained for over 90% reaction and c_{pm} calculated using equation 6.14 agreed well with the observed value.

The precision of the rate constants were normally better than $\pm 2.5\%$, and the acid concentration was known to within $\pm 0.001 N$. These values were used in assigning weights to the observations (Section 7.2). Reaction rates measured in solutions containing organic buffer components were assigned a different error, since the acid concentration is now known relatively more accurately.

Examples of the decarboxylation rates for all three compounds studied are given in Tables 6.12 to 6.14 .

TABLE 6.12 Protodecarboxylation of indole-3-carboxylic acid at 25°C. $I = 1.0$ $[H^+] = 0.0089N$. Run 154.

<i>Time/min.</i>	<i>cpm</i>	<i>cpm(Calc)</i>	<i>% reaction</i>
0	2021	2020	0
89	1984	1975	1.8
209	1898	1917	6.1
458	1811	1801	10.4
1261	1465	1475	27.5
1534	1391	1379	31.2
2870	993	995	50.9
4580	663	663	67.2
∞	8	65 ± 45	100

$$k_0 = 4.06 \pm 0.19 \times 10^{-6} s^{-1}.$$

TABLE 6.13 Protodecarboxylation of 2-methylindole-3-carboxylic acid at 25°C. $I = 1.0$
 $[H^+] = 1.003N$. Run 234.

<i>Time/min.</i>	<i>cpm</i>	<i>cpm(Calc)</i>	<i>% reaction.</i>
0	3536	3560	0
2	3084	3040	12.8
4	2581	2595	27.0
7	2041	2044	42.3
10	1602	1607	54.7
15	1075	1071	69.6
20	707	708	80.0
∞	0	-60 ± 43	100

$$k_0 = 13.5 \pm 0.37 \times 10^{-4} \text{ s}^{-1}.$$

TABLE 6.14 Deuteriodecarboxylation of 5-chloroindole-3-carboxylic acid at 25°. $I = 1.0$
 $[D^+] = 1.016$ N. Run 409 .

<i>Time/min.</i>	<i>cpm</i>	<i>cpm(Calc)</i>	<i>% reaction.</i>
0	10113	10088	0
1050	6466	6468	36.1
2505	3520	3502	65.2
3045	2770	2792	72.6
3930	1909	1930	81.1
4395	1594	1591	84.2
5460	1043	1027	89.7
6960	561	564	94.5
∞	0	45 ± 14	100

$$k_0 = 7.01 \pm 0.07 \times 10^{-6} \text{ s}^{-1}.$$

6.4 HYDROGEN EXCHANGE OF 2-INDOLINONES.

6.4.1 PREPARATION AND PURIFICATION OF SUBSTRATES.

N-Methylindolin-2-one¹²⁶.

Treatment of oxindole (Aldrich) with one equivalent of sodium hydride in benzene, followed by one equivalent of iodomethane gave an oil on workup, which on fractional distillation gave a fraction, b.p. 82-90°/0.3 mm, m.p. (hexane) 87-88° (Lit.¹²⁶ 88-90°C).

δ (Ref. 100) 3.10 (3H, s), 3.32 (2H, s), 7.0 (4H, m).

ν_{\max} 1700, 1609, 1560 cm^{-1} .

1,3-Dimethylindolin-2-one¹⁰¹ (Scheme 5.4).

N-Methylaniline was treated with one equivalent of triethylamine in ether and 2-bromopropanoyl chloride (1 equiv.) and the precipitated amine salt was filtered off. Removal of the ether gave a residual oil which was treated at 160° with freshly sublimed aluminium chloride for 20 minutes. Ice was added and ether extraction followed by distillation gave the product (65%), b.p. 84°/0.3 mm; m.p. (hexane) 56°; m.p. (zone refined) 56° (Lit.¹⁰¹ 55°).

δ 1.30, 1.40 (3H, d, J 7Hz), 3.07 (3H, s), 3.15, 3.28 (1H, m, J 7 Hz), 6.9 (4H, m).

m/e 161 (M^+), 146, 118 (Lit.⁹⁹ 161, 146, 118).

ν_{\max} (Nujol/hexachlorobutadiene) 3040, 2970, 2940, 2880, 1720, 1700, 1605, 765 cm^{-1} .

4,6-Di^tbutylindolin-2-one (Scheme 5.5).

Ethyl 2-methylthioacetate¹²⁶ was prepared by treating a solution of ethyl 2-mercaptoacetate (12g) with sodium (2.3g) in ethanol (30ml), followed by slow addition of iodomethane (14.2g). After one hour reflux, the ethanol was removed and the residue washed with water and ether extracted. Careful fractionation of the ether extract gave a pale yellow liquid (50%), b.p. 61°/10.5 mm (Lit.¹²⁸ 60°/12mm).

δ 1.28 (3H, t), 2.19 (3H, s), 3.09 (2H, s), 4.14 (2H, q).

This thioester was used in the Gassman synthesis of indolinones⁵³. Treatment of ethyl 2-methylthioacetate (8g) with chlorine (3.5g) in dichloromethane at -78°, followed by slow addition of a solution of 3,5-di^tbutylaniline (10g) and triethylamine (5g) in dichloromethane gave the azasulphonium salt. Cyclisation was achieved by adding a solution of sodium (3g) in ethanol (20ml) and warming to room temperature. The organic solution was shaken with water several times till clear and evaporated to give a viscous oil.

δ 1.30, 1.48 (18H, d), 2.17 (3H, s), 4.27 (1H, s), 6.83, 7.07 (2H, dd).

m/e 291 (M⁺), 262, 244 (M⁺ - CH₃S⁺).

Desulphurisation was carried out with Raney Nickel¹¹⁷ (from 100g of 50% Ni/Al alloy) giving a viscous oil. Addition of hexane fraction

precipitated a buff solid, of which the total yield was eventually 2.5g (20%). The mother liquors contained an appreciable quantity, which could have been extracted if desired by column chromatography. m.p. (CHCl_2 /hexane) 209-210°C.

δ (CDCl_3) 1.32, 1.37 (18H, d), 3.70 (2H, s), 6.85, 7.10 (2H, dd).

m/e 245 (M^+), 230 ($\rightarrow 174$, m.s. 131.6), 174.

ν_{max} 3130, 1701, 1621, 1579, 877 cm^{-1} .

Found C, 78.25; H, 9.45; N, 5.53%. $\text{C}_{16}\text{H}_{23}\text{NO}$ requires C, 78.32; H, 9.44; N, 5.70%.

1-Methyl-4,6-di^tbutylindolin-2-one (Scheme 5.5).

The unalkylated indolinone (1g) was refluxed for one hour with sodium hydride (80% in oil, washed twice beforehand with hexane, 300mg) and iodomethane (5g)¹²⁶ in hexane. The solution was then poured into ice and washed well with water. Removal of the solvent gave about 500mg of a brown solid, which gave white needles on crystallisation from hexane, m.p. 176°C.

δ 1.33, 1.37 (18H, d), 3.17 (3H, s), 3.58 (2H, s), 6.60, 6.98 (2H, dd).

m/e 259 (M^+), 244 ($\text{M} - 15$).

ν_{max} 1696, 1616, 1580, 858 cm^{-1} .

Found C, 78.62; H, 9.52; N, 5.19%. $\text{C}_{17}\text{H}_{25}\text{NO}$ requires C, 78.70; H, 9.71; N, 5.40%.

1,3-Dimethyl-4,6-di^tbutylindolin-2-one (Scheme 5.3).

Treatment of the N-methylindolinone (500 mg) with a large excess of sodium hydride and methyl iodide in toluene at reflux for 2.5 hours, followed by workup as above gave a golden yellow oil which solidified (350mg). This solid was crystallised several times from pentane at 0°C., m.p. 101-102°C.

δ 1.33, 1.43 (18H, d), 1.50 (3H, d, J 7Hz), 3.12 (3H, s),
3.50 (1H, q, J 7Hz), 6.56, 7.04 (2H, dd, J 1.6Hz).

m/e 273 (M^+), 258 ($M^+ - 15$).

ν_{\max} 1704, 1618, 1580, 1005, 862 cm^{-1} .

Purification of Reagents.

Iodine was sublimed once before use. Potassium iodide, sodium tetraborate and methanol were all AnalaR reagents. Methanol-d₁ (Aldrich) contained > 99% d and was used as such. Ionic strength was maintained with either AnalaR sodium chloride or potassium iodide.

6.4.2 LABELLED INDOLINONES.

The 3-³H derivatives of 1-methyl and 1,3 dimethylindolinone were prepared by shaking a solution in ether with 1 N NaOH containing THO (1ml, 20mCi/ml) overnight. The ether was then separated, washed and evaporated. The 3-²H₁ labelled 1,3-dimethylindolinone was prepared by shaking an ethereal solution with 1 N NaOD in D₂O, and an isotopic

purity of >98% was obtained by renewing the NaOD solution twice. Nmr confirmed that the site of exchange was indeed the 3-position. 1,3-Dimethyl-4,6-di^tbutylindolinone was labelled by shaking with a cocktail of t-butanol (1ml) , ether (2ml) and NaOD (2ml) or NaOH/THO as required for 36 hours. Evaporation of the organic layer gave the required product.

6.4.3 OXIDATION PRODUCTS OF ALKYLINDOLINONES.

A solution of sodium (200mg) in methanol (5ml) was mixed with 1,3-dimethylindolinone (500mg) and ether added (25ml). Overnight, silky needles were precipitated. The reaction was almost complete in five minutes if oxygen gas was bubbled through. The white solid, presumed to be the sodium salt of the 3-hydroperoxide, was filtered off and dried. The solid gave a clear solution in water initially, but white crystals were rapidly deposited and the supernatant liquid liberated iodine from acidified potassium iodide solution. The crystals were filtered, dried and crystallised from chloroform/hexane to give white prisms of *1,3-dimethylindolin-2-on-3-ol*, m.p. 156° (Lit. ¹⁰⁹ 152° C).

δ 1.57 (3H,s), 3.17(3H,s), 3.6 (1H, br, exchanges with D₂), 7.0 (4H, m).

ν_{\max} 3300, 1700 cm⁻¹.

m/e 177 (M⁺), 162 (M-15), 149 (M-28), 134 (M-43).

Found C, 67.65; H, 6.18; N, 8.01%. Calculated for C₁₀H₁₁NO: C, 67.78; H, 6.26; N, 7.91%.

6.4.4 MEASUREMENT OF RATES.

a) Rates of protodetritiation.

The reaction solution was prepared by taking 20ml of sodium tetraborate solution (0.05M.), methanol (57.0ml) and the necessary amount of stock potassium iodide or sodium chloride solution to maintain the ionic strength. The desired pH was obtained by addition of sodium hydroxide solution. Runs were started by adding the $3\text{-}^3\text{H}_1$ labelled indolinone ($\sim 1\text{mg}$ in 0.7ml methanol) and making the volume up to 100 ml. Periodic aliquots (7-8 x 10ml) were withdrawn and assayed for tritium by extraction into xylene and scintillation counting. Air was always bubbled through before counting to remove excess tritium.

b) Rates of iododeprotonation and iododeuteriation^{38a}.

A solution containing borate buffer (0.05M, 5 ml) and methanol (14.4 - x, where x is the number of ml of stock indolinone to be added) was prepared in duplicate, and to both were added 3 ml of a degassed solution of iodine ($5 \times 10^{-4}\text{M}$) in potassium iodide (1.0N). The pH of the solutions was adjusted at this point by addition of 1.0N HCl or NaOH and the run started by adding the appropriate volume of stock $2.5 \times 10^{-2}\text{N}$ indolinone solution in methanol. The control solution had an equivalent amount of methanol added, was made up to a total volume of 25 ml and was placed in the sample cell (10mm) of the spectrometer.

The reaction solution was placed in the reference beam and the subsequent apparent increase in optical density monitored at 356 nm. This arrangement of the cells helps to overcome the problem caused by the slight decomposition of I_3^- at these pH values¹²⁹. The pH was measured at the end of the run.

c) Deuterium exchange by Mass Spectrometry.

The dedeuteriation of 1,3-dimethyl-4,6-di^tbutyl-3-²H₁-indolinone was followed by the following method, in essence the same as that adopted for methyl-dibutylindole.

The 3-²H indolinone (~10mg) and the 3-³H substrate (~1.5 mg) was dissolved in methanol (0.7 ml) and added to a solution containing methanol (57.0ml), and 0.1N in sodium chloride and about 0.01N in sodium hydroxide. The volume was made up to 100 ml and periodic aliquots (8 x 3ml) removed for tritium assay and (8 x ~7ml) for deuterium assay. The latter were shaken with 2,2,4 trimethylpentane (~2ml) and sodium chloride (~1g). After separation of the octane and careful removal under vacuum the samples were analysed by mass spectrometry (Section 6.1.6). The natural isotopic abundances were measured for an undeuteriated sample and incorporated in equation 6.17, which gives the deuterium content.

$$\%d_1 = \frac{100(R - 0.202)}{1 + (R - 0.202)} \quad 6.17$$

The deuteriation run was analogous, except that D₂O (>99.7%d) and methanol-d₁ ('Diaprep' Aldrich, >99%d) were used as solvents.

The deuterium content was estimated from a comparison of the areas of the HOD and ^{13}C satellite nmr peaks of the methanol to be >99.5% at the end of the run.

A typical mass spectral analysis is illustrated in Figure 6.3 .

6.4.5 ANALYSIS OF THE KINETIC DATA.

The rate of tritium loss was plotted according to equation 6.7, which was found to give linear plots for more than 90% reaction. Deuterium exchange kinetics were plotted according to equation 6.8 . The experimental data for a simultaneous dedeuteriation and detritiation is given in Table 6.15, taken partially from the results shown in Figure 6.3 .

The optical iodination data were fitted to the integrated form of equation 5.6

$$|A_{\infty} - A_t| = a \cdot t - b \cdot \ln |A_{\infty} - A_t| + c \quad 6.17$$

where A_t is the optical density at 356 nm.

$$a = k_1^{-H} [\text{Indolinone}] [\text{OH}^-] / \epsilon \cdot \ell$$

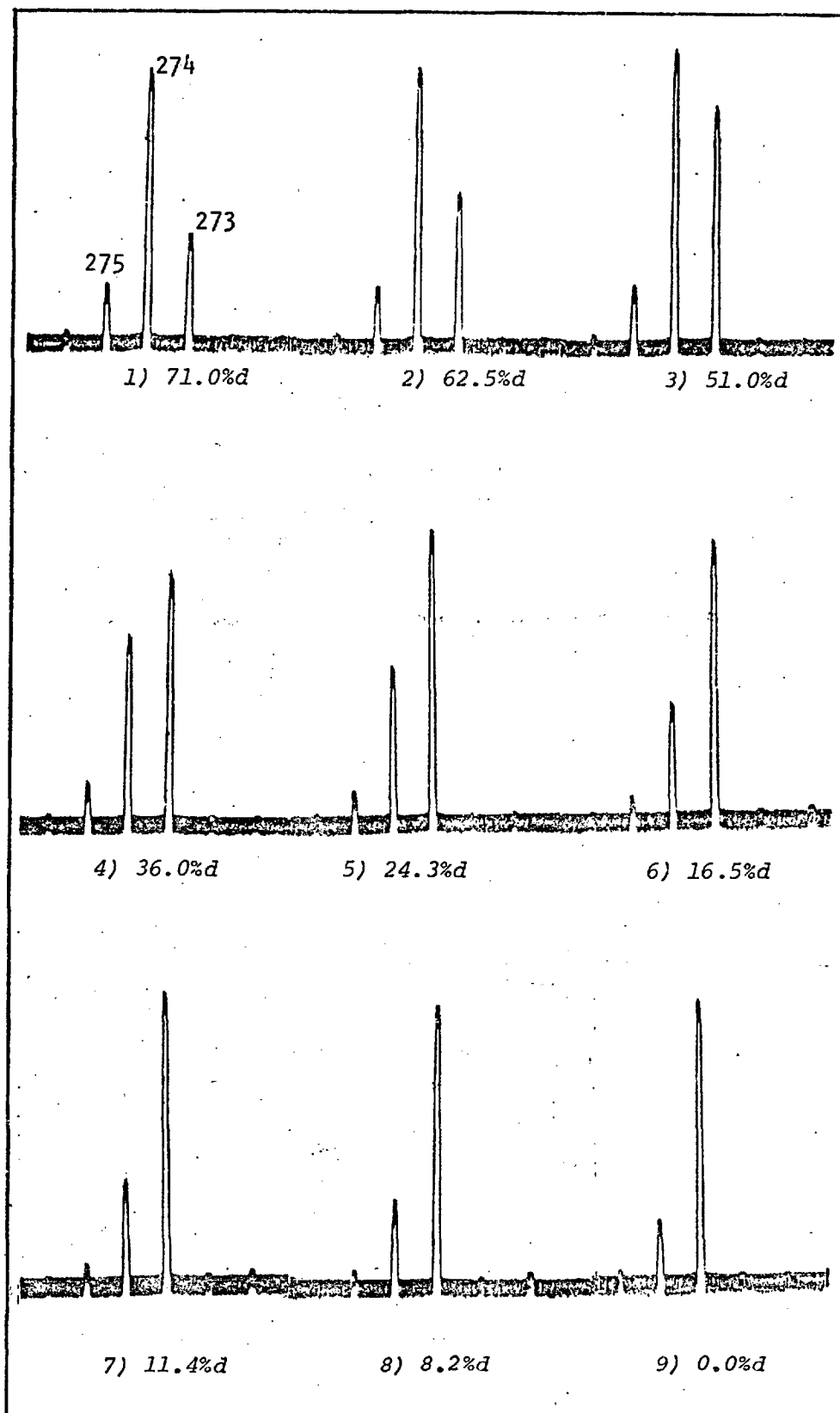
$$b = 715k_{-1} [\text{I}^-] / k_2 \cdot \epsilon \cdot \ell$$

ϵ = extinction coefficient of the tri-iodide ion.

ℓ = optical path length.

Figure 6.3 Mass Spectral analysis of 1,3-Dimethyl-4,6-di^tbutyl-3-²H₁ indolinone. Run 496.

The sequence 1) to 9) represents decreasing deuterium content.



Equation 6.17 was analysed by a linear least squares regression analysis. Strictly speaking equation 6.17 is a non-linear system, since the variable $|A_{\infty} - A_t|$ appears twice, however no explicit solution is available for this variable and a rigorous regression analysis could not be made. By making the approximation that $|A_{\infty} - A_t|$ and $\ln |A_{\infty} - A_t|$ are two independent variables the system can be treated by linear multiple regression analysis. The validity of this approximation was demonstrated when analysing the decarboxylation data (Section 7.2), where the agreement between the linear and non-linear analyses of the same data was good, though not perfect.

To guard against a spurious analysis, equation 6.17 was also analysed in a different form (Equation 6.18).

$$\ln |A_{\infty} - A_t| = \frac{a}{b} \cdot t - \frac{|A_{\infty} - A_t|}{b} + c \quad 6.18$$

The difference in the two equations is that in the former, residuals in the optical density were minimised, in the latter it is the logarithm of the optical density that has the residuals minimised. The values for the constants obtained by these methods agreed closely.

It is worth mentioning that standard errors obtained by the non-rigorous method outlined above may be 2 or 3 times too low. Also, in several cases where non-random variations in the fit of data were observed, it was found a slight adjustment in A_{∞} improved the fit considerably. This was normally not necessary. An example of this analysis is given in Table 6.16 .

TABLE 6.15 Simultaneous protodetrition and protodeuteriation of 1,3-Dimethyl-4,6-di^tbutylindolinone in 50%(w/w) aqueous methanol/sodium hydroxide solution at 25^oC.

[NaCl] = 0.1N, $pH_m = 12.151$. Run 496

Time/min.	Dedeuteriation		Detritiation	
	%d ₁	%d ₁ (Calc)	cpm	cpm (Calc)
-1	71.0	73.5		
5			6381	6375
10	62.5	63.4		
25	51.0	50.8		
35			5253	5237
50	36.0	35.1		
65			4273	4306
75	24.3	24.3		
100	16.5	16.7		
105			3342	3320
125	11.4	11.5		
148	8.2	8.1		
150			2475	2483
200			1797	1805
250			1329	1318
306			932	935
∞	0.0	-0.3 ± 0.7	60	84 ± 28

$$k_o^{-D} = 2.45 \pm 0.08 \times 10^{-4} \text{ s}^{-1} \quad k_o^{-T} = 1.10 \pm 0.015 \times 10^{-4} \text{ s}^{-1}.$$

TABLE 6.16 Iododeprotonation of 1,3-Dimethylindolin-2-one in 50%(w/w) aqueous methanol/sodium tetraborate solution at 25°C and pH_m 9.118 . Run 445

$$[\text{Indolinone}] = 2 \times 10^{-3} \text{M}, \text{ Initial } [\text{I}_3^-] = 6 \times 10^{-5} \text{M}, \quad \epsilon_{\text{I}_3^-} = 2.54 \times 10^4 \text{M}^{-1} \text{cm}^{-1}.$$

Time/s	Minimisation of $ A_\infty - A_t $				Minimisation of $\ln A_\infty - A_t $		
	$0.5A_t$	$ A_\infty - A_t $	Calc.	Difference	$-\ln A_\infty - A_t $	Calc.	Diff.
80	0.156	0.564	0.563	-0.001	0.573	0.576	-0.003
100	0.220	0.500	0.502	0.002	0.693	0.687	0.006
120	0.278	0.442	0.441	-0.001	0.816	0.821	-0.004
140	0.337	0.383	0.386	0.003	0.960	0.951	0.009
160	0.388	0.332	0.330	-0.002	1.103	1.109	-0.007
180	0.439	0.281	0.281	0.000	1.269	1.268	0.001
200	0.484	0.236	0.235	-0.001	1.444	1.448	-0.004
250	0.579	0.141	0.140	-0.001	1.969	1.962	-0.003
300	0.645	0.075	0.078	0.003	2.590	2.581	0.009
350	0.683	0.037	0.036	-0.001	3.297	3.301	-0.004
∞	0.720	0.000					

$$*k_1^{-H} = 37.19 \pm 0.38 \times 10^{-8}; k_{-1}/k_2^* = 2.168 \pm 0.038 \times 10^{-5} \quad | \quad *k_1^{-H} = 37.24 \times 10^{-8}; k_{-1}/k_2^* = 2.178 \times 10^{-5}$$

P A R T F O U R

APPENDIX

CHAPTER VII

7.1 NON-LINEAR LEAST SQUARES ANALYSIS OF KINETIC DATA.

The mathematical technique of Deming^{124a} was applied to equation 7.1

$$y = a + e^{(-k_0 t + b)} \quad 7.1$$

The residual F_i is defined;

$$F_i = a + e^{(-k_0 t + b)} - y_i \quad 7.2$$

The residual F_i is only an approximation, since in order to initiate the method estimates of \underline{a} , k_0 and \underline{b} are employed. F_i therefore deviates from the 'most probable' value (at which point $\sum F_i^2$ is a minimum) by the amount δF_i . To evaluate δF_i we make use of Taylor's Theorem (equation 7.3).

$$f(x + \delta x) = f(x) + \delta x \cdot f'(x) + \frac{(\delta x)^2}{2} \cdot f''(x) \quad 7.3$$

To simplify the argument only the first two terms of the expansion are used, and since

$$\delta f(F_i) = \frac{\partial F_i}{\partial a} + \frac{\partial F_i}{\partial b} + \frac{\partial F_i}{\partial k_0} \quad 7.4$$

equation 7.3 becomes

$$G_i = F_i + \delta a.(\partial F_i/\partial a) + \delta b.(\partial F_i/\partial b) + \delta k_o(\partial F_i/\partial k_o) \quad 7.5$$

G_i now represents the corrected value for the residual F_i and is the quantity which the least squares principle requires to be minimised, such that $\sum F_i^2/L_i > \sum G_i^2/L_i = \text{minimum}$. The quantity L_i is the weight of the observation and will be defined later. To obtain the condition under which $\sum G_i^2/L_i$ is a minimum we differentiate w.r.t. each adjustable parameter.

$$\text{Hence} \quad \sum \frac{G_i}{L_i} \cdot \frac{\partial G_i}{\partial(\delta a)} = 0 \quad \text{w.r.t.} \quad \delta a \quad 7.6a$$

$$\sum \frac{G_i}{L_i} \cdot \frac{\partial G_i}{\partial(\delta b)} = 0 \quad \text{w.r.t.} \quad \delta b \quad 7.6b$$

$$\sum \frac{G_i}{L_i} \cdot \frac{\partial G_i}{\partial(\delta k_o)} = 0 \quad \text{w.r.t.} \quad \delta k_o \quad 7.6c$$

$$\text{Also} \quad \partial G_i/\partial(\delta a) = \partial F_i/\partial a \quad 7.7a$$

$$\partial G_i/\partial(\delta b) = \partial F_i/\partial b \quad 7.7b$$

$$\partial G_i/\partial(\delta k_o) = \partial F_i/k_o \quad 7.7c$$

$$\text{And} \quad \partial F_i/\partial a = 1 \quad 7.8a$$

$$\partial F_i/\partial b = e^{(-k_o t_i + b)} \quad 7.8b$$

$$\partial F_i/\partial k_o = -k_o \cdot e^{(-k_o t_i + b)} \quad 7.8c$$

Substituting equation 7.8 in equation 7.6 and expressing in matrix notation

$$\begin{pmatrix} \frac{n}{L_i} & \sum \frac{e^{(-k_o t_i + b)}}{L_i} & - \sum k_o \frac{e^{(-k_o t_i + b)}}{L_i} \\ \sum \frac{e^{(-k_o t_i + b)}}{L_i} & \sum \frac{e^{2(-k_o t_i + b)}}{L_i} & - \sum k_o \frac{e^{2(-k_o t_i + b)}}{L_i} \\ - \sum k_o \frac{e^{(-k_o t_i + b)}}{L_i} & - \sum k_o \frac{e^{2(-k_o t_i + b)}}{L_i} & \sum k_o^2 \frac{e^{2(-k_o t_i + b)}}{L_i} \end{pmatrix} \begin{pmatrix} \delta a \\ \delta b \\ \delta k_o \end{pmatrix}$$

$$= \begin{pmatrix} - \sum \frac{F_i}{L_i} \\ \sum \frac{F_i e^{(-k_o t_i + b)}}{L_i} \\ \sum \frac{k_o F_i e^{(-k_o t_i + b)}}{L_i} \end{pmatrix} \quad 7.9$$

Equation 7.9 can be expressed in shorthand as

$$A.X. = M \quad 7.10$$

Also A^{-1} is defined as the inverse of A, and has the property

$$A^{-1}.A = I, \text{ where } I.X. = X.$$

By multiplying equation 7.10 by A^{-1} we obtain

$$X = M.A^{-1}. \quad 7.11$$

The summations in equation 7.9 are obtained, using estimates for the parameters a , b and k_0 , and the experimental values for t_i and y_i . The matrix A is then inverted, using a pivotal method to minimise roundoff errors and equation 7.11 solved to obtain X , which can be seen from equation 7.9 to represent the increments δa , δb and δk_0 . The new estimate for the parameters is found, ie $k_0^1 = k_0 + \delta k_0$ and the whole cycle is repeated using as estimates k_0^1 etc till the corrections become small in relation to the parameters.

Weighting of data.

For two variables related by $y = f(x)$ Deming defined^{124a}

$$1/\text{Weight} = L_i = \frac{(\partial F / \partial x_i)^2}{W_{x_i}} + \frac{(\partial F / \partial y_i)^2}{W_{y_i}} \quad 7.12$$

$$\text{where } F = f(x_i) - y_i, \quad W_{x_i} = \sigma_0^2 / \sigma_x^2 \quad \text{and} \quad W_{y_i} = \sigma_0^2 / \sigma_y^2 \quad 7.13$$

σ_x and σ_y are the variances assigned to the variables and σ_0^2 is the internal variance of unit weight (an arbitrary constant).

Application to equation 7.1 gives

$$\sigma_{x_i} = 0, \quad \sigma_{y_i} = m$$

We have assigned no error to the time variable and an error of $\pm m$ to a reaction ordinate such as optical density.

By defining the internal variance $\sigma_o = m$, we obtain from equation 7.13

$$W_{y_i} = \left(\frac{m}{y_i}\right)^2 = 1 \quad \text{and equation 7.12 reduces to}$$

$$L_i = 1, \text{ since } \partial F / \partial y_i = -1$$

The value for L_i of 1 is inserted into the matrix elements of equation 7.9.

When equation 7.1 is used to treat data with relative errors, then we use

$\sigma_{x_i} = 0$, $\sigma_{y_i} = m \cdot y_i$ where m is now the fractional error assumed in y_i and by defining $\sigma_o = m$ we obtain

$$W_{y_i} = m^2 / m^2 \cdot y_i^2 \quad \text{and hence} \quad L_i = y_i^2.$$

Standard errors.

When the iteration is complete, since $\delta F_i = 0$ then $F_i = G_i$. The external variance is defined (independently or from equation 7.15) as

$$\sigma_{\text{ext}}^2 = \frac{\sum F_i^2 / L_i}{n - 3} \quad 7.14$$

At this point a comparison of σ_o and σ_{ext} can be made, where σ_o as defined above equals m , the fractional or absolute internal error estimate of y and σ_{ext} represents the external error of the variable y . Generally σ_o and σ_{ext} should be approximately equal, though a rigorous F test can be applied if sufficient data to define σ_o is available (ie spectrophotometric accuracy of the instrument).

Normally, since this is not the case the simple assumption that $\sigma_o = \sigma_{ext}$ is made and equation 7.15 can be applied using σ_{ext} rather than σ_o . It should be noted that σ_{ext} is often termed the standard error of the variable y.

$$\begin{aligned} \sigma_a^2 &= A^{-1}(1,1) \sigma_o^2 \\ \sigma_b^2 &= A^{-1}(2,2) \sigma_o^2 \\ \sigma_{k_o}^2 &= A^{-1}(3,3) \sigma_o^2 \end{aligned} \quad 7.15$$

The elements of A^{-1} are often termed the variance co-variance elements.

7.2 NON-LINEAR LEAST SQUARES ANALYSIS OF DECARBOXYLATION DATA.

The technique discussed previously was applied to equation 7.16 .

$$y = \frac{a + b.x}{1 + cx} \quad 7.16$$

As seen from the previous section initial estimates are required for a, b and c and these were obtained by rearranging equation 7.16 to 7.17 and analysing this function by linear least squares analysis.

$$y = a + b.x - c.x.y. \quad 7.17$$

The regression equations 7.18 used to calculate $\delta a, \delta b,$ and δc were obtained by a process analogous to equation 7.9

$$\begin{pmatrix} \sum \frac{1}{(1 + c \cdot x_i)^2 L_i} & \sum \frac{x_i}{(1 + c \cdot x_i)^2 L_i} & \sum \frac{(a + b \cdot x_i)}{(1 + c \cdot x_i)^3 L_i} \\ (1,2) & \sum \frac{(a + b \cdot x_i)^2}{(1 + c \cdot x_i)^2 L_i} & \sum \frac{(a + b \cdot x_i) x_i}{(1 + c \cdot x_i)^3 L_i} \\ (1,3) & (2,3) & \sum \frac{(a + b \cdot x_i)^2}{(1 + c \cdot x_i)^4 L_i} \end{pmatrix} \begin{pmatrix} \delta a \\ \delta b \\ \delta c \end{pmatrix}$$

$$= \begin{pmatrix} \sum \frac{F_i}{(1 + c \cdot x_i) L_i} \\ \sum \frac{F_i \cdot x_i}{(1 + c \cdot x_i) L_i} \\ \sum \frac{F_i (a + b \cdot x_i) x_i}{(1 + c \cdot x_i)^2 L_i} \end{pmatrix} \quad 7.18$$

Weighting of data

From equation 7.12 we obtain;

$$F_i = \frac{a + b \cdot x_i}{1 + c \cdot x_i} - y_i$$

and so $(\partial F_i / \partial x_i)^2 = (b - ac)^2 / (1 + c \cdot x_i)^4$

and $(\partial F_i / \partial y_i)^2 = 1$

For decarboxylation data we assume

$$\sigma_{y_i} = 0.025 y_i \quad (\text{ie a 2.5\% error in rate constant}) \text{ and}$$

$$\sigma_{x_i} = 0.001 \quad (\text{ie an error of 0.001 N in the acid conc.})$$

Since $W_{x_i} = \sigma_o^2 / \sigma_x^2$ we define $\sigma_o = 0.001$ and hence

$$W_{x_i} = 1 \quad . \text{ It follows then that}$$

$$W_{y_i} = \frac{\sigma_o^2}{\sigma_y^2} = 1 / 625 y_i^2 \quad . \text{ Equation 7.12 becomes}$$

$$L_i = \frac{(b - ac)^2}{(1 + c.x_i)^4} + 625 y_i^2$$

and this function is inserted in the matrix elements of equation 7.18 and solved as previously described.

Standard errors.

σ_{ext} is obtained from equation 7.14 and the standard errors obtained from equation 7.15, but using the value obtained for σ_{ext} rather than σ_o . The ratio $\sigma_{\text{ext}}/\sigma_o = \sigma_{\text{ext}}/0.001 = F$ was generally found to be between 0.9 and 0.3. If σ_o is given ∞ degrees of freedom and σ_{ext} about 7 then normally a fairly good level of significance is obtained (~ 0.2) on application of the F test.

BIBLIOGRAPHY

1. F.H.Westheimer, *Chem. Rev.*, 1961, 61, 265.
2. J.Bigeleisen, *Pure. Appl. Chem.*, 1964, 8, 217.
3. M.Wolfsberg, *Ann. Rev. Phys. Chem.*, 1969, 449.
4. W.A. van Hook in ' *Isotope effects in Chemical reactions*', Chapter 1 (C.J.Collins & W.S.Bowman, Eds) 1970, Van Nostrand, N.Y.
5. R.A.More O'Ferrall and J.Kouba, *J. Chem. Soc.B*, 1967, 985.
6. R.A.More O'Ferrall, *ibid*, 1970, 785.
7. W.J.Albery, *Trans. Faraday Soc.*, 1967, 63, 200.
8. R.P.Bell, W.H.Sachs and R.L.Tranter, *ibid*, 1971, 67, 1995.
9. a) A.Bromberg, K.Muszkat, E.Fisher and F.S.Klein, *JCS Perkin II*, 1972, 588
b) F.Williams and J.T.Wang, *J. Amer. Chem. Soc.*, 1972, 94, 2930.
10. a) A.V.Willi and M.Wolfsberg, *Chem. and Ind.*, 1964, 2097.
b) M.J.Stern and M.Wolfsberg, *J. Chem. Phys.*, 1966, 45, 4105.
11. a) A.J.Kresge, *Chem. Soc. Rev.*, 1973, 2, 475.
b) A.J.Kresge, *Can. J. Chem.*, 1974, 52, 1897.
c) D.S.Kemp and M.L.Casey, *J. Amer. Chem. Soc.*, 1973, 95, 6670
and references cited within.
12. J.N.Brønsted and E.A.Guggenheim, *ibid*, 1927, 49, 2552.
13. F.G.Bordwell and W.J.Boyle, *ibid*, 1972, 94, 3907; *ibid*, 1970, 92, 5926; *ibid*, 1969, 91, 4002.
14. R.A.Marcus, *ibid*, 1969, 91, 7224 and references within.
15. a) G.W.Koepp1 and A.J.Kresge, *JCS Chem. Commun.*, 1973, 371

- b) J.R.Murdock, *J. Amer. Chem. Soc.*, 1972, 94, 4410.
16. J.L.Kurtz and L.C.Kurtz, *ibid*, 1972, 94, 4451.
17. D.J.Barnes and R.P.Bell, *Proc. Roy. Soc. A*, 1970, 318, 421
and numerous references cited within.
18. F.G.Bordwell and W.J.Boyle, *J. Amer. Chem. Soc.*, 1971, 93, 511
and 512.
19. a) R.P.Bell and B.G.Cox, *J. Chem. Soc. B*, 1971, 783.
b) *ibid*, 1970, 194.
c) J.E.Dixon and T.C.Bruice, *J. Amer. Chem. Soc.*, 1970, 92, 905.
20. a) J.R.Keefe and N.H.Munderloh, *JCS Chem. Commun.*, 1974, 17.
b) J.H.Kim and K.T.Leffek, *Can. J. Chem.*, 1974, 52, 592.
21. H.Wilson, J.D.Caldwell and E.S.Lewis, *J. Org. Chem.*, 1973, 38,
564 and earlier papers cited within.
22. a) J.P.Calmon, M.Calmon and V.Gold, *J. Chem. Soc. B*, 1971, 659.
b) V.Gold and S.Grist, *JCS Perkin II*, 1972, 89.
23. F.Hibbert, F.A.Long and E.A.Walters, *J. Amer. Chem. Soc.*, 1971,
93, 2829 & 2833.
24. a) L.Melander and N.A.Bergman, *Acta. Chem. Scand.*, 1971, 25, 2264.
b) L.Melander, *ibid*, 1972, 26, 1130.
25. D.J.McLennan and R.J.Wong, *JCS Perkin II*, 1974, 526.
26. P.J.Smith and S.K.Tsui, *J. Amer. Chem. Soc.*, 1973, 95, 4760.
27. C.A.Pollock and P.J.Smith, *Can. J. Chem.*, 1971, 49, 3856.
28. L.F.Blackwell, P.D.Buckley and K.W.Jolley, *JCS Perkin II*, 1973,
169.
29. W.A.Pryor and K.G.Kneipp, *J. Amer. Chem. Soc.*, 1971, 93, 5584.
30. E.S.Lewis and M.M.Butler, *Chem. Commun.*, 1971, 941.

31. A.Streitwieser, M.R.Granger, F.Mares and R.A.Wolf, *J. Amer. Chem. Soc.*, 1973, 95, 4257 and earlier references cited within.
32. A.J.Kresge and Y.Chiang, *ibid*, 1969, 91, 1025.
33. L.C.Gruen and F.A.Long, *ibid*, 1967, 89, 1287; J.L.Longridge and F.A.Long, *ibid*, 1967, 89, 1292.
34. S.Olsson, *Arkiv Kemi*, 1970, 32, 105 and earlier papers.
35. a) B.C.Challis and E.M.Millar, *JCS Perkin II*, 1972, 1111.
b) *Ibid*, 1116.
c) *Ibid*, 1618.
d) *Ibid*, 1625.
36. S.B.Hanna, C.Jermini and H.Zollinger, *Tet. Letters*, 1969, 4415.
37. E.F.Caldin, *Chem. Rev.*, 1969, 69, 135.
38. J.R.Jones, ' *The Ionisation of Carbon Acids*', 1973, Academic Press, London.
a) p 7 b) p 152 c) p 139 d) pp 171-180 e) p 179 f) pp 203-207 g) pp 41-44.
39. E.F.Caldin and S.Mateo, *JCS Chem. Commun.*, 1973, 854.
40. E.S.Lewis and J.K.Robinson, *J. Amer. Chem. Soc.*, 1968, 90, 4337.
41. M.J.Stern and P.C.Vogel, *ibid*, 1971, 93, 4664.
42. C.G.Swain, E.S.Stivers, J.F.Reuwar and L.J.Schaad, *ibid*, 1958, 80, 5855.
43. A.J.Kresge and S.G.Mylonakis, *ibid*, 1972, 94, 4197.
44. H.V.Ansell and R.Taylor, *JSC Chem. Commun.*, 1973, 936.
45. J.Bangor, C.D.Johnson, A.R.Katritzky and B.R.O'Neill, *JCS Perkin II*, 1974, 394 and earlier papers.
46. R.L.Hinman and E.B.Whipple, *J. Amer. Chem. Soc.*, 1962, 84, 2534.
47. B.C.Challis and F.A.Long, unpublished results.

48. A.J.Kresge and Y.Chiang, *J. Amer. Chem. Soc.*, 1962, 84, 3976.
49. A.J.Kresge and Y.Chiang, *ibid*, 1967, 89, 4411.
50. R.J.Sundeberg, ' *The Chemistry of Indoles*', 1970, Academic Press, London. a) Chapter 3 b) Chapter 7.
51. M.Chastrette, *Ann. Chim.*, 1962, 7, 643.
52. a) F.T.Tyson, *J. Amer. Chem. Soc.*, 1941, 63, 2024.
b) L.Marion and C.W.Oldfield, *Can. J. Res.*, 1947, 25B, 1.
53. P.G.Gassman, G.Gruetzmacher, T.J. van Bergen, *J. Amer. Chem. Soc.*, 1973, 95, 6508. I am grateful to Professor Gassman for details of the experimental method.
54. a) D.D.Perrin ' *Dissociation Constants of Organic Bases in Aqueous Solution*', 1965, Butterworths, London.
b) G.Kortum, W.Vogel and K.Andrussow, ' *Dissociation Constants of Organic Acids in Aqueous Solution.*' , 1961, Butterworths, London.
55. E.M.Millar, Ph.D. Thesis, 1968, London.
56. R.Bates, *J. Phys. Chem.*, 1965, 69, 2750; *ibid*, 1966, 70, 2073.
57. R.Bates, ' *The Determination of pH.*' , 1964, p 224. Wiley, N.Y.
58. P.J.Krueger and J.Jan, *Can. J. Chem.*, 1970, 48, 3226.
59. R.L.Hinman and J.Lang, *J. Amer. Chem. Soc.*, 1964, 86, 3796.
60. R. iqbal, Ph.D. Thesis, 1971, London.
61. A.J.Kresge and Y.Chiang, *J. Amer. Chem. Soc.*, 1967, 89, 4418.
62. G.Yagil and M.Anbar, *ibid*, 1963, 85, 2376.
63. H.Zollinger, *Helv. Chim. Acta.*, 1955, 38, 1597; *ibid*, 1617 ;
ibid, 1623; *ibid*, 1958, 41, 2274. For a recent review see
H.Zollinger, *Angew. Chem.*, 1972, 11, 874.
64. J.A.Feather and V.Gold, *J. Chem. Soc.*, 1965, 1752.

65. E.A.Walters and F.A.Long, *J. Amer. Chem. Soc.*, 1969, 91, 3733.
66. a) G.Yagil, *J. Phys. Chem.*, 1967, 71, 1034 & 1045.
b) G.Yagil, *Tetrahedron*, 1967, 23, 2855.
67. J.H.Binks and J.H.Ridd, *J. Chem. Soc.*, 1957, 2398.
68. T.Hino and N.Nakagawa, *Tetrahedron*, 1970, 26, 4491.
69. J.Harley-Mason and T.J.Leeney, *Proc. Chem. Soc.*, 1964, 363.
70. a) F.Snychers and H.Zollinger, *Tet. Letters*, 1970, 2759.
b) F.Snychers and H.Zollinger, *Helv. Chim. Acta*, 1970, 53, 1294.
71. L.Meurling, *Acta Chem. Scand.*, 1974, B28, 369.
72. R.J.Higgins, Ph.D. Thesis, 1972, London.
73. a) G.Castanati, A.Dossena and A.Pochini, *Tet. Letters*, 1972, 5227.
b) R.Iyer, A.H.Jackson, P.V.R.Shannon and B.Naidoo, *JCS Perkin II*, 1973, 872.
c) V.G.Avramenko, V.D.Nazina, S.Sherif and N.N.Suvorov, *Tr. Mosk. Khim. Tekhnol. Inst.*, 1970, 132.
74. a) N.N.Bubnov, K.A.Bilevich, L.A.Polyakova and O.Y.Okhlobystin, *JCS Chem. Commun.*, 1972, 1058.
b) S.McLean and G.I.Dmitrienko, *Can. J. Chem.*, 1971, 49, 3642.
75. P.Burri, H.Loewenschuss, H.Zollinger and G.K.Zwolinski, *Helv. Chim. Acta*, 1974, 57, 395.
76. K.Valter and V.Sterba, *Coll. Czech. Chem. Comm.*, 1972, 37, 270.
77. a) V.Beranek, H.Korinkova, P.Vetesnik and M.Vecera, *ibid*, 1972, 37, 282 report a study of N-methylaniline.
b) V.Beranek, M.Vecera, *ibid*, 1969, 34, 2753 report a study of N,N-dimethylaniline.
78. J.Panchartek and V.Sterba, *ibid*, 1969, 34, 2971.

79. V.Beranek, V.Sterba and K.Valter, *ibid*, 1973, 38, 257.
80. E.Berliner in '*Prog. in Phys. Org. Chem.*', 1964, 2, p 306.
81. O.Sziman and A.Messmer, *Tet. Letters*, 1968, 1625.
82. J.R.Penton and H.Zollinger, *Helv. Chim. Acta*, 1971, 54, 573.
83. R.W.Franck and Y.Yanagi, *J. Amer. Chem. Soc.*, 1968, 90, 5814
report a similar decomposition of 2,5 di^tbutylaniline.
84. L.G. Van Uitert and C.G.Hass, *ibid*, 1953, 75, 451.
85. E.Helgstrand and B.Lamm, *Arkiv Kemi*, 1963, 20, 193.
86. a) P.G.Farrell and S.F.Mason, *Nature*, 1963, 197, 590.
b) D.G.Pradham, *Ind. J. Chem.*, 1973, 11, 894.
87. A.V.Willi, C.M.Won and P.Vilk, *J. Phys. Chem.*, 1968, 72, 3142.
88. A.V.Willi, C.M.Won and M.H.Cho, *Helv. Chim. Acta*, 1970, 53, 663.
89. M.Zielinski, *Rocz. Chem.*, 1968, 42, 1725.
90. D.S.Noyce, L.M.Gortler, F.B.Kirby and M.D.Schiavelli, *J. Amer. Chem. Soc.*, 1967, 89, 6944.
91. a) J.L.Longridge and F.A.Long, *ibid*, 89, 1292.
b) *Ibid*, 1968, 90, 3092.
c) F.A.Long and H.H.Huang, *ibid*, 1969, 91, 2872.
92. a) G.E.Dunn and S.K.Dyal, *Can. J. Chem.*, 1970, 48, 3349.
b) G.E.Dunn and K.J.G.Lee, *ibid*, 1971, 49, 1032.
c) G.E.Dunn, K.J.G.Lee and H.Thimm, *ibid*, 1972, 50, 3017.
93. G.R.Allen, C.Pidacks and M.J.Weiss, *J. Amer. Chem. Soc.*, 1966, 88, 2536.
94. J.C.Powers, *Tet. Letters*, 1965, 655.
95. S.Kasperek and R.A.Heacock, *Can. J. Chem.*, 1967, 45, 771.
96. M.S.Melzer, *J. Org. Chem.*, 1962, 27, 496.

97. B.M.Lowe and D.G.Smith, *JCS Faraday I*, 1974, 362.
98. C.G.Swain, D.A.Kuhn and R.L.Showen, *J. Amer. Chem. Soc.*, 1965, 87, 1553.
99. T.Hino, M.Nakagawa, K.Tsuneoka, S.Misawa and S.Akuboshi, *Chem. Pharm. Bull.*, 1969, 17, 1651.
100. B.Witkop, *J. Org. Chem.*, 1970, 35, 3981 and references within.
101. P.L.Julian, J.Pikl and D.Boggess, *J. Amer. Chem. Soc.*, 1934, 56, 1797.
102. E.A.Halevi and F.A.Long, *ibid*, 1961, 83, 2877.
103. R.R.Li and S.I.Millar, *J. Chem. Soc. B*, 1971, 2269.
104. J.Toullec and J.E.Dubois, *J. Amer. Chem. Soc.*, 1974, 96, 3524 and previous papers cited within.
105. R.P.Bell, D.W.Earls and B.A.Timini, *JCS Perkin II*, 1974, 811.
106. K.F.Bonhoeffer, K.H.Geib and O.Reitz, *J. Chem. Phys.*, 1939, 7, 664.
107. J.R.Jones, *Trans. Faraday Soc.*, 1965, 61, 95.
108. D.W.Earls, J.R.Jones and T.G.Rumney, *JCS Faraday I*, 1972, 925.
109. P.L.Julian and J.Pikl, *J. Amer. Chem. Soc.*, 1935, 57, 539.
110. M.A.Winnik, V.Stoute and P.Fitzgerald, *ibid*, 1974, 96, 1977 who report results on hemiketal formation of analogous compounds.
111. N.Gravitz and W.P.Jencks, *ibid*, 1974, 96, 489.
112. V.Golj and S.Grist, *J. Chem. Soc. B*, 1971, 2282.
113. A.Jönsson, *Svensk. Kem. Tid. Skv.*, 1955, 67, 188.
114. N.B.Chapman, K.Clarke and H.Hughes, *J. Chem. Soc.*, 1965, 1424.
115. J.Geuze, C.Ruinard, J.Soeterbroek, P.E.Verkaide and B.M.Wepster, *Rec. Trav. Chim.*, 1956, 75, 301.
116. T.W.Elder and R.P.Mariella, *Can. J. Chem.*, 1963, 41, 1653.
117. L.F.Fieser and M.Fieser, ' *Reagents for Organic Synthesis* ', 1967, 1, p 729.

118. D.P.Perrin, W.L.F.Armarego and D.R.Perrin ' *Purification of Laboratory Chemicals* ', 1966, Pergamon.
119. R.P.Bell and D.M.Goodall, *Proc. Roy. Soc. A*, 1966, 294, 273.
120. J.H.Beynon and A.E.Williams, ' *Mass and Abundance Tables for use in Mass Spectrometry* ', 1963, Elsevier, N.Y.
121. V.Machacek, O.Machackova and V.Sterba, *Coll. Czech. Chem. Comm.*, 1971, 36, 3186.
122. M.Sukigara and S.Kikuchi, *Bull. Chem. Soc. Jap.* , 1967, 40, 1077.
123. A.Zenhausern and H.Zollinger, *Helv. Chim. Acta*, 1962, 45, 1882.
124. a) W.E.Deming, ' *Statistical Adjustment of Data* ', 1943, Wiley, N.Y.
b) W.E.Wentworth, *J. Chem. Ed.*, 1965, 42, 96 & 162.
125. C.J.Collins in ' *Adv. in Phys. Org. Chem.* ', 1964, 2, p 67.
126. E.Wenkert, N.K.Bhattachargya, T.L.Reid and T.E.Stevens, *J. Amer. Chem. Soc.*, 1956, 78, 797.
127. R.B.Wagner and H.D.Zook, ' *Synthetic Organic Chemistry* ', 1953, Wiley, N.Y.
128. A.Schoenberg and K.Praefcke, *Chem. Ber.*, 1966, 99, 2371.
129. E.S.Lewis and L.H.Funderburk, *J. Amer. Chem. Soc.*, 1967, 89, 2322.